INFORMATION TO USERS

This manuscript has been reproduced from the microfilm master. UMI films the text directly from the original or copy submitted. Thus, some thesis and dissertation copies are in typewriter face, while others may be from any type of computer printer.

The quality of this reproduction is dependent upon the quality of the copy submitted. Broken or indistinct print, colored or poor quality illustrations and photographs, print bleedthrough, substandard margins, and improper alignment can adversely affect reproduction.

In the unlikely event that the author did not send UMI a complete manuscript and there are missing pages, these will be noted. Also, if unauthorized copyright material had to be removed, a note will indicate the deletion.

Oversize materials (e.g., maps, drawings, charts) are reproduced by sectioning the original, beginning at the upper left-hand corner and continuing from left to right in equal sections with small overlaps. Each original is also photographed in one exposure and is included in reduced form at the back of the book.

Photographs included in the original manuscript have been reproduced xerographically in this copy. Higher quality 6" x 9" black and white photographic prints are available for any photographs or illustrations appearing in this copy for an additional charge. Contact UMI directly to order.

UMI

A Bell & Howell Information Company
300 North Zeeb Road, Ann Arbor MI 48106-1346 USA
313/761-4700 800/521-0600

LABYRINTHINE CONTROL OF THE VESTIBULO-OCULAR REFLEX IN THREE DIMENSIONS

by

Sergei Yakushin

A dissertation submitted to the Graduate

Faculty in Psychology in partial fulfillment of the requirements for the degree of

Doctor of Philosophy

The City University of New York

1996

This manuscript has been read and accepted for the Graduate Faculty in Psychology in satisfaction of the dissertation requirement for the degree of Doctor of Philosophy.

1/29/96
date

Theodore Raphan Theodore Raphan
Chairman of Examining Committee

1-30-96
date

Executive Officer

Professor Israel Abramov

Professor Bernard Cohen

Professor Louise Hainline

Professor John Simpson

Theodore Raphan
Professor Theodore Raphan
Supervisory Committee

The City University of New York

Abstract

LABYRINTHINE CONTROL OF THE VESTIBULO-OCULAR REFLEX IN THREE DIMENSIONS

by

Sergei Yakushin

Advisor: Professor Theodore Raphan

This study determined the contribution of individual semicircular canals to the generation of horizontal and roll components of angular vestibulo-ocular reflex (aVOR). Animals were tilted forward or backward 0° to ±90° around an interaural axis from upright, and rotated with sinusoids of 0.2-4.0 Hz around a vertical axis. At 0.2 Hz the gain of the horizontal aVOR was maximal at 11° tilt forward and decreased as animals were pitched forward or backward. Torsional gain was maximal at 90° tilt forward. After plugging of all vertical canals, the gains were zero at about -60° backward tilt. After both lateral canals were plugged, peak gains were shifted from the normal data, reaching a peak at approximately -56° tilted back. The same was true for the animals with an anterior and corresponding contralateral posterior canal intact.

The data were compared to predictions of a model based on the geometric organization of the canals and their relation to a head coordinate frame. The model used the normal to the canal planes to form a non-orthogonal coordinate basis for representing eye velocity. An analysis of variance was used to define the goodness of fit of model predictions to the data. Model predictions and experimental data agreed closely for both

normal animals, and after canal lesions. This implies that there was no adaptation of the response planes of the individual canals after plugging. When the operated animals were tested in light, vision compensated for the lack of spatial adaptation of the response planes after plugging at 0.2 Hz.

There was also an approximate linear rise of horizontal and roll aVOR gain with regard to frequency in the all canal plugged animals up to 4 Hz. Thus, the changes in gain and phase as a function of frequency is likely due to the frequency response of the plugged canal and not to adaptation.

These results indicate that both the vertical and lateral canals contribute to the horizontal and roll component of the aVOR in the monkey, there is little or no central adaptation when canals are inactivated, and canal plugging may change the frequency characteristics of the canal response without abolishing its response to rotation.

ACKNOWLEDGEMENTS

I wish to express my extreme gratitude to my mentor, Professor Theodore Raphan, for his guidance and encouragement throughout the course of this research. The many hours of technical discussions and many valuable criticisms and suggestions are most appreciated. I also wish to thank him for guiding me in developing the simulations used in this work.

I would like to thank all the members of my doctoral guidance and examination committee, Professors Louise Hainline (Brooklyn College), Israel Abramov (Brooklyn College), Bernard Cohen (Mt. Sinai School of Medicine), and John Simpson (New York University) for the time and effort each has taken to read and constructively criticize this dissertation.

I would especially like to thank Professor Bernard Cohen for his support and making available the resources in his laboratory for carrying out the experiments. The many hours of informative discussions about physiology of eye movements and the vestibular system is greatly appreciated. I am also indebted to him for teaching me the surgical procedures for implanting search coils which were essential in carrying out this work.

I would like to greatfully acknowledge the help of Dr. Mingjia Dai for implementing the data acquisition program utilized in this study. He was also a collaborator in the initial stages of this work. I would also like to thank Professor David Owen (Brooklyn College, CUNY) for helpful discussion on statistics.

I would like to thank Professor Jun Ichi Suzuki (Teikyo University, Tokyo, Japan)

for performing the canal plugging used in this work.

I would like to thank Professor Yasuko Arai, (Women's Medical College, Tokyo, Japan) for doing the anatomy which verified the plugging procedure and for allowing me to use her data as morphological control figures.

I would like to thank Dr. Evgeney Buharin (NYU, New York) for implementing the program to help analyze the high frequency sinusoidal data, Mr. Victor Rodriguez for surgical assistance and helping to make some of the figures, Nicholas Pasquale and Philip Cook for technical assistance in electronics and machining.

I would like to especially thank my wife, Svetlana, for her encouragement throughout the course of this work.

I would like to also thank the faculty of the Dept. of Experimental Psychology at Brooklyn College of the City University of New York and the faculty of the Dept. of Higher Nervous Activity of Moscow State University for giving me fundamental training in physiology and experimental techniques. I would also like to thank Prof. I. B. Kozlovskaya and the members of the Institute for Biomedical Problems where I received my basic training in neurophysiology.

Finally, I would like to acknowledge the support given me by The National Aeronautics and Space Administration (NASA) under grant numbers NAG 2-573 (Bernard Cohen) and NAG 2-703 (Bernard Cohen), and the National Institutes of Health under grants NS00294 (Bernard Cohen), EY04148 (Theodore Raphan), and EY01867 (Oscar Candia, Core Center).

TABLE OF CONTENTS

LIST OF ILLUSTRATIONS

CHAPTER 1:

INTRODUCTION

The vestibulo-ocular reflex (VOR) normally functions to maintain orientation and stable gaze while subjects are moving. The VOR can be divided into several subreflexes: the angular VOR (aVOR) generated through activation of semicircular canal afferents by angular acceleration and the linear VOR (lVOR) generated by activation of the otolith organs by linear acceleration. During normal behavior these subreflexes interact and complement each other. The aVOR compensates for head movement in space by rotating the eyes in the opposite directions to the head. Although much work has been done on characterizing the function of the aVOR, it is still not clear how specific canal activation drives the oculomotor system in three dimensions and how it adapts to lesions. Studies have indicated that the aVOR drives the oculomotor system according to the relationship of the semicircular canals in the head (Böhmer et al. 1985; Baker et al. 1987; Angelaki et al. 1995). Based, on these studies, it has been suggested that there is increased sensitivity of the remaining canals to the damaged canal plane (Böhmer et al. 1985; Baker et al. 1987; Angelaki et al. 1995). There has also been a suggestion that the adaptation is frequency selective (Angelaki et al. 1995). This suggestion is in contradiction to the Pavlovian notion that when sensors are destroyed, the reflex cannot be adaptively changed. In addition, no model-based analysis has been done to test the validity of the Pavlovian suggestion.

The purpose of this study was to perform experiments on normal animals as well as those with plugging of individual semicircular canals. Our hypothesis is that the

semicircular canals act as independent sensor. The loss of sensor function is not compensated by central reorganization of signals from the remaining semicircular canals. The data were compared to a model in which head velocity is projected onto each canal pair. These canal activations then project back to head coordinates multiplied by specific gains. We determined whether superposition held for responses due to each pair of push-pull canals to give the normal response or whether the model gain parameters had be modified to predict the data. The data and model were compared statistically. We also examined the aVOR frequency response of animals with plugged canals and determined their frequency dependencies.

CHAPTER 2

BACKGROUND:

The aVOR is comprised of three components: an afferent or sensory component, a central nervous system component, and a motor component which rotates the eye. The first model of the aVOR was based on the idea that it comprised a simple three neuron arc (Lorente de No 1933). The first neuron innervates the sensory hair cells of the semicircular canals. The cell bodies are located in Scarpa's ganglion (also called primary vestibular neurons) whose axons activate the central vestibular system via the vestibular nerve. The second neuron (the target neurons of the primary afferents) is located in the ipsilateral vestibular nuclei. The third neuron is located in the oculomotor nuclei which activates the eye muscles ipsi- and contralaterally. Further work on the aVOR indicated a more complicated organization which involved mathematical integrator functions for changing eye velocity to eye position in the motoneurons (Skavenski and Robinson 1973) and for generating storage properties (Raphan et al. 1977; Raphan et al. 1979). Integrator function had also been infered for generation of the optokinetic nystagmus (OKN) and optokinetic afternystagmus (OKAN) (Collewijn, 1972). However, the spatial organization of the semicircular canals to a large extent determines the planes of compensatory eye movements (Suzuki et al. 1964). One purpose of this study was to determine from behavioral observations how the spatial organization of the sensory part determines the planes of eye movement.

There are three semicircular canals on each side of the head (Fig 2.1): lateral, anterior and posterior. Figure 2.1 shows the approximate position of the three pairs of

Figure 2.1:

Approximate position of the three pairs of semicircular canals in the head. The **vertical dashed line** represents the mid-sagittal plane. The **dashed circle** represents the lateral canal plane. **RALP** and **LARP** planes are determined by the anterior canal on one side and posterior canal on the contralateral side. These planes are rotated approximately 45° from the mid-sagittal plane. Arrows on the canals represent direction of the head movement that exited this canal (see legend of Figure 2.2 for details). Therefore, each pair of canals: left anterior/ right posterior, right anterior/ left posterior and left/right lateral canals, operate as a push-pull pair.

Approximate Position of the Three Pairs of SemicircularCcanals in the Head

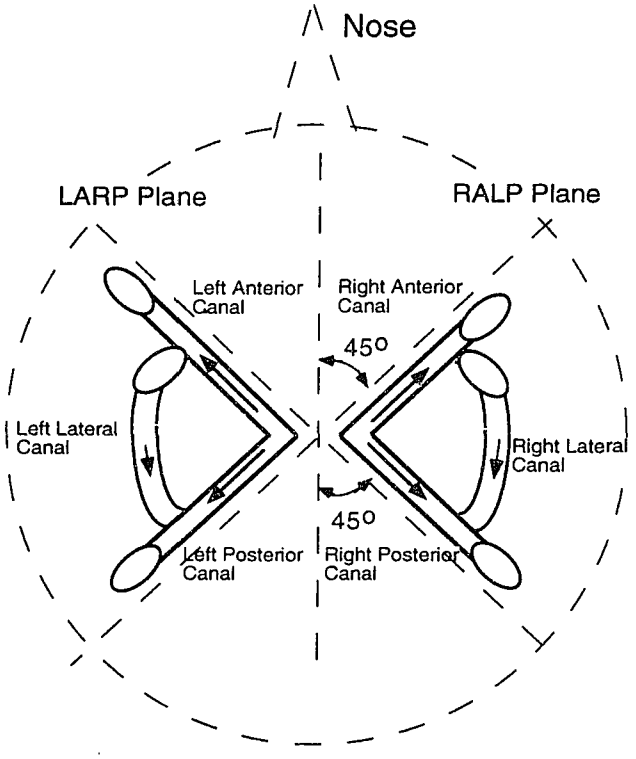

semicircular canals in the head. The vertical dashed line represents the sagittal plane. The dashed circle represents the lateral canal plane. **RALP** and **LARP** planes are determined by the anterior canal on one side and posterior canal on the contralateral side. These planes are rotated approximately 45° from the mid-sagittal plane. Arrows on the canals represent direction of the head movements that excited this canal. Opposite direction of the head movement inhibits the canal. Each pair of canals: left anterior/ right posterior, right anterior/ left posterior and left/right lateral canals, operate as a push-pull pair. Afferents of the lateral canals are activated when head is moved ipsilaterally in the horizontal plane and inhibited during contralateral rotation. Therefore the lateral semicircular canals on both side serve as a push-pull pair during head movement in the horizontal plane. The signal associated with afferent firinigs of the anterior canal on one side of the head combines with the signal from the posterior canal on the contralateral in a push-pull manner when head is displaced in that plane. Therefore the six semicircular canals functionally serve as three push-pull pairs, which are activated by head movement in three approximately orthogonal planes. This converts any head movement into a combination of three vectors in the planes of the push-pull pairs. As will be shown, however, deviations from true orthogonality can have important influences on the eye movements induced by head movement in these canal planes.

Afferent fibers of the primary vestibular neurones project to secondary vestibular neurones that are located in one of the vestibular nuclei. The lateral canal afferents primarily project to the medial vestibular nucleus while the anterior and posterior canal afferents project to the superior vestibular and rostral part of the medial vestibular nuclei

(Stein and Carpenter, 1967; Gacek, 1969; Büttner-Ennever 1992). The planar organization of the canal-recipient neurons conforms to the push-pull organization described above. That is, three push-pull pairs are represented in the secondary neural activity which characterizes all head movements (Reisine et al. 1988; Reisine and Raphan 1992). The secondary vestibular nuclei neurons activate neurons in the oculomotor nuclei (abducens, trochlear and oculomotor) to drive six pair of the oculomotor muscles (lateral and medial recti, superior and posterior recti, inferior and posterior obliques) which rotate the eyes.

This model of aVOR function describes it as an open loop system. This means that activation of the semicircular canals will produce a preprogrammed eye counter-rotation which is not corrected instantaneously by either direct feedback from the muscle proprioceptors or other parts of the oculomotor system. Despite its open-loop characteristics, the labyrinth has an efferent innervation (Gacek and Lyon 1974). Efferent fibers originate on both sides of the brainstem lateral to the abducens nucleus (Goldberg and Fernandez 1980). In anaesthetized preparations, electrical stimulation of the efferent fibers alters the activity of afferent fibers (Goldberg and Fernandez 1980). The functional role of the efferent system is not clear. It has been suggested that spontaneous activity of the efferent vestibular system functions to raise the level of spontaneous firing rate prior to impending motion. The higher level of firing would prevent inhibitory silencing during rotation which would inhibit the canal (Highstein and Baker, 1985). A role during eye movements and active head movements has been postulated, but evidence for this could not be demonstrated in alert, behaving animals (Khalsa et al. 1987).

Quantitative models of the aVOR have elucidated the signal processing done in implementing the aVOR. These have been derived from the physics of the motion of the sensory epithelium in response to acceleration and the transduction to the hair cells (Hudspeth and Corey 1977) (Fig 2.2). The bundles of the hair cells are embedded in the sensory epithelium and the displacement of their tips transduces the forces due to acceleration into a modulating signal that drives the central nervous system (Fig 2.2A). The signal transduction is dependent on the inertia, viscous damping and elasticity of the associated membrane and surrounding fluid. There are specific differences in the way the otoliths, semicircular canals, and organ of Corti are activated (Fig 2.2A). The otolithic membrane is attached to otoconia which have a relatively high density compared to the surrounding fluid or endolymph. In response to a linear acceleration, the otoconia are displaced, moving the membrane and consequently bending the tips of the hair bundles (Fig 2.2A, left). The transduction process within the semicircular canal is somewhat different than otolith transduction. For the semicircular canals, the hair cells lie in the cristae which is in the bulbous part of the canal called the ampulla. The hair bundles are embedded in a gelatinous membrane called the cupula (Fig 2.2A, Middle) which completely blocks the canal. Fluid motion within the canal due to angular acceleration can deform the cupula and in turn bend the tips of the hair bundles. For auditory stimuli, the transduction of hair cell activation in the organ of Corti due to pressure changes is the same as for vestibular stimulation. However, the mechanical activation of the hair cell bundle is different (Fig 2.2A, right). In this instance the bending of the hair cell is due primarily to the relative shearing between the basilar membrane on which the hair

Figure 2.2: Information processing in inner ear sensory organs. **A**, Displacement of the hair bundle by stimulus in all three types of sensory organs in the inner ear: utriculus and sacculus (left), the semicircular canals (middle) and the cochlea (right). **B**, Position of the sensory organs that contain the hair cells (dense color) in a human inner ear (From Hudspeth and Corey 1977). Excitation of the lateral canal is caused by endolymph flow in the utriculopetal (towards utricle) direction. Endolymph motion in the utriculofugal direction (away from utricle) inhibits the hair cell activity. Exitation of the vertical canal is caused by endolymph flow in the utriculofugal direction, and flow in the opposite direction inhibits the hair cell activity.

A

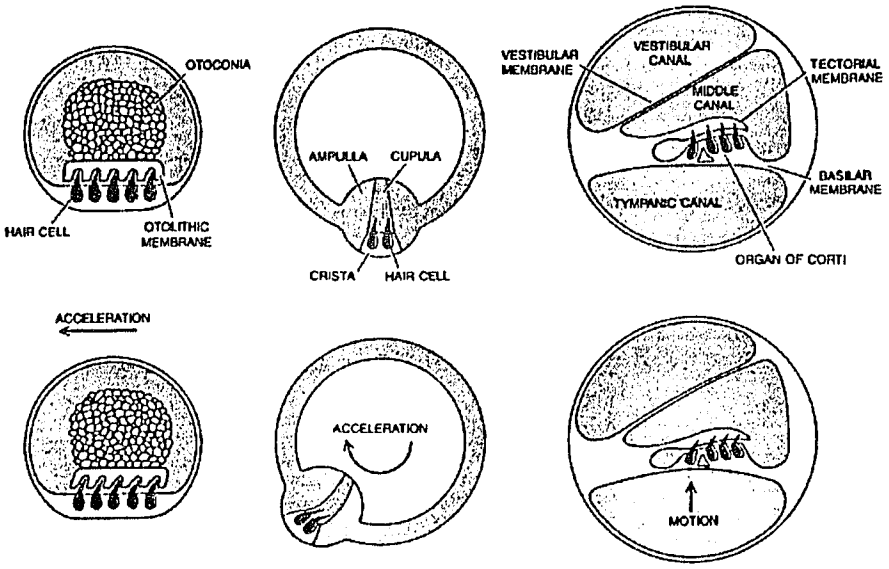
OTOCONIA
HAIR CELL
OTOLITHIC MEMBRANE
AMPULLA
CUPULA
CRISTA
HAIR CELL
VESTIBULAR MEMBRANE
VESTIBULAR CANAL
TECTORIAL MEMBRANE
MIDDLE CANAL
BASILAR MEMBRANE
TYMPANIC CANAL
ORGAN OF CORTI
ACCELERATION
ACCELERATION
MOTION

B

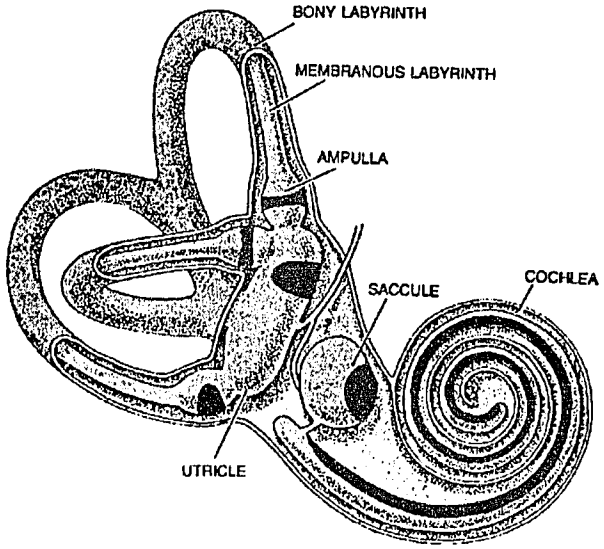
BONY LABYRINTH
MEMBRANOUS LABYRINTH
AMPULLA
SACCULE
COCHLEA
UTRICLE

cells lie and the tectorial membrane which holds the tips of the hair cell bundles (Fig 2.2A, right). The vestibular and auditory hair cell transduction operate over different frequency ranges and there is no cross-talk between the two systems.

The vestibular portion of the inner ear on each side contains three semicircular canals that respond to angular acceleration along an axis normal to their corresponding planes (Fig 2.2B). The planes of the canals relative to the head are discussed in more detail in section 2.6. The utriculus part of the otolith organs responds to linear acceleration which lies close to the horizontal plane of the head. The sacculus responds to acceleration predominantly along the vertical axis (See Wilson and Melvill Jones (1979) for review). The main subject of this thesis relates to aVOR function based on semicircular canal activation.

Steinhausen (Steinhausen 1933) has shown that the semicircular canals can be modelled as a simple torsion pendulum which can explain the frequency domain characteristics of the aVOR. Subsequent work showed that if the appropriate stimulus for activating the semicircular canals is angular head acceleration, it must be integrated twice to obtain the eye position related signal found in oculomotor neurons (Skavenski and Robinson 1973). For frequencies of head movement above 0.1 Hz, the first integration is done mechanically by the cupula-endolymph system. Accordingly, a "head velocity" related signal can be recorded from afferent vestibular nerve fibers at frequencies above 0.1 Hz (Fernandez and Goldberg 1971). The second integration to a position signal has to take place centrally and is hypothesized to be performed by a central "neural integrator" (Skavenski and Robinson 1973).

Canal afferent responses, which represent the dynamics of the cupula-endolymph system, have time constants of 3-6 sec (Goldberg and Fernandez 1971; Büttner and Waespe 1981; Reisine and Henn 1984; Correia et al. 1992) in monkey. Thus, the cupula-endolymph system would limit the range of good compensation of the aVOR to the high-frequency range above 0.2 - 0.3 Hz. However, monkeys have stable horizontal gains (eye velocity/stimulus velocity) of the aVOR for head movements ocurring over a frequncy range 0.02 - 1.5 Hz (Skavenski and Robinson 1973; Miles and Eighmy 1980a). An additional integrator which stores velocity information from the semicircular canals gives compensation at frequencies below 0.2 Hz. (Raphan et al. 1979).

In humans, the gain of the aVOR is in the range of 0.4 to 0.7 (Gonshor and Melvill-Jones 1976a; Cohen et al. 1981; Jäger and Henn 1981; Misslisch et al. 1994; Tweed et al. 1994; Fetter et al. 1995) and is particularly dependent on the state of alertness (Collins 1962). However, during rotation in light, the aVOR combines with visual information to produce compensation with a gain approximately equal to 1.0 (Robinson 1976; Raphan et al. 1979; Dai et al. 1994). The visual component is probably mediated through cerebellar circuits, through the flocculus and ventral paraflocculus (Ito 1970; Ito 1972; Maekawa and Simpson 1973; Ito 1974; Kimura and Maekawa 1981; Zee et al. 1981). The gain of the aVOR is also higher during active head movement (Grossman et al. 1989).

To extend the model of the aVOR to three dimensions, it is necessary to consider how each canal is oriented in the head and how they work together to implement the compensatory function. Several studies have described the position of the semicircular

canals relative to a stereotaxic head coordinate frame as well as the planes of their maximal activation (Curthoys et al. 1977; Blanks et al. 1985; Reisine et al. 1988). Blanks et al (1985) demonstrated that the lateral semicircular canals on both sides of the head are approximately coplanar (within 2°). There is an 11° difference in the orientation of the planes of the anterior canal on one side and posterior canal on another side. Anterior and posterior canals on one side are orthogonal to each other. The plane of the posterior semicircular canal is almost orthogonal to the lateral canal plane, but the anterior canal plane makes a bigger angle with a lateral canal plane (99°). This is probably due to the bending of the anterior canal. Relative to a stereotaxic head coordinate system, the lateral canals of rhesus monkeys are tipped up approximately 22°. Thus, the normal to this plane is tipped back 22° from the yaw axis of the head. The anterior and posterior canal are rotated approximately 45° from the sagittal plane. Morphological and physiological recordings from canal afferents are in general agreement with these findings, but demonstrate some differences from these values (Reisine et al. 1985; Reisine et al. 1988). Morphological measurement demonstrated that vertical canals were tilted back about 25° (22.8°and 26.3° for each of two monkeys) while the lateral canals were tilted up only 12° (14.5° and 8.8°, respectively) relative to a head coordinate frame which is tilted down 15°. This would orient the lateral canal approximately 27° up from the stereotaxic coordinate frame. According to measurements of maximal sensitivity vectors for primary afferents, the vertical canals are tilted back about 18° (14,1° and 21.5°) while the lateral canals are tilted up only 14° (15.4° and 13.4°). These measurements were again relative to a head coordinate frame tilted 15° down relative to the stereotaxic.

Differences between morphological and physiological findings of 7° were consistent with those found in the cat (Blanks et al. 1975).

During head movement, each semicircular canal afferent is activated according to the projection of the angular velocity vector along the normal to the average plane of the canal. Thus, the angular velocity vector can be represented in a canal coordinate frame whose axes are the normals to the anterior, posterior, and lateral canals. The transformation of the head velocity vector in head coordinates to that in canal coordinates can be represented as 3x3 matrix (Robinson 1982; Yakushin et al. 1995).

It has been known that each semicircular canal can activate every eye muscle (Szentagothai 1950; Cohen et al. 1964; Suzuki et al. 1964; Cohen et al. 1965; Suzuki and Cohen 1966). However, there are some dominant projections which have been emphasized. The lateral canals mainly activate the lateral and medial rectus muscles to generate horizontal eye velocity. The left anterior and right posterior canal project to the left vertical recti and right oblique muscles, and the right anterior and left posterior canal to the right vertical recti and left oblique muscles (Szentagothai 1950; Cohen et al. 1964; Suzuki et al. 1964; Cohen et al. 1965; Suzuki and Cohen 1966; Graf and Ezure 1986). Thus any head rotation leads to a specific pattern of muscle activation and inhibition determined by the activated canal pairs. It has been suggested that collaterals of vestibular nuclei neurons projecting to additional motoneuron pools correct for the slight misalignment of canal and muscle planes (Ezure and Graf 1984a; Graf and Ezure 1986). Eye movements are produced by activation of the push-pull pair of the eye muscles, but they are not simply related as semicircular canal push-pull pairs. However, a meaningful

functional description can be implemented by assuming that each antagonist pair of muscles rotates the eye about an approximately head fixed axis. This leads to a representation of the muscle-eye transformation as a 3x3 matrix (Robinson 1975) (see Section 2.6.1).

There is some difficulty with this approach. The muscle matrix was derived from theoretical considerations about muscle slip (Robinson 1975). It is now clear that there are pulley effects associated with rectus muscles (Simonsz 1990; Miller et al. 1993) and therefore the muscle matrix is different than originally proposed (Raphan 1995). This would impact on the computation of the brainstem matrix. Thus, it would seem reasonable to lump the brainstem and muscle matrix into a composite matrix for analyzing the system (See also Section 2.6.2).

2.1 MODIFICATION OF THE aVOR:

The aVOR can be adapted in a variety of ways. The gain of the horizontal component can be enhanced when wearing magnifying glasses or reduced when wearing reducing lenses (Miles and Fuller 1974; Gonshor and Melvill-Jones 1976a, b; Miles and Eighmy 1980a; Miles and Lisberger 1981; Melvill-Jones et al. 1984; Cohen et al. 1992). Miles and Eighmy (Miles and Eighmy 1980a) demonstrated that monkeys wearing lenses can increase or decrease the gain of the aVOR in a few hours. Similar result were found for different species from rabbit (Ito 1974; Nagao 1989) to human subject (Gauthier and Robinson 1975). These experiments showed that the aVOR could be adapted, but did not isolate the mechanisms of adaptation. For example, the gain of the aVOR is increased by viewing close objects in light (Virre et al. 1986). Therefore, it is possible that the

lenses changed viewing distance, and that this was the effector in changing the gain. However, the gain can also be reduced by activating the vestibular system and forcing the subject to view a subject stationary surround without lenses (Miles and Eighmy 1980a; Nagao 1989; Cohen et al. 1992). This suggests that the retinal slip to the oculomotor system is the important signal that modifies the gain of the aVOR (Ito 1970; Gonshor and Melvill-Jones 1976a, b; Robinson 1976; Miles and Eighmy 1980a).

The gain of the aVOR can be adaptively reduced by about 30% from initial levels during 3-4 hours (in some cases after 8 hour) rotation in a subject- stationary surround (Miles and Eighmy 1980a; Lisberger et al. 1984; Nagao 1989; Cohen et al. 1992). There were additional changes in the gain after 20-40 hours of rotation (Miles and Eighmy 1980a). Rotation in darkness by itself did not cause any changes in the aVOR gain (Cohen et al. 1992).

The most dramatic changes in the aVOR gain were obtained with prisms that reversed the visual field (Gonshor and Melvill-Jones 1976a, b). Objects seen through such lenses move in a reversed direction, relative to the head, when the head turns. The normal action of the aVOR is to rotate the eyes at the same speed as the head but in the opposite direction. This keeps images from moving on the retina during head movements, allowing one to move and see at the same time. With reversing prisms, the reflex now does more harm than good. If, say, the head turns to the left, the world seen through the prisms is also moving to the left, while normal compensation through the aVOR would be to move the eyes to the right relative to the head. This creates increased retinal slip and retinal error signals which degrade vision.

Gonshor and Melvill-Jones demonstrated gain change and phase reversal in humans (Gonshor and Melvill-Jones 1976a, b; Melvill-Jones et al. 1984). After wearing reversing prisms for only a few days, their subjects' eye movements, tested in the dark, changed phase and went with the head instead of against it. Dynamics of gain adaptation due to reversing prisms was also studied in cats (Robinson 1976). Forced rotation in light at low frequency (0.05 Hz, 28°/s. peak velocity) caused substantial decreases in aVOR gain. The largest decrease occurred in the first two hours. After removal of the prism goggles, the gain returned to normal within one hour. Prolonged adaptation lasting for several days reduced the gain rapidly in the first day. The gain then declined slowly over the next 7 days. In all of these studies, the adaptation was always so as to better stabilize images on the retina when the head is moved. In terms of the gain matrix description of the aVOR, the elements of the [VOR] matrix were modified by visual vestibular conflict. We will now consider how adaption is accomplished centrally.

2.2 NEURONAL BASIS FOR aVOR GAIN ADAPTATION.

All of the studies cited have shown that the aVOR is mainly an open-loop control system (Szentagothai 1950) (See Szentagothai and Arbib (1974) for review). It compensates for dysmetria by modifying the parameters of the system. Studies in monkey demonstrated that changes in the aVOR gain are not accompanied by changes in the vestibular afferent activity (Miles and Eighmy 1980a). It is also unlikely that the changes in gain of the aVOR can be explained by decreasing sensitivity of eye muscle contraction in response to activation of motoneurons, since there are no changes in saccade amplitude or changes in oculomotor behavior in light (Frens and van Opstal 1994). Therefore,

adaptive changes in the aVOR gain must occur in the CNS which transduces the afferent signals from the canals to the eye velocity commands.

One of the hypotheses of aVOR gain adaptation is based on the more general hypotheses of cerebellar learning. Mossy fiber signals coming into the cerebellum transfer across the cerebellar cortex, through granule cells whose axons (parallel fibers) in turn activate Purkinje cells. Marr (Marr 1969) and Albus (Albus 1971) postulated that these connections can be functionally reorganized by "instruction" signals from climbing fiber afferents. Utilizing the Marr-Albus hypothesis, Ito (Ito 1970; Ito 1972; Ito 1974) proposed that the visual system could modify the parameters of the aVOR using the retinal slip during head motion as the corrective error signal. In support of this hypothesis and based on axonal degeneration techniques, it was believed that the flocculus of the rabbit (Alley et al. 1975), rat (Blanks et al. 1983) and cat (Brodal et al. 1962) receives information about head movements from primary vestibular fibers. As in the monkey, the vestibular input or information about head velocity comes only from the vestibular nuclei (Waespe et al. 1981; Langer et al. 1985). However, more recent studies do not confirm the earlier assumption about direct vestibular projections to the flocculus (Epema et al. 1988). The flocculus was postulated to receive visual signals monitoring the constancy of retinal images (Ito 1970). Thus, it was suggested that the flocculus is the site of parameter adaptation associated with the aVOR. Following this suggestion, Maekawa and Simpson (Maekawa and Simpson 1973) found a visual pathway to the flocculus mediated by climbing fiber afferents. Later, another visual pathway to the flocculus via mossy fiber afferents was found (Maekawa and Takeda 1975). Output

signals from the flocculus via Purkinje cell axons activate the vestibular nuclei, which involve neurons that are responsible for the aVOR.

One possible way that floccular Purkinje cells can modify the elements of the aVOR gain matrix is by changing cell sensitivity during the adaptation process. To test this hypothesis, Lisberger and Miles (1980) recorded in the medial vestibular nuclei of monkeys before and after adaptation to the higher and lower gain condition (Lisberger and Miles 1980). The results of these studies showed no statistically significant differences in resting discharge rate, phase shift, or sensitivity to head velocity between the high- and low-gain samples of any of the cell types. There were also no changes in the phase shift or resting discharge rates of recorded cells in the MVN. Nonetheless, they found a consistent tendency in the functionally defined cell groups for the sensitivity to be about 20% greater in the high-gain samples. The conclusion was that this difference was small by comparison with the fourfold difference in aVOR gain and therefore "the major changes underlying VOR plasticity occur after the first central synapse in the VOR pathways."

There are several arguments against this conclusion. Keller and Precht (Keller and Precht 1979) recorded from the medial vestibular nucleus of cats before and after the gain of the aVOR was decreased by 4-5 hours of sinusoidal oscillation while the animals were wearing left-right reversing prisms. They found differences in sensitivity to vestibular input that were both statistically significant and considerably larger than in the Lisberger and Miles (Lisberger and Miles 1980) study. In addition, they found differences in the phase shift of cells. One possibility is that there is a species difference.

However, the vestibular responses and the visual-vestibular interaction of cats (Keller and Precht 1979) have the same general characteristics as in the monkey (Chubb et al. 1984) both in the frequency and time domain. In addition, the time course of adaptive changes due to prism reversal are the same in cats as in monkeys (Miles and Fuller 1974; Robinson 1976; Cohen et al. 1992). The differences between findings in the Keller and Precht (Keller and Precht 1979) and Lisberger and Miles (Lisberger and Miles 1980) studies are not clear.

A further complicating feature of the flocculus gain control of the aVOR is the presence of multiple parallel component pathways arising from different labyrinths and terminating in different extraocular muscles. In flocculus, five zones (I-V) have been distinguished (Yamamoto 1979). Only one of them (zone II) is involved in the horizontal aVOR gain control (Dufosse et al. 1978). An adaptive increase of the aVOR gain is accompanied by an increase in the out-phase modulation of simple spike discharges from H-zone Purkinje cells. Similarly, an adaptive decrease of the aVOR gain is accompanied by a decrease in out-phase modulation. Population studies for all zones revealed a statistically significant difference in the amplitude of out-phase modulation before and after adaptation (Dufosse et al. 1978).

An important characteristic of the flocculus horizontal gaze velocity Purkinje cells in the normal monkey is that they are, on average, equally sensitive to head velocity and slow phase eye velocity (Lisberger and Fuchs 1978; Miles et al. 1980c). During the aVOR in darkness Purkinje cells showed negligible modulation under normal conditions. Long-term changes to x2 telescopic spectacles or dove prism spectacles showed changes

in activity of Purkinje cells in the monkey flocculus (Miles et al. 1980c). Miles (Miles et al. 1980c) have argued that such changes in Purkinje cell responsiveness could not underlie the adaptive changes in the aVOR and are likely to be a secondary consequence of adaptive changes. In a recent single cell recording study of the flocculus and ventral paraflocculus (Lisberger et al., 1994b), it was also concluded that the flocculus may not be responsible for the underlying adaptive changes that take place in the aVOR. It has been suggested that flocculus target neurons may be primarily responsible for adaptation (Lisberger et al., 1994a). These studies in monkey have not, however, related recordings to the microzonal structure of the flocculus. Watanabe (Watanabe 1984) reinvestigated the monkey's flocculus and uncovered a modification of simple spike vestibular responsiveness of H-zone Purkinje cells during the aVOR adaptation. Those observations made on the primate flocculus (Watanabe 1984) are in agreement with the previously reported rabbit's data (Dufosse et al. 1978) and support the "flocculus hypothesis of aVOR control". Thus, the structural aspects of adaptation mediated by the flocculus are still not clear and more work is necessary to elucidate the role of the flocculus and vestibular nuclei in the adaptive behavior of the aVOR.

2.3 ADAPTATION TO MICROGRAVITY:

Effects of microgravity on the horizontal aVOR gain which is presumably an adaptive phenomenon has led to a different interpretation of aVOR adaptive behavior. Over the last twenty years, Russian investigators have studied oculomotor behavior in rhesus monkey before and after space-flight. The eye velocity during counter-rotation immediately following an on-target saccade (Bizzi et al. 1971; Bizzi et al. 1972) was

compared with head velocity during the time period when the head is moving towards the target and the eye is rotating back to the midposition. The ratio of (eye velocity)/(head velocity) during this time period remained approximately constant. This was taken as a measure of the gain of the aVOR (Kozlovskaya et al. 1984). Under normal circumstances, eye position is on target during the counter-rotation period, giving a gain of 1.0. In microgravity, this paradigm generates eye position at the end of the saccade which overshoots the target position. The corresponding gain of the counter-rotation of the eye relative to the head is therefore much larger than normal. This behavior was maximal during the first day and gradually returned to normal over the course of one to two weeks. The same sequence of changes occurred during readaptation to the normal gravitational conditions (Kozlovskaya et al. 1984, 1985, 1989, 1990, 1991; Sirota et al. 1987, 1988, 1989a, 1989b, 1990a, 1990b, 1990c, 1991a, 1991b; Yakushin et al. 1989, 1992a). The interpretation that these alterations due to microgravity are the results of gain change in aVOR (Kozlovskaya et al. 1984) would contradict other studies on rhesus monkeys where aVOR gain during or after exposure to microgravity was measured in darkness during head oscillation (Correia et al. 1990a, 1990b, 1991, 1992a, 1992b; Cohen et al. 1991, 1992). A possible explanation for this discrepancy is that the apparent increased gain during the eye-head coordination test was due to the added target-induced input which drove the eyes more rapidly back to the target when there was saccadic overshoot. This coupled with the slower head movement could have been responsible for the increased ratio of counter-rotation eye velocity to head velocity. Thus, differences in conclusions about adaptation of the aVOR gain in microgravity are

probably due to different experimental conditions.

2.4 CROSS-AXIS ADAPTATION:

Another mode of plastic modification of the aVOR that has significant bearing on the three dimensional structure of the aVOR, has been referred to as "cross-axis adaptation" (Schultheis and Robinson 1981; Baker et al. 1986, 1987; Harrison et al. 1986; Peterson et al. 1991; Peng et al. 1994). Cross-axis adaptation is measured as a cross-axis velocity ratio, (horizontal eye velocity)/(vertical eye velocity), in response to vestibular stimulation in a vertical plane; or (vertical eye velocity)/(horizontal eye velocity) for vestibular stimulation in a horizontal plane. Shultheis and Robinson (1981) demonstrated that cats could be adapted with continued sinusoidal pitching while an optokinetic surround sinusoidally oscillated in a horizontal plane. When animals were later tested in darkness with a pitching stimulus (Fig 2.3), eye velocity had a horizontal component. The magnitude of the vertical component of eye velocity could be adaptively increased from zero and the magnitude of the horizontal component reduced at the same time. When the adaptation paradigm was applied with animals on their sides, there was a small increase (about 0.1) in the cross-axis adaptation (Baker et al. 1986, 1987) as compared with cross-axis adaptation with the animal upright. This demonstrates that cross-axis adaptation is greater when the otolith organs are reoriented relative to a spatial vertical during head rotation.

One important finding on normal animals from these studies was that the axis of adaptation was independent of the axis of stimulation. That is, since all canals contribute to the horizontal and vertical gains, it is possible to change the contribution of the lateral

Figure 2.3:

Determination of the three rotational axis. **A.** Pitch axis is along the interaural axis. The positive direction of rotation is nose down rotation (arrow). **B.** The roll axis is inline with naso-occipital axis and the positive direction is counter-clockwise from the subject point of view (arrow). **C.** The yaw axis is inline with long body axis with the positive direction leftward (arrow). See Fig 2.8 for a details of the vector description of these rotations and the corresponding head coordinate frame.

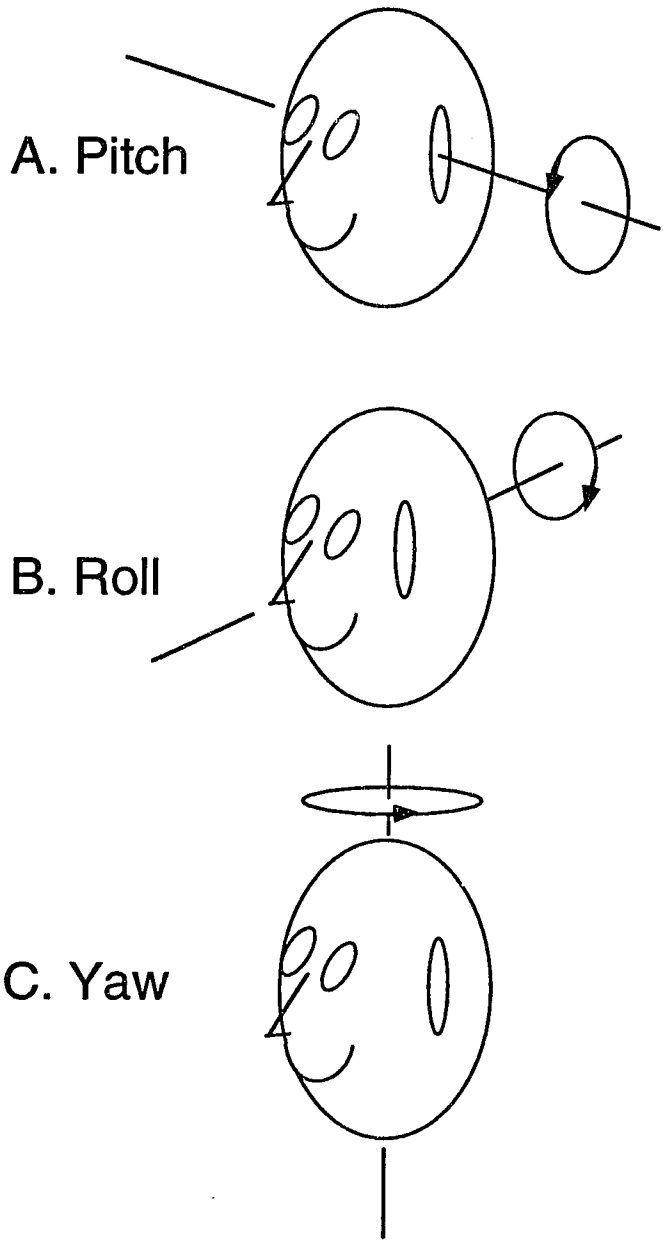
A. Pitch
B. Roll
C. Yaw

semicircular canal to the vertical aVOR gain without changing contribution of the vertical semicircular canals for that plane of rotation (Schultheis and Robinson 1981). The same should hold for horizontal aVOR gain. It also demonstrated that changes in one geometrical plane can not be related to any changes in another planes. The authors proposed that mechanisms of aVOR gain "repairing" due to plugging of individual semicircular canals could work without affecting the undamaged part of the aVOR. Moreover, it was demonstrated that the cross-axis adaptation is frequency dependent and cross-axis ratio is greater for lower frequency (Baker et al. 1986, 1987). Similar results have now been described in humans (Peng et al. 1994). Whether there is cross-axis adaptation of the aVOR after specific canals have been plugged has been a subject of considerable controversy (Baker et al. 1982; Yakushin et al. 1992b, 1995). This issue is addressed in this dissertation.

2.5 CANAL-PLUGGING:

Originally described by Ewald (Ewald 1892), and modified by Money (Money and Scott 1962), it has been possible to produce a strong bony plug that blocks the flow of endolymph when the head is turned. Another technique using implanted silver spindels which compress the membranous labyrinth and inhibits the flow of endolymph (Barmack and Pettorossi, 1988a,b). Canal plugging can isolate the role of each semicircular canal in the function of the aVOR, by interrupting the sensor without damaging the hair cells or nerve which might affect central processing. Canal plugging does not abolish central visual-vestibular processing such as OKAN (Cohen et al. 1983; Raphan et al. 1983). In contrast, bilateral labyrinthectomy or neurectomy abolishes OKAN and normal visual-

vestibular interaction (Uemura and Cohen 1975; Collewijn 1976; Cohen et al. 1983; Raphan et al. 1983). Canal plugging, therefore, allows the exclusion of responses to specific angular accelerations along canal axes, while maintaining a relatively normal spontaneous discharge of the afferents of the plugged canals (Money and Scott 1962; Correia and Money 1970; Goldberg and Fernandes 1975; Baker et al. 1982, 1986, 1987; Cohen et al. 1983, 1988; Paige 1983; Raphan et al. 1983; Böhmer et al. 1985; Igarashi et al. 1987; Baker and Peterson 1991). Study of animals during normal conditions and after different semicircular canal plugging explored the importance of each pair of the semicircular canals for the aVOR gain (Baker et al. 1982; Böhmer et al. 1985). It was demonstrated that when canal plugged animals were rotated around a spatial vertical axis with the head pitched stationary forward or backward, the remaining gain represents "normal or increased coupling" of the vertical semicircular canal to the horizontal aVOR response (Baker et al. 1982). Recently, there has also been a suggestion that the adaptation is frequency selective (Angelaki et al. 1995).

When the lateral canals of the cat were plugged, the minimum horizontal gain occurred when head was pitched about 30-35.0° relative to stereotaxic plane. The authors pointed out that Robinson's matrix approach can probably describe the gain behavior for the plugging conditions. However, a clear methodology for doing this was not put forward. The main difficulties in generalizing the Robinson approach was that the canal matrix was fixed based on data of Curthoys et al (Curthoys et al. 1977) and no general scheme was developed for arbitrary canal configurations due to individual differences between animals. In similar experiments performed on a rhesus monkey (Böhmer et al.

1985), it was found that the horizontal aVOR gain curve as a function of head tilt was similar to that of the cat. Böhmer et al (1985) pointed out that there are "possible plastic changes to adapt to the different sensory input after canal plugging ....." (p. 296). They also conclude that "a specific, but currently unknown gain element exists which couples vertical canal input to the horizontal nystagmus generator. The gain of this element has been increased as a compensatory mechanism to obtain a better response in the range of the missing horizontal canal input" (p. 297). The conclusion from the latter study is that the gain of the aVOR in the plane of the missing semicircular canal is a result of increased contribution from the intact canals. Thus, while a great deal is known about the canal response to rotation and to stimulation and how it activates the aVOR, canal contribution to horizontal, vertical and roll components of coordinated compensatory eye movements has not been completely elucidated.

2.6 MODELING THE CANAL CONTRIBUTIONS TO THE aVOR

Modeling the semicircular canal contribution to the aVOR utilizes the geometrical relationship of the individual canals to the head frame in which eye movements are measured. This approach was first used by Robinson (1982) using specific measurements of canal planes relative to the head (Blanks et al. 1975, 1985; Curthoys et al. 1977) and the muscle transformation derived from the approximate muscle torques on the eye (Robinson 1975). The transformations were represented by two matrices from which Robinson derived a brainstem matrix to give an overall aVOR reflex gain of -1.0 (Robinson 1982).

2.6.1 ROBINSON FORMULATION OF THE aVOR TRANSFORMATION

Head Velocity, Eye Velocity, and the Canal Referenced Head Velocity can be described as a vector $\underline{\omega}_H$ $\underline{\omega}_E$ $\underline{\omega}_C$ (Eq. 1):

$$\underline{\omega}_H = \begin{bmatrix} \omega_{H_{pit}} \\ \omega_{H_{roll}} \\ \omega_{H_{yaw}} \end{bmatrix} \qquad \underline{\omega}_E = \begin{bmatrix} \omega_{E_{pit}} \\ \omega_{E_{roll}} \\ \omega_{E_{yaw}} \end{bmatrix} \qquad \underline{\omega}_C = \begin{bmatrix} \omega_{C_{ant}} \\ \omega_{C_{post}} \\ \omega_{C_{lat}} \end{bmatrix} \qquad \textbf{(Eq. 1)}$$

For the ideal aVOR the head velocity and eye velocity vectors must have equal size but be directed oppositely (Eq. 2).

$$\underline{\omega}_E = \begin{bmatrix} \omega_{E_{pit}} \\ \omega_{E_{roll}} \\ \omega_{E_{yaw}} \end{bmatrix} = [VOR]\ \underline{\omega}_H = \begin{bmatrix} -1 & 0 & 0 \\ 0 & -1 & 0 \\ 0 & 0 & -1 \end{bmatrix} \begin{bmatrix} \omega_{H_{pit}} \\ \omega_{H_{roll}} \\ \omega_{H_{yaw}} \end{bmatrix} = [-I]\ \underline{\omega}_H \qquad \textbf{(Eq. 2)}$$

The aVOR matrix [VOR] is a product of the canal [C], brain-stem [B] and eye muscles [M] (Eq. 3-5). The canal matrix [C], represents the head velocity, $\underline{\omega}_H$, in term of neuronal activity of primary afferents of pairs of semicircular canals and is a projection transformation into vectors normal to the canal planes (Eq. 3).

Eye velocity $\underline{\omega}_E$ is generated from $\underline{\omega}_C$ through the transformation by a brain-stem matrix [B] and a muscle matrix [M] (Eq. 3-5).

$$\underline{\omega}_C = [C]\ \underline{\omega}_H \qquad \textbf{(Eq. 3)}$$

$$\underline{\omega}_E = [M]\ [B]\ \underline{\omega}_C \qquad \textbf{(Eq. 4)}$$

$$\underline{\omega}_E = [M]\ [B]\ [C]\ \underline{\omega}_H \qquad \textbf{(Eq. 5)}$$

This model assumed a specific matrix for the canal transformation and does not give the matrix in terms of specific orientations of the canals relative to the head.

2.6.2 RAPHAN GENERALIZATION OF MATRIX APPROACH TO CONSIDER ARBITRARY RELATIONSHIP BETWEEN HEAD AND CANAL AXES

To model data obtained from behavioral studies, Raphan (Yakushin et al. 1995) derived a canal transformation in terms of general angles between the canals as observed physiologically (Reisine et al. 1988). This model is described in Fig 2.4A, B. Because this model forms the basis for the model-data comparisons in this thesis, we will describe it in detail.

In the model, it was assumed that the normal to the lateral canal (Z_c) is tilted back relative to the head yaw axis (Z) by an angle θ_l. The normals to the anterior and posterior canal planes (X_c and Y_c, Fig 2.4B) are tilted back relative to the yaw axis of the head (Z) by an angle θ_v, which is greater than θ_l. These normals are also rotated by an angle ψ_v about a virtual axis (broken line, Fig 2.4B) which is normal to the plane determined by X_c and Y_c. Thus, the vertical canals were assumed to be perpendicular to each other (Yakushin et al. 1995). Together, the lateral and vertical canals form a non-orthogonal coordinate frame for encoding the head velocity vector (Blanks et al. 1975; Simpson and Graf 1981; Ezure and Graf 1984a, 1984b; Blanks et al. 1985; Reisine et al. 1988).

A head velocity vector $\underline{\omega}_H$ relative to the head coordinate frame can be mapped onto the canal frame by taking each of the components of ω (ω_{Hpit}, ω_{Hroll}, ω_{Hyaw}) and projecting each component onto the normals of the canals according to the rotation of the

Figure 2.4: A, Position of the left labyrinth of a monkey relative to its head. The coordinate frame of the head has been taken as the stereotaxic frame. It is the coordinate frame in which pitch (vertical), roll (torsion), and yaw (horizontal) eye movements are measured. X represents the pitch axis, Y the roll axis and Z the yaw axis. **B,** Representation of the relative orientation of the coordinate axes of the stereotaxic frame (X, Y, Z) and the coordinate axes determined by the normals to the semicircular canal planes. The positive direction of these normals are determined by using a right hand rule for the rotation direction which excites an individual canal. X_c represents the positive direction for the anterior canal, Y_c the posterior canal, and Z_c the lateral canal. Θ_l is the angle between stereotaxic vertical axis (Z) and the average direction of the lateral canal axis (Z_c). Θ_v is the angle between Z and the normal to the plane determined by X_c and Y_c. The X_c and Y_c axes are orthogonal to each other and rotated relative to the head frame about an axis normal their plane (dashed axis) by an angle Ψ_v. The difference between Θ_v and Θ_l represents the non-orthogonality of the canal system coordinate frame.

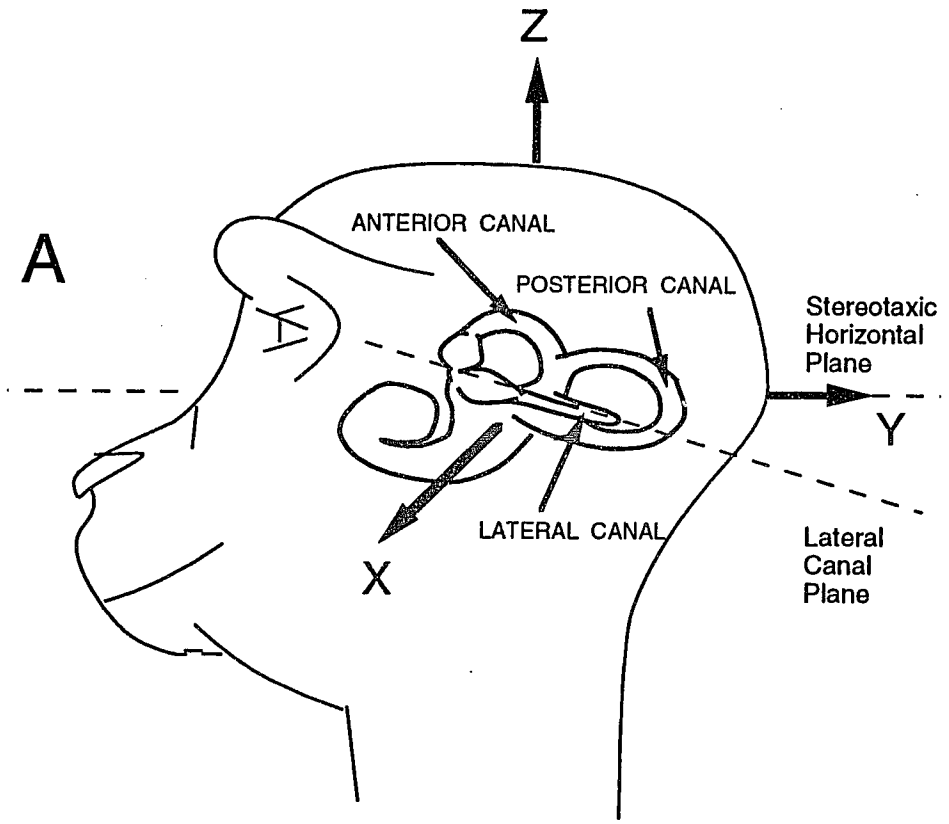
A
Z
ANTERIOR CANAL
POSTERIOR CANAL
Stereotaxic
Horizontal
Plane
Y
LATERAL CANAL
Lateral
Canal
Plane
X

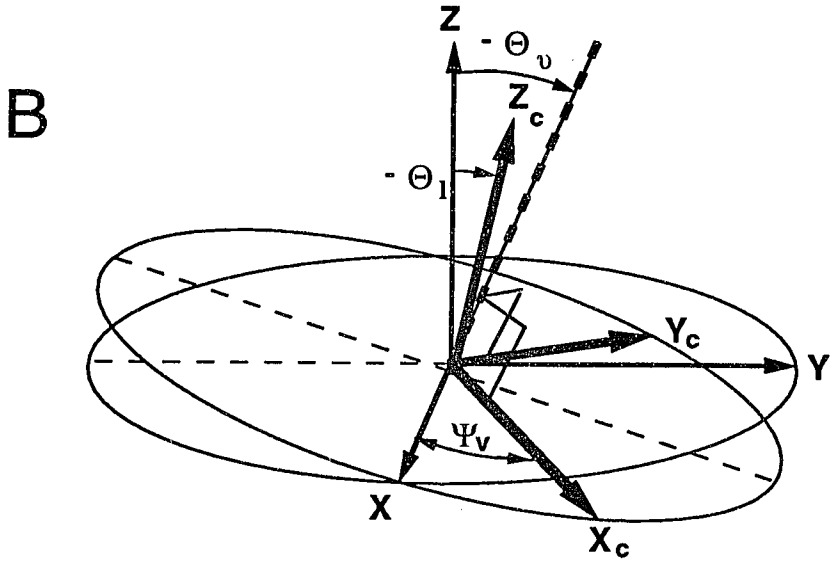
B
Z
- Θυ
Zc
- Θl
Yc
Y
Ψv
X
Xc

canal plane within the head frame. The component ω_{Hpit} has no projection along the normal to the lateral canal and will have a projected value of zero. The following relationships between the velocity components along the anterior, posterior and lateral canal normals can then be given in terms of the pitch, yaw and roll head velocities as follows:

$$\begin{bmatrix} \omega_{C_{ant}} \\ \omega_{C_{post}} \\ \omega_{C_{lat}} \end{bmatrix} = \begin{bmatrix} \cos\psi_v & \sin\psi_v\cos\theta_v & \sin\psi_v\sin\theta_v \\ -\sin\psi_v & \cos\psi_v\cos\theta_v & \cos\psi_v\sin\theta_v \\ 0 & -\sin\theta_1 & \cos\theta_1 \end{bmatrix} \begin{bmatrix} \omega_{H_{pit}} \\ \omega_{H_{roll}} \\ \omega_{H_{yaw}} \end{bmatrix} \quad \textbf{(Eq. 6)}$$

where ω_{Hpit}, ω_{Hroll}, ω_{Hyaw} are the pitch, roll and yaw components of head velocity in head coordinates and ω_{Cant}, ω_{Cpost}, ω_{Clat} are the head velocity components in canal coordinates.

The [B] and [M] matrices of the Robinson (1982) model (See above) were collapsed into a [G] matrix that transforms the canal based signals into the head frame:

$$[G]=[M][B] \quad \textbf{(Eq. 7)}$$

It has been assumed that the complementary canals on both sides act in a push-pull combination that they are coplanar, and that they contribute equally to the compensatory eye velocity vector (Cohen et al. 1964). The **g** parameters are:

g_{00} - anterior canal contribution in to the pitch plane,

g_{01} - posterior canal contribution into the pitch plane,

g_{02} - lateral canal contribution into the pitch plane,

g_{10} - anterior canal contribution into the roll plane,

g_{11} - posterior canal contribution into the roll plane,

g_{12} - lateral canal contribution into the roll plane,

g_{20} - anterior canal contribution into the yaw plane,

g_{21} - posterior canal contribution into the yaw plane,

g_{22} - lateral canal contribution into the yaw plane.

The canal activations are mapped back to the stereotaxic head frame by projecting their activations to each of the head coordinate basis vectors. They are given by the following equations:

$$\begin{bmatrix} \omega_{E_{pit}} \\ \omega_{E_{roll}} \\ \omega_{E_{yaw}} \end{bmatrix} = \begin{bmatrix} g_{00}\cos\psi_v & -g_{01}\sin\psi_v & 0 \\ g_{10}\dfrac{\cos\theta_l\sin\psi_v}{\cos(\theta_v-\theta_l)} & g_{11}\dfrac{\cos\theta_l\sin\psi_v}{\cos(\theta_v-\theta_l)} & -g_{12}\dfrac{\sin\theta_v}{\cos(\theta_v-\theta_l)} \\ g_{20}\dfrac{\sin\theta_l\sin\psi_v}{\cos(\theta_v-\theta_l)} & g_{21}\dfrac{\sin\theta_l\cos\psi_v}{\cos(\theta_v-\theta_l)} & g_{22}\dfrac{\cos\theta_v}{\cos(\theta_v-\theta_l)} \end{bmatrix} \begin{bmatrix} \omega_{C_{ant}} \\ \omega_{C_{post}} \\ \omega_{C_{lat}} \end{bmatrix}$$

(Eq.8)

where ω_{Epit}, ω_{Eroll}, ω_{Eyaw} are the pitch, roll and yaw components of eye velocity in head coordinates.

The orientation of a canal relative to a head coordinate axis multiplied by a gain (g) is the percentage of that canal activation along that coordinate axis of the head. The sum of the projections multiplied by its associated gain from all canals determines the gain of each component of eye velocity (Yakushin et al. 1995).

CHAPTER 3

METHODS:

Experiments were performed on ten cynomolgus monkeys (Macaca fascicularis). Nine of them had one or more semicircular canal pairs plugged. The experiments conformed to the Principles of Laboratory Animal Care (NIH Publication 85-23, Revised 1985), and were approved by the Institutional Animal Care and Use Committee of the Mount Sinai Medical Center.

3.1 SURGICAL PROCEDURES:

Under anaesthesia (ketamine induction, halothane/NO_2 gas anaesthesia) using sterile surgical conditions, head bolts were implanted on the skull in dental acrylic cement in the stereotaxic vertical plane. The bolts provided painless fixation of the head in stereotaxic coordinates during testing. With the animals upright, the normal to the horizontal stereotaxic plane or the yaw axis was along the spatial vertical. During the same surgery, two three-turn coils were implanted on one eye. One 14 mm coil was placed symmetrically around the iris in a plane such that its normal is approximately aligned with the visual axis[1] (Robinson 1963; Judge et al. 1980). This coil was used to measure horizontal and vertical eye position. An 11-12 mm coil, threaded under the superior rectus muscle, was implanted on top of the same eye (Cohen et al. 1992; Dai et al. 1994). The top coil, which was used to measure roll eye position, was placed approximately orthogonal to the frontal coil. The animals were allowed to recover and receive baseline testing.

---

[1]For purposes of this dissertation, the visual and optic axis are used interchangeably.

About a month after coil implantation, monkeys were anesthetized again, and the semicircular canals were plugged. This part of the surgery was performed by Dr. J-I. Suzuki (Cohen et al. 1964; Suzuki et al. 1964; Cohen et al. 1965; Suzuki and Cohen 1966). The middle ear was approached posteriorly. The canals were identified under an operating microscope. Plugging was accomplished by grinding across each canal with a diamond burr until the membranous canal was interrupted. The region of the canal was packed with bone and covered with a small piece of muscle. Five types of plugged canal animals were prepared: 1) All vertical canals plugged (**LC**) 2) both lateral canals plugged (**VC**) 3) both lateral and left anterior-right posterior canals plugged (**RALP**) 4) both lateral and right anterior-left posterior canals plugged (**LARP**) 5) animal for which all six semicircular canals were plugged (**NC**).

Animals received steroids for 3 days, antibiotics for 5 days and analgesics (morphine) for 2 days to reduce swelling, infection and pain, respectively. Animals were allowed to recover for one month after plugging before testing began, and testing continued at monthly intervals until the results stabilized. Following this, animals were tested up to 24 months after surgery. During the recovery period, the animals moved freely in their cages, which were 77 cm wide x 77 cm height x 88 cm deep. By the time of testing, postural control was good, and the uncoordinated head movements in the plane of the plugged canals observed in the first weeks after surgery had largely disappeared. Thus, the results that will be reported were from animals that had recovered from the effects of operation.

Canal plugging was verified physiologically by examining the response to

sinusoidal rotation at 0.2 Hz, 60°/s. in a plane perpendicular to the average plane of the remaining canals. This midband frequency was high enough to activate the direct vestibular pathway, but not velocity storage. It was low enough so that there were immeasurable responses for this plane of activation. At the end of testing, three animals were deeply anaesthetized and perfused through the heart with saline and a paraformaldehyde/formalin solution. The temporal bones were removed, decalcified, embedded in celloidin and processed for anatomical study. Morphological studies were performed by Drs. Kodama, Arai and Suzuki of Teikyo University, Tokyo, Japan (Suzuki et al. 1995). The plugged canals were verified, and the condition of the ampullae and nerves were examined. Figures 3.1 and 3.2 show an example of the canals and otolith organs in a bilateral lateral canal plugged animal (M1126) that was utilized in other studies (Cohen et al, 1983; Raphan et al, 1983). This animal was not tested using the paradigm utilized in this study. However, its results are shown because a complete set of end organs was available for display. Moreover, the surgery was done using the same technique on the same species by the same surgeon and are typical of all other animals in the series. The lateral canals were plugged in the portion of the canal farthest away from the ampullae by dense bone that completely filled the canal and would not allow passage of endolymph (Fig 3.1 C, D, arrows). Plugging of the canals was local, however, and the crista and hair cells of both lateral canals were intact (Fig 3.1 A, B). The ampullae of the anterior canals (Fig 3.2 C, D) and the posterior canals (Fig 3.2 E, F) and the macula of the utriculus and sacculus (Fig 3.2 A, B) were also unaffected by the plugging. (Suzuki et al. 1995). The Organ of Corti was also intact in this animal.

Figure 3.1: Anatomic verification of the semicircular canal plugging in a bilateral lateral canal plugged (VC) animal (M1126). Dense bone completely filled the canal in the portion farthest away from the ampullae. This would inhibit passage of endolymph (**C, D**). Plugging of the canals was local, however, and the crista and hair cells of both lateral canals were intact (**A, B**). Cr-Crista, Lc-Lateral canal, Plugged canal is indicated by an arrow. This demonstrates that both lateral canals were plugged.

LATERAL CANALS

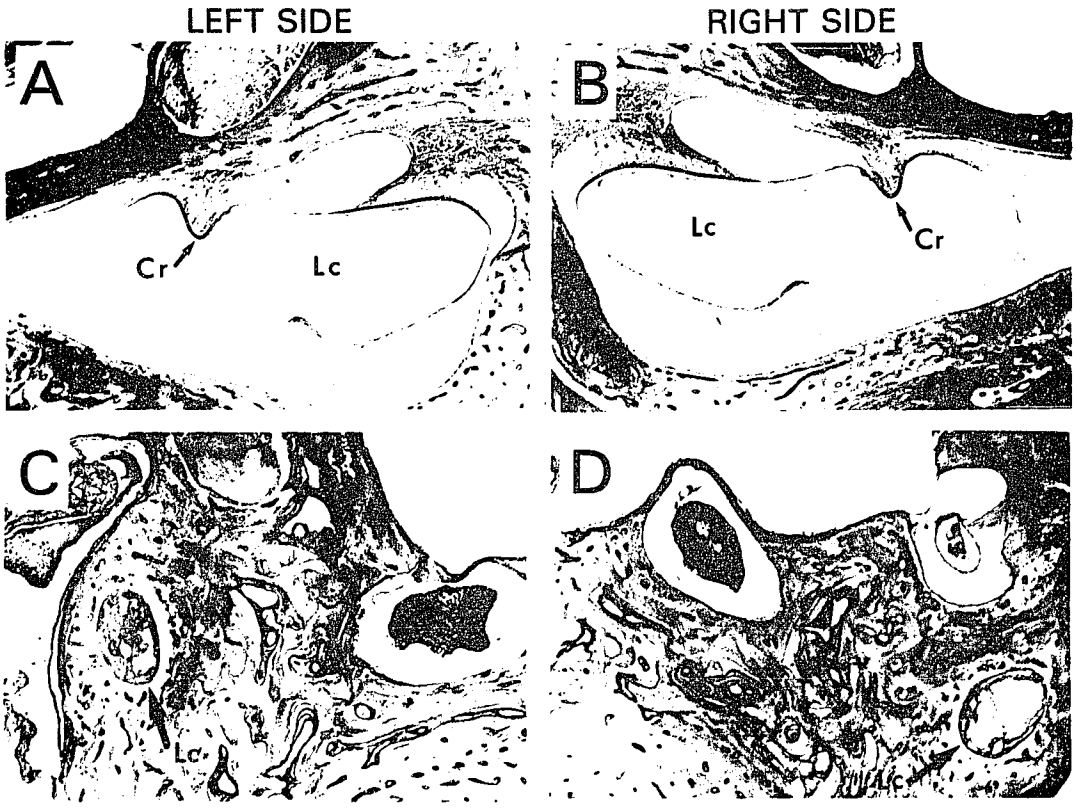

Figure 3.2: Anatomic verification that the anterior and posterior canals were intact following bilateral lateral canal plugging (VC animal, M1126). This typical result demonstrates that the maculae of the utricle and saccule (**A**, **B**), the ampullae of the anterior canals (**C**, **D**) and the posterior canals (**D**, **E**) were unaffected by the plugging. It could be seen that ampullae nerves of the anterior canals were intact on both sides. Ot- otolith organ, MU- maculae of the utricle, MS- maculae of the saccule, Cr- crista, Lc- lateral canal, Ac- anterior canal, Pc- posterior canal, AcN- anterior canal ampullae nerve.

CANALS AND OTOLITHS

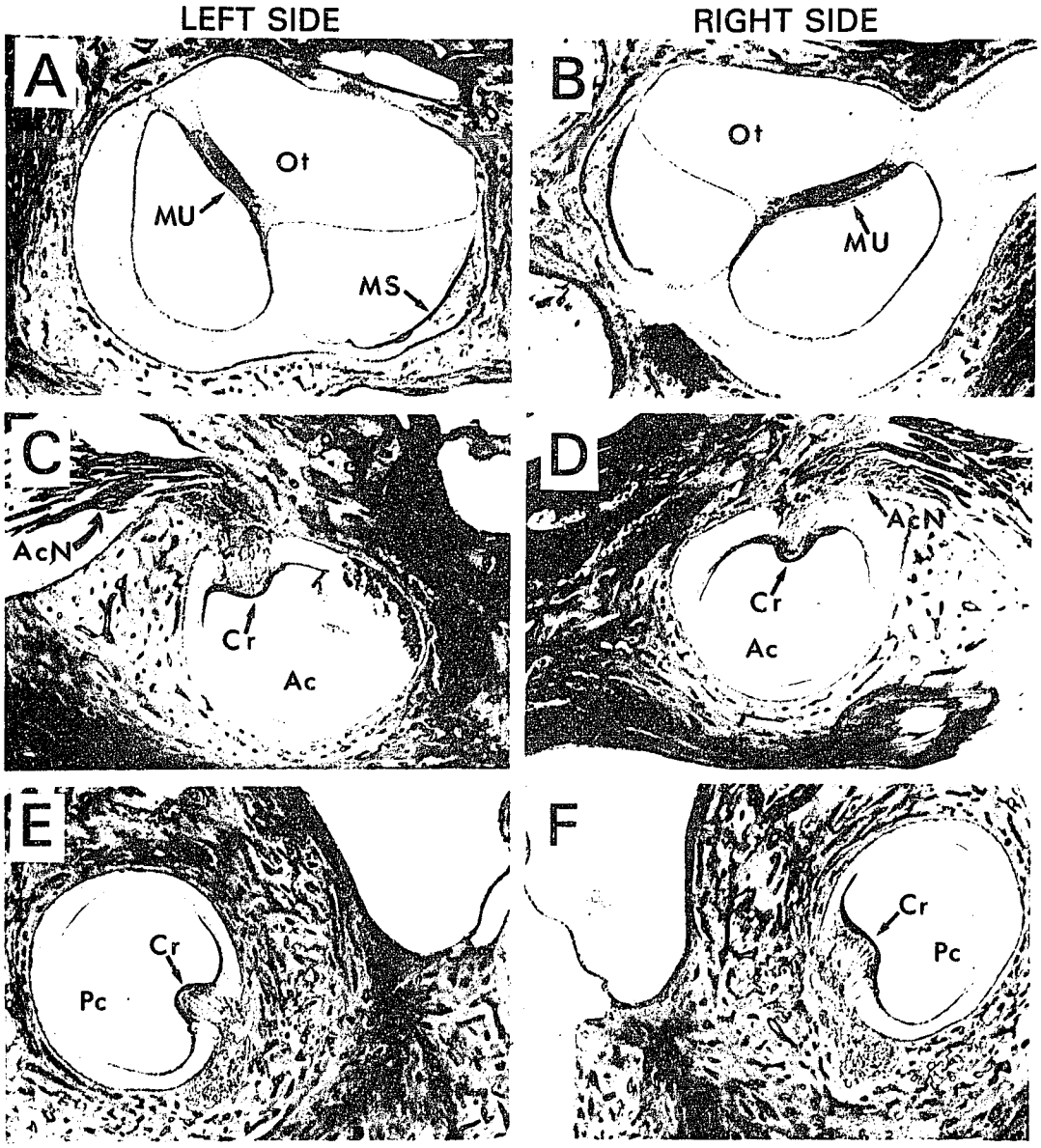

Canal plugs were similarly verified in the other animals used in this series. The histology report (Y. Arai and J-I. Suzuki, personal communication), showed the following:

In monkey M9008 (LC animal), the plugging of the four vertical canals were complete. Plugging of the right anterior canal was close to the crista ampullaris and the top area of the crista was missing sensory hair cells. However, the top area was surrounded by normal-looking haircells and no pathology was found in the right posterior and lateral canals, any of the three semicircular canals on the left side, or organ of Corti. Nerves and ganglion cells appeared intact.

In monkey M9006 (LARP animal), both horizontal, right anterior and left posterior canals were completely plugged. No pathology was found in the haircells of the six ampullae, the four maculae or organ of Corti. No changes in the dark cell area were found. The otolithic membranes were not smooth, but the sensory cells looked intact. Nerves and ganglion cells appeared intact.

In monkey M9003 (VC animal), both lateral canals were completely plugged. No pathology was found in the haircells of the ampullae, maculae and the organ of Corti. No changes in the dark cell area were found. Nerves and ganglion cells were intact (Suzuki et al. 1995).

3.2 TECHNIQUES FOR MEASURING EYE POSITION AND EYE VELOCITY:

During testing, the monkey's head was fixed in a 13 cm plastic frame which hold two sets of field coils that generated orthogonal oscillating magnetic fields at the same frequency (24.7 kHz). The axes of the field coils were along the interaural and

dorsoventral axes of the head, establishing a head fixed reference frame for measuring the orientation of the frontal and top search coils. The head frame axes for the field coils were defined to be the X and Z directions, respectively.

It should be noted that the coordinate frame utilized in this study was different from that used by Böhmer et al. (Böhmer et al. 1985), Minor and Goldberg (Minor and Goldberg 1990) and Baker and Peterson (Baker and Peterson 1991). They pitched the head at various angles relative to the horizontal stereotaxic plane to bring the lateral canals to the presumed spatial horizontal.

The monkeys were positioned so that the eye with the search coils was at the center of the magnetic fields. Its orientation relative to the head was determined from the orientation of the search coils within the fixed coil frame. During rotation about a vertical axis, a portion of the horizontal voltage was fed back and subtracted from the roll coil voltage. As a result, there was minimal cross talk in the roll recording when the upright animal was rotated around a spatial vertical axis. This method electronically "orthogonalized" the eye axes so that the effective normal to the top coil was aligned with axis from the bottom to the top pole of the eye. Studies on monkeys have shown that there is a small ($< 3°$) nonorthogonal relationship between the maximum direction for roll and yaw (Crawford and Vilis 1991), but the angles are well within the error bounds of the data reported in this study. Therefore orthogonalization was warranted.

3.3 CALIBRATION PROCEDURES:

To calibrate eye movements, the animals were rotated in light at 30°/s. about the pitch, roll and yaw axis. It was assumed that horizontal and vertical gains were close to

unity in this condition (Robinson 1963; Raphan et al. 1979; Crawford and Vilis 1991; Dai et al. 1991). Roll gains were assumed to be 0.6 when rotation was around a naso-occipital axis aligned with the spatial vertical (Crawford and Vilis 1991; Henn et al. 1992). This agrees with roll gains determined for monkeys using other techniques (Dai et al. 1994; Yue et al. 1994). This procedure was adopted because the apparatus does not allow for training animals and there was no absolute registration of eye position. However, this study depended only on eye velocity and this method was applicable (See Appendix A for calibration and computation of eye velocity in head coordinates, and for a comparison of these velocities with eye velocity derived from differentiation of coil voltages). Calibration values that were determined before surgery for each animal were used after canal plugging. Calibrated eye velocities obtained during sinusoidal rotation at 0.2 Hz, with a peak velocity 60°/s. in light after plugging matched the preoperative values. Eye velocities to the left, down, and counterclockwise (from the animal's point of view) are represented by downward deflections in the velocity traces in the figures.

In order to determine eye velocity in a head frame coordinate system, eye orientation was determined relative to a reference position. The horizontal reference eye position was obtained from the average voltage of each coil during 10 cycles of sinusoidal rotation about a vertical axis at 0.2 Hz in darkness (60°/s. peak velocity) with animals sitting upright (stereotaxical horizontal plane). The references for vertical and torsional eye positions were obtained in the same fashion, by positioning an animal on its left side or face down, respectively, and oscillating the animal about a spatial vertical. We then determined the slope of the voltage change for a slow phase during step rotation

at 30°/s. in light about a yaw axis at a point where the other two voltages were close to the reference value. The same was done for pitch and roll during rotation about the pitch and roll axes of the head, respectively. The average absolute value of the slope corresponded to an eye velocity of 30°/s. for yaw and pitch (Robinson 1963; Raphan et al. 1979; Crawford and Vilis 1991; Dai et al. 1991) and 18°/s. for roll (roll gain 0.6) (Berthoz et al. 1981; Ferman et al. 1987a, 1987b; Collewijn et al. 1988; Crawford and Vilis 1991; Henn et al. 1992; Dai et al. 1994; Yue et al. 1994).

3.4 DATA COLLECTION:

During testing animals sat in a primate chair with the head fixed in a four-axis vestibular stimulator surrounded by an optokinetic drum. The drum has a diameter of 91 cm and contains vertical black and white stripes of 10° width each. Each axis of the stimulator went through the center of rotation of the head. The stimulator capabilities have been described in detail in previous publications (Raphan et al. 1981; Dai et al. 1991; Reisine and Raphan 1992). Therefore, only part of the stimulator's capability utilized in these experiments is described.

The monkey could be sinusoidally oscillated around a spatial vertical axis inside the optokinetic drum. When the animal was rotated about its yaw axis in light, it produced full field visual stimulation. The monkey could also be statically positioned at pitch angles from -90° to 90° and rotated about a spatial vertical axis (see cartoons on Fig 3.7 A, B). In the experiments performed during this research, animals were pitched about their interaural axes (Fig 2.3A) to a given angle and then rotated about a spatially vertical axis (Fig 3.7 A, B). This stimulus induced yaw eye movements when animals

were upright and both yaw and roll eye movements when the animals were pitched forward or back. This paradigm is similar to that utilized in previous studies of horizontal eye movements induced after semicircular canal plugging (Baker et al. 1982, 1986; Böhmer et al. 1985; Cohen et al. 1988; Minor and Goldberg 1990; Baker and Peterson 1991). Unless otherwise specified (as in Fig 4.14), all testing was done in darkness. In one set of experiments, however, the stimulus was applied in light.

The calibrations that were determined before surgery were used after canal plugging. Once the amplifier gains had been set at the first testing, they were maintained throughout. Our assumption was that the eye movement recording system had the same gain in the pre- and post-operative periods. This was supported by the following: 1) The settings and gains of the instrument and the eye coil system were noted and maintained constant throughout the experiment. 2) There was no change in the resistance of the coil, measured in each experiment. 3) Voltages representing change in a position for $\pm 40°$ horizontal, $\pm 30°$ vertically and torsionally of the standard coil were the same on any experimental days for the same amplifier settings. 4) Utilizing the same system for recording eye movements, there were no difference in the pre- and post-operative gains, when the animals were rotated in light at 30°/s. and 60°/s.

Eye position voltages and voltages related to the velocity of chair oscillation as well as position of the tilt axes were recorded with amplifiers having a bandpass of DC to 40 Hz. Data were acquired with an MS-DOS based, PC/AT computer, running programs written by Dr. M. Dai in DAOS (Data Acquisition and Operating System, Mycon Technology, Australia). Voltages were digitized at 600 Hz/channel with 12 bit

resolution, and stored on optical disk. Eye position voltages were smoothed by sequentially averaging four sampling intervals. The smoothed waveform was digitally differentiated by finding the slope of the least squares linear fit to 11 data points. This corresponds to a filter which has a 3 dB cutoff above 40 Hz, the cutoff frequency of the filters used for data acquisition. Saccades were then determined using a maximum likelihood detection criterion (Singh et al. 1981), and replaced in the velocity trace with a straight line.

3.5 TESTING PROTOCOL AND DATA ANALYSIS:

All animals were tested during sinusoidal rotation at 0.2 Hz, 60°/s. in darkness before and after the surgery. Some of the animals were tested in light. One animal with all six canals plugged (NC Animal), one LARP, one RALP and one VC animal were tested at several other frequencies of sinusoidal rotation in darkness: 0.5 Hz and a peak velocity 60°/s., 1.0 Hz and 30°/s., 2.0 Hz and 15°/s., 4.0 Hz and 5°/s. The animals were tested upright (0°) and statically tilted forward (nose down, +) or backward (nose up, -) in 10° increments up to 90°. Ten cycles or more were collected in each position.

Eye velocities for sinusoidal data were processed in two steps. First, an average of ten cycles of desaccaded eye velocity traces were fit with a sinusoid at the given frequency of oscillation. From this, the average value of eye velocity and the phase relative to the stimulus (Fig 3.3, phase shift) were determined. The time of occurrence of the peak value of the fitted curve (Fig 3.4A) was also computed. The maximum and minimum values of the data for each of at least 10 cycles of eye velocity were obtained at the times of the peaks of the fitted curves. Fig 3.4 shows examples of data and fits

Figure 3.3: Determining temporal gain and phase of the aVOR. Horizontal eye velocity was averaged over 10 cycles during rotation of a **RALP** animal about a vertical axis in light at 0.2 Hz with 60°/s. peak velocity. The least mean square fit to the data was compared to stimulus velocity to determine temporal phase shift. The stimulus velocity is shown reversed by 180° to facilitate comparison. The positive peak stimulus velocity on the graph corresponded to 0° on the abscissa. The dashed line shows the zero level. Negative values correspond to leftward eye velocity. The phase in degrees is along the abscissa. The ordinate represents velocity in degrees/sec.

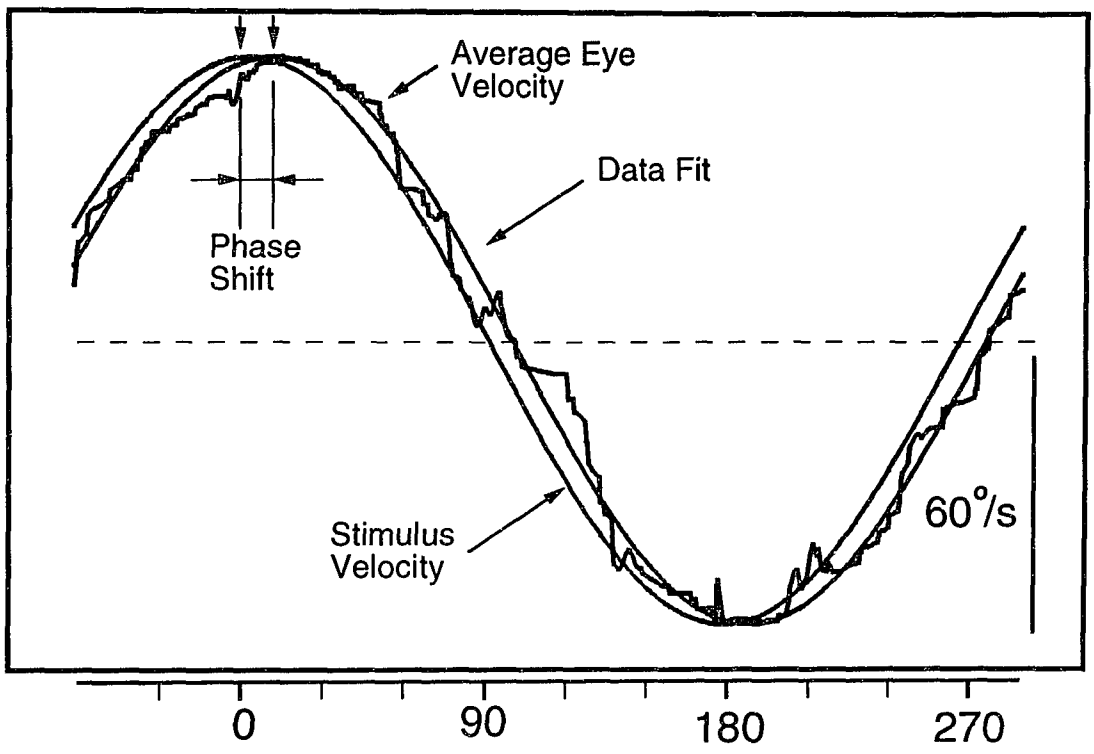
Average Eye Velocity
Data Fit
Phase Shift
Stimulus Velocity
60°/s
0
90
180
270

Figure 3.4: Measuring peak slow phase eye velocity at different frequencies of rotation. **A.** Sample of data obtained from normal monkey at 0.2 Hz 60°/s. The solid line shows desaccaded eye velocity which overlays the data (jagged line). **B.** Samples of data obtained from normal monkey at 4.0 Hz, 5°/s. Arrows represent points of maximum eye velocity, which were used in the computation of gain.

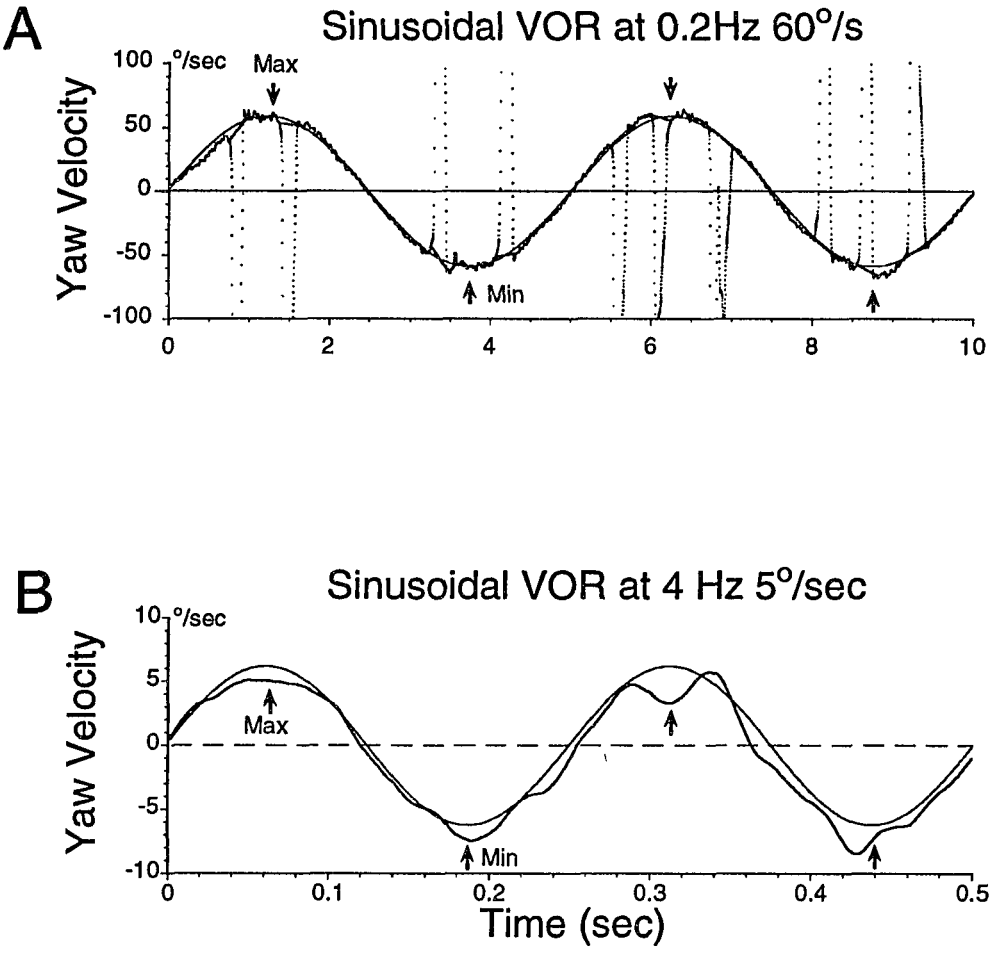
A
Sinusoidal VOR at 0.2Hz 60°/s
Yaw Velocity
°/sec
Max
Min
100
50
0
-50
-100
0
2
4
6
8
10
B
Sinusoidal VOR at 4 Hz 5°/sec
Yaw Velocity
°/sec
Max
Min
10
5
0
-5
-10
0
0.1
0.2
0.3
0.4
0.5
Time (sec)

obtained at 0.2 Hz (Fig 3.4A) and at 4.0 Hz (Fig 3.4B). The horizontal and torsional gains were obtained for each cycle as (peak-to-peak eye velocity)/ (peak-to-peak stimulus velocity). The individual estimates of maximum and minimum values were taken at the peak eye velocity because eye position was close to the reference at this time (Fig 3.5). This minimized any effects of eye position on the velocity (Misslisch, Tweed et al. 1994). Mean gain and standard deviations were obtained over all peak values.

The step response gain of the aVOR was also tested by rotating animals at a constant velocity over short periods of time in darkness. Pulses of angular velocity lasting five seconds at 60°/s. were repeated ten times for left and right rotation (Fig 3.6D). After each rotation, the animal was stopped in light (Fig 3.6C) for at least 5 sec to suppress any post-rotatory nystagmus (Fig 3.6 A, B). According to the Raphan model (Raphan et al. 1979), the dominant time constant of the aVOR step response is the sum of two modes each having a different time constant. One mode originates in the peripheral labyrinth and has the time constant of the cupula dynamics ($\approx$3-6 sec; Fernandez and Goldberg 1971; Goldberg and Fernandez 1971; Büttner and Waespe 1981; Correia et al. 1992). The second mode arises from central integration of this activity by velocity storage (Raphan et al. 1979). The velocity storage integrator does not contribute to the initial jump in eye velocity which is mediated over a direct vestibular pathway (Raphan et al. 1979). In addition, the five second period in light following the five second pulse of constant velocity rotation was sufficient to completely abolish any residual horizontal (Fig 3.6A) or roll (Fig 3.6B) eye velocity stored in the velocity-storage integrator (Raphan et al. 1979). Therefore, the initial jump in eye velocity was

Figure 3.5: Comparison of coil voltages (solid lines, **A-C**) and derivatives of coil voltages (solid lines, **D-F**) with Euler angle derivations of eye position (dotted lines, **A-C**) and eye velocity (dotted lines, **D-F**) in head coordinates. See Appendix A for derivation of Euler angle representations. Stimulus velocity is shown in **G**. The dashed horizontal lines in **A-C** represent the reference position of the eye. The dashed horizontal lines in **D-G** are zero velocity. The arrows in **A** and **C** are the points at which gain measurements were taken. The solid and dotted lines were indistinguishable in **A**, **B**, and **D**, **E**. There were small differences between them in torsional position (**C**) and velocity (**F**), but these where minimal at the points were measurements were taken. The ordinates in **A-C** represent deviation in degrees around the reference position. In **D-G**, the ordinates represent eye velocity in degrees/sec.

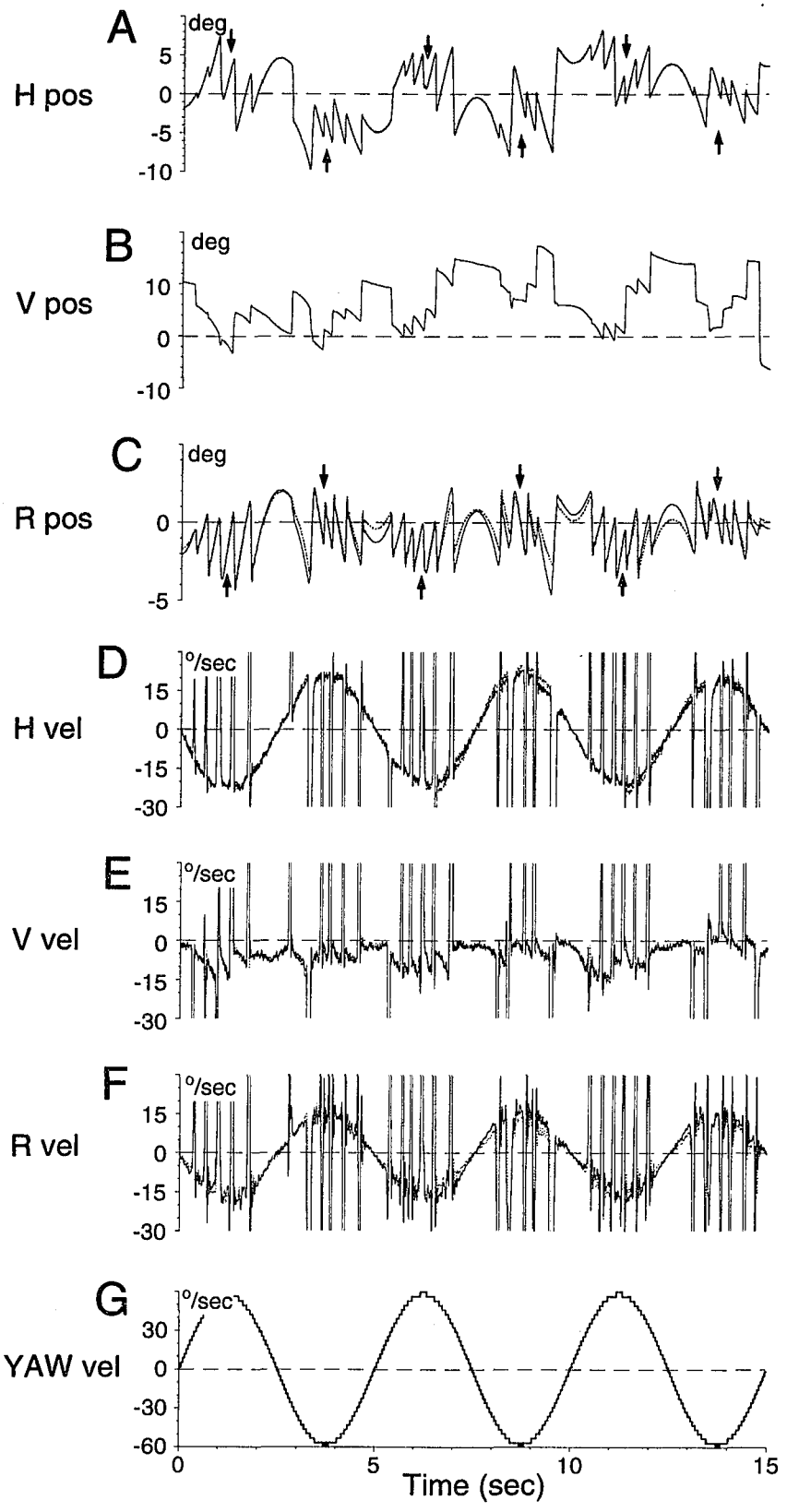
A
deg
5
0
-5
-10
H pos
B
deg
10
0
-10
V pos
C
deg
0
-5
R pos
D
°/sec
15
0
-15
-30
H vel
E
°/sec
15
0
-15
-30
V vel
F
°/sec
15
0
-15
-30
R vel
G
°/sec
30
0
-30
-60
YAW vel
0
5
10
15
Time (sec)

Figure 3.6: Horizontal (**A**) and roll (**B**) eye velocity during 60°/s. constant velocity rotation around the spatial vertical axis (**D**). When the normal animal is rotated in darkness (**C**) in an upright position, the response of the aVOR has predominantly a horizontal component. Animals were rotated for 5 seconds in darkness and then stopped in light (**C, D**). The light was turned off 2 seconds before the beginning of the next rotation.

Constant Velocity Rotation of the Normal Animal

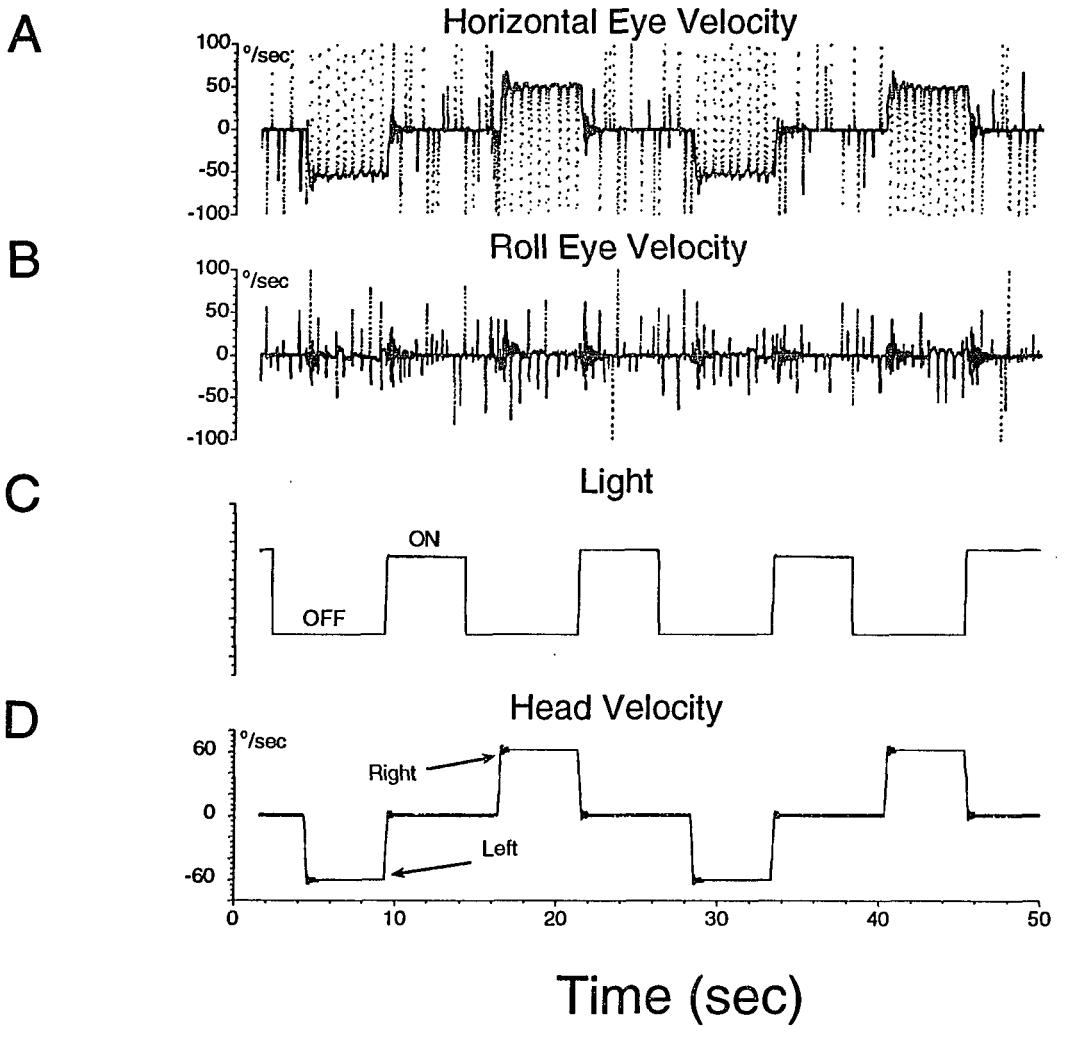

completely determined by the direct vestibular pathway and velocity storage had no influence. The gain of the step response is defined as the (Eye Velocity)/(Head Velocity) at the beginning of constant velocity of rotation.

An equal number of individual gain values were obtained for each tilt position both for sinusoidal and constant velocity stimulation paradigms. Processed files were transferred to a Macintosh computer for statistical analysis using Kaleidograph 3.0 (Abelbeck Software). The gain values as a function of tilt angle were fit with a sinusoid $y=A*Cos(x+B)$. The peak value (spatial gain) and its phase relative to the upright (0°) (spatial phase) were obtained from the fit. The spatial gains and phases of the horizontal and torsional aVOR were the variables of interest of this study.

3.6 SMALL ANGLE APPROXIMATION USED FOR MEASUREMENT OF EYE VELOCITY:

We calculated eye velocity in two ways. One way by differentiating the search coil signals used to represent eye position. The coil voltages are close approximations of eye position for small angular deviations, usually taken as 15° from some reference position (Ferman et al. 1987a; Paige and Tomko 1991). This is dictated by the fact that the cosine of 15° is approximately 1 and the sine is approximately linear over $\pm 15°$. In this study, eye position shifts were less than 15° from the reference position on average.

For five monkeys, we also computed the Euler angles from the coil voltages and used these variables to compute eye velocity in head coordinates (Appendix A, C). Eye velocity in head coordinates was compared to the derivative of the coil voltages for the 5 monkeys and differences were negligible. Figure 3.5 shows sample presurgery data

from monkey M9223 tilted 50° forward where the gain of each component was close to maximum, and the eyes were maximally deviated vertically. Coil voltages in Fig 3.5 are shown by solid lines and the values of the Euler angle by dotted lines. The two horizontal representations of eye position (Fig 3.5 A) and eye velocity (Fig 3.5 D) were indistinguishable. The same was true for vertical position and velocity (Fig 3.5 B, E). There were small differences between the voltage and Euler angle representations of torsion (Fig 3.5 C) at times when there were large horizontal and vertical deviations. The roll velocities, however, were indistinguishable at the peaks where the measurements for roll velocity were taken (Fig 3.5 F, arrows).

The conclusion is that because the computed eye velocity represents changes in eye orientation that remain within 15° of the reference position, eye velocity in head coordinates was not significantly different from the derivatives of the coil voltages. Thus, we used the coil voltage derivatives to represent eye velocity in head coordinates in this study because they could be obtained easily. A similar approximation was used by Paige and Tomko (Paige and Tomko 1991).

3.7 CONVENTIONS FOR DATA REPRESENTATION:

The coordinate frame for the semicircular canals, described by the normals to the canal planes, is approximately an orthogonal frame, rotated 45° and tilted up relative to the pitch, roll and yaw axes of the head (Blanks et al. 1975; Blanks et al. 1985; Reisine et al. 1988). The pitch axis is interaural, the roll axis is naso-occipital, and the yaw axis lies in the sagittal and coronal planes perpendicular to the pitch and roll axes. Because the horizontal stereotaxic plane is perpendicular to the coronal plane, we define

horizontal eye movements as movements that are confined to the horizontal stereotaxic plane. They are about the yaw axis and have no roll or vertical components. The conventions for describing eye velocity in the head followed a right-hand rule. The positive direction for the stimulus is along the spatial vertical (Fig 3.7 A,B), and peak positive values occur during rotations to the left (Fig 3.7 C, D). Horizontal or yaw eye velocity, which is also positive for rotations to the left, has a vector pointing out the top of the head (Fig 2.4A; Fig 3.7A, B, Z-axis). The positive direction for roll or torsion is along the naso-occipital axis, towards the back of the head (Fig 2.4A; Fig 3.7A, B, Y-axis). This represents a counterclockwise rotation from the animal's perspective. The positive direction for the vertical or pitch component is out of the left ear (Fig 2.4A, X-axis).

When the animal is tilted forward (Fig 3.7A, C, E, G), the horizontal (Yaw, Fig 3.7E) and torsional (Roll, Fig 3.7G) components are 180° out of phase with the stimulus velocity (Fig 3.7C). When the animal is tilted backward (Fig 3.7B, D, F, H), the reference sinusoid (Fig 3.7D) is the same as in Fig 3.7C. The horizontal component has the same phase relationship to the stimulus sinusoid (Compare Fig 3.7E to Fig 3.7F), but the torsional component oscillates in phase with the stimulus (Fig 3.7H).

In each case all components of eye velocity are either in phase or 180° out of phase with the reference sinusoid. The phase difference between the stimulus sinusoid and the eye velocity sinusoid is the temporal phase. For forward tilts (Fig 3.7A), when the horizontal and roll components of eye velocity are out of phase with the reference sinusoid (Fig 3.7C, E, G), the gain is considered as positive. With the animal tilted back

Figure 3.7: Conventions for describing eye velocity in the head. The reference sinusoid for computing gains was along the spatial vertical (**A** and **B**). For the tilted forward condition, the components of head velocity (**C**) along the yaw (**E**) and roll (**G**) axes are positive, and the corresponding compensatory eye velocity components are 180° out of phase. This has been taken as a positive gain. With the head tilted backwards, the component of head velocity (**D**) along the yaw axis (**F**) is positive and the component along the roll axis (**H**) is negative. This corresponds to a yaw eye velocity (**F**) which is 180° out of phase with the reference and a roll eye velocity (**H**) which is in phase with the reference sinusoid.

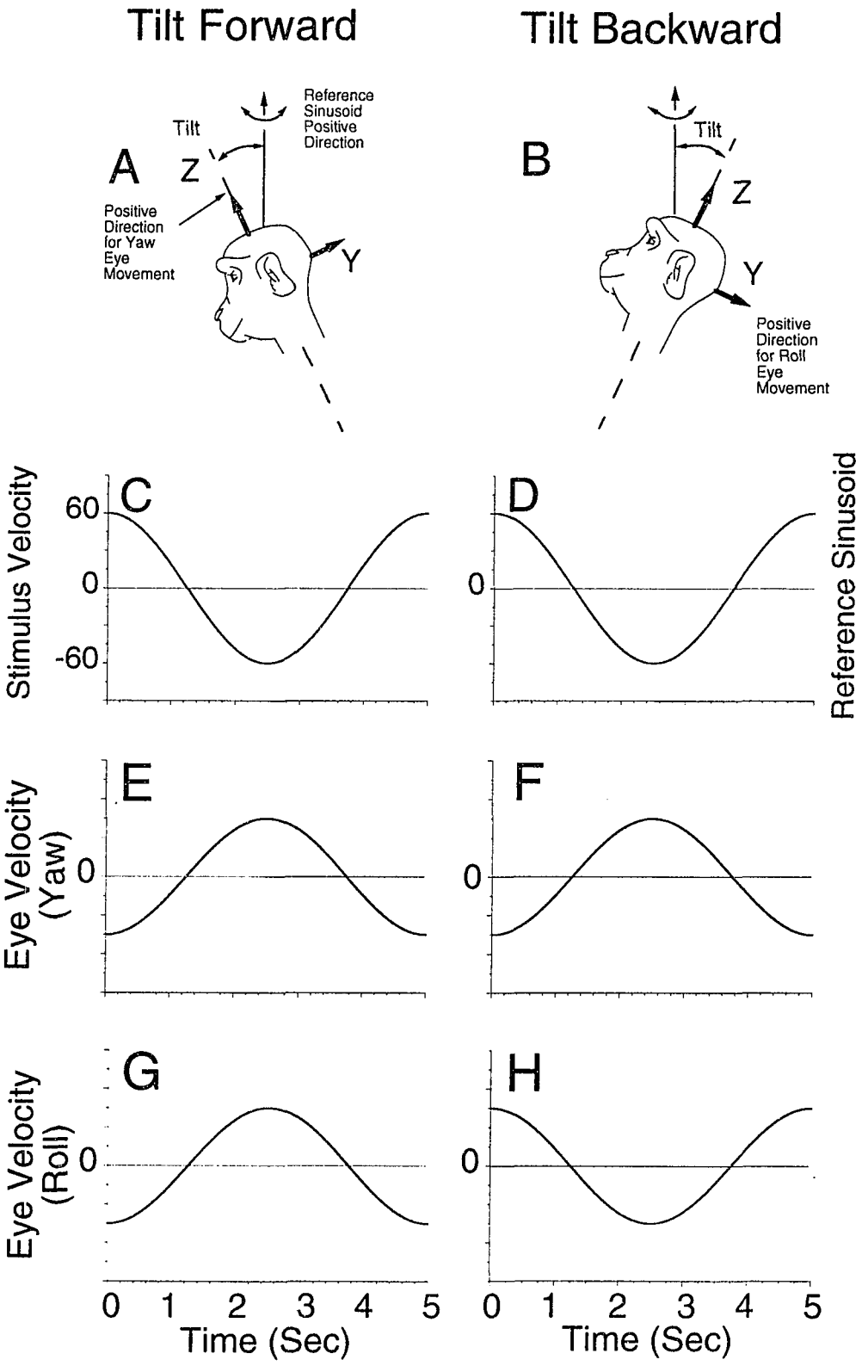
Tilt Forward
Tilt Backward
A
B
Tilt
Z
Y
Reference Sinusoid Positive Direction
Positive Direction for Yaw Eye Movement
Positive Direction for Roll Eye Movement
C
D
E
F
G
H
60
0
-60
Stimulus Velocity
Reference Sinusoid
Eye Velocity (Yaw)
Eye Velocity (Roll)
0 1 2 3 4 5
Time (Sec)

(Fig 3.7B), when the zero phase of the torsional component is in phase with the reference sinusoid (Fig 3.7B, F), the roll gain is considered negative. The positive and negative gains are represented on the ordinates of graphs displaying the average gains of horizontal and torsional (roll) eye velocity as functions of tilt with regard to gravity (Figs 4.7-4.16; Fig 4.18; Figs 4.20-4.22; Figs 4.28-4.29). The abscissa shows the direction of tilt (0° upright; + forward; - backward).

3.8 STATISTICAL ANALYSIS OF DATA

3.8.1 MOTIVATION

The data were evaluated by comparing a control data set to one under a specific treatment condition. The control experiment consisted of average data obtained from a normal group of animals which were described by gain vs. tilt angle. The **treatment** consisted of plugging specific semicircular canals and evaluating the gain vs. tilt angle curves under the treatment condition. In order to make model-data comparisons, a two step procedure was adopted.

We first evaluated whether the gain as a function of tilt was significantly close to a reference function which was chosen to be sinusoidal. The function used to fit the data is:

$$Y_{FIT} = A\cos(x + B) \qquad \textbf{(Eq.9)}$$

where **x** is the tilt angle, **A** is the spatial gain and **B** is the spatial phase. This was done to insure that the data were normally distributed around the best sinusoidal fit to the data. The reference sinusoid is characterized by two parameters, amplitude and phase, and

allowed us to develop a specific alternate hypothesis for computing power, based on specific variation of these parameters. For this purpose, we computed the best fitting sinusoid in the mean square sense to the gain vs. tilt angle curve for each monkey and each treated condition.

Based on this fit, we computed the deviation of each data point from the reference function and averaged over all tilt angles (μ_1). The mean of the deviation of each data point from its mean averaged over all tilt angles (μ_0) is zero, by definition. The null hypothesis was:

H_0: $\mu_0 = \mu_1 = 0$

The alternate hypothesis was:

H_1: $\mu_1 \neq 0$

If the null hypothesis could not be rejected ($p < 0.05$), we concluded that the data could be fit by a sinusoid. The power associated with accepting the null hypothesis (Keppel 1991) was evaluated by considering a specific alternate hypothesis that some mean value was different due to a sampling error for computing the phase or amplitude of the fitted sinusoid. The effect size, ω^2, was computed as a ratio of the between group variance to within group variance (See (Keppel 1991), Eq. 4-1). Power could then be estimated from the effect size (Keppel 1991). An effect size greater than 0.15, implies that power is quite high if the N is large (Keppel 1991). The conclusion that the data were indeed sinusoidal enabled us to make comparisons with the model, which predicted sinusoidal variations in gain as a function of tilt angle.

The model consists of predictions of gain as a function of forward and backward

tilt angles based on the geometry of the semicircular canals relative to the head and fixed gain parameters that generate the compensatory eye velocity. The model predictions of gain vs tilt are sinusoidal functions. Model parameters were identified from data taken from normal monkeys. Based on the established model parameters, the various treatment effects due canal plugging were simulated and compared to the data for corresponding treatment conditions. We then statistically evaluated the null hypothesis in the same manner as described above except that the reference function was the model prediction rather than the minimum mean square error fit. The power of the test was estimated in the same fashion using ω^2.

3.8.2 METHODOLOGY

In the experimental design, we considered the data arising from testing normal animals as being generated by one population, the control group. Although there is no physiological reason for expecting the variance around the mean at each tilt angle to be different, we cannot a priori dismiss this possibility. The model predictions are based on the normal data. The variances of the data for the treated conditions could also be different from normal. Therefore, because the data and model generated values could be derived from populations with different variances, it is appropriate to use an analysis of variance (ANOVA) (Keppel 1991). We utilized a reduced case ANOVA (F statistic) in the model-data comparisons performed in this work, since the analysis compares two sets of data. Because each measurement of gain at each tilt angle is done independently, the ratio of the variance of the data relative to the fit and the variance relative to the mean follows an F distribution (Keppel 1991). The F statistic could then be used to evaluate

how closely the model-generated sinusoid describing gain as a function of tilt angle fit the data (Keppel 1991). A similar analysis was used to compare the model predicted curves when canal contributions were removed from the data.

The F statistic is a ratio of the mean square error of the data relative to the reference prediction and the mean square error of the data relative to mean value of the data ($F = MS_{err\ ref}/MS_{err\ data}$). Where,

$$MS_{err\ model} = \sum_{i=1}^{M} \sum_{j=1}^{L} (x_{ij} - x_{im})^2 \qquad \textbf{(Eq.10)}$$

$$MS_{err\ data} = \sum_{i=1}^{M} \sum_{j=1}^{L} (x_{ij} - \bar{x}_{iL})^2 \qquad \textbf{(Eq.11)}$$

L is the number of cycles (L=10);

M is the number of stationary tilt positions (M=19);

i - A particular stationary tilt position, (-90, -80, -70, ...+80, +90);

j - A particular cycle of sinusoidal rotation for a given tilt position;

x_{ij} - observed gain value for tilt position **i** and cycle of rotation **j**;

x_{ir} - reference gain value denoted by **r**, for stationary tilt position (**i**). The reference is the same value for all N cycles of rotation for a given M.

$\bar{x}_{iL}$ - average gain value observed for stationary tilt position **i**.

Since the mean value of the data at a given tilt position, i, is given by:

$$\bar{x}_{iL} = \frac{1}{L} \sum_{j=1}^{L} x_{ij} \qquad \textbf{(Eq.12)}$$

then:

$$F=\frac{MS_{err\ ref}}{MS_{err\ data}}=\frac{\sum_{i=1}^{M}\sum_{j=1}^{L}(x_{ij}-x_{ir})^2}{\sum_{i=1}^{M}\sum_{j=1}^{L}(x_{ij}-\bar{x}_{iL})^2} \qquad \textbf{(Eq.13)}$$

The F statistic is not affected by variance of data around the mean, but simply measures the goodness of fit of the model to the data. As long as the data follow the sinusoidal fit, an increase in variance will not cause an increase in the F value or an increase in the phase error term. This implies that the F statistic is not sensitive to the normality of the data distribution. Therefore, if the model-predicted gain values are equal to the average observed gain values at each stationary tilt position, then the F statistic would be 1. When the data deviate from the sinusoidal fit, however, the F statistic will increase. The critical value (95% confidence level) can then be calculated. If the F statistic is less than the critical value, we assume that there is no significant difference between the data and the model prediction. The power will detrmine to what extent we can accept the model as fitting the data (See below).

In this study two distributions (data around the mean value and data around the reference) are compared with the F value. Because the variances of each distributions are derived from the same data set using the hypothesis that it could be fit by a sine function, the F statistic has 1 degree of freedom (df=2-1) and is given by $F_{1,N}$ (where N is the number of data points i*j). If this value is larger than the critical value at the 95% confidence level, then the null hypothesis is rejected, and the data are considered to be not well fit (F_{cr}; Table A-1 of Keppel, (Keppel 1991).

The best fit curve was shifted in both directions in increments of 1° on the abscissa until a critical value is obtained for the F statistic (Fig 3.8). The maximum deviation of the spatial phase from the optimal fit that maintains the F statistic within critical limits ($p < 0.05$) were computed and defined as the phase error. The criterion for assessing model fits was that the phase predicted by the model should fall within the range of the phase error.

Fig 3.8A shows the change in the F statistic for phase shifts of the fit to the data from the horizontal aVOR of one of the normal monkeys (M9003). The horizontal dashed line is the critical value, above which the fits were considered significantly different from the data ($p < 0.05$). The largest phase shift that had an F statistic below the critical values was $\pm 16°$ (Fig 3.8, up arrows). The size effect, ω^2, was about 0.62 for the smallest phase shift and reached about 0.8 at the critical value for F (Fig 3.8B). This typical example shows that our test has considerable power and the probability of accepting the null hypothesis when it is false (Type II error) is small. We also estimated power due to amplitude errors (Fig 3.8C,D). When reference amplitude was changed by 0.16, the F statistic exceeded the critical value (Fig 3.8C). The size effect was greater than 0.8 at the critical value. This indicates that our test has considerable power.

Data from pairs of monkeys with different canal plugging were summated to compare with data from normal monkeys or with data from monkeys with the same plugging of individual semicircular canals. To create the summated response, ten individual gain measurements that were taken from each pair of monkeys in each tilt position were sequentially summated to get ten gain values. These gain values are used

Figure 3.8: **A**, F value as a function of spatial phase shift (abscissa) for sine fits to the data from a normal animal tested in darkness. 0° on the abscissa represents the F value for the minimum mean square error fit of the data. The points to the right and left of 0° represent values where the curve used for fitting the data was shifted by the number of degrees shown on the abscissa. The dashed line represents the critical value above which the fits were considered significantly different from the data at a 95% confidence level. The up arrows represent the maximum possible angular shift of the curve at which the data were significantly fit. This defines the phase error. **C**, F value as a function of spatial gain variation (abscissa) for sine fits for the same data as in **A**. **B**, **D**. Estimated measurement of the power of F statistic ω^2 for cases **A** and **C**, respectively. Power is considered strong if ω^2 is above 0.15 ("large").

Shift of the Best Fit Curve in Phase

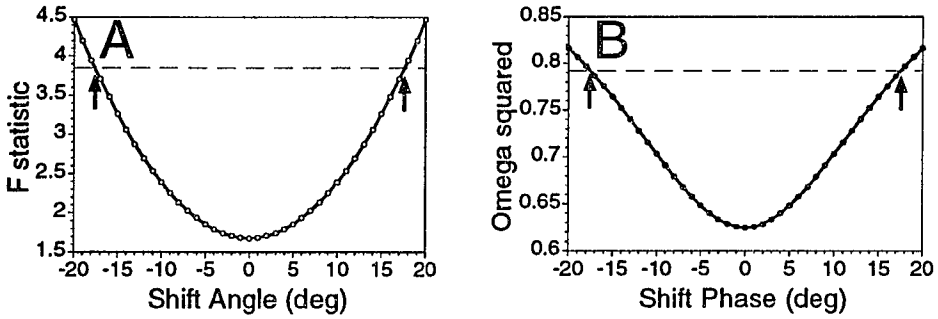

Shift of the Best Fit Curve in Gain

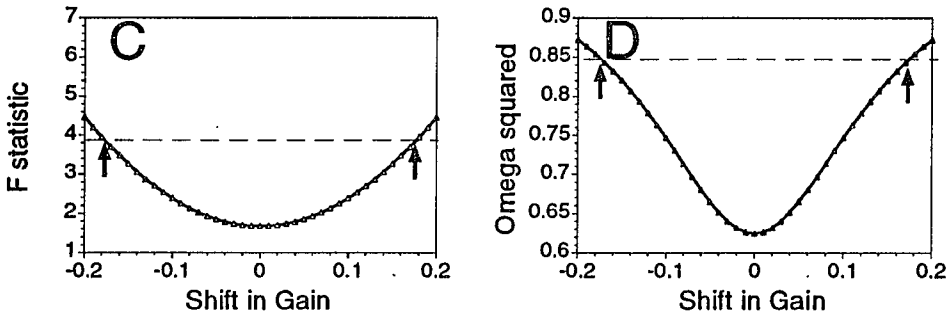

to construct a best fit curve. This curve is then compared to preoperative data from all monkeys using the F statistic described above. The vertical bars in all of the graphs represent $\pm$1SD.

In one set of experiments, the gain of the aVOR was determined at five different frequencies. In this case, each frequency was considered as a separate treatment and ANOVA was used to determine whether there was a significant effect of frequency on the gain of the aVOR. The null hypothesis was that the average gain at each frequency was the same. If the null hypothesis was rejected at the 0.05 significance level, the effect of each specific frequency was tested by using the method of orthogonal contrasts (Keppel 1991), to determine the specific set of frequencies that were the main contributors to the rejection of the null hypothesis. The set of orthogonal contrasts (Table 4.7) were evaluated using a post-hoc Scheffe approach which modifies the critical F value according to the number of compared groups (Keppel 1991).

CHAPTER 4

RESULTS:

Normal monkeys and those with five types of treatments were studied to determine the contribution of individual canals to the total eye velocity response (Fig 4.1). We first considered the spatial gain and phase of the responses produced by the lateral canals after the vertical canals were plugged (**LC M9008**) (Fig 4.1B). We then determined the response due to the vertical canals by plugging the lateral canals (**VC M9003, M9354**) (Fig 4.1C). We also studied animals that only had one pair of vertical canals intact (**LARP M9006, M9306, M9356; RALP M9223, M9355**) (Fig 4.1D, E). We compared results from the **VC** animals to the summated responses of the **RALP** and **LARP** animals. The results obtained from the **LC** and **VC** animals were summated and compared to the responses of normal animals. These determinations were done in animals in which the canal plugging was both physiologically and anatomically verified (**LC M9008; VC M9003**). One animal was studied that had all six canals plugged (**NC M9308**). The complete canal plugged animal (**NC**) was used as a control to determine the response characteristics of the plugged canal as a function of frequency (Fig 4.1F).

4.1 QUALITATIVE LOW FREQUENCY BEHAVIOR OF NORMAL AND CANAL PLUGGED ANIMALS

Sinusoidal rotation of normal monkeys about a spatial vertical produced compensatory sinusoidal eye velocity. When the animal was in the upright position (Fig 4.2A), the response was predominantly in the horizontal plane (Fig 4.2A, **Ḣ**) and 180° out of phase with stimulus velocity (Fig 4.2A, **St**). There was negligible vertical and roll

Figure 4.1: Five type of canal plugging and their relationship to the normal animal. **A. Normal Animals.** This group comprises all animals that were used in this study before canal plugging. **B. LC animal.** Only one animal was prepared with this type of plugging. **C. VC animal.** Two animals were available in this study. **D, E. RALP** and **LARP animals.** Three **LARP** and two **RALP** animals were prepared with this type of plugging. **F. NC animal.** This animal was used as a control to another type of canal plugging.

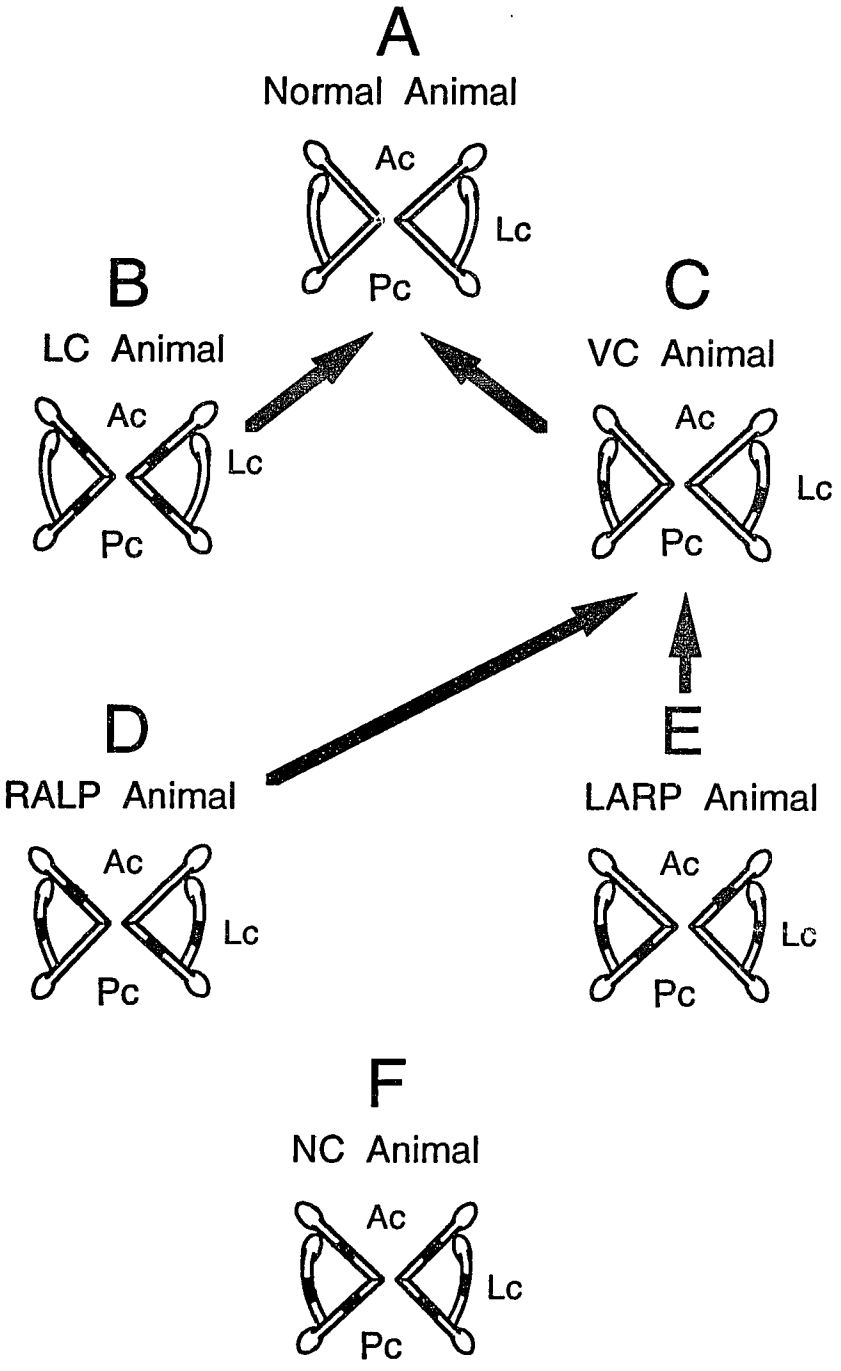
A
Normal Animal
Ac
Lc
Pc
B
LC Animal
Ac
Lc
Pc
C
VC Animal
Ac
Lc
Pc
D
RALP Animal
Ac
Lc
Pc
E
LARP Animal
Ac
Lc
Pc
F
NC Animal
Ac
Lc
Pc

Figure 4.2: Horizontal (yaw) ($\dot{H}$), vertical ($\dot{V}$) and torsional (roll) ($\dot{R}$) eye velocity of the **LARP** animal before (**A**) and after (**B**) canal plugging when animals were rotated upright in darkness or in light (**C**). Before surgery (**A**) and after surgery when animals were tested in light (**C**) upright rotation produced predominantly horizontal eye velocity. This component was markedly reduced after the surgery (**B**). The dashed line shows the zero level. Deviation up represents right eye velocity on horizontal traces, upward on vertical traces and clockwise direction on torsional traces from the animal's view. **St** - represents rotation of the primate chair around the spatial vertical axis. Upward deviation corresponds to clockwise rotation from the animal's view.

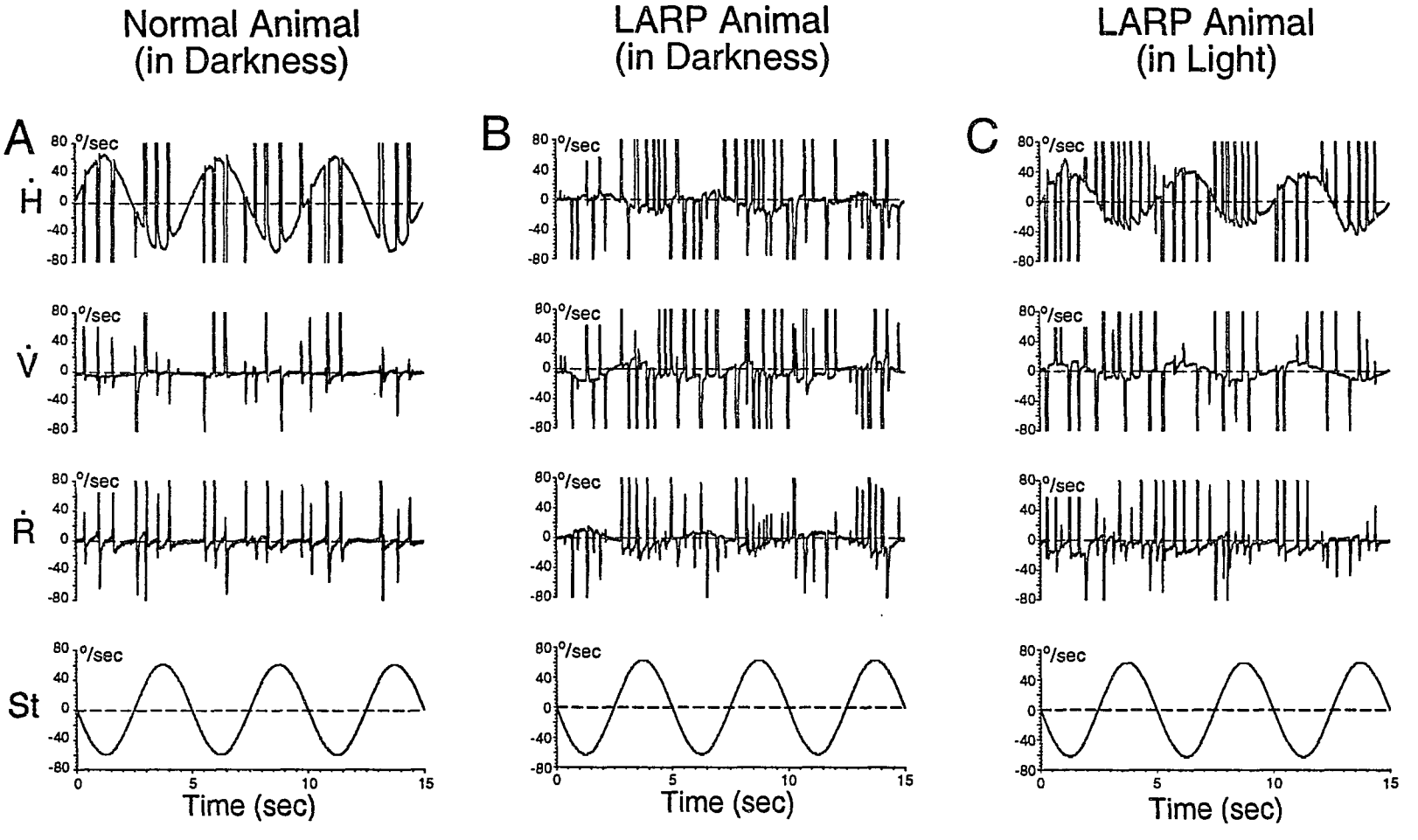
Normal Animal
(in Darkness)
LARP Animal
(in Darkness)
LARP Animal
(in Light)
A
B
C
Ḣ
V̇
Ṙ
St
80 °/sec
40
0
-40
-80
0
5
10
15
Time (sec)

components (Fig 4.2A, $\dot{V}$ and $\dot{R}$). When animals were tilted -80°, the dominant component was torsional (Fig 4.3A, $\dot{R}$), with small horizontal and vertical components (Fig 4.3A, $\dot{H}$, $\dot{V}$). The horizontal component of eye velocity gradually decreased as the monkey was tilted forward (Fig 4.4A, $\dot{H}$) or backward (Fig 4.5A, $\dot{H}$). The torsional eye velocity response complemented the horizontal response with an increase in amplitude as the animal was gradually tilted forward (Fig 4.4A, $\dot{R}$), or backward (Fig 4.5A, $\dot{R}$). It was out of phase with the stimulus sinusoid when the animal was tilted forward (positive gain) and in phase when the animal was tilted back (negative gain) (See Convention in Methods, Section 3.7, Fig 3.7).

After surgery, leaving only the left anterior and right posterior canals intact (**LARP** animal) (Fig 4.2B, C and 4.3B) or leaving only the right anterior and left posterior canals intact (**RALP** animal) (Fig 4.4B, C; Fig 4.5B, C), rotation in the upright position generated all three components of eye velocity (Fig 4.2B). When tilted -80°, all three components increased in amplitude (Fig 4.3B). For a wide range of head positions relative to gravity, the amplitude of the horizontal, vertical and torsional eye velocity components were proportional to each other (Fig 4.4B, Fig 4.5B) and were not compensatory. When a **LARP** animal was rotated in light, it produced predominantly horizontal (Fig 4.2C, $\dot{H}$) and a small vertical and torsional component (Fig 4.2C, $\dot{V}$ and $\dot{R}$). Eye velocity responses in light for **RALP** animals were identical to the **LARP** animal responses (Fig 4.4C and Fig 4.5C). The responses were also similar to those obtained from normal animals tested in dark (Compare A and C, Fig 4.4 and Fig 4.5).

Vertical velocities were small or absent in normal monkeys during the sinusoidal

Figure 4.3: Similar to Fig 4.2, horizontal (yaw) ($\dot{H}$), vertical ($\dot{V}$) and torsional (roll) ($\dot{R}$) eye velocity of the **LARP** animal before (**A**) and after (**B**) canal plugging when animals were rotated at -80° tilted back in darkness. When normal animals were tilted back (**A**) eye velocity was predominantly torsional ($\dot{R}$). After canal plugging (**B**) this stimulus produced all three eye velocity components ($\dot{H}$, $\dot{V}$, $\dot{R}$). The dashed line shows the zero level. Deviation up represents right eye velocity on horizontal traces, upward on vertical traces and clockwise direction on torsional traces from the animal's view. **St** - represents rotation of the primate chair around the spatial vertical axis. Upward deviation corresponds to clockwise rotation from the animal's view.

Normal Animal in Darkness (-80° Tilt Backward)

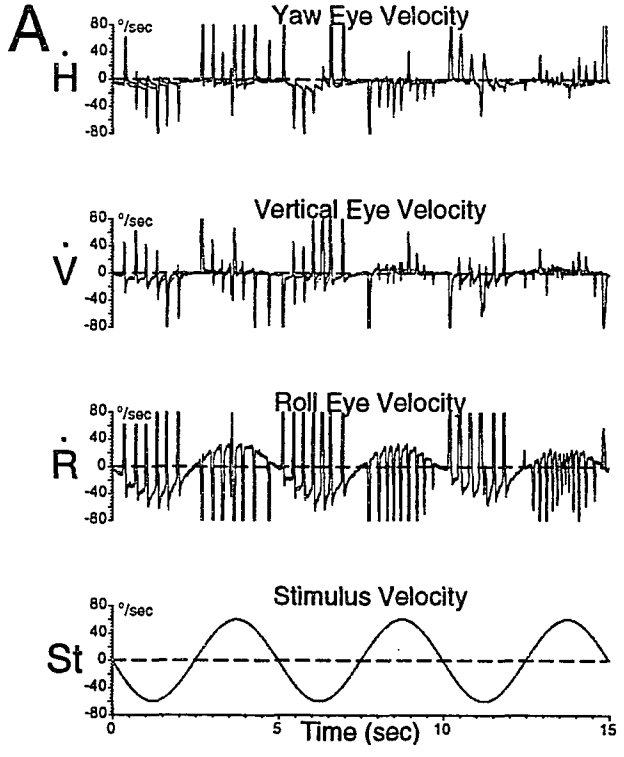

LARP Animal in Darkness (-80° Tilt Backward)

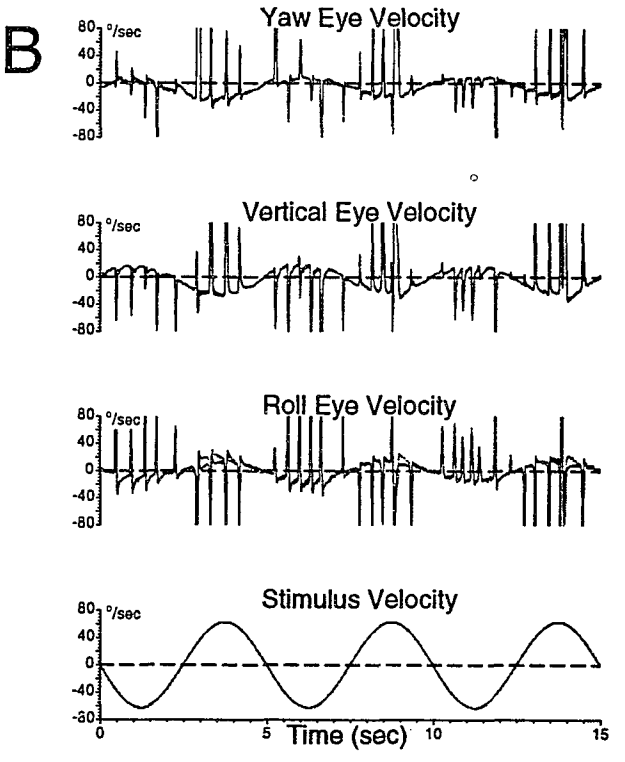

Figure 4.4: Horizontal (Ḣ), vertical (V̇) and roll (Ṙ) eye velocity of a **RALP** animal (**M9223**) during sinusoidal rotation about a spatial vertical axis (**Turntable**). Represented are responses upright (left), and during forward tilts along the **pitch axis** at angles of 30°, 60°, and 90°. The attitude of tilt and the axes of rotation are shown by the position of the monkey's head in the inserts below. The vertical line below the monkey represents the axis of gravity which was coincident with the axis of rotation. Three conditions are represented, **Pre-Op in Darkness** (**A**), **Post-Op in Darkness** (**B**) and **Post-Op in Light** (**C**). Before operation (**A**) and in light after operation (**C**), there was a decrease in the peak horizontal component and an increase in the peak roll component with increases in tilt angle along the pitch axis. **B**, When the animal was rotated in darkness after operation, horizontal and roll eye velocity decreased toward zero with 30° tilt forward and reversed at larger tilt angles (60° and 90°). There was a vertical component during the rotation at all angles that was also predicted by the model (see text). The calibrations for eye velocity and turntable velocity, which are the same for each component and for each panel are shown on the right of **A**.

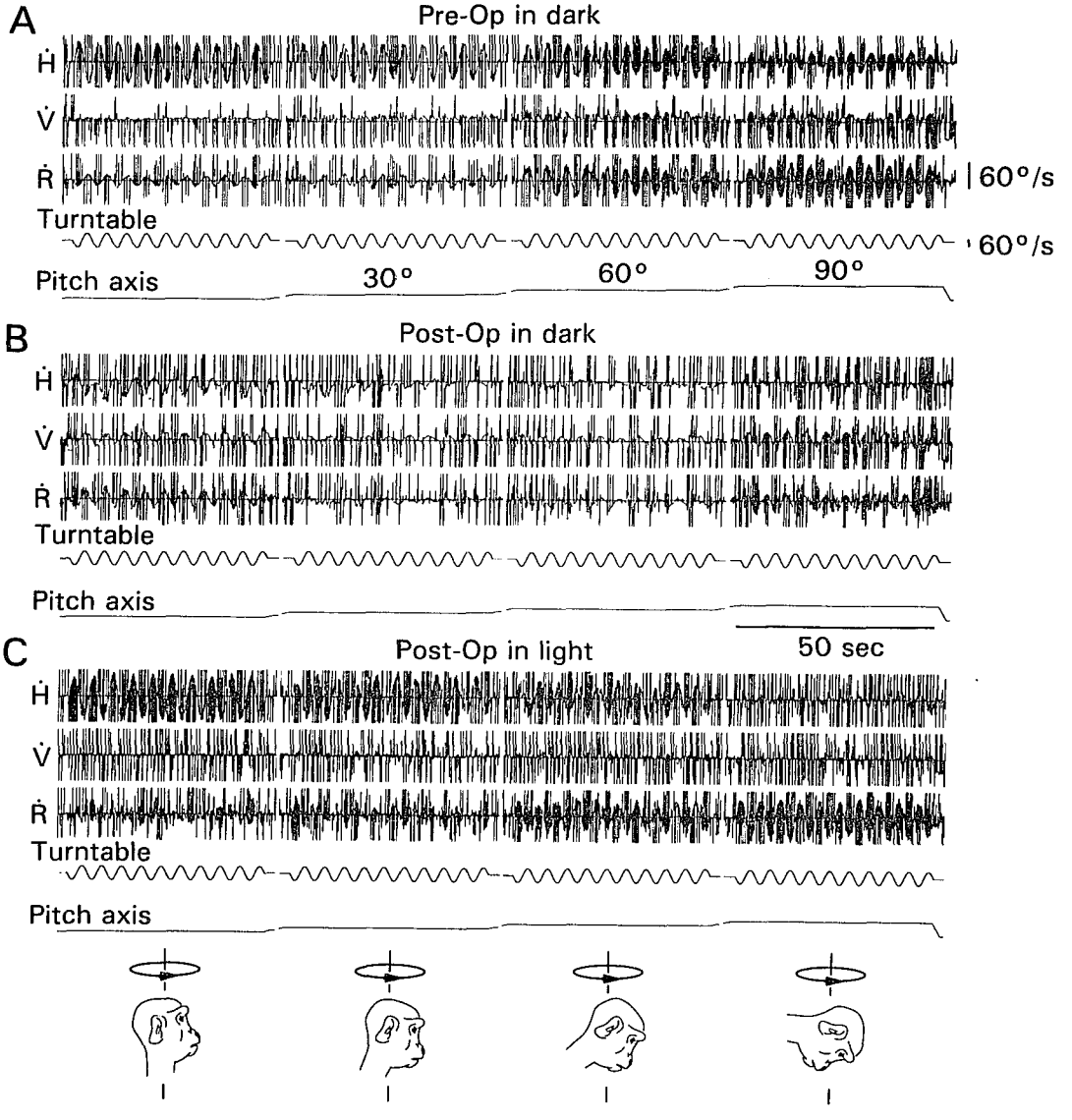
A
Pre-Op in dark
Ḣ
V̇
Ṙ
60°/s
Turntable
60°/s
Pitch axis
30°
60°
90°
B
Post-Op in dark
Ḣ
V̇
Ṙ
Turntable
Pitch axis
50 sec
C
Post-Op in light
Ḣ
V̇
Ṙ
Turntable
Pitch axis

Figure 4.5: Schema similar to that in Fig 4.4 except that the **RALP** animal (**M9223**) was pitched backward (-). Before operation (**A**) and in light after operation (**C**), there was a decrease in the peak horizontal component and an increase in the peak roll component with increases in tilt angle along the pitch axis. When the animal was rotated in darkness after operation (**B**), horizontal and roll eye velocity both reached a maximum at about -60° (tilt backward). Note the appearance of a vertical component in darkness after the lesion.

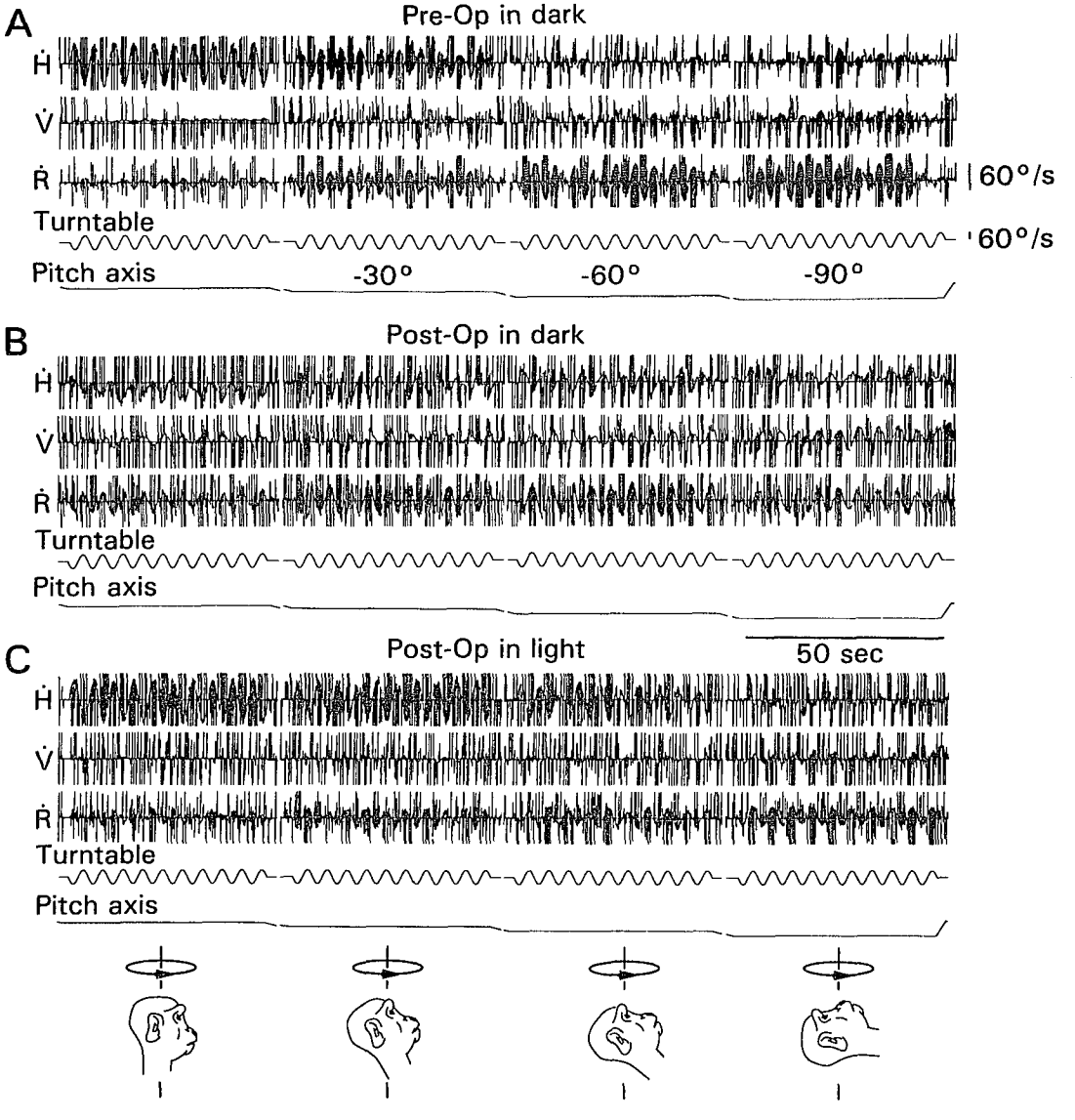
A
Pre-Op in dark
Ḣ
V̇
Ṙ
60°/s
Turntable
60°/s
Pitch axis
-30°
-60°
-90°
B
Post-Op in dark
Ḣ
V̇
Ṙ
Turntable
Pitch axis
C
Post-Op in light
50 sec
Ḣ
V̇
Ṙ
Turntable
Pitch axis

rotation (Fig 4.2A, Fig 4.3A, $\dot{V}$). Therefore, we concentrated on horizontal and torsional velocities in this study. There were vertical components in the **LARP** and **RALP** animals after surgery when they were tested in darkness (Fig 4.2-4.5, B). These will be considered below.

4.1.1 TEMPORAL ASPECTS OF RESPONSE

One purpose of this study was to determine whether summations of the gain as a function of tilt angle of complementary treated monkeys would give the normal response when summated. It, therefore, was important to insure that the temporal responses of animals used for summation were not significantly different from each other.

The mean values for the temporal phase between stimulus velocity and horizontal and torsional eye velocity for normal animals were -5° ± 2° and -7° ± 2°, respectively, over all tilt angles (Table 4.1). After vertical canal plugging (**LC**), the temporal phases were 0° and 3° for horizontal and roll eye velocity, respectively. After lateral canal plugging (**VC**), the phases were 6° for horizontal and 2° for torsional eye velocity. Differences in phase angles were similarly small for the **LARP** and **RALP** animals (8° ± 3° horizontal, 5° ± 4° torsion). Therefore, the differences in phase angles before and after plugging were not significant, and the peak gain values would not be significantly affected by correcting for temporal phases.

Recent work has indicated that vertical eye position can affect the axis of compensation, producing larger roll components of eye velocity when the eyes look up or down (Misslisch et al. 1994). There was on average a shift in vertical eye position as

Table 4.1: Temporal phase and bias for the horizontal (**A**) and torsional components of the aVOR (**B**) before and after surgery for the eight monkeys of this study tested at 0.2 Hz with a peak velocity 60°/s. Each mean represents the average value for all 19 tilt positions $\pm$ 1 SD. Six animals were tested in light as well as in darkness.

Table 4.1

A. Temporal Phase and Bias for Horizontal aVOR.

TYPE OF SURGERY	MONKEY'S ID	BEFORE SURGERY		AFTER SURGERY			
		IN DARKNESS		IN DARKNESS		IN LIGHT	
		PHASE	BIAS	PHASE	BIAS	PHASE	BIAS
LC Animal	M9008	4 ± 2	2 ± 4	0 ± 5	0 ± 2	-	-
VC Animals	M9003	3 ± 5	1 ± 3	3 ± 4	1 ± 4	5 ± 10	1 ± 2
	M9354	7 ± 2	2 ± 1	8 ± 9	2 ± 2	15 ± 8	-1 ± 2
LARP Animals	M9006	4 ± 6	0 ± 2	6 ± 6	-2 ± 4	-	-
	M9306	3 ± 3	1 ± 2	13 ± 28	3 ± 2	11 ± 4	1 ± 2
	M9356	8 ± 2	1 ± 1	3 ± 12	2 ± 3	26 ± 8	-1 ± 3
RALP Animals	M9223	6 ± 4	0 ± 2	6 ± 13	0 ± 2	10 ± 6	0 ± 1
	M9355	5 ± 3	1 ± 3	10 ± 11	13 ± 8	15 ± 16	-5 ± 3

B. Temporal Phase and bias for the Torsional aVOR

TYPE OF SURGERY	MONKEY'S ID	BEFORE SURGERY		AFTER SURGERY			
		IN DARKNESS		IN DARKNESS		IN LIGHT	
		PHASE	BIAS	PHASE	BIAS	PHASE	BIAS
LC Animal	M9008	7 ± 10	0 ± 6	3 ± 6	1 ± 1	-	-
VC Animal	M9003	8 ± 9	-1 ± 3	1 ± 12	-2 ± 6	7 ± 11	1 ± 3
	M9354	6 ± 2	0 ± 1	3 ± 6	1 ± 2	6 ± 3	0 ± 1
LARP Animal	M9006	7 ± 6	1 ± 1	3 ± 8	0 ± 3	-	-
	M9306	2 ± 3	0 ± 1	7 ± 6	-2 ± 2	9 ± 6	0 ± 2
	M9356	9 ± 3	0 ± 3	2 ± 6	1 ± 7	14 ± 9	3 ± 6
RALP Animal	M9223	8 ± 4	0 ± 1	1 ± 4	0 ± 2	9 ± 3	0 ± 2
	M9355	7 ± 2	-1 ± 3	11 ± 15	7 ± 14	20 ± 4	1 ± 9

a function of tilt for oscillations at 0.2 Hz (Fig 4.6). When the animals were tilted forward, the eyes were on average up and when tilted back, the eyes were on average down. Consistent with Haslwanter et al. (1992), the magnitude of average vertical eye deviation as a function of tilt tended to saturate at $\approx 6°$ shift at about $\pm 50°$ of tilt (Fig 4.6, shaded area). Variance was large, however, and the difference between the upright and tilted positions was significant only for backward tilts ($p < 0.05$). For these angular deviations, the expected tilt in the axis of rotation would be less than 1-3° (Misslisch et al. 1994). The amount of error this would introduce in computing the roll gain is negligible.

4.1.2 CONTRIBUTION OF THE LATERAL CANALS (LC ANIMALS, ANTERIOR/POSTERIOR CANALS PLUGGED)

When the anterior and posterior canals are plugged (LC), all compensatory eye movements due to the aVOR originate in the lateral canals. As a result the horizontal and roll velocities produced by the lateral canals should be in phase at each tilt angle and direction-fixed with regard to the head. Gains were plotted as a function of tilt angle to determine spatial phases (Fig 4.7A, D). The standard deviations of the gains were small. Data were approximated with sine curves (Fig 4.7A, D, solid line; Table 4.3A, **M9008**). Therefore, these curves could be used to measure the gain and phase of the response. The maximum gain of the horizontal component was 0.71 after plugging, and it occurred at 30° pitch forward (up arrow, Fig 4.7A; Table 4.3A; Table 4.2, $\pm 9°$ phase error). Similarly, the peak gain of the roll component due to lateral canal activation was 0.37, and it occurred at 39° pitch forward (up arrow, Fig 4.7D; Table 4.3 ;Table 4.2, $\pm 11°$

Figure 4.6: Average vertical eye position at different pitch angles for eight normal animals. Eye position was calculated from 10 cycles of rotation in darkness at 0.2 Hz. The positive value on the ordinate represent upward eye deviation. The abscissa represents pitch angles in forward (positive values) and backward (negative values) directions. It was assumed that the average vertical eye position was zero when the animal was upright. The vertical bars in this and subsequent graphs represent $\pm$ 1 SD. The shaded area encompasses the range of vertical eye deviation for forward and backward tilts.

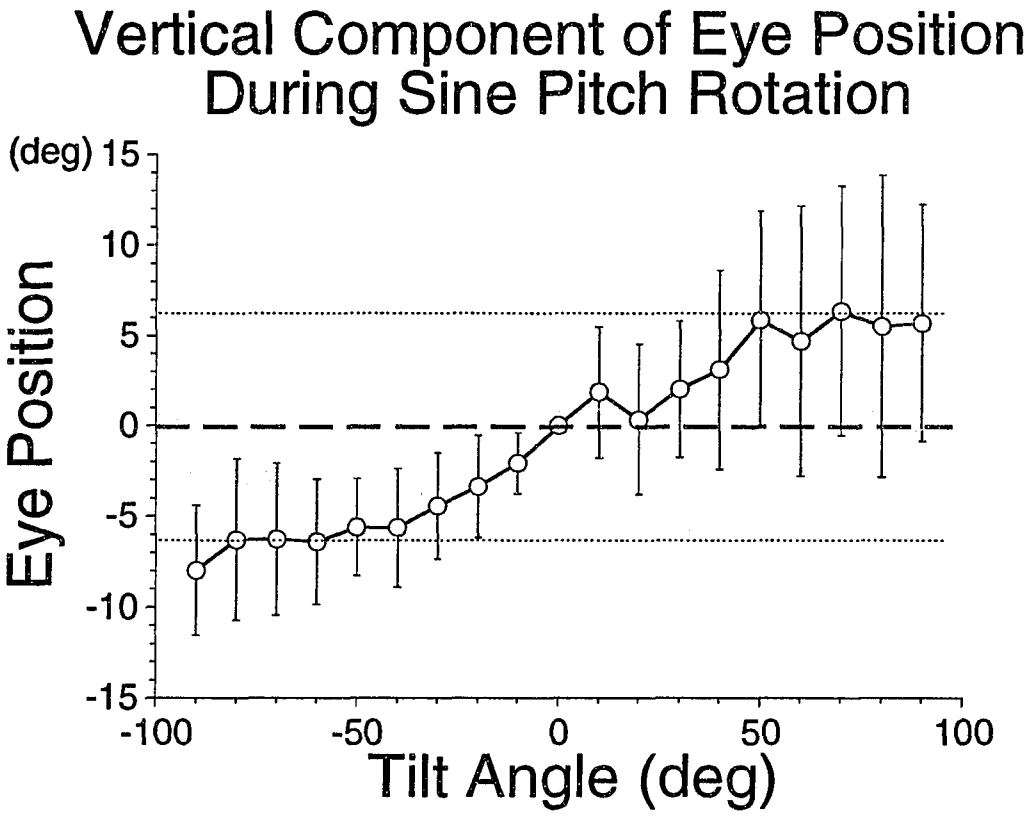
Vertical Component of Eye Position
During Sine Pitch Rotation
(deg) 15
10
5
0
-5
-10
-15
Eye Position
-100
-50
0
50
100
Tilt Angle (deg)

Figure 4.7: Gain vs tilt angle of yaw (**A** - **C**) and roll (**D** - **F**) eye velocity over tilt angles of -90° to +90° in 10° intervals. Yaw and roll gains after plugging the vertical canals (**A**, **D**, **LC** animal(**M9003**)) and two animals with the lateral canals plugged (**VC** animal) **M9008** (**B**, **E**) and **M9354** (**C**, **F**). Monkey heads at the bottom of the graphs **D** and **F** show head position at these pitch angles. Each symbol represents the mean of gain values obtained at that tilt angle. Standard deviations (± 1 SD) about each value are denoted by the vertical bars. In this and subsequent graphs, the two dotted lines show the region over which the approximation curve can be shifted and still significantly fit the data. Arrows point to the tilt position with maximal gain response.

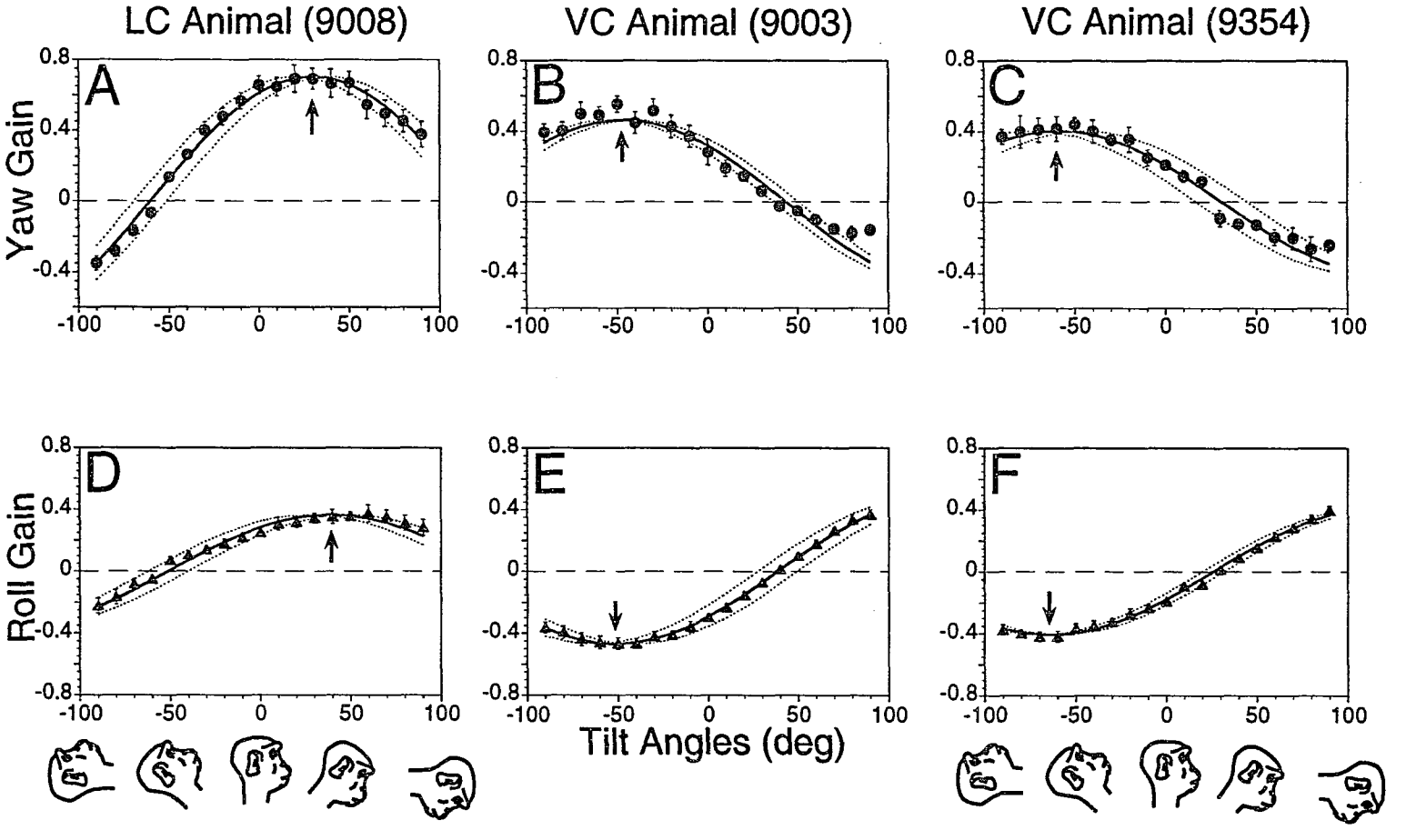
LC Animal (9008)
VC Animal (9003)
VC Animal (9354)
A
B
C
D
E
F
Yaw Gain
Roll Gain
Tilt Angles (deg)
0.8
0.4
0
-0.4
-0.8
-100
-50
0
50
100

Table 4.2: Significance of the sinusoidal fits for the horizontal and roll aVOR gains of eight monkeys before and after canal plugging. The **F** statistic represents a value estimated from the data, **df** represents degrees of freedom, F_{cr} is the critical value for these data (p=0.05), and P_{err} is the phase error. Underlined values corresponding to P_{err} =0, exceed critical value and are significantly different. See text for explanation.

Table 4.2

M9006 (LARP)		F	df	Fcr	Perr
Hor	Before	3.74	1,169	3.90	1
	After	1.42	1,303	3.87	25
Roll	Before	2.15	1,169	3.90	7
	After	1.31	1,303	3.87	10

M9008 (LC)		F	df	Fcr	Perr
Hor	Before	6.18	1, 69	3.90	0
	After	1.62	1,379	3.87	9
Roll	Before	2.37	1,113	3.91	5
	After	1.76	1,379	3.87	11

M9306 (LARP)		F	df	Fcr	Perr
Hor	Before	4.97	1,189	3.84	0
	After	1.13	1,169	3.84	15
Roll	Before	1.36	1,189	3.84	8
	After	1.44	1,189	3.84	11

M9003 (VC)		F	df	Fcr	Perr
Hor	Before	13.58	1, 69	3.90	0
	After	2.91	1,303	3.87	7
Roll	Before	2.37	1,113	3.91	5
	After	1.76	1,379	3.87	11

M9356 (LARP)		F	df	Fcr	Perr
Hor	Before	1.47	1,170	3.84	8
	After	1.82	1,189	3.84	9
Roll	Before	1.73	1,170	3.84	12
	After	1.18	1,189	3.84	9

M9354 (VC)		F	df	Fcr	Perr
Hor	Before	3.06	1,189	3.84	4
	After	1.77	1,189	3.84	14
Roll	Before	1.41	1,189	3.84	8
	After	1.60	1,189	3.84	6

M9223 (RALP)		F	df	Fcr	Perr
Hor	Before	1.85	1,189	3.84	7
	After	3.48	1,169	3.84	5
Roll	Before	3.55	1,189	3.84	4
	After	1.43	1,169	3.84	17

M9355 (RALP)		F	df	Fcr	Perr
Hor	Before	2.80	1,189	3.84	3
	After	2.70	1,189	3.84	12
Roll	Before	1.49	1,189	3.84	16
	After	1.31	1,189	3.84	11

Table 4.3 A, Maximal yaw and roll spatial gains and angles of tilt at which the peak gains and zero crossings occurred in the eight animals before and after surgery. Testing was done in darkness at 0.2 Hz with 60°/s. peak velocity. **B,** Same values as in **A** derived from predictions based on the geometric model of the canals and their projections to the oculomotor system. Using only the gains and phases of the normal monkeys, the model predicted the results after canal plugging.

Table 4.3

A EXPERIMENTAL DATA

Intact canals	YAW BEFORE Gain	YAW BEFORE Spatial Phase Zero Crossing Deg	YAW BEFORE Spatial Phase Max Deg	YAW AFTER Gain	YAW AFTER Spatial Phase Zero Crossing Deg	YAW AFTER Spatial Phase Max Deg	ROLL BEFORE Gain	ROLL BEFORE Spatial Phase Zero Crossing Deg	ROLL BEFORE Spatial Phase Max Deg	ROLL AFTER Gain	ROLL AFTER Spatial Phase Zero Crossing Deg	ROLL AFTER Spatial Phase Max Deg	Monkey ID
Lateral Canals (LC Animal)	.88	89	-1	.71	-60	30	.53	2	-88	.37	-51	39	M9008
Vertical Canals (VC Animals)	.83	-80	10	.46	44	-46	.53	-12	78	.47	38	-52	M9003
	.94	-76	14	.40	31	-59	.42	9	-81	.39	26	-64	M9354
LARP Canals (LARP Animals)	.71	-87	3	.20	35	-55	.64	3	-87	.26	23	-67	M9006
	.94	-81	9	.23	33	-57	.56	2	-88	.23	24	-66	M9306
	.89	-73	17	.28	30	-60	.58	-5	85	.32	26	-64	M9356
RALP Canals (RALP Animals)	.81	-71	19	.36	46	-44	.48	4	-86	.29	38	-52	M9223
	.97	-74	16	.29	32	-58	.41	-1	89	.31	28	-62	M9355

B MODEL PREDICTION

Intact canals	YAW BEFORE Gain	YAW BEFORE Spatial Phase Zero Crossing Deg	YAW BEFORE Spatial Phase Max Deg	YAW AFTER Gain	YAW AFTER Spatial Phase Zero Crossing Deg	YAW AFTER Spatial Phase Max Deg	ROLL BEFORE Gain	ROLL BEFORE Spatial Phase Zero Crossing Deg	ROLL BEFORE Spatial Phase Max Deg	ROLL AFTER Gain	ROLL AFTER Spatial Phase Zero Crossing Deg	ROLL AFTER Spatial Phase Max Deg	
LC Animal	.87	± 90	0	.68	-60	30	.52	0	± 90	.34	-60	30	
VC Animal				.44	40	-50				.46	40	-50	
LARP/RALP				.22	40	-50				.23	40	-50	

phase error). Considering the variation, there was no significant difference between these sinusoidal data fits. Therefore, both sets of data could be approximated with a single curve that could have phase shifts between 28° and 39° ($p=0.05$). This is consistent with the postulate that only the lateral canals were active in this animal.

4.1.3 CONTRIBUTIONS OF THE ANTERIOR AND POSTERIOR CANALS (VC ANIMALS, LATERAL CANALS PLUGGED)

With the lateral canals plugged, only the vertical canals can generate the aVOR. Since the vertical canals are tilted back relative to the stereotaxic coordinate frame (Blanks et al. 1975, 1985; Reisine et al. 1988), they should produce both horizontal and roll components during sinusoidal rotation in the upright condition. As with the lateral canal animal, the horizontal and roll velocities should be in phase, direction-fixed with regard to the head, and their gains should also reflect the projection of the vertical canals into head coordinates.

The peak gain of the horizontal velocity was 0.46 after lateral canal plugging in **M9003** (Fig 4.7B, up arrow). This was achieved for -46° tilt back (Table 4.3 A; Table 4.2, ±7° phase error). The peak gain of the roll component was 0.47 at -52° tilt back (Fig 4.7E, down arrow; Table 4.3; Table 4.2, ±7° phase error). Discounting the phase difference of 180° and phase error of ± 7°, the difference between the horizontal and torsional curves was not significant for fits with phases between -45° and -53°. Differences between the horizontal and torsional phases in a second **VC** animal (**M9354**) were similar (Fig 4.7C, F; Table 4.3).

Horizontal and torsional components obtained from two **VC** animals were

averaged. The averaged horizontal spatial gain was 0.43, the peak occurring at -52° (Fig 4.8A). The torsional gain was 0.44 with peak at -58° tilt (Fig 4.8C).

These findings confirm those of Baker et al. (1982) and Böhmer et al. (1985) which show that a horizontal component of eye velocity is produced by the vertical canals after lateral canal plugging. The data demonstrate that the lateral and vertical canals each contribute both horizontal and roll components to the aVOR, and except for the fact that there is a 180° phase difference between the horizontal and roll components, their spatial gain characteristics are not significantly different ($p < 0.05$).

4.1.4 RALP AND LARP ANIMALS

The characteristics of the compensatory eye movements in the three **LARP** and two **RALP** animals were similar to each other (Fig 4.9). The horizontal aVOR gain after the surgery ranged from 0.20 to 0.36; spatial phase ranged from -44° to -60° (Table 4.3). When the three **LARP** animal responses were averaged, the horizontal gain was 0.24 occurring at -57° tilt ($F_{1,190}=2.87$; Phase Error ±7°) (Fig 4.10A). The averaged torsional gain was 0.27 occurring at -65° ($F_{1,190}=1.86$; Phase Error ±5°) (Fig 4.10D). Similarly, when the two **RALP** animal responses were averaged, the horizontal gain was 0.32 occurring at -51° tilt ($F_{1,190}=3.64$; Phase Error ±3°) (Fig 4.10B). The averaged torsional gain was 0.30 occurring at -57° ($F_{1,190}=1.38$; Phase Error ±10°) (Fig 4.10E). While there were individual differences between the **LARP** and **RALP** animals, there was no significant differences in horizontal and torsional gains and phases between the two groups on average. Both the **LARP** and **RALP** animals have only one pair of vertical canals remaining. We assumed that they produce equivalent eye velocity

Figure 4.8: Average horizontal (**A**) and torsional (**C**) gains of the **VC** animals and summated average gains of three **LARP** and two **RALP** animals (**B**, **D**, respectively) as a function of tilt angle. Solid line represent model prediction. The spatial gains were slightly higher in the summed data. Arrows point to the tilt position with maximal gain response (**heavy arrows**) or to the tilt position with maximal model predicted gains (**thin arrows**). The spatial phases were similar in all cases. The phase error in **B** could not be determined since F exceeded the critical value. Monkey heads at the bottom of the graph **D** show head position at these tilt angles.

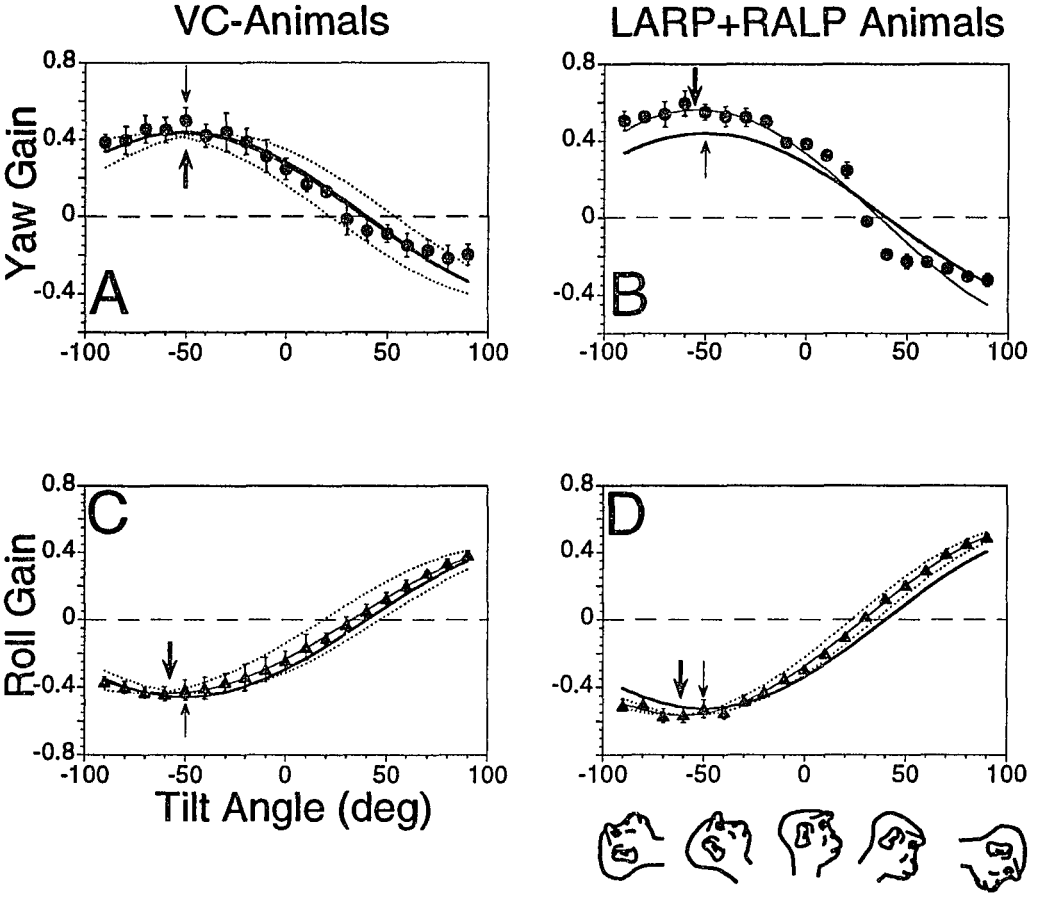
VC-Animals
LARP+RALP Animals
Yaw Gain
Roll Gain
Tilt Angle (deg)
A
B
C
D
0.8
0.4
0
-0.4
-0.8
-100
-50
0
50
100

Figure 4.9: Average gains of yaw (**A, B, C, D, E**) and roll (**F, G, H, I, J**) eye velocity over tilt angles of -90° to +90° in 10° intervals after plugging the lateral and right anterior-left posterior canals (**LARP** animal)(**M9006**, **A**, **F**; **M9306**, **B**, **G**; **M9356**, **C**, **H**) and after plugging the lateral and left anterior-right posterior canals (**RALP** animal)(**M9223**, **D**, **I**; **M9355**, **E**, **J**). Each symbol represents the mean of gain values obtained at that tilt angle. Standard deviations ($\pm$1 SD) about each value are denoted by the vertical bars. The two dotted lines show the region over which the approximation curve can be shifted and still significantly fit the data.

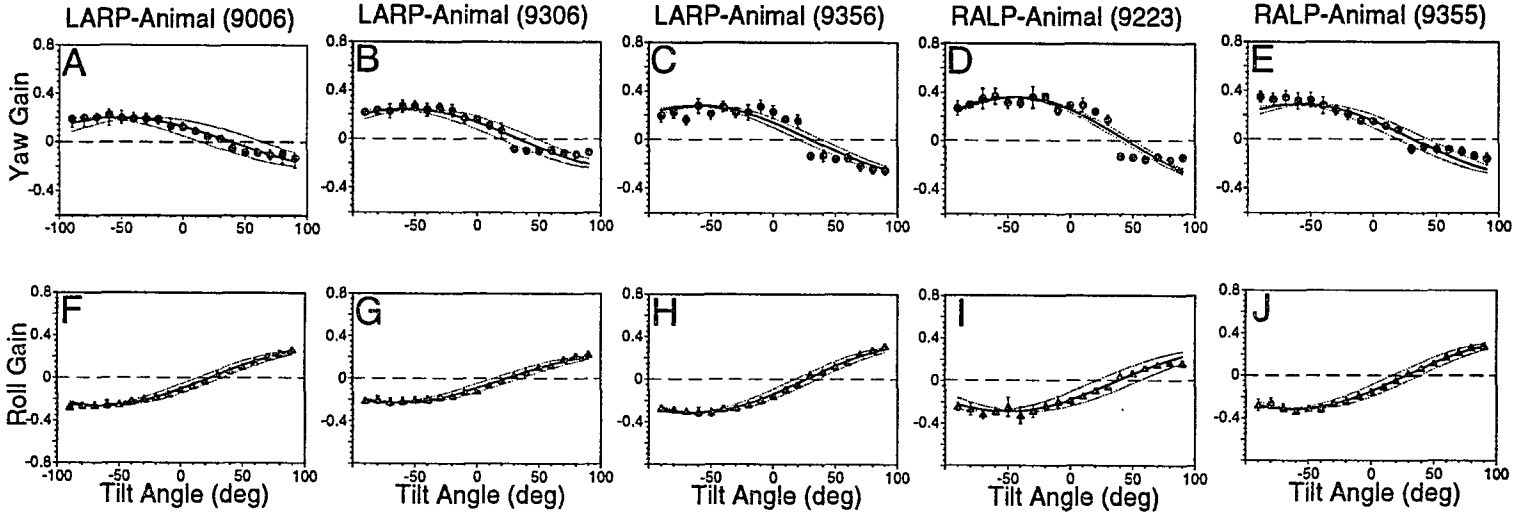
LARP-Animal (9006)
LARP-Animal (9306)
LARP-Animal (9356)
RALP-Animal (9223)
RALP-Animal (9355)
A
B
C
D
E
F
G
H
I
J
Yaw Gain
Roll Gain
Tilt Angle (deg)
Tilt Angle (deg)
Tilt Angle (deg)
Tilt Angle (deg)
Tilt Angle (deg)

Figure 4.10: Average horizontal and torsional gains for all **LARP** animals (**A**, **D**) and all **RALP** animals (**B**, **E**) in comparison to average gain for all five **LARP** and **RALP** animals (**C**, **F**). The spatial phases of the horizontal (**A**, **B**, **C**) and roll (**D**, **E**, **F**) responses were similar to the **VC** animal responses (Fig 4.8). Average gain for graphs **C** and **F** were compared to the model prediction (**heavy line**). The spatial gains were not significantly different from the model predicted values. Arrows point to the tilt position with maximal gain response (**heavy arrows**) or to the tilt position with maximal model predicted gains (**thin arrows**).

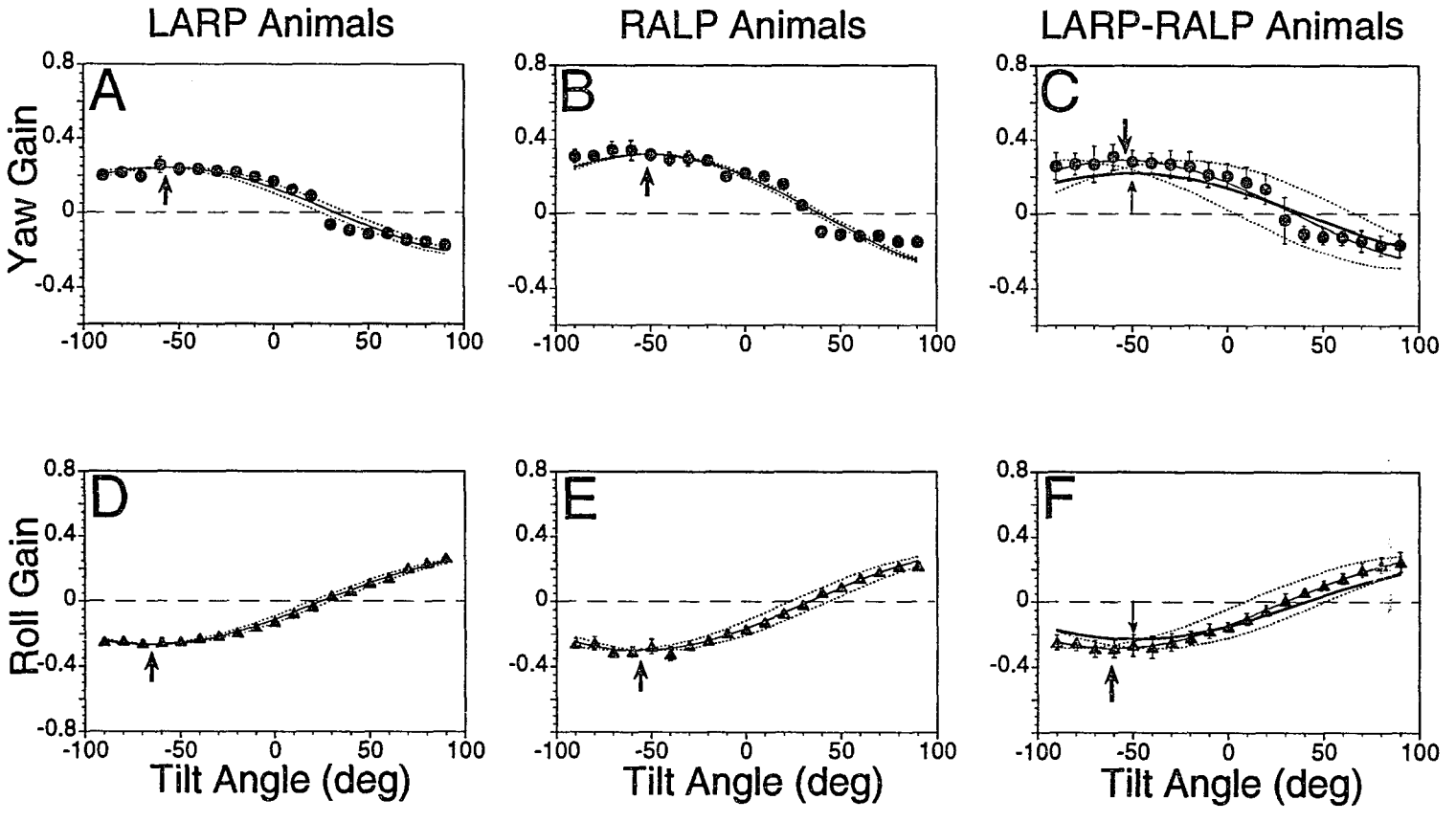
LARP Animals
RALP Animals
LARP-RALP Animals
A
B
C
D
E
F
Yaw Gain
Roll Gain
0.8
0.4
0
-0.4
-0.8
-100
-50
0
50
100
Tilt Angle (deg)

responses and that the differences were due to physiological variance. We, therefore, averaged data obtained from all five monkeys (Fig 4.10C, F). The average peak horizontal gain was 0.27, occurring at -55° ± 6° tilt backward with a null point at 35° ± 6° tilt forward (Fig 4.10C). On average roll gain was 0.28, at -62° ± 5° tilt with a null point at 28° ± 5° tilt forward. As for the VC animals, if the 180° phase difference between horizontal and roll was discounted, the spatial gain curves of the horizontal and roll components were not significantly different (compare -55° ± 6° and -62° ± 5°).

4.1.5 SPATIAL CHARACTERISTICS OF THE HORIZONTAL AND TORSIONAL aVOR OF NORMAL ANIMALS:

The averaged gains of the horizontal and torsional components for the eight normal monkeys are shown in Fig 4.11A, C. The peak gain of the horizontal component of the aVOR was 0.87 ± 0.08, occurring at 11° tilt forward (up arrow, Fig 4.11A; phase error ±14°). The peak torsional gain was 0.52 ± 0.07. The zero crossing occurred at 0° tilt (down arrow, Fig 4.11C; phase error ±21°).

We also compared the spatial gain characteristics when computing eye velocity in head coordinates and using derivatives of coil voltages for each type of plugging condition (Appendix A) (Fig 4.12). Comparisons for normal monkeys (Fig 4.12A,E), LC monkey (Fig 4.12B,F) and VC animals (Fig 4.12C,G) had no significant differences ($p=0.05$). There was only a small difference for the horizontal spatial gain characteristic for the RALP animal, but not for the torsional component.

4.1.6 SIX CANALS PLUGGED ANIMAL (NC ANIMAL):

As a control, we tested one animal with all of its semicircular canals plugged.

Figure 4.11: Averaged gains of the yaw (**A**) and roll (**C**) components from eight normal monkeys and corresponding yaw (**B**) and roll (**D**) gains summated from two canal-plugged monkeys (**M9008+M9003**). One had its lateral canals plugged (**VC** animal), another had anterior and posterior canal plugging (**LC** animal). These two animals were chosen for summation, because they were operated and tested over the same time period. The solid lines represent the best sinusoidal fit to the horizontal and torsional gains. The dotted lines represent the range over which the fit for horizontal and roll gains could be phase shifted and still significantly fit the data ($p=0.05$). The range of fits for both normal and summated responses overlap, and they are not significantly different from each other. Arrows point to the tilt position with maximal (for horizontal) and minimal (for roll) gain responses. Monkey heads at the bottom of the graph **D** show head position at these tilt angles.

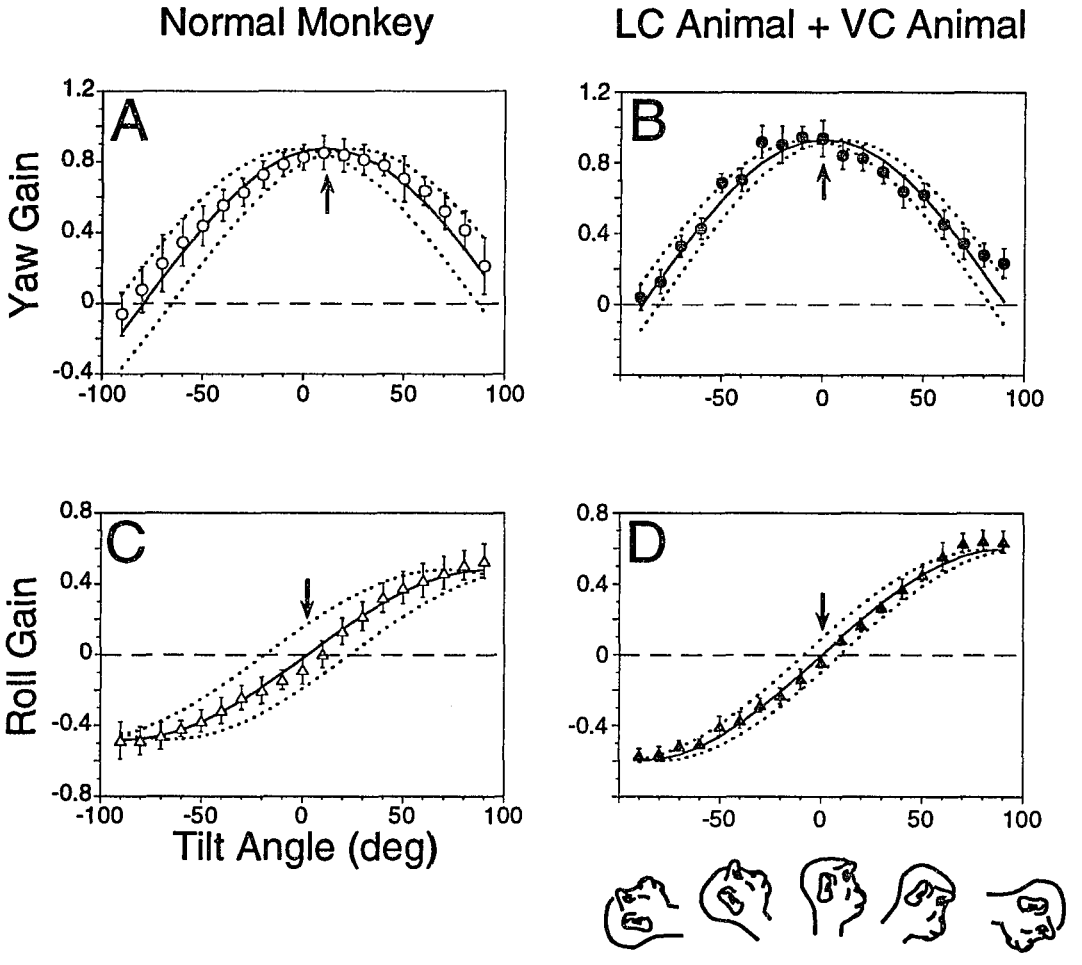
Normal Monkey
LC Animal + VC Animal
A
B
C
D
Yaw Gain
Roll Gain
Tilt Angle (deg)
1.2
0.8
0.4
0
-0.4
-0.8
-100
-50
0
50
100

Figure 4.12: Comparison of spatial gains derived from measurements of derivatives of coil voltages (circles) with derived Euler angle velocities (triangles). The solid lines are best fitting curves for the derivatives of the coil voltages, and the dashed lines, the best fitting curves for the Euler angle velocities. The curves overlap, and small differences between them were not significant ($p=0.05$). Monkey faces on a bottom of the graphs **E** and **H** show head position at this pitch angles.

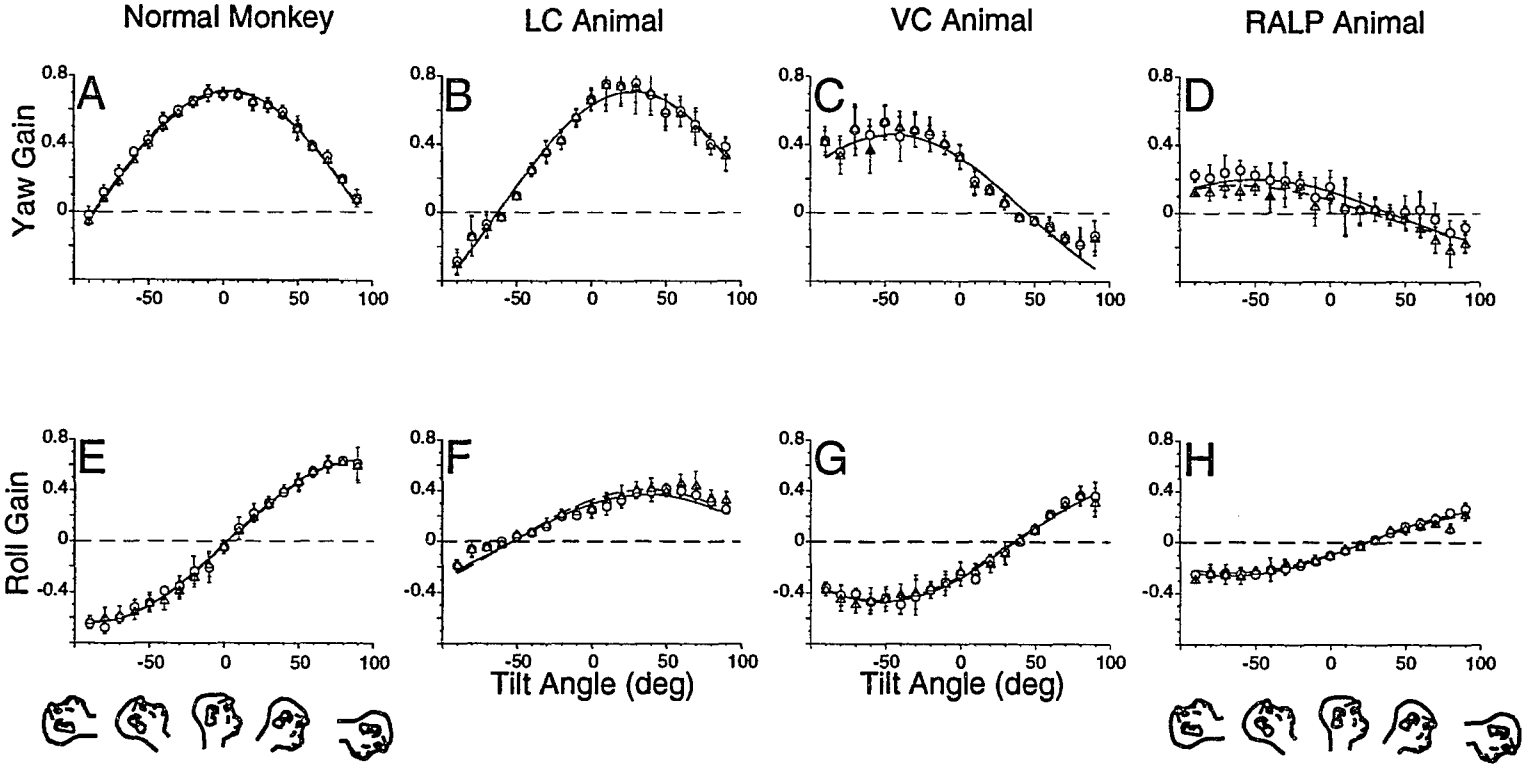
Normal Monkey
LC Animal
VC Animal
RALP Animal
A
B
C
D
E
F
G
H
Yaw Gain
Roll Gain
0.8
0.4
0
-0.4
-50
0
50
100
Tilt Angle (deg)

Before surgery, the spatial horizontal gain was 0.89 occurring at 22° tilt forward (Fig 4.13). The maximum of the spatial roll gain was 0.59 occurring at -83°. After all canals were plugged, the aVOR gain was reduced to zero for both the horizontal and torsional components (Fig 4.13A, E). The spatial gain curve was not significantly different from zero gain over all tilt angles considered ($F_{1,190}$=2.76 and $F_{1,190}$=2.35, for horizontal and torsional respectively). This indicates that at 0.2 Hz, the semicircular canals are necessary for eliciting the aVOR and the otoliths do not significantly contribute to the aVOR at that frequency. This, together with the data on individual canal-induced spatial characteristics, indicates that each canal contributes to the aVOR according to its geometric orientation in the head.

4.1.7 ROTATION IN LIGHT FOLLOWING PI

The previous data show that when animals ed in darkness after canal plugging, the roll and horizontal movements were approximately in spatial phase so that there were significant roll eye movements associated with horizontal eye movements (Fig 4.7- Fig 4.9). This was different from the normal animals where the roll and horizontal eye movements were 90° out of phase (Fig 4.11A, C). Therefore, the horizontal and roll components of the aVOR recorded in darkness after surgery were anticompensatory in that they would not have improved stabilization of gaze on the surround during head movement (Fig 4.11B).

We determined whether vision would alter the spatial relationship between horizontal and roll components to improve retinal stability during rotation. In six animals with various canal plugging available for testing in this paradigm, vision caused the

Figure 4.13: Spatial responses of the monkey with all six canals plugged (**NC** Animal; **M9308**) tested at 0.2 Hz, 60°/s. of sinusoidal rotation. Average gains of the yaw (**A**) and roll (**B**) components from the **NC** Animal (filled symbols) compared to the spatial curves based on data obtained from the same animal before surgery during sinusoidal rotation at 0.2 Hz, 60°/s. (open symbols). The solid lines represent the best sinusoidal fit to the horizontal and torsional gain obtained before surgery. Arrows point to the tilt position with maximal gain responses. Standard deviations ($\pm$ 1SD) about each value are denoted by the vertical bars.

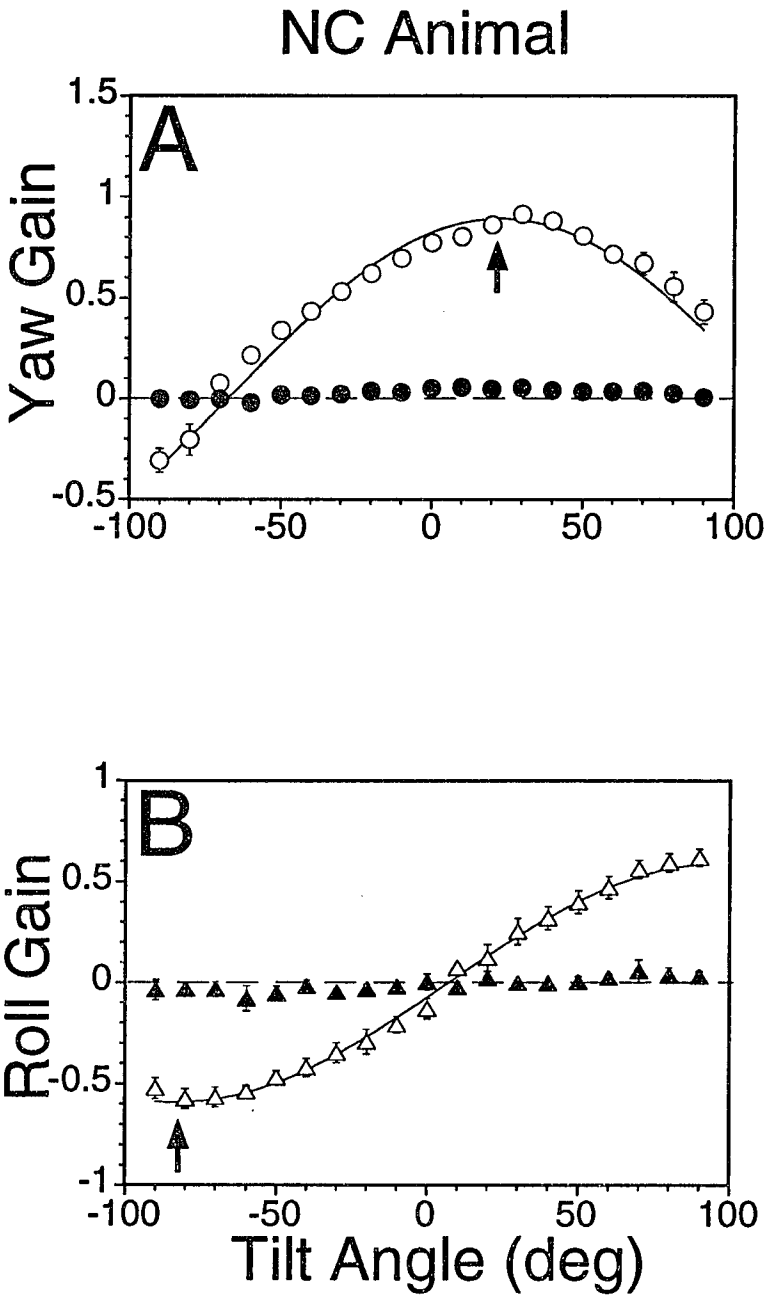
NC Animal
A
Yaw Gain
1.5
1
0.5
0
-0.5
-100
-50
0
50
100
B
Roll Gain
1
0.5
0
-0.5
-1
-100
-50
0
50
100
Tilt Angle (deg)

spatial phases to return to those recorded in the normal animals in darkness (Fig 4.14A, B; horizontal: spatial phase ±14°, roll: spatial phase ±21°). The peak spatial gain for canal plugged animals in light at 10° forward was 0.93 for horizontal and 0.60 for roll at +90° tilt forward.[2] This can be compared to gains and phases of 0.87 at 11° and 0.48 at ±90° for the normal animals, respectively. This demonstrates that the visual system can compensate for the plugging of individual semicircular canals. It also indicates that the horizontal and torsional components of the aVOR had not been cross adapted in any of the canal plugged animals when tested in darkness, although the ocular compensatory movements were correctly phased in light in all of them.

4.2 COMPARISONS OF THE DATA OBTAINED FROM THE MONKEY WITH DIFFERENT CANALS PLUGGED:

The aVOR can be spatially adapted by interacting vestibular and optokinetic inputs (Schultheis and Robinson 1981). This has been termed, "cross-axis adaptation" (Baker et al. 1986; Baker et al. 1987). It is possible that the responses of the canals after plugging represented spatial adaptation of the aVOR. If so, there should be a significant difference between the spatial gain characteristic of the intact animal and that of a sum

---

[2] Data in Fig 4.14, derived from rotation of the canal plugged monkeys in light, were not fitted. When the animals were tilted more than -60° back, they faced a frame on the ceiling of the drum that attached the primate chair to the primate axis. This provided a stationary field that covered the optokinetic stimulus and caused suppression of the VOR. It accounts for the sharp drop in the gain of the horizontal VOR for tilts between -70° and -90°. Therefore, the data could not be approximated with a single best fit line, and only the mean values at the other tilt angles are shown (open symbols ± 1 SD). The solid and dotted lines in this figure show the fitted cosine curve and the phase error calculations for the eight normal monkeys for comparison.

Figure 4.14: Average yaw (**A**) and roll (**B**) aVOR gains of 6 canal-plugged animals as a function of head tilt when tested in light (open symbols ± 1 SD). Also shown is the best fit curve for the 8 normal monkeys tested in darkness (solid line) and the phase error for the normal data (dotted lines). The mean values and phase error of the data obtained from the canal-plugged monkeys recorded in light were close to the mean and phase error of the data obtained from the normal monkeys recorded in darkness.

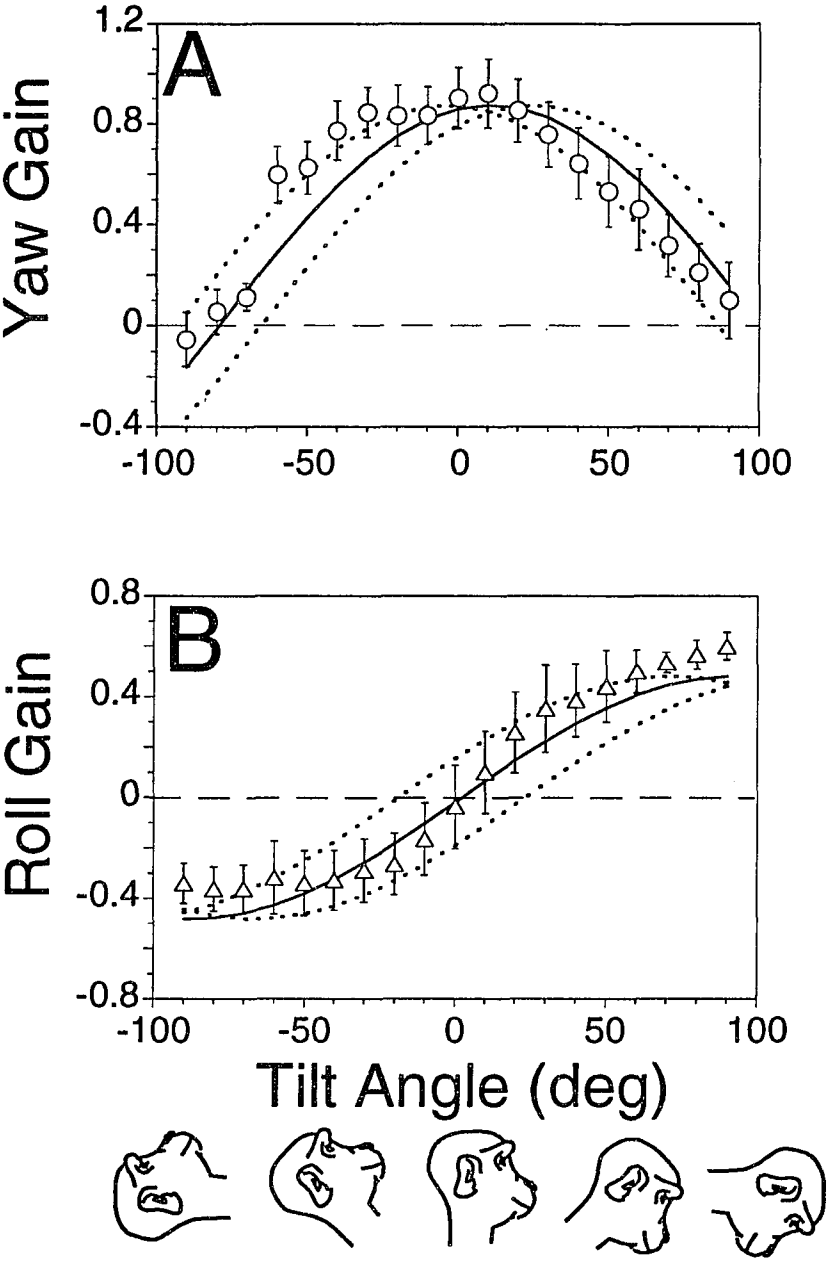
A
Yaw Gain
1.2
0.8
0.4
0
-0.4
-100
-50
0
50
100
B
Roll Gain
0.8
0.4
0
-0.4
-0.8
-100
-50
0
50
100
Tilt Angle (deg)

of the spatial gain curves from animals with their lateral and vertical canals plugged. Similarly, there would be differences between the spatial gain characteristic of **VC** animals and the summed spatial gain characteristic of **LARP** and **RALP** animals. If not, the spatial gain characteristics of the summed responses in both cases should be approximately equal to the corresponding gain characteristic of the animals with the appropriate intact canals. This would demonstrate that the spatial gain is determined solely according to the vector projection of head velocity onto the normals of the individual canals and that there was essentially no spatial adaptation.

4.2.1 COMPARISON OF THE RESPONSES OBTAINED FROM VC ANIMALS TO THE SUMMATED RESPONSES OBTAINED FROM THE LARP AND RALP ANIMALS:

Data from three **LARP** (Fig 4.10A, D) and two **RALP** (Fig 4.10B, E) animals were summated (Fig 4.8B, D) and compared to the those from the **VC** animals (Fig 4.8A, C). The summated horizontal gains for the two types of monkeys had a maximum at 0.56 for -54° tilt (Fig 4.8B). However, the summated data could not be well fit with a sinusoid at $p<0.05$ ($F_{1,190}=4.34$). This was not the case when the **LARP** and **RALP** animals were analyzed individually or treated as one group. This is probably due to an accumulated error when measuring small amplitudes of gain (Figs 4.8 - 4.10), and could probably be reduced by computing eye velocity in head coordinates using the Euler angle method (Appendix A, Fig 4.12D). The summated torsional gains were 0.57 at -61° (±6° phase error; Fig 4.8D; $F_{1,190}=1.33$). The gains were slightly higher than the gains in the two **VC** animals but the phases were comparable. This indicates that although there was

some increase in temporal gain after surgery in the **LARP** and **RALP** animals, there was little or no change in the spatial gains and phases after the plugging of individual semicircular canals despite the long period of recovery after surgery. From this, we conclude that to a large extent the **VC** animal response comprises the responses due to the **LARP** and **RALP** canal planes.

4.2.2 COMPARISON OF THE RESPONSES OBTAINED FROM NORMAL ANIMALS TO THE SUMMATED RESPONSES OBTAINED FROM THE LC AND VC ANIMALS:

Data from **LC** and **VC** animals were summated to form the curves shown in Fig 4.11B, D. The spatial phasor representing the gain and angle of one of the vertical canal plugged animals (0.71 at 30°; Table 4.3, **M9008**) was added to the horizontal canal plugged animals (0.46 at -46°, Table 4.3, **M9003**). To do this, ten gain values measured at each tilt condition for monkey **M9008** were summated in order tith ten gain values for monkey **M9003**. New average gains and standard deviation were calculated and fitted with a sine curve. The summed gain was 0.93 at 1° tilt forward (phase error ±8°; $F_{1,303}=2.06$). The summed spatial roll gain was 0.60 with a zero crossing at -1° tilt backward (phase error ±9°; $F_{1,303}=1.63$). Differences between the curves from the normal and summed canal-plugged data were not significant ($p<0.05$). Thus, the average summated gains and phases of both horizontal and roll components of the canal plugged animals matched the corresponding gains and phases of the normal monkeys.

From these comparisons, we conclude that disregarding small changes in gain, the normal or plugged canal responses can be approximated by summating the response

from animals with different canal plugging.

4.3 MODEL-DATA COMPARISONS:

The data were compared to a model which projects the head velocity into a coordinate frame defined by the normals to the average canal planes, and projects the eye velocity command into the head coordinate frame to drive the oculomotor system (See Section 2.6.2).

The spatial properties of the eye velocity characteristics were simulated with this model using θ_l = -30° and θ_v = -40°. A program was written in BASIC 7.1 (Appendix B) to simulate these equations. The parameters, g_{00} and g_{01}, were arbitrarily chosen as 0.83 corresponding to the gain of the anterior and posterior contribution to the vertical aVOR which has a gain of about 0.85 (Crawford and Vilis 1991; Henn et al. 1992), although no data on vertical eye velocity was obtained.

Each lateral canal and a *fortiori* the average plane of the lateral canals on both sides are close to 90° with respect to the midsagittal plane in the monkey (Blanks et al. 1985). Therefore, they do not significantly contribute to generating a vertical velocity (Suzuki et al. 1964), and g_{02} which represents the gain of the lateral canal contribution to the vertical aVOR, was set to zero. Because g_{10}, g_{11}, and g_{12} represent the anterior, posterior and lateral canal gain contributions to roll, they can be chosen as 0.52, corresponding to the average gain value of the torsional aVOR when it was recorded in darkness (Crawford and Vilis 1991; Henn et al. 1992; Dai et al. 1994; Yue et al. 1994). The gain parameters g_{20}, g_{21}, and g_{22} represent the anterior, posterior and lateral canal gain contributions to the horizontal aVOR. They were chosen as 0.87 corresponding to

the yaw axis gain in our data.

For animals with normal labyrinths, the model predicted that the aVOR gain of yaw and roll would vary sinusoidally as a function of tilt angle (Fig 4.15A, E), although the yaw and roll components were shifted 90° relative to each other. The peak of the yaw gain occurred at 0° and corresponded to the zero crossing of the roll gain. The normal monkeys had peak yaw and roll gains at 11° ± 14° and 90° ± 21°, respectively (Fig 4.11A, C). Differences between the model predictions and the data were not significant. Thus, despite the fact that the canals are non-orthogonal and are tipped up 30°, the reflex still has a peak at 0°. This corresponds to our data which peaked on average at 11° tilt forward.

When the model parameters were set for a vertical canal plugged condition leaving the lateral canals intact (**LC**; Fig 4.15B, F), the model predicted a gain of 0.68 and 0.34 for yaw and roll aVOR respectively. This occurred for both components at 30° tilt forward (Table 4.3 B). Corresponding gains in the **LC** animal (**M9008**) were 0.71 (yaw) and 0.37 (roll), occurring at 30° and 39°, respectively (Table 4.3 A). When the model parameters were set for a lateral canal plugged condition, leaving the vertical canals intact (**VC**; Fig 4.15C, G), the model predicted 0.44 and 0.46 peak yaw and roll gains, respectively, occurring at -50° tilt back (Table 4.3 B). Corresponding average gains for the two **VC** animals were 0.43 for horizontal and 0.44 for the torsional components (Fig 4.8A,C). The average phases were -52° for horizontal and -58° for torsional (**M9003** & **M9354**, Table 4.3 A). When the model parameters were set for a lateral and **LARP** canal plugged condition, leaving a **RALP** (Fig 4.15D, H), the model

Figure 4.15: Model prediction for the gains of yaw (**A** - **D**) and roll (**E** - **H**) eye movements at various tilt angles for the normal animals (**A**, **E**), after bilateral anterior and posterior canals plugging (**B**, **F**), bilateral lateral canal plugging (**C**, **G**) and bilateral lateral and left anterior, right posterior canal plugging (**D**, **H**). Schematics at the top of graphs **A** - **H** and **G** indicate which canals were plugged. **Ac** - anterior canal, **Lc** - lateral canal and **Pc** - posterior canal. Monkey heads at the bottom of graphs **F** - **H** show head position at each pitch angle. Abscissas for each graph represent stationary head tilt position when animals were rotated around the spatial vertical. Negative values correspond to the tilt back position, positive value correspond to tilting forward. Ordinates on all graphs represent the aVOR gains.

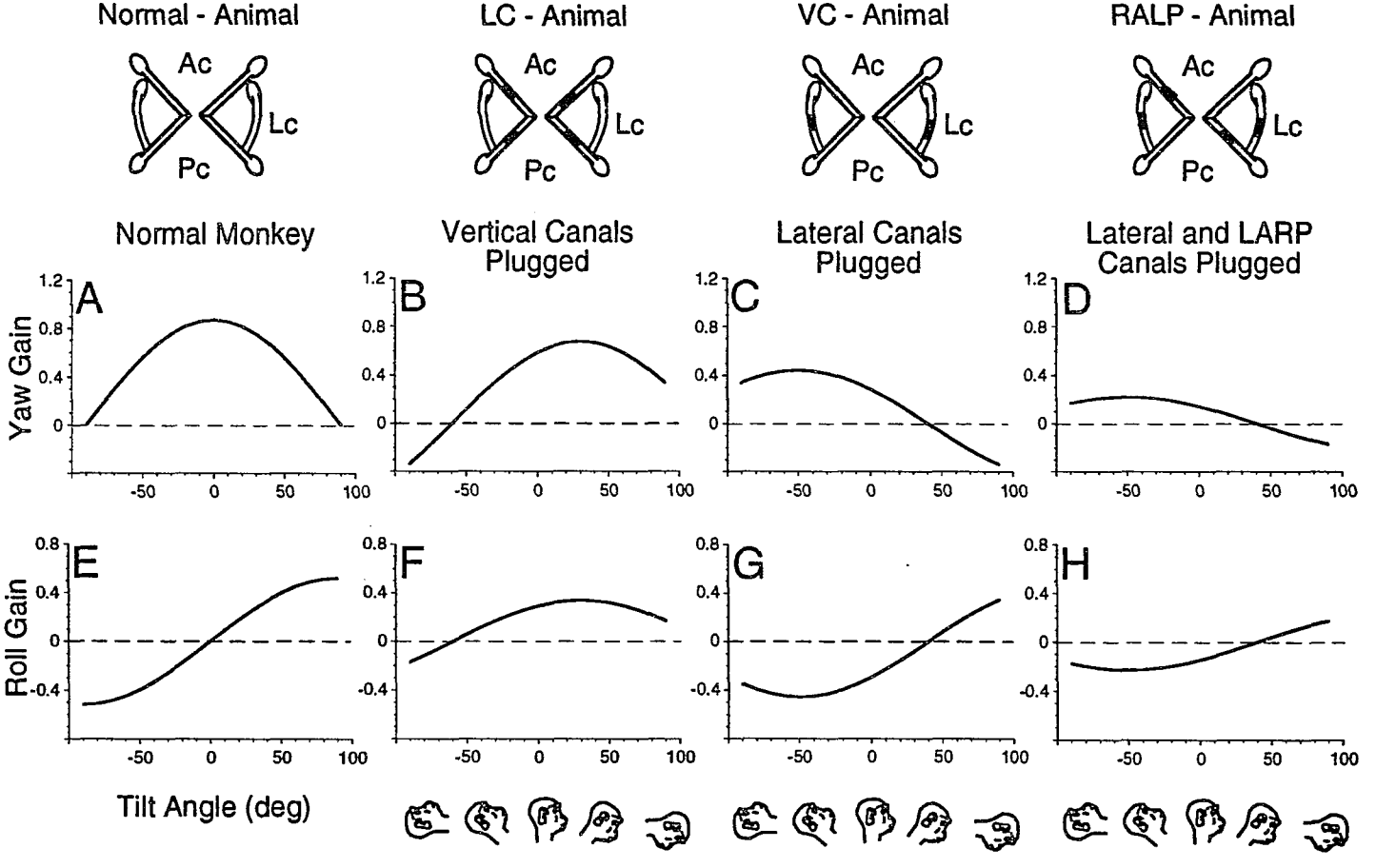
Normal - Animal
LC - Animal
VC - Animal
RALP - Animal
Ac
Lc
Pc
Normal Monkey
Vertical Canals Plugged
Lateral Canals Plugged
Lateral and LARP Canals Plugged
A
B
C
D
E
F
G
H
Yaw Gain
Roll Gain
1.2
0.8
0.4
0
-0.4
-50
0
50
100
Tilt Angle (deg)

predicted a reduction in the gain of both components to 0.22 and 0.23 for yaw and roll respectively. The peak gains for both occurred at -50° tilt backward. The average peak yaw and roll gains for the five **LARP** and **RALP** animals were 0.27 and 0.28 occurring at -55° and -62° (Fig 4.10C,F).

Thus, even though the model was based on average rather than specific normal responses, it was capable of approximately predicting both the normal and the plugged canal data with a single set of parameters. Although the model predicted that the phases would occur at the same angle, there were small discrepancies in the **LC** and **LARP** and **RALP** animals. These were not significant, however. The model also predicted the appearance of a vertical component with the same spatial phase as the horizontal component in the **LARP** and **RALP** animals at -50° tilt back. This vertical component was also present in the experimental data ($\dot{V}$, Fig 4.2-4.5B).

4.4 SPATIAL GAIN BEHAVIOR OF aVOR AS A FUNCTION OF FREQUENCY:

Work on the aVOR in rhesus monkeys has shown that the gain of the horizontal aVOR in dark slightly increases for frequencies up to 2.0 Hz. There was a significant increase in horizontal aVOR gain when animals were tested at 4.0 Hz (Keller 1978). Above 4.0 Hz, the gain declined toward the values obtained at low frequencies (Keller 1978). To determine whether the conclusions about individual canal contributions to the aVOR extend over a wide frequency range, we studied the spatial gain characteristics of the aVOR over a frequency range of 0.2 to 4.0 Hz for normal and all types of plugged conditions. We also examined the spatial gain characteristics for the step response. This was done to determine whether the periodicity of the stimulus would affect the gain.

The animals that were available for this part of the study were: one **VC**, one **LARP**, one **RALP**, and one animal with all six semicircular canal plugged. None of these animals were tested before surgery at a frequency other that 0.2 Hz. Therefore another normal animal **M9357** was prepared for this study and used as a control.

4.4.1 NORMAL ANIMAL:

Figure 4.16 summarizes the results from a normal animal that was tested at frequencies of 0.2 - 4.0 Hz. Temporal phases of the sinusoidal aVOR relative to the stimulus were $2° \pm 7°$ for horizontal and $1° \pm 5°$ for torsional components (Table 4.4). Increasing the frequency did not effect the phase ($p=0.05$). The peak of the spatial horizontal gain curve at 0.2 Hz was 1.0, occurring at 3° (Phase error $\pm 4°$) tilt forward (Fig 4.16A). There was no significant variation ($p<0.05$, ANOVA, Tabl 4.7) in the peak value for frequencies at 0.5 Hz (Fig 4.16B), 1.0 Hz (4.16C), 2.0 Hz (Fig 4.16D) and 4.0 Hz (Fig 4.16E) (Table 4.5A). Torsional aVOR gain was 0.46, when animal was tested at 0.2 Hz (Fig 4.16F) and gradually increased up to 0.85 at 4.0 Hz (Fig 4.16F-J). Spatial phase, for the torsional component, however, had no frequency dependent trend. It was -71°, when the animal was tested at 0.2 Hz and -73°, when it was tested at 4.0 Hz (Fig 4.16J), ranging from -69° to -78° (Table 4.5,B). A statistical analysis showed that only the spatial curve of the torsional aVOR gain curve tested at 4.0 Hz is different from all others ($p<0.05$, ANOVA based on post-hoc contrasts, with Scheffe adjustment, Table 4.7).

The results indicate that over a range from 0.2 - 4.0 Hz, the horizontal spatial gain did not vary as a function of frequency (Fig. 4.17A-E). The torsional gain increased

Figure 4.16: Spatial gain responses of the normal animal tested at different frequencies of sinusoidal rotation. Averaged gains of the yaw (**A** - **E**) and roll (**F** - **J**) components of the normal monkey (**M9357**). **A**, **F** - tested at 0.2 Hz, 60°/s; **B**, **G** - tested at 0.5 Hz, 60°/s; **C**, **H** - tested at 1.0 Hz 30°/s; **D**, **I** - tested at 2.0 Hz, 15°/s. and **E**, **J** - tested at 4.0 Hz, 5°/s. Spatial gain curves for the horizontal aVOR were the same at any tested frequency. Spatial phases of torsional (roll) curves were similar to each other, but spatial gains increased as a function of stimulus frequency and were significantly higher at 4.0 Hz rotation then at any other frequency. The solid lines represent the best sinusoidal fit to the horizontal and torsional gains at tested frequency. Arrows point to the tilt position with maximal gain responses.

Spatial Gain of aVOR as a Function of Frequency (Normal Monkey, M9357)

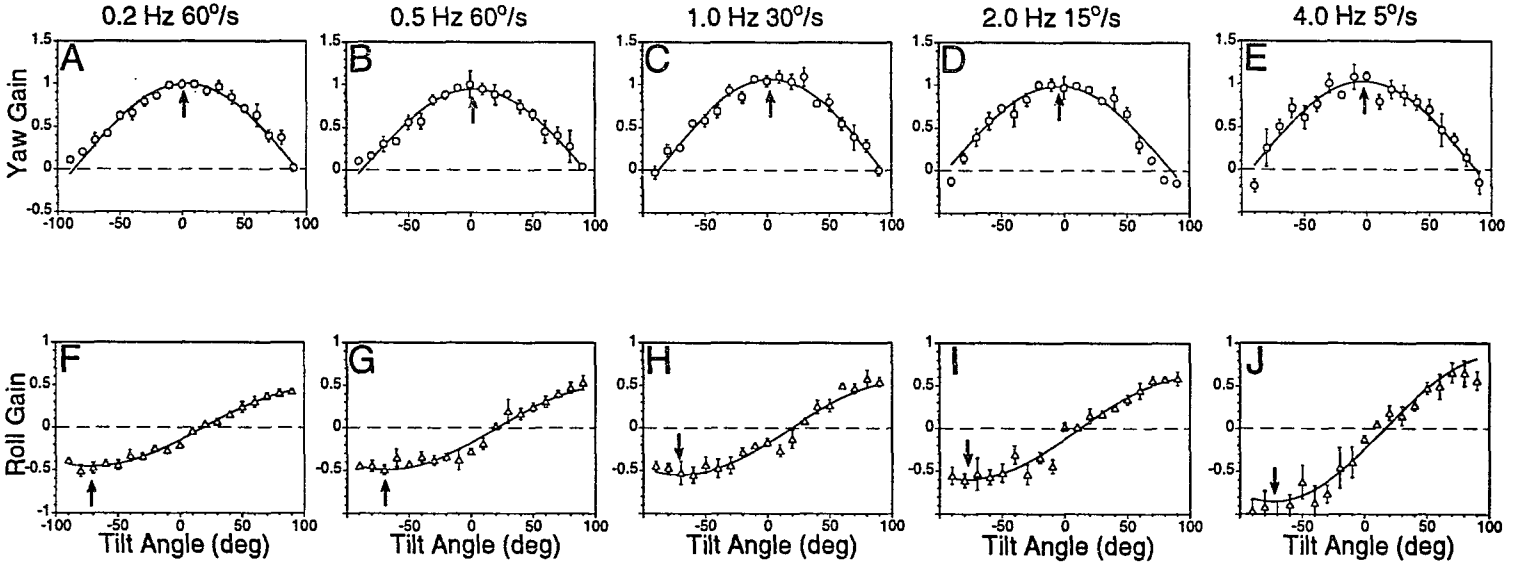

Figure 4.17: Peak spatial gains (**A**, **C**) and phases (**B**, **D**) of the horizontal (**A**, **B**) and torsional (**C**, **D**) components of the aVOR of the normal monkey (**M9357**) tested in darkness at different frequencies. Horizontal dashed lines represent average values obtained for normal animals tested at 0.2 Hz 60°/s.

Horizontal aVOR. Normal Monkey (M9357)

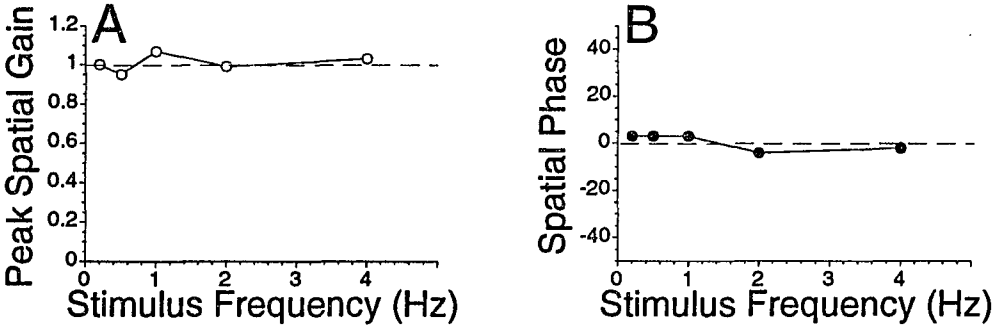

Roll aVOR. Normal Monkey (9357)

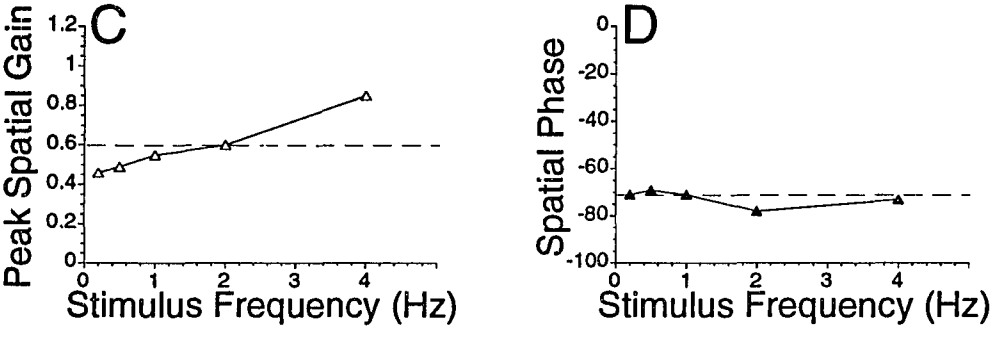

Table 4.4: Temporal phases of the horizontal aVOR gain of the normal and canal plugged animals tested at different frequencies in darkness. Since temporal phases of eye velocity were not correlated with the tilt position, they were averaged for a given frequency of rotation. Average value and $\pm$ 1 SD are shown in each table cell. The six canals plugged animal (NC) was not tested at 0.5 Hz, 60°/s., these values are missing in the table.

Table 4.4

	Horizontal aVOR				Roll aVOR				
	0.5 Hz	1.0 Hz	2.0 Hz	4.0 Hz	0.5 Hz	1.0 Hz	2.0 Hz	4.0 Hz	
Normal Animal	2 ± 7	0± 5	-8±17	0± 6	1 ± 5	0± 6	1± 7	-3± 8	M9357
VC Animal	6 ± 14	1±16	2±11	-6±13	2 ± 6	1± 8	1± 6	0± 4	M9354
LARP Animal	-1 ± 11	-4±16	-10±14	-15±10	-3 ± 8	-6± 8	-10± 8	-6±10	M9306
RALP Animal	-6 ± 8	9±11	14±10	-12± 5	-4 ± 6	-9± 4	-16± 6	-14± 9	M9355
NC Animal	-	-19± 7	-38± 6	-26±15	-	-25± 7	-45± 9	-21± 9	M9308

Table 4.5: Spatial phases and gains of the horizontal (**A**) and torsional (**B**) aVOR of the normal and canal plugged animals tested at different frequencies in darkness. The six canals plugged animal (**NC**) was not tested at 0.5 Hz, 60°/s. These values are missing in the table.

4.5

A. Spatial phases and gains of the horizontal aVOR of the normal and canal plugged animals tested at different frequencies in darkness.

	Spatial Phase				Spatial Gain				
	0.5 Hz	1.0 Hz	2.0 Hz	4.0 Hz	0.5 Hz	1.0 Hz	2.0 Hz	4.0 Hz	
Normal Animal	3	3	-4	-2	0.95	1.07	0.99	1.03	M9357
VC Animal	-23	0	1	11	0.30	0.50	0.71	0.86	M9354
LARP Animal	-8	-7	6	6	0.17	0.28	0.45	0.74	M9306
RALP Animal	-20	-9	-3	-2	0.35	0.57	0.81	0.94	M9355
NC Animal	-	3	10	10	-	0.24	0.44	0.73	M9308

B. Spatial phases and gains of the torsional aVOR of the normal and canal plugged animals tested at different frequencies in darkness.

	Spatial Phase				Spatial Gain				
	0.5 Hz	1.0 Hz	2.0 Hz	4.0 Hz	0.5 Hz	1.0 Hz	2.0 Hz	4.0 Hz	
Normal Animal	-69	-71	-78	-73	0.49	0.55	0.60	0.85	M9357
VC Animal	-66	-66	-73	-82	0.41	0.46	0.55	0.70	M9354
LARP Animal	-67	-70	-68	-74	0.34	0.33	0.42	0.59	M9306
RALP Animal	-65	-67	-78	-77	0.47	0.44	0.60	0.84	M9355
NC Animal	-	-43	-43	-45	-	0.24	0.44	0.78	M9308

Table 4.6: Significance of the F statistic and value of the phase error of the horizontal and torsional components of the aVOR obtain at different frequencies for normal monkey and animals with different canal plugging. $F_{0.05}$ - represent calculated values of the F statistic. P_{err} - represent phase error.

Table 4.6

HORIZONTAL aVOR								
Stimulus	0.5 Hz, 60°/s		1.0 Hz, 30°/s		2.0 Hz 15°/s		4.0 Hz 5°/s	
	$F_{0.05}$	P_{error}	$F_{0.05}$	P_{error}	$F_{0.05}$	P_{error}	$F_{0.05}$	P_{error}
Normal Animal (M9357)	$F_{1,114}=1.60$	±9°	$F_{1,133}=2.16$	±6°	$F_{1,152}=3.18$	±4°	$F_{1,190}=2.27$	±8°
VC Animal (M9354)	$F_{1,133}=10.5$	-	$F_{1,152}=5.95$	-	$F_{1,228}=3.56$	±3°	$F_{1,228}=4.14$	-
LARP Animal (M9306)	$F_{1,114}=2.15$	±18°	$F_{1,114}=4.96$	-	$F_{1,152}=2.13$	±12°	$F_{1,209}=5.84$	-
RALP Animal (M9355)	$F_{1,152}=4.97$	-	$F_{1,209}=3.85$	-	$F_{1,152}=3.63$	±3°	$F_{1,152}=2.05$	±12°
NC Animal (M9308)	-	-	$F_{1,266}=2.09$	±24°	$F_{1,209}=1.18$	±25°	$F_{1,247}=1.65$	±16°
ROLL aVOR								
Stimulus	0.5 Hz 60°/s		1.0 Hz 30°/s		2.0 Hz 15°/s		4.0 Hz 5°/s	
	$F_{0.05}$	P_{error}	$F_{0.05}$	F_{error}	$F_{0.05}$	P_{error}	$F_{0.05}$	P_{error}
Normal Animal (M9357)	$F_{1,133}=2.46$	±11°	$F_{1,133}=2.60$	±10°	$F_{1,133}=1.80$	±17°	$F_{1,152}=2.01$	±15°
VC Animal (M9354)	$F_{1,152}=1.59$	±6°	$F_{1,152}=1.57$	±6°	$F_{1,171}=1.44$	±12°	$F_{1,247}=1.21$	±14°
LARP Animal (M9306)	$F_{1,114}=3.79$	±4°	$F_{1,171}=1.49$	±16°	$F_{1,133}=1.32$	±14°	$F_{1,247}=1.21$	±19°
RALP Animal (M9355)	$F_{1,152}=1.90$	±10°	$F_{1,209}=2.01$	±17°	$F_{1,114}=3.21$	±6°	$F_{1,209}=2.34$	±13°
NC Animal (M9308)	-	-	$F_{1,209}=1.32$	±39°	$F_{1,190}=1.23$	±28°	$F_{1,209}=1.11$	±26°

Table 4.7: Summary tables of ANOVA for the horizontal (**A**) and torsional (**B**) components of the aVOR gain of the normal monkey tested at 0.2Hz (μ_1), 0.5Hz (μ_2), 1Hz (μ_3), 2Hz (μ_4) and 4Hz (μ_5) of the normal monkey M9357.

Table 4.7 RESULTS OF STATISTICAL ANALYSIS (ANOVA).

A. Yaw aVOR Gains.

Source	SS	df	MS	F_{comp}	$F_{0.05}$
Between data	0.0830	3	0.0277	1.80	2.68
Within data	1.0939	71	0.01541		

B. Roll aVOR Gains.

Source	SS	df	MS	F_{comp}	$F_{Scheffe}$
Between data	0.7528	4	0.1882	4.3780	2.5300
$\mu_1=\mu_2=\mu_3$	0.0349	2	0.0612	1.4243	9.8000
$⅓\mu_1+⅓\mu_2+⅓\mu_3=\mu_4$	0.0527	1	0.0527	1.2257	9.8000
$⅓\mu_1+⅓\mu_2+⅓\mu_3=\mu_5$	0.6652	1	0.6652	15.470	9.8000
Within data	3.869	90	0.0430		

when tested at 4.0 Hz. (Fig. 4.17F-J). However, the spatial phase of both the horizontal and torsional aVOR gain did not vary (Fig 4.17B, D). We, therefore, used the average spatial gain characteristics obtained at 0.2 Hz for all normal monkeys as a reference. This was compared to the spatial gain curves of the horizontal and torsional aVOR of **NC, VC, LARP** and **RALP** plugged conditions over the complete range of frequencies.

4.4.2 SIX CANALS PLUGGED ANIMAL (NC ANIMAL):

As already described, the horizontal aVOR at 0.2 Hz was not significantly different from 0 (See Section 4.1.6 and Fig 4.13). At higher frequencies, the spatial response characteristics could be well approximated with a sinusoid for all cases ($p<0.05$)(Table 4.6). When tested at 1.0 Hz, the horizontal and torsional peak spatial gain rose to 0.24 (Fig 4.18A,D) and a spatial phase of $+3°$ (Phase error $\pm 24°$) for horizontal and $-43°$ (Phase error $\pm 39°$) for torsional (Table 4.5). For 2.0 Hz, the peak spatial gain was 0.44 for horizontal and torsional aVOR (Fig 4.18B,E). Horizontal phase was $+10°$ (Phase error $\pm 25°$) and torsional phase was $-43°$ (Phase error $\pm 28°$). At 4.0 Hz, the peak horizontal spatial gain rose to 0.73, at $+10°$ (Phase error $\pm 16°$; Fig 4.18C). The peak torsional spatial gain was 0.78, occurring at $-45°$ (Phase error $\pm 26°$; Fig 4.19F). In summary, the horizontal and torsional spatial gains of an NC animal increased as a function of frequency and approached values obtained before surgery (Fig 4.19A,C). The horizontal spatial phase of the NC animal was not different from the normal animal (M9357) for all frequencies (Fig 4.19B). The torsional spatial phase was different from normal (Fig 4.19D). However, the spatial phase of horizontal and torsional aVOR did not vary with frequency (Fig 4.19B,D). The gradual increase in gain

Figure 4.18: Spatial responses of the monkey with all six canals plugged (NC Animal) tested at different frequencies of sinusoidal rotation. Average gains of the yaw (**A** - **C**) and roll (**D** - **F**) components from the NC Animal (**M9308**) (filled symbols) compared to the normal animals responses recorded at 0.2 Hz 60°/s. **A**, **D** - tested at 1.0 Hz, 30°/s.; **B**, **E** - tested at 2.0 Hz 15°/s.; **C**, **F** - tested at 4.0 Hz, 5°/s. When this animal was tested after surgery at 0.2 Hz, 60°/s., it had no responses at any tilt position (Fig 4.13), but responses appeared at higher frequency. The gains and spatial phases had a tendency to shift to normal responses. The dashed lines represent the minimum mean square error fit to the horizontal and torsional gains at the tested frequencies. Arrows point to the tilt position with maximal gain response.

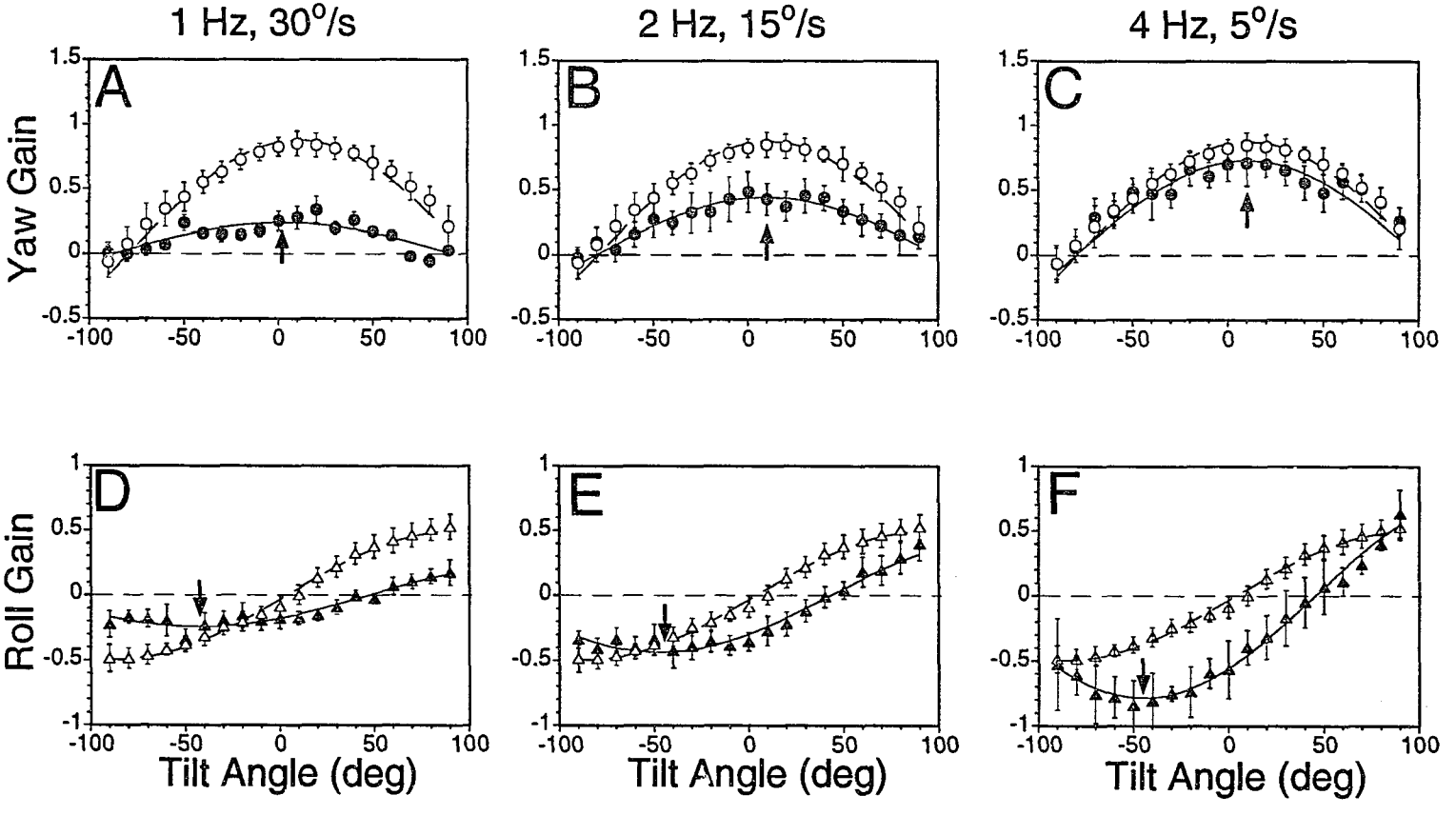
NC Animal Tested at Different Frequencies
1 Hz, 30°/s
2 Hz, 15°/s
4 Hz, 5°/s
A
B
C
D
E
F
Yaw Gain
Roll Gain
Tilt Angle (deg)
Tilt Angle (deg)
Tilt Angle (deg)

Figure 4.19: Peak spatial gains (**A**, **C**) and phases (**B**, **D**) of the horizontal (**A**, **B**) and torsional (**C**, **D**) components of the aVOR of the **NC** animal (**M9308**) tested in darkness as a function of frequency. Horizontal dashed lines represent average values obtained for this animal at 0.2 Hz 60°/s.

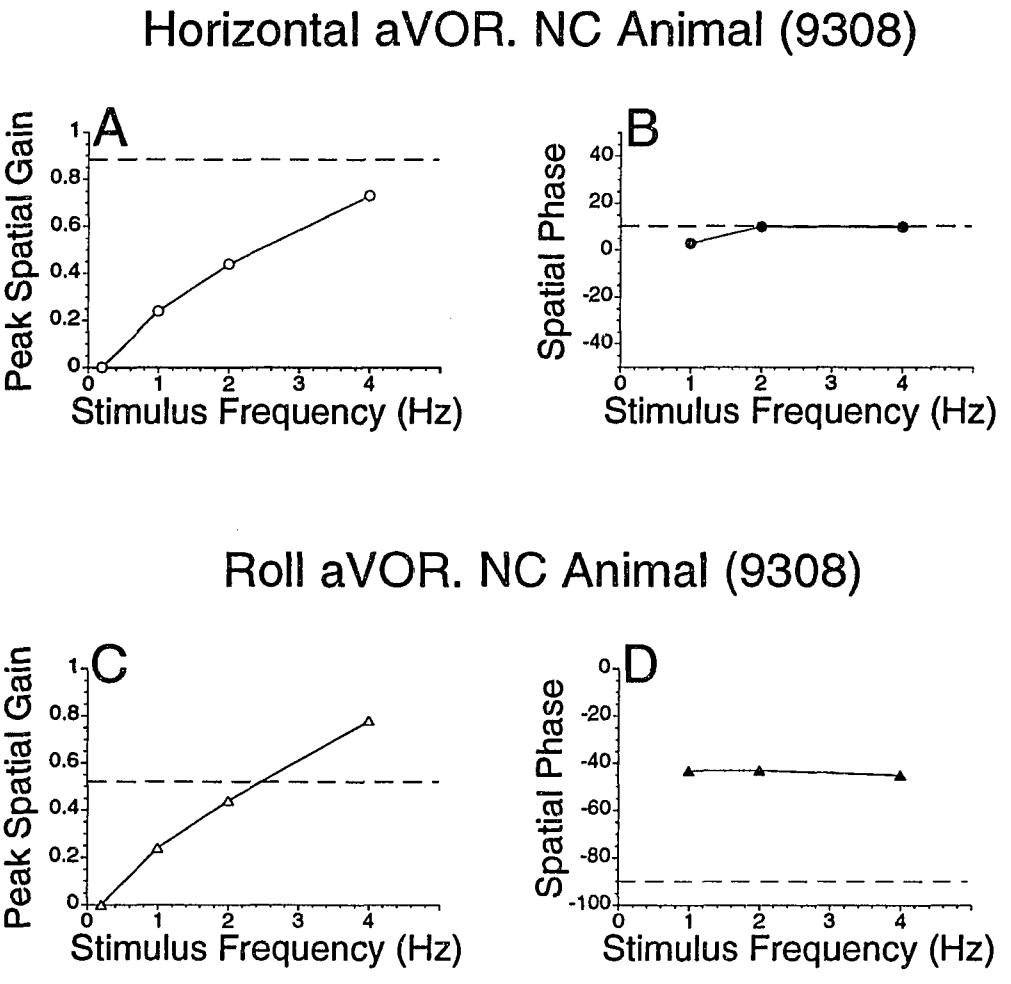
Horizontal aVOR. NC Animal (9308)
A
Peak Spatial Gain
1
0.8
0.6
0.4
0.2
0
0
1
2
3
4
Stimulus Frequency (Hz)
B
Spatial Phase
40
20
0
-20
-40
0
1
2
3
4
Stimulus Frequency (Hz)
Roll aVOR. NC Animal (9308)
C
Peak Spatial Gain
1
0.8
0.6
0.4
0.2
0
0
1
2
3
4
Stimulus Frequency (Hz)
D
Spatial Phase
0
-20
-40
-60
-80
-100
0
1
2
3
4
Stimulus Frequency (Hz)

with frequency suggests that the time constant of the canal response had been drastically reduced due to plugging. The data of Fig 4.19A,C suggest that the 3 db break point is higher than 3 Hz. This would correspond to a dominant time constant smaller than 0.3 sec. The time constant will be considered for the step response (See Section 4.5).

4.4.3 LARP, RALP AND VC ANIMALS:

The spatial gain characteristic of **LARP**, **RALP**, and **VC** animals were different at 0.2Hz as described in Section 4.1. However, each of the animals had a tendency to normalize with increasing frequency of stimulation (Figs 4.20 - 4.22).

The peak horizontal spatial gain of the **LARP** animal (**M9306**) decreased to 0.17 at 0.5 Hz compared to 0.23 at 0.2 Hz (Fig 4.23A). The spatial phase which was -57° at 0.2 Hz moved to -8°, and was considerably closer to the average normal condition of +11° (Fig 4.23B). At higher frequencies, gain and phase continued to normalize and at 4 Hz reached a peak spatial gain of 0.74 at +6° tilt (Fig 4.23A,B). The peak torsional spatial gain gradually increased from 0.23 at 0.2 Hz to 0.59 at 4 Hz (Fig 4.23C). However, spatial phase remained the same at all frequencies (Fig 4.23C,D).

The horizontal and torsional spatial gain characteristics of the **RALP** (Fig 4.24A,B) and **VC** (Fig 4.25A,B) animals behaved essentially the same as the **LARP** animal. That is, the horizontal and torsional peak spatial gain increased as a function of frequency. Both the horizontal and torsional spatial phase shifted towards normal (Fig 4.24C,D; Fig 4.25C,D).

The data indicate that canal plugging is a frequency dependent operation which eliminates rotational responses at 0.2 Hz, but not at higher frequencies. Thus, plugging

Figure 4.20: Spatial responses of the monkey with both horizontal, right anterior and left posterior canal plugged (**LARP** Animal) tested at different frequencies of sinusoidal rotation. It demonstrates average gains of the yaw (**A** - **D**) and roll (**E** - **H**) components from the **LARP** Animal (**M9306**). **A**, **E** - tested at 0.5 Hz, 60°/s; **B**, **F** - tested at 1.0 Hz 30°/s; **C**, **G** - tested at 2.0 Hz, 15°/s. and **D**, **H** - tested at 4.0 Hz, 5°/s. When this animal was tested after surgery the responses (gains and spatial phases) tended to shift to normal responses as testing frequency increased. The solid lines represent the minimum mean square error fit to the horizontal and torsional gains at the tested frequencies. Arrows point to the tilt position with maximal gain response.

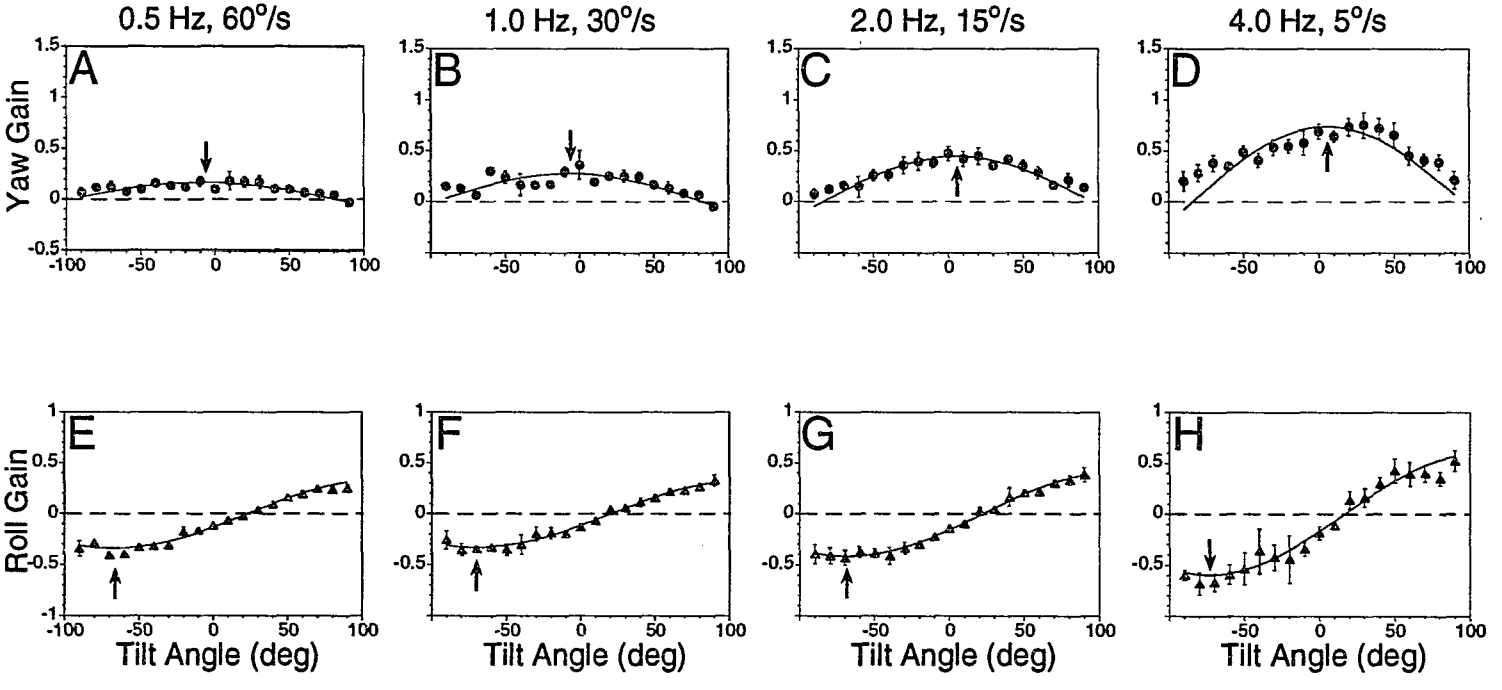
0.5 Hz, 60°/s
1.0 Hz, 30°/s
2.0 Hz, 15°/s
4.0 Hz, 5°/s
A
B
C
D
E
F
G
H
Yaw Gain
Roll Gain
Tilt Angle (deg)
Tilt Angle (deg)
Tilt Angle (deg)
Tilt Angle (deg)

Figure 4.21: Spatial responses of the monkey with both horizontal, left anterior and right posterior canal plugged (**RALP** Animal) tested at different frequencies of sinusoidal rotation. Average gains of the yaw (**A**, **B**, **C**, **D**) and roll (**E**, **F**, **G**, **H**) components from the **RALP** Animal (**M9355**). **A**, **E** - tested at 0.5 Hz, 60°/s; **B**, **F** - tested at 1.0 Hz 30°/s; **C**, **G** - tested at 2.0 Hz, 15°/s. and **D**, **H** - tested at 4.0 Hz, 5°/s. When this animal was tested after surgery the responses (gains and spatial phases) tended to shift to normal responses as testing frequency increased. The solid lines represent the minimum mean square error fit to the horizontal and torsional gains at the tested frequencies. Arrows point to the tilt position with maximal gain response.

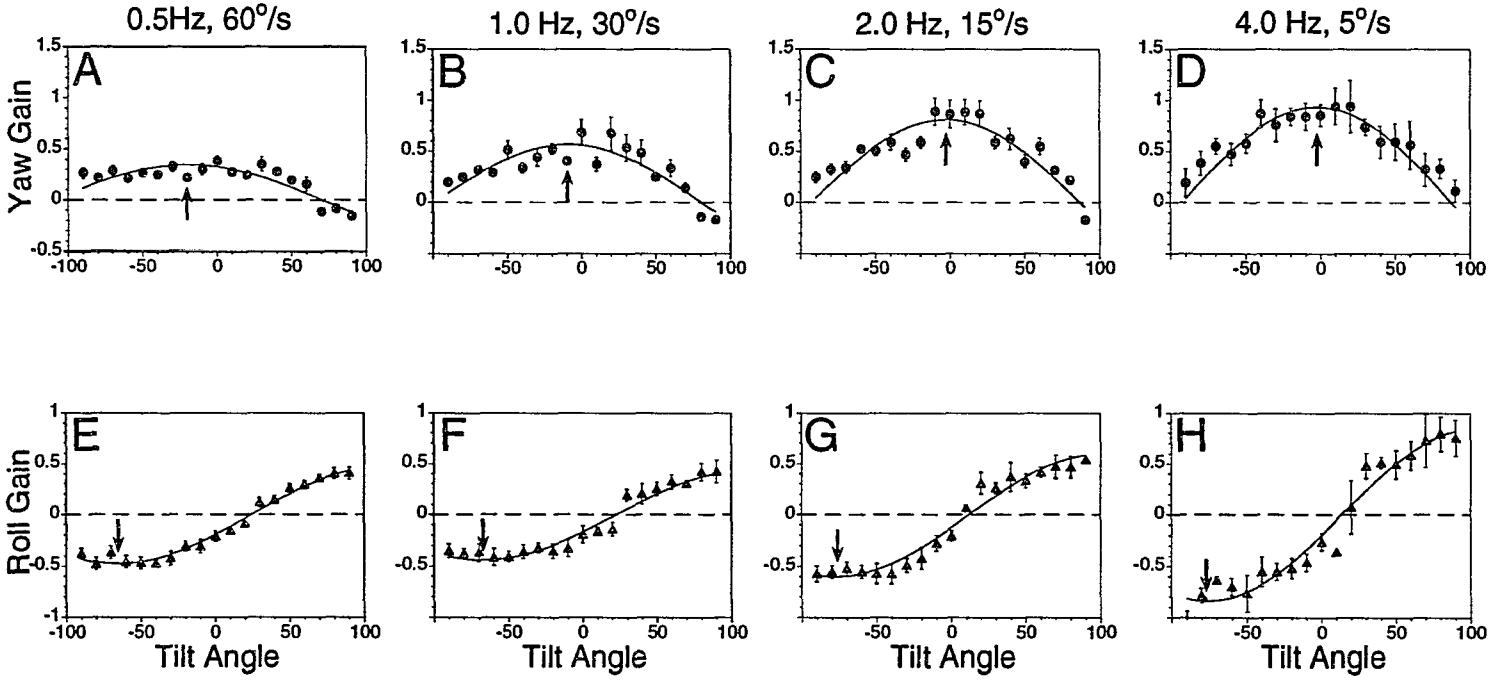
0.5Hz, 60°/s
1.0 Hz, 30°/s
2.0 Hz, 15°/s
4.0 Hz, 5°/s
A
B
C
D
Yaw Gain
E
F
G
H
Roll Gain
Tilt Angle
Tilt Angle
Tilt Angle
Tilt Angle

Figure 4.22: Spatial responses of the monkey with all four vertical canals plugged (**VC** animal) tested at different frequencies of sinusoidal rotation. Average gains of the yaw (**A** - **D**) and roll (**E** - **H**) components from the **VC** animal (**M9354**). **A**, **E** - tested at 0.5 Hz, 60°/s; **B**, **F** - tested at 1.0 Hz 30°/s; **C**, **G** - tested at 2.0 Hz, 15°/s. and **D**, **H** - tested at 4.0 Hz, 5°/s. When this animal was tested after surgery the responses (gains and spatial phases) tended to shift to normal responses as testing frequency increased. The solid lines represent the minimum mean square error fit to the horizontal and torsional gains at the tested frequencies. Arrows point to the tilt position with maximal gain response.

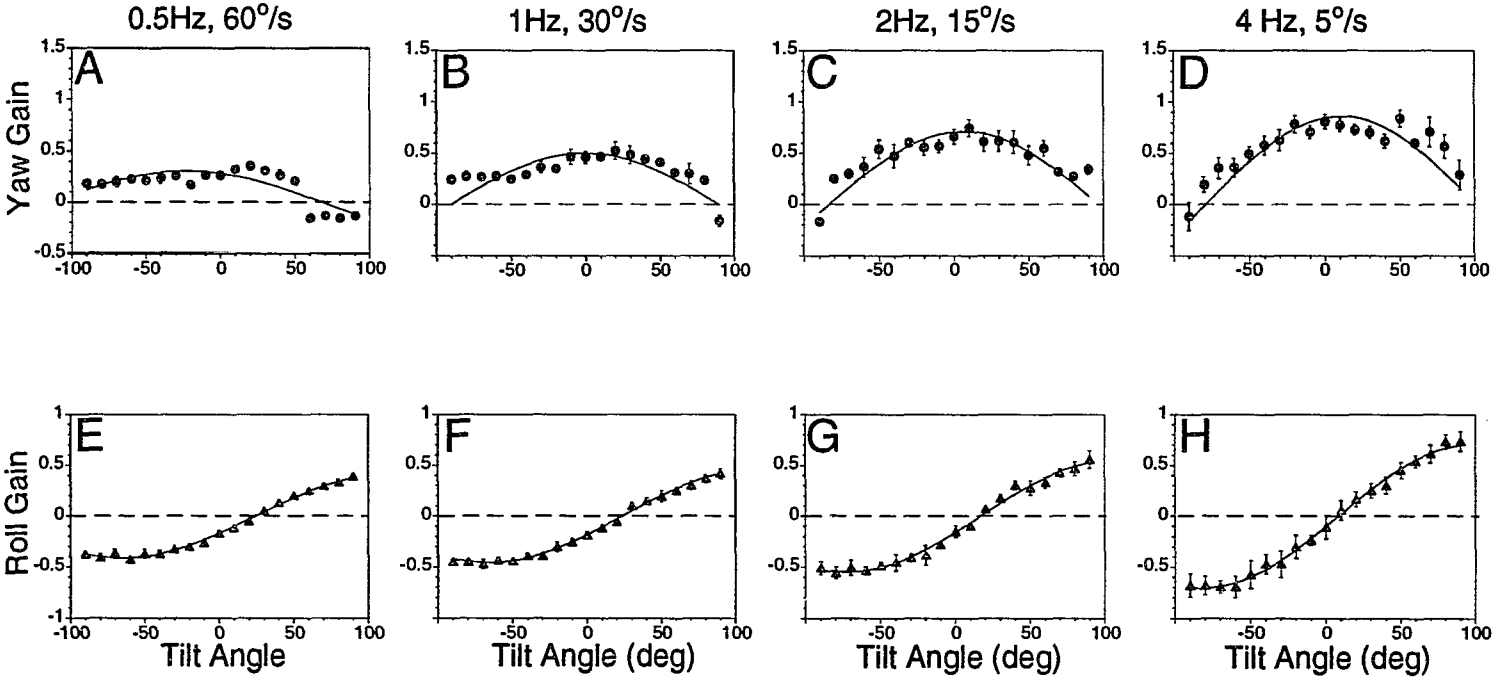
0.5Hz, 60°/s
1Hz, 30°/s
2Hz, 15°/s
4 Hz, 5°/s
A
B
C
D
Yaw Gain
E
F
G
H
Roll Gain
Tilt Angle
Tilt Angle (deg)
Tilt Angle (deg)
Tilt Angle (deg)

Figure 4.23: Peak spatial gains (**A**, **C**) and phases (**B**, **D**) of the horizontal (**A**, **B**) and torsional (**C**, **D**) components of the aVOR of the **LARP** animal (**M9306**) tested in darkness as a function of frequency. The horizontal dashed lines represent the average values obtained for normal animals tested at 0.2 Hz 60°/s.

Horizontal aVOR. LARP Animal (9306)

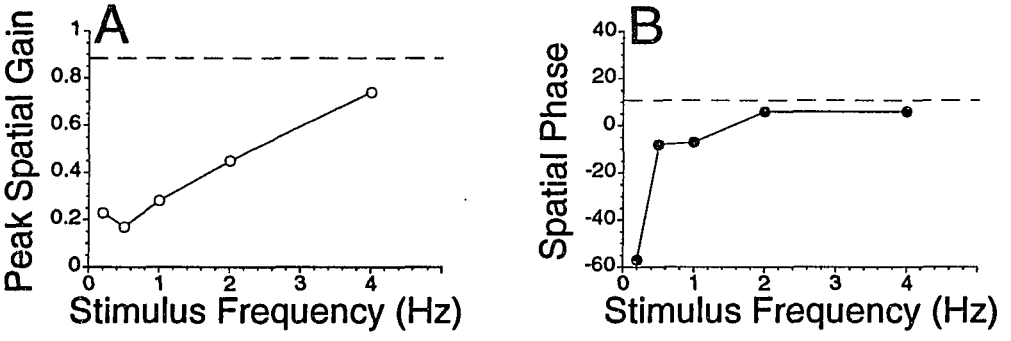

Roll aVOR. LARP Animal (9306)

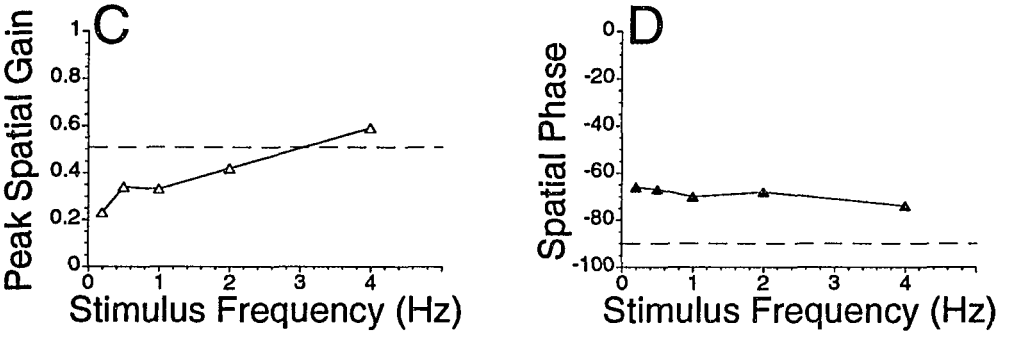

Figure 4.24: Peak spatial gains (**A**, **C**) and phases (**B**, **D**) of the horizontal (**A**, **B**) and torsional (**C**, **D**) components of the aVOR of the **RALP** animal (**M9355**) tested in darkness as a function of frequency. The horizontal dashed lines represents the average values obtained for normal animals tested at 0.2 Hz 60°/s.

Horizontal aVOR. RALP Animal (9355)

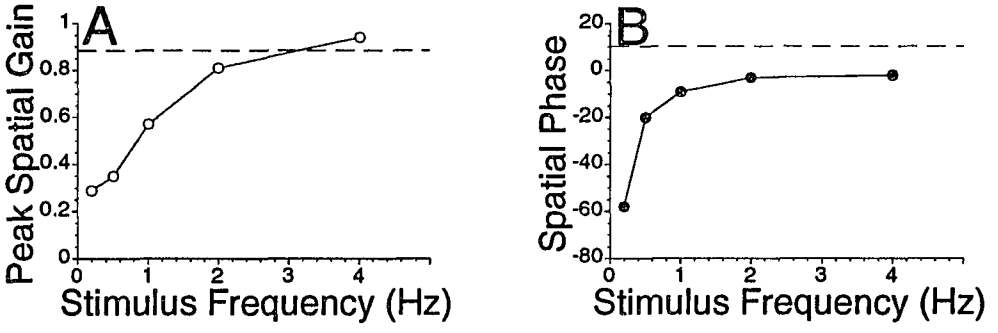

Roll aVOR. RALP Animal (9355)

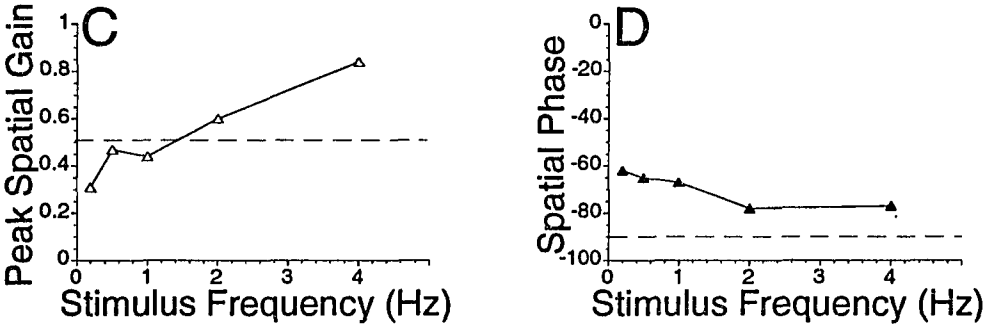

Figure 4.25: Peak spatial gains (**A**, **C**) and phases (**B**, **D**) of the horizontal (**A**, **B**) and torsional (**C**, **D**) components of the aVOR of the **VC** animal (**M9354**) tested in darkness as a function of frequency. The horizontal dashed lines represent the average values obtained for normal animals tested at 0.2 Hz 60°/s.

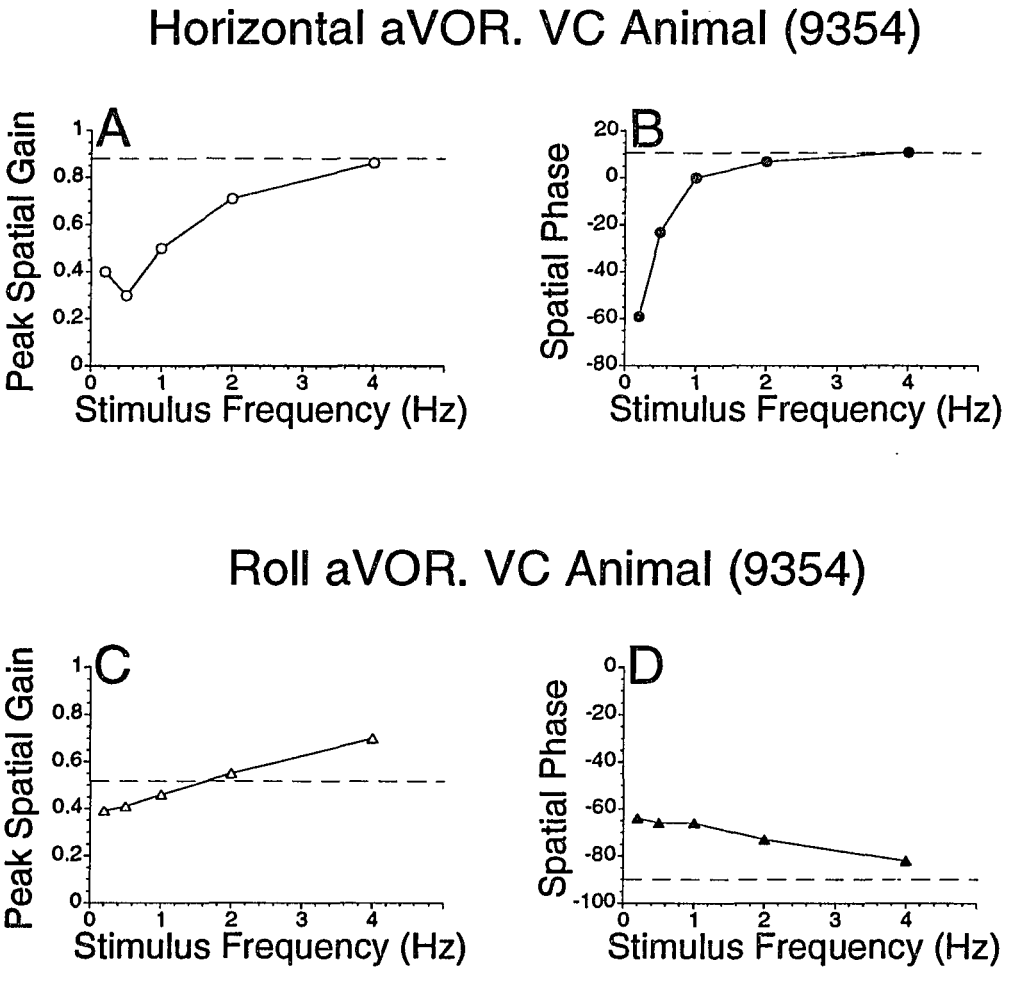
Horizontal aVOR. VC Animal (9354)
A
Peak Spatial Gain
1
0.8
0.6
0.4
0.2
0
0 1 2 3 4
Stimulus Frequency (Hz)
B
Spatial Phase
20
0
-20
-40
-60
-80
0 1 2 3 4
Stimulus Frequency (Hz)
Roll aVOR. VC Animal (9354)
C
Peak Spatial Gain
1
0.8
0.6
0.4
0.2
0
0 1 2 3 4
Stimulus Frequency (Hz)
D
Spatial Phase
0
-20
-40
-60
-80
-100
0 1 2 3 4
Stimulus Frequency (Hz)

individual canals does not necessarily isolate their contribution to the aVOR at higher frequencies.

4.5 RESPONSES TO CONSTANT VELOCITY ROTATION:

When animals were given steps of rotation at 60°/s., slow phase eye velocity, contralateral to the direction of rotation, was generated. The slow phase eye velocity was interapted by ipsilaterally directed saccades which were identified and removed from the velocity traces (See Section 2.4). Desaccaded eye velocities in response to steps of rotation were synchronized to the beginning of rotation and 10 responses were overlaid (Fig 4.26)(Program was written in BASIC 7.1, see Appendix D). For the upright condition, the step of rotation produced essentially horizontal compensatory eye velocity which remained stable for at least one second during the constant velocity period (Fig 4.26A,B). It should be noted that the chair response was underdamped and oscillated with a frequency of 10 Hz (Fig 4.26E,F). Individual eye velocity responses followed these oscillations, but the average response was constant over the period of oscillation (Fig 4.22A,B).

The step of rotation velocity had a rise time of approximately 200 msec for 60°/s. peak velocity. This corresponds to an acceleration of 300°/s^2. Average eye velocity was computed during the first 200 msec after the stimulus achieved constant velocity of rotation. The gain of the step response for the individual responses was computed by taking the average eye velocity of the individual responses and dividing by the average stimulus velocity. The gains were averaged over 10 responses to obtain the average gain and standard deviation of the step response for each tilt position. For the animal with all

Figure 4.26: Horizontal (**A**, **B**) and torsional (**C**, **D**) eye velocity during constant velocity rotation to the right (**A**, **C**, **E**) and to the left (**B**, **D**, **F**), when a normal animal (**M9308**) is in the upright position. Rotation in this position produced predominantly a horizontal component of eye velocity. Each graph represents the superposition of several eye velocity responses. **E** and **F** are the velocities of the head rotation. The abscissa represents time in msec and is synchronized to the start of head rotation. The ordinate is velocity in °/s.

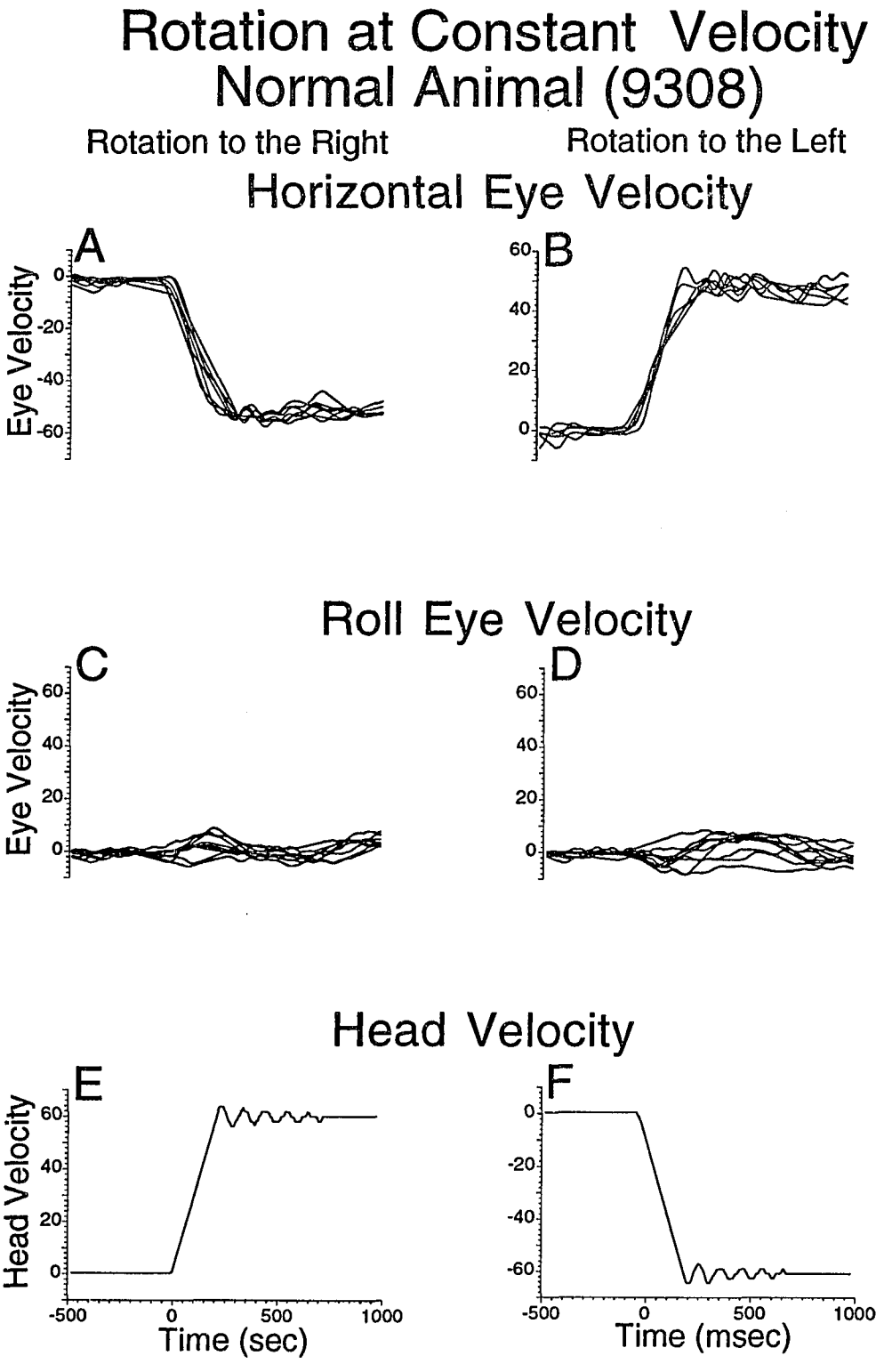
Rotation at Constant Velocity
Normal Animal (9308)
Rotation to the Right
Rotation to the Left
Horizontal Eye Velocity
A
B
Eye Velocity
0
-20
-40
-60
60
40
20
0
Roll Eye Velocity
C
D
Eye Velocity
60
40
20
0
Head Velocity
E
F
Head Velocity
60
40
20
0
0
-20
-40
-60
-500
0
500
1000
Time (sec)
Time (msec)

canals plugged, the eye velocity response was transient (Fig 4.27) and the gain of the step response was computed as peak eye velocity due to the step of rotation divided by the velocity of rotation. The average gains and standard deviations were computed based on ten responses as shown overlaid in Fig 4.27. In all cases, the gains were computed for rotation to the left and right independently.

4.5.1 NORMAL RESPONSE CHARACTERISTICS:

The spatial gain characteristics for the normal animal in response to steps of velocity were similar to these during sinusoidal stimulation (Fig 4.28A, D, **M9308**; Fig 4.29A, D, **M9306**). For rotations to the left (Fig 4.28A, open symbols), peak horizontal spatial gain was 0.85 occurring at 15° tilt forward. For rotations to the right (Fig 4.28A, filled symbols), peak horizontal spatial gain was 0.93 occurring at 13° tilt forward. These were not significantly different from each other ($F_{1,171}=3.69$). The peak torsional gain for rotation to the left was 0.45, occurring at +83° (Fig 4.28D, open symbols). The peak torsional gain for rotation to the right was 0.40, occurring at +78° (Fig 4.28D, filled symbols). These were significantly different from each other ($F_{1,171}=4.00$) and represent an asymmetry in the torsional response.

Another normal animal had peak horizontal spatial gain of 1.01, occurring at -5° and gain 0.98 occurring at +5°, for left and right respectively (Fig 4.29A). These responses were significantly different from each other ($F_{1,171}=4.20$). The peak torsional gains were 0.53 occurring at +89° and 0.55 occurring at +93°, for left and right respectively (Fig 4.29D). The torsional gain curves were not significantly different from each other ($F_{1,171}=2.12$).

Figure 4.27: Horizontal (**A**, **B**)and torsional (**C**, **D**) eye velocity during constant velocity rotation to the right (**A**, **C**, **E**) and to the left (**B**, **D**, **F**), when animal (**M9308**) was tested in upright position after plugging all six canal. Rotation in this position produced predominantly a horizontal component of eye velocity. Each graph represents the superposition of several eye velocity responses. **E** and **F** are the velocities of the head rotation. The abscissa represents time in msec and is synchronized to the start of head rotation. The ordinate is velocity in °/s.

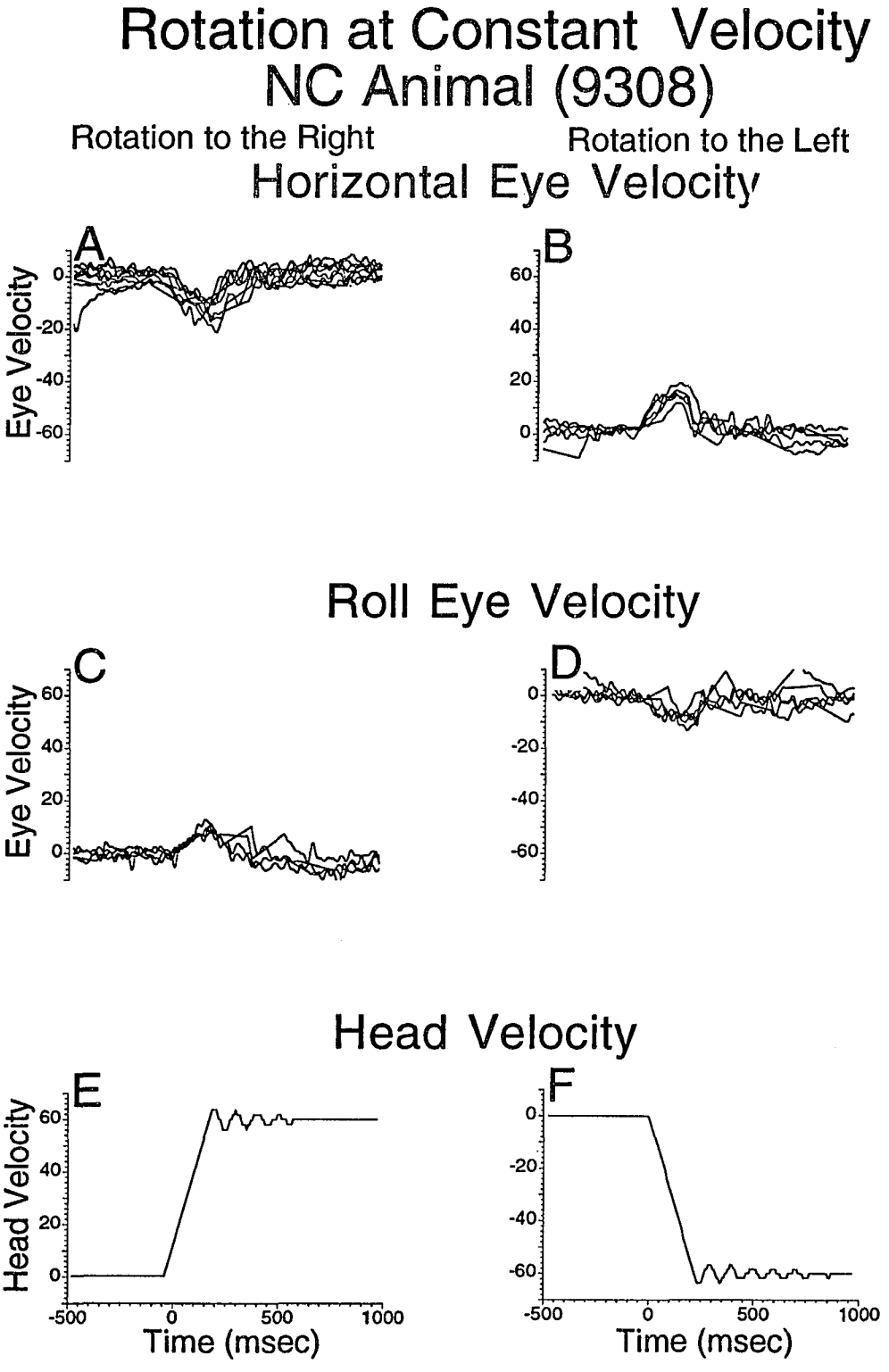
Rotation at Constant Velocity
NC Animal (9308)
Rotation to the Right
Rotation to the Left
Horizontal Eye Velocity
A
B
Eye Velocity
0
-20
-40
-60
60
40
20
0
Roll Eye Velocity
C
D
Eye Velocity
60
40
20
0
0
-20
-40
-60
Head Velocity
E
F
Head Velocity
60
40
20
0
0
-20
-40
-60
-500
0
500
1000
Time (msec)
-500
0
500
1000
Time (msec)

Figure 4.28: Average gains of the yaw (**A** - **C**) and roll (**D** - **F**) components from monkey (**M9308**) before plugging the canals (**A**, **D**) and corresponding yaw and roll gains from the same monkey after all six semicircular canal were plugged (**B** - **C**, **E** - **F**). Open symbols on **A** and **D** correspond to rotations to the left, while filled symbols correspond to rotations to the right. When the monkey was tested with step of velocity before surgery the gains were the same as obtained from sinusoidal rotation at 0.2 Hz, 60°/s. in darkness (dotted line) (**A**, **D**). After surgery, gains were reduced for rotation in both directions (filled symbols; **B**, **E** and **C**, **F**), but spatial phases of the responses were close to pre-surgical values. Gain curves for rotation to the left (**B**, **E**) were not different from the gain curves for rotation to the right (**C**, **F**). The solid lines in **B**, **C**, **E** and **F** represent the average gain for steps of rotation obtained before surgery and shown in **A** and **D** as symbols. Dashed lines represent zero velocity.

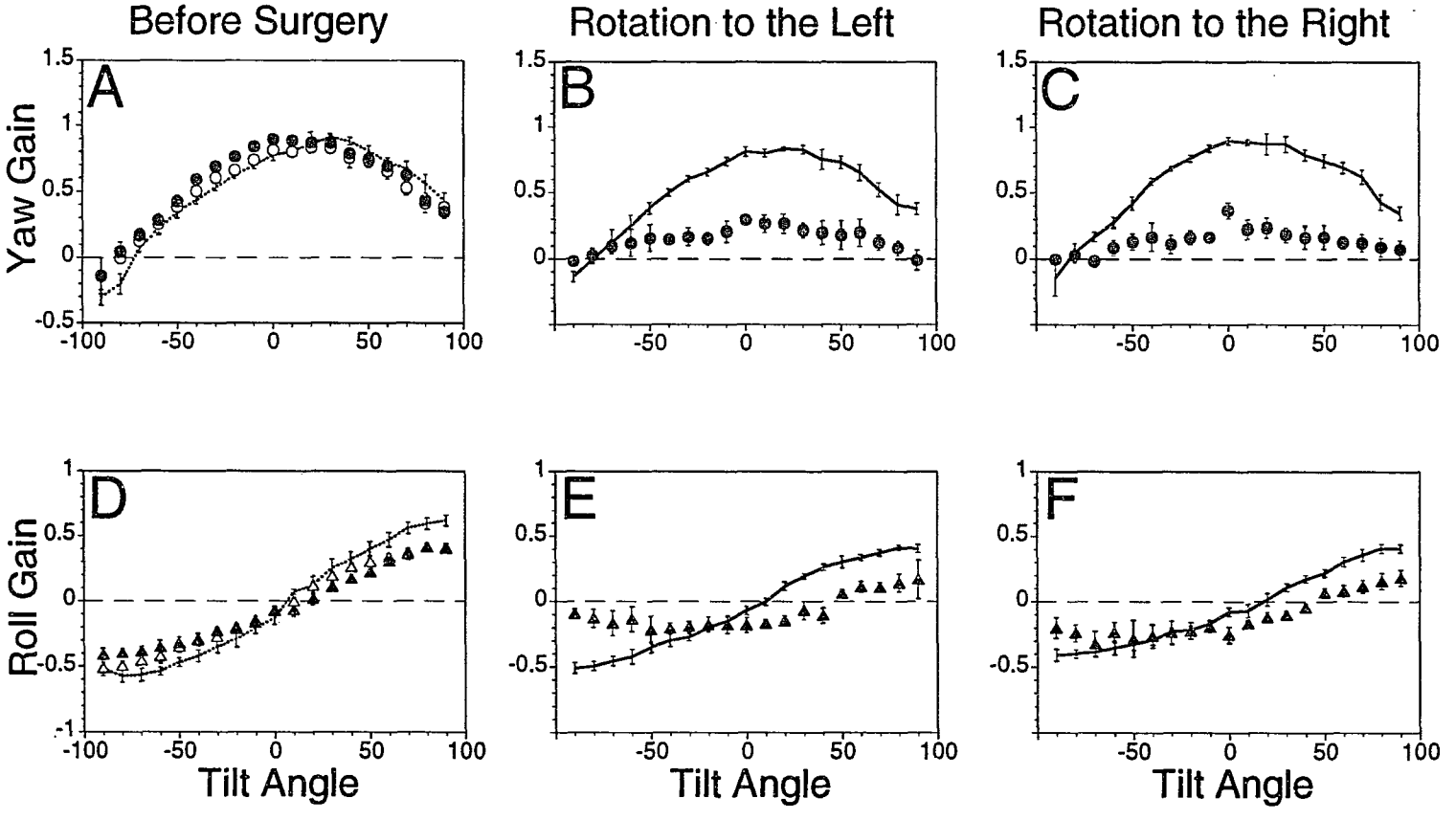
Before Surgery
Rotation to the Left
Rotation to the Right
A
B
C
D
E
F
Yaw Gain
Roll Gain
Tilt Angle
Tilt Angle
Tilt Angle
1.5
1
0.5
0
-0.5
-1
-100
-50
0
50
100

Figure 4.29: Average gains of the yaw (**A** - **C**) and roll (**D** - **F**) components from monkey (**M9306**) before plugging the canals (**A**, **D**) and corresponding yaw and roll gains from the same monkey after all six semicircular canal were plugged (**B** - **C**, **E** - **F**). Open symbols on **A** and **D** correspond to rotations to the left, while filled symbols correspond to rotations to the right. When the monkey was tested with step of velocity before surgery the gains were the same as obtained from sinusoidal rotation at 0.2 Hz, 60°/s. in darkness (dotted line) (**A**, **D**). After surgery, gains were reduced for rotation in both directions (filled symbols; **B**, **E** and **C**, **F**), but spatial phases of the responses were close to pre-surgical values. Gain curves for rotation to the left (**B**, **E**) were different from the gain curves for rotation to the right (**C**, **F**). The solid lines in **B**, **C**, **E** and **F** represent the average gain for steps of rotation obtained before surgery and shown in **A** and **D** as symbols. Dashed lines represent zero velocity.

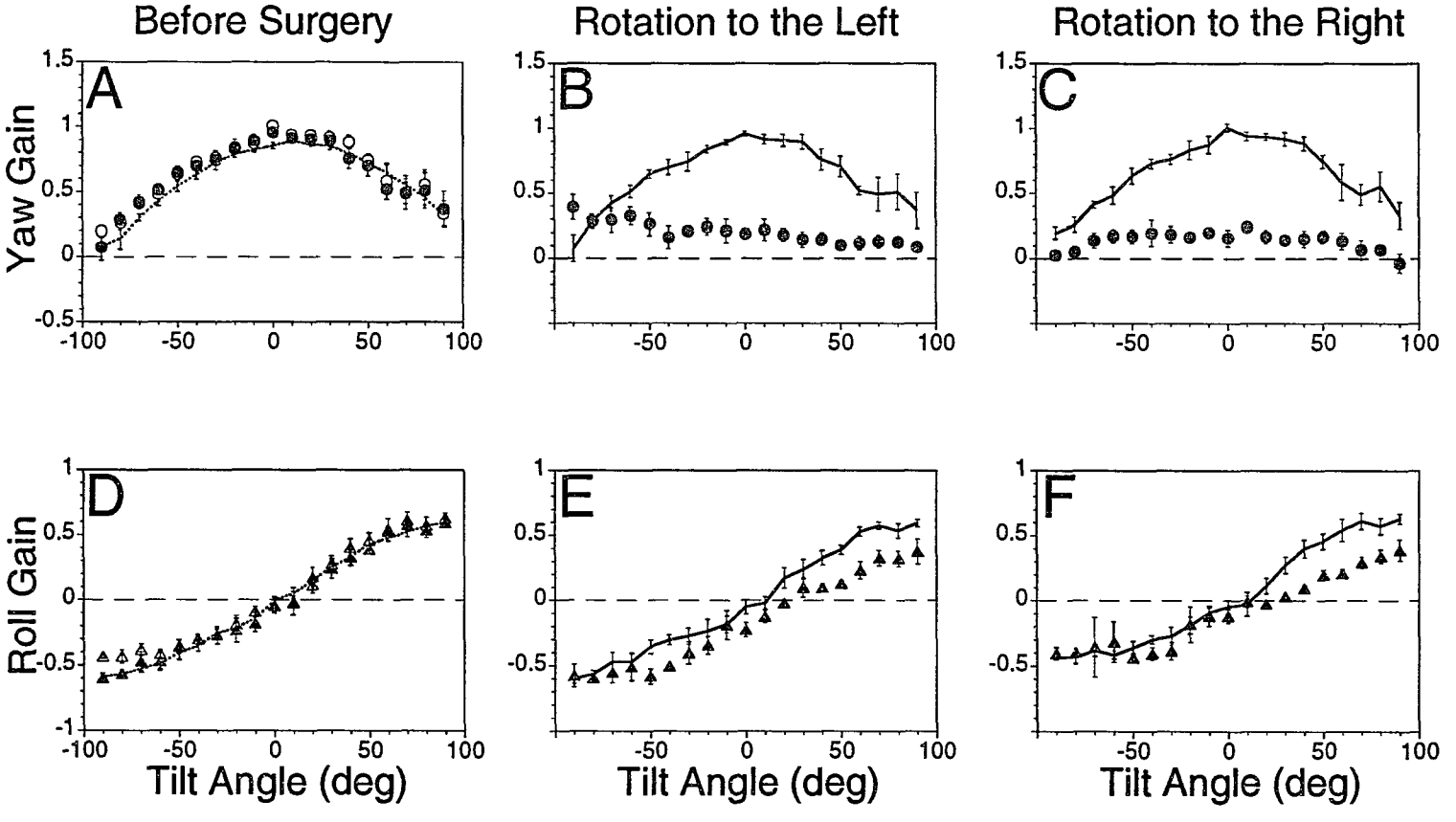
Before Surgery
Rotation to the Left
Rotation to the Right
A
B
C
D
E
F
Yaw Gain
Roll Gain
Tilt Angle (deg)
Tilt Angle (deg)
Tilt Angle (deg)

4.5.2 CANAL PLUGGED CHARACTERISTICS:

The step response spatial gain characteristics were obtained for the **NC** and **LARP** animals. For the NC animal, rotation to the left produced a peak horizontal spatial gain of 0.25 occurring at +7° tilt forward (Fig 4.28B, symbols). For rotations to the right (Fig 4.28C, symbols), peak horizontal spatial gain was 0.23 occurring at +10° tilt forward. These were not significantly different from each other ($F_{1,171}=1.31$). However, both of the responses were significantly different from corresponding normal responses ($F_{1,171}=5.34$, rotation left; $F_{1,171}=6.73$, rotation right). The peak torsional gain for rotation to the left was 0.28, occurring at -44° (Fig 4.28E, symbols). The peak torsional gain for rotation to the right was 0.21, occurring at -59° (Fig 4.28F, symbols). These were not significantly different from each other ($F_{1,171}=2.09$). However, both of the responses were significantly different from corresponding normal responses ($F_{1,171}=11.42$, rotation left; $F_{1,171}=20.00$, rotation right).

The spatial gain characteristics for the step response had a peak gain which was close to the peak gain obtained at 1 Hz of sinusoidal rotation for the same animals after canal plugging. It was smaller than the gain obtained at higher frequencies of rotation. This is probably due to the fact that the plugged canal had a short time constant. From Fig 4.27A,B it could be estimated as approximately 75 msec. As noted above, the step of rotation velocity had a rise time of approximately 200 msec for 60°/s. peak velocity. This corresponds to an acceleration of 300°/s^2. Under these circumstances eye velocity would rise towards a final velocity of 22.5°/s. (0.075*300), due to the acceleration. During the interval of 200 msec with time constant of 0.075 sec, the final eye velocity

should be 22.5(1-exp(-0.2/0.075)). This would give a peak velocity of approximately 21°/s. and correspond to a gain of 0.3. The measured gain was approximately 0.25. The implication is that the 3 db cutoff for the frequency response would be at 1/0.075 or 13 Hz. The range of frequencies tested in the sinusoidal spatial gain experiments only ranged to 4.0 Hz. Although there was a rising trend in the gain vs frequency characteristic, the 3 dB point was difficult to determine. Studies at high frequencies could address this question.

For the **LARP** animal, rotation to the left produced a peak horizontal spatial gain 0.25 but data could not be fit by a sinusoid (Fig 4.29B, symbols). For rotations to the right (Fig 4.29C, symbols), peak horizontal spatial gain was 0.21 occurring at -5° tilt backward. These were significantly different from each other ($F_{1,171}=6.16$) and both of the responses were significantly different from corresponding normal responses ($F_{1,171}=4.61$, rotation left; $F_{1,171}=6.48$, rotation right). The peak torsional gain for rotation to the left was 0.51, occurring at -64° (Fig 4.29E, symbols). The peak torsional gain for rotation to the right was 0.39, occurring at -60° (Fig 3.25F, symbols). These were not significantly different from each other ($F_{1,171}=2.72$). Rotation to the left after canal plugging was not significantly different from the data obtained before surgery ($F_{1,171}=2.28$). However, for rotation to the right it was significantly different from corresponding normal responses ($F_{1,171}=4.23$).

CHAPTER 5

DISCUSSION:

The experiments support the idea that when the head is rotated, there is a geometrical projection of the head velocity vector onto the planes of the semicircular canals to drive eye velocity. They show that each semicircular canal contributes horizontal and torsional components of eye velocity to the compensatory aVOR independently according to its geometrical orientation within the head in the normal or canal-plugged animal. It was possible to predict the data from the model for the normal and plugged animals using a non-orthogonal coordinate frame and a single set of parameters obtained from modelling the normal animals' data. Had there been significant spatial gain or phase adaptation following plugging, the spatial phases of the summated curves would be different from the model predictions. Therefore, we conclude that there was no spatial adaptation after canal-plugging, and that the geometric association between the canals and the oculomotor system, represented by the gain parameters of the model, was not altered by plugging. Regardless of variation from any source, the average phase error for the 95% confidence level in the 32 data sets from the eight animals was $\pm$ 8°. The analysis of variance indicated that on average the model fits to the data were within this resolution. There was also sufficient power to detect changes of phase of one degree and amplitude of 0.01.

Although the yaw and roll eye velocity components were spatially out of phase by $\approx$90° in the normal animals, they were in phase or 180° out of phase when the aVOR was produced by one or more single canal pairs. As a result, the eyes had a

torsional component associated with rotation about a yaw axis in darkness after lateral or vertical canal plugging (Figs 4.7-4.10 and Fig 4.12) where there was none in the normal animal (Fig 4.11A, C) or during rotation in light (Fig 4.14). This inappropriate roll component must have caused visual-vestibular conflict when the animals moved their heads in light after plugging. That the animals did not adaptively suppress the roll component during yaw axis rotation in darkness was surprising, considering the remarkable plasticity of the vestibular system, as well as the ability of the brain to alter spatial responses during visual-vestibular conflict stimulation (Schultheis and Robinson 1981; Baker et al. 1986, 1987).

The fact that both the horizontal and torsional gains were phase shifted in the same way when the vertical canals were plugged and only the lateral canals were intact demonstrates that a torsional component is produced by the lateral canals in the normal animal. When the normal animal is upright and rotated, the torsional component generated by the lateral canals superposes with that from the vertical canals to produce a zero torsional response. Similarly, there is a superposition of the yaw component of eye velocity produced by the lateral and vertical canals to generate a maximum response at zero spatial phase or close to the upright position.

Peak horizontal gains for the normal animal, calculated by Böhmer et al. (1985), occurred at 15° tilt forward. This value is close to the angle at which peak horizontal gains occurred in our normal animals (11°, range -1° to 19°, Table 4.3). It is different from the mean lateral canal orientation in our animals, however, which was predicted to be about 30°. The latter is close to predictions from the physiological data of Miles and

Braitman (1980b). Data in both Böhmer et al. (1985) and this study are consistent with the interpretation that the peak horizontal aVOR response is dependent on activation of both the lateral and vertical canals. This would explain why the null point for the horizontal gain curve crossed zero away from the 15° tilt position after lateral canal plugging.

After surgery, the animals initially had postural instability as well as head titubation in the planes of the plugged canals. After recovery, their behavior was close to that of normal animals, with the exception of slight instability of the head during movement in the plugged canal planes. There were small differences between the normal gains and those obtained from a summation of the responses after canal-plugging. These differences were also present in a comparison of model predictions and observed post-canal plugging responses. These small gain increases could not have been responsible for the behavioral adaptation that was present in each of the animals. Rather, recovery was likely to be due to the dependence on visual-oculomotor reflexes (Fig 4.14), on enhanced cervico-ocular reflexes (Dichgans et al. 1973; Böhmer et al. 1985) and on adaptation of posture (for review, see Curthoys and Halmagyi 1995). This may have clinical significance in that recovery after labyrinthine lesions in humans may mask the effects of the lesion, and deficits may be expressed during appropriate stimulation.

There is evidence that the axis of eye velocity is not aligned with the axis of rotation when the eye looks up or down during rotation of the head about a yaw axis (Henn et al. 1992; Misslisch et al. 1994). However, the axis shift is variable and for small vertical shifts of the eyes ($<$7-8°), the axis shift will be less than 3° in both

monkeys and humans (Crawford and Vilis 1991; Misslisch et al. 1994). Thus, our method of orthogonalization of the coils would not significantly impact our analysis or the conclusions drawn from it, particularly since our analysis is focussed on the relative changes in horizontal and torsional changes in eye velocity before and after plugging of individual semicircular canals. Computation of spatial gains using eye velocity in head coordinates (Appendix A) would also not alter our results or conclusions. Data plotted for yaw and roll eye velocities as a function of tilt angle in the normal animal (Fig 4.12A, E), and after canal plugging (Fig 4.12B-D, F-H), confirmed that there was no significant difference between the results derived from a differentiation of coil voltages and from computation of eye velocity in head coordinates for any of the canal-plugged conditions (ANOVA, $p=0.05$).

The zero crossings of the model predictions for the normal responses occurred at $\pm$ 90° for yaw (Fig 4.15A). These were close to the experimental data. Variation increased for yaw at $\pm$ 90° (Fig 4.11A). A likely explanation for the increase in variance is the change in vertical eye position when the animals were tilted forward or back due to compensatory static otolith-ocular reflexes (Fig 4.6). The horizontal component of eye velocity induced by rotation around a spatial vertical varied as the cosine of the angle between the axis of eye rotation and the yaw axis. The nature of the sine function is such that the amplitude of the horizontal component is largest with the animal upright, but the sensitivity of change in the horizontal component is largest with the animal supine or prone and smallest with the animals upright. Thus, small upward or downward movement of the eyes could easily increase the horizontal component of the aVOR when the animals

were in forward or backward pitch, although the same vertical deviations would have little effect when the animals were upright.

The peak yaw gain after vertical canal plugging occurred at approximately 30° (Fig 4.7A). The maximum yaw gain after lateral canal plugging occurred at ≈ -50° (Table 4.3). From these values, we estimated that the average horizontal canal planes were tilted about 30° back relative to the stereotaxic horizontal plane, whereas the vertical canals were tipped back ≈ 40°, the values used in simulating the data. There were variations among the monkeys that could easily be simulated by changing these angles in the model. In some instances, there were phase shifts between the yaw and roll peaks for the plugged animals which could not be encompassed by this model. These phase shifts were not significant from a statistical point of view, and at present we have ignored them. The angles of the lateral and vertical canal planes are about 10° more in our data than in the study of Reisine et al. (1988). They are in general agreement with calculations of others, however (Blanks et al. 1975; Blanks et al. 1985). Differences between the various studies may be due to individual variation based on species or differences between animals or to differences in the placement of the head in the stereotaxic frames (Curthoys et al. 1977).

A critical factor in predicting the results was incorporating a non-orthogonal coordinate frame in the model. This was necessary to explain the finding that the maximal horizontal and roll components occurred at ≈30° tilt forward when the lateral canals were intact as compared the maximal components at - 50° tilt back when only the vertical canals were intact. The difference between the two is not 90°. As a result, it is

not possible to activate the lateral canals maximally with rotation without activating the vertical canals. Conversely, it is not possible to activate the vertical canals maximally with rotation without activating the lateral canals. Despite the fact that there is a non-orthogonal frame, the normal animal would have a peak in the upright at 0° because of the contributions of all of the canals.

The non-orthogonality found in this behavioral study is supported by both anatomical and physiological data. In the rhesus monkey, the non-orthogonality of the relationship between the lateral and the vertical canals was in the order of 10° (Blanks et al. 1985; Reisine et al. 1988), as in this study. The non-orthogonality is greater in the guinea pig and in man (Blanks et al. 1975). Minor and Goldberg (1990) tested the horizontal contribution to the aVOR when the lateral canals were presumed vertical. They concluded that "signals from the horizontal, but not the vertical canals contribute to the HVOR.", whereas we have inferred an important vertical canal contribution. Differences between the studies are that Minor and Goldberg (1990) assumed orthogonality of the vertical and lateral canals, whereas we found that a non-orthogonal canal coordinate frame was better able to approximate the data in our animals.

Baker and Peterson (1991) assumed from the data of Curthoys et al. (1977) that the amount of non-orthogonality between the vertical and lateral canals in the cat was 6°. By tipping animals forward by 28°, they further assumed that the vertical canals were vertical. A larger angle of tilt of the vertical canals with regard to the lateral canals in individual cats could cause a greater contribution of the individual canals in the activation of individual muscles, perhaps accounting for differences between their study and those

utilizing mechanical or electrical stimulation of the canals (Szentagothai 1950; Cohen et al. 1964; Suzuki et al. 1964; Tokumasu et al. 1965).

There were differences in the gain values between the data from the normal animals and the summed **LC** and **VC** animals, and between the **VC** animals and the summed **LARP** and **RALP** animals (Figs 4.8 and 4.11). The spatial gains were slightly greater for the operated animals. This can be explained by an adaptive increase in the gains of the horizontal and torsional components. Such adaptation, however, would have to occur concurrently in the torsional and roll components, otherwise it would cause a change in the spatial phases of the response, which did not occur.

The conclusion about the spatial invariance of canal induced components of the aVOR with regard to the head is limited to the direct vestibular pathway which is predominantly active during frequencies of sinusoidal rotation between 0.1 and 8 Hz, the range of normal head movements. Below this frequency, cross-coupling of velocity storage would have converted the head-fixed, directional responses after canal plugging into responses that were oriented around gravity (Dai et al. 1991; Raphan and Sturm 1991; Raphan et al. 1992).

The model also predicted that a vertical component would appear in the **RALP** and **LARP** animals. This was observed as is shown in Figs 4.1B-4.4B ($\dot{V}$). The reason for this vertical component is that the activated canal pair in the **RALP** and **LARP** animals is shifted $\approx 45°$ from the midline, causing a vector projection on the X axis.

One question which had arisen during the course of this work was whether the spatial invariance of canal induced components of the aVOR extended over a wide range

of frequencies. Recent work has suggested that central adaptation due to canal plugging is frequency dependent and occurs mainly at higher frequencies (Angelaki et al. 1995). The work presented here indicates that the response characteristic of a plugged canal is frequency dependent and its response gain goes up with frequency. At 0.2 Hz, the response is essentially abolished. Canal plugging, therefore, does not abolish the response of the canal, but merely alters its response characteristics as a function of frequency of stimulus. The physiological mechanism by which this is accomplished requires further study.

Our results indicate that there is an approximate linear rise of horizontal aVOR gain with regard to frequency in the all canal plugged animal up to 4 Hz. Whether the gain continues to rise and where it levels off would be of interest in predicting the step response of the all canal plugged animals. For example, if the 3 db cutoff of the plugged canal animal response would be at 8-10 Hz, it would correlate well with the step response which has a time constant of about 100 msec. The step response spatial characteristics had a lower gain, but maintained the same spatial phase characteristics as the normal. This supports our contention, because the step response has spectral power at high frequencies. The gain would be expected to be lower because the low frequency power would be cut off. Thus, the changes in gain and phase as a function of frequency attributed to central adaptation (Baker et al. 1982; Böhmer et al. 1985; Angelaki et al. 1995) is due to the frequency response of the plugged canal and not to adaptation.

There were differences between the horizontal and torsional spatial gain responses in the canal plugged animals. If canal plugging at different distances relative to the

ampulla alters the frequency characteristics of the plugged canal in different ways, it could explain the observed differences between the horizontal and torsional components of the aVOR over a wide range of plugged conditions.

In summary, the data support the hypothesis that the individual canal pairs encode the projection of head velocity onto the normals of their planes. They then contribute eye velocity components according to their vector projections along the head coordinate frame in which eye movements are measured. The gains and the spatial phases of the horizontal component were the same after lateral canal plugging at low frequencies (0.2 Hz) as in previous studies (Baker et al. 1982; Böhmer et al. 1985; Cohen et al. 1988). At higher frequencies, the plugged canal contributes to the response. The finding that the data from separate animals with different combinations of plugging of individual semicircular canals could be combined to predict the response of the normal and the canal plugged monkeys was internally consistent. These data suggest that despite considerable plasticity in the aVOR, the canal coordinate system is hard-wired, and that the innate coordinate frame with regard to the head is not altered in adult animals by inactivation of the individual canals.

CHAPTER 6

SUMMARY AND CONCLUSIONS

6.1 SUMMARY

We studied the contribution of the individual semicircular canals to the generation of horizontal and torsional eye movements in cynomolgus monkeys (Macaca fascicularis). Eye movements were elicited by sinusoidal or constant velocity rotation of the monkey about a vertical (gravitational) axis with the animals tilted in various attitudes of static forward or backward pitch. The gains of the horizontal and torsional components of the angular vestibulo-ocular reflex (aVOR) were measured for each tilt position. The gain as a function of tilt position was fit with a sinusoidal function, and the spatial gain and phase were determined. After recording control responses, the semicircular canals were plugged, animals were allowed to adapt and the test procedure was repeated. Animals were prepared with only the anterior and posterior canals intact (vertical canal (VC) animals), only the lateral canals intact (lateral canal (LC) animal) and only one anterior and the contralateral posterior canals intact (right anterior and left posterior canal (RALP) animals; left anterior and right posterior canal (LARP) animals). One animal was prepared with all six semicircular canals plugged (NC animal).

The gain of the horizontal (yaw axis) velocity of the compensatory movements of normal animals was determined at 0.2 Hz and 60°/s. The gain was maximal at 11° tilt forward and decreased as they were pitched forward or backward. Torsional gains were maximal when animals were tilted 90° forward and minimal at 90° tilt backward. Torsional gains decreased to zero, when animals were upright. Gain value as a function

of tilt were plotted and fit with sinusoids. Spatial gain (peak value) and spatial phase (phase shift relative to stimulus) were calculated for each graph. Horizontal and torsional gains tested with constant velocity of rotation had the same spatial gain and phases as described above. After the anterior and posterior canals were plugged (**LC** animal), the horizontal component was reduced when the animal was tilted backward; the gain was zero with about -60° backward tilt. The spatial phase of the torsional component had the same characteristics. This is consistent with the fact that both responses are produced by the lateral canals which from our results are tilted between 28° and 39° above the horizontal stereotaxic plane.

After both lateral canals were plugged (**VC** animals), horizontal velocity was reduced in the upright position but increased as the animals were pitched backward relative to the axis of rotation. Torsional velocities, which were zero in the upright position in the normal animal, were now 180° out of phase with the horizontal velocity. The peak values of the horizontal and torsional components were significantly shifted from the normal data and were closely aligned with each other, reaching a peak value at approximately -56° pitched back (-53° horizontal, -58° torsional). The same was true for the **LARP** and **RALP** animals; the peak values were at -59° pitched back (-55° horizontal, -62° torsional). Likewise, in the **LC** animal, the peak yaw and roll gains occurred at about the same angle of forward tilt, 35° (30° horizontal, 39° torsional). Thus, in each case, the canal plugging had transformed the aVOR from a compensatory to a direction-fixed response with regard to the head. Thus, there was no adaptation of the response planes of the individual canals after plugging.

The data were compared to eye velocity predictions of a model based on the geometric organization of the canals and their relation to a head coordinate frame. The model used the normal to the canal planes to form a non-orthogonal coordinate basis for representing eye velocity. An analysis of variance was used to define the goodness of fit of model predictions to the data. Model predictions and experimental data agreed closely for both normal animals and for the animals after canal plugging. Moreover, if horizontal and roll components from the **LC** and **VC** animals were combined, the summation overlay the response of the normal monkeys and the predictions of the model. In addition, a combination of the **RALP** and **LARP** animals predicted the response of the lateral canal plugged (**VC**) animals. If significant adaptation of central organization of the aVOR had occurred after plugging, then the summed responses from the **LC** and **VC** animals would have been significantly different from the data obtained from the normal animals. This inability to reconstruct normal responses from the plugged responses would have been reflected in the models inability to fit the data without changing the model parameters.

When the operated animals were tested in light, the gains, peak values and spatial phases of horizontal and roll eye velocity returned to the preoperative values, regardless of the type of surgery performed. This indicates that vision, perhaps utilizing smooth pursuit, had compensated for the lack of spatial adaptation of the response planes after plugging. It converted a non-compensatory, direction-fixed response with regard to the head to an appropriate compensatory response.

There was also an approximately linear rise of horizontal aVOR gain with regard

to frequency up to 4 Hz in the animal for which all six canals were plugged. However, there were differences between the horizontal and torsional spatial gain responses in the canal plugged animals. The step response spatial characteristics had a lower gain, but maintained the same spatial phase characteristics as the normal. Thus, the changes in gain and phase as a function of frequency attributed to central adaptation (Baker et al. 1982; Böhmer et al. 1985; Angelaki et al. 1995) is due to the frequency response of the plugged canal and not to adaptation.

These results indicate that :

1. Each pair of semicircular canals contributes to eye velocity by its projection to head coordinates and there is no adaptation of the response due to the remaining semicircular canals.

2. Otoliths do not contribute to angular vestibulo-ocular reflex when rotation is about a spatial vertical axis. This has been shown for low frequencies and we conjecture that it holds at high frequencies.

3. Vision compensates at low frequencies for canal inactivation.

4.Commonly accepted method of canal plugging has a limitation in that it does not inactivate the response at high frequencies.

6.2 RECOMMENDATION FOR FUTURE RESEARCH

Future research in this area could take several directions:

1. The present study deals with horizontal and torsional gain components of the aVOR. Raphan's model (Yakushin et al. 1995) predicts that if animals are tilted on the side during rotation around the spatial vertical axis, the horizontal and vertical, rather

than torsional components would be varied as a function of tilt angle. However, behavioral studies to test the model have not been done. If the data fit the model with unmodified parameters, it would strengthen our hypothesis about how the semicircular canals control the aVOR at low frequencies.

2. The present study has indicated that sinusoidal and step velocity stimulations could be explained by one model. To do this the 3 dB cutoff of the aVOR gain should be evaluated for the monkeys with different canal plugging and compared to the time constant of the step response. To evaluate this important parameter the stimulus frequency should be increased up to 10-13 Hz.

3. The work presented here indicates that the response characteristic of a plugged canal is frequency dependent and its response gain goes up with frequency. At 0.2 Hz, the response is essentially abolished. Canal plugging, therefore, does not abolish the response of the canal, but merely alters its response characteristics as a function of frequency of the stimulus. However, this was not directly proven. To demonstrate it, the primary afferent's activity should be recorded at different frequencies of rotation of the animal for which all six canals were plugged. If modulation of canal afferents are activated by high frequency stimulation but not at low frequencies, it would directly support our hypothesis. It is unlikely that the otolith system significantly contributes to the high frequency responses, but it can not be rejected without actual testing of the primary vestibular fiber activity of the animal for which all six canals were plugged. Unit recording could be done during studies of canal plugged animals as suggested above (2).

4. This study demonstrates that there is no aVOR gain adaptation to plugging the

push-pull pair of the semicircular canals. Whether the system adapts to neurectomy of specific branches of the nerve is not known. If this kind of lesion does generate adaptation it would further enhance our understanding of the mechanisms of central adaptation.

APPENDIX A:

COMPUTATION OF EYE VELOCITY IN HEAD COORDINATES AND COMPARISON WITH DERIVATIVES OF COIL VOLTAGES

The voltages, V_{fx}, and V_{fz}, derived from the frontal coil are proportional to the inner products of the normal to the frontal coil, $\hat{n}_f$, with unit vectors, e_x, e_z, along the X and Z axes, respectively. The voltage V_{tx}, is proportional to the inner product of the normal to the top coil, $\hat{n}_t$, with the unit vector along the X axis, e_x. These voltages can be related to the rotation matrix which describes the orientation of the eye with respect to the head using various parameterization techniques, including quaternions (Westheimer 1957, Tweed and Vilis, 1987; Crawford and Vilis, 1991; Tweed et al., 1990), rotation vectors (Haustein 1989, Haslwanter et al. 1992), Euler angles (Collewijn et al., 1988) and axis-angle (Schnabolk and Raphan, 1994). These different representations are not different coordinate frames but relate the eye coordinate frame to the head frame. These different parameterizations can in turn be related to each other. Since the computation of eye velocity is uniquely determined as a vector in head coordinates, it is independent of the formalism for describing eye orientation, which is not a vector. That is, any representation of eye position would lead to the same eye velocity which is the primary interest of this paper.

A simple parameterization of the rotation matrix is through Euler angles (Euler 1748). These can be chosen in a variety of ways, one of which corresponds to Fick angles (1854). This describes the rotation about a fixed point as a sequence of rotations given by three matrices:

$$R_{\phi}=\begin{bmatrix}\cos\phi & -\sin\phi & 0\\ \sin\phi & \cos\phi & 0\\ 0 & 0 & 1\end{bmatrix} \qquad \textbf{(Eq.14)}$$

$$R_{\theta}=\begin{bmatrix}1 & 0 & 0\\ 0 & \cos\theta & -\sin\theta\\ 0 & \sin\theta & \cos\theta\end{bmatrix} \qquad \textbf{(Eq.15)}$$

$$R_{\psi}=\begin{bmatrix}\cos\psi & 0 & \sin\psi\\ 0 & 1 & 0\\ -\sin\psi & 0 & \cos\psi\end{bmatrix} \qquad \textbf{(Eq.16)}$$

where ϕ, θ, and ψ are the Euler angles representing rotations about the head yaw axis, a line of nodes axis (rotated pitch axis) of the eye, and the optic axis (doubly rotated axis). The positive direction for the head based axes are shown in Figs 2.4 and 3.7 and the rotations are in accordance with the right hand rule. A vector in eye-based coordinates can be expressed in the head coordinate frame by the following transformation (Goldstein, 1980):

$$R=R_{\phi}R_{\theta}R_{\psi}=\begin{bmatrix}\cos\phi\cos\psi-\sin\phi\sin\theta\sin\psi & -\sin\phi\cos\theta & \cos\phi\sin\psi+\sin\phi\sin\theta\cos\psi\\ \sin\phi\cos\psi+\cos\phi\sin\theta\sin\psi & \cos\phi\cos\theta & \sin\phi\sin\psi-\cos\phi\sin\theta\cos\psi\\ -\sin\psi\cos\theta & \sin\theta & \cos\theta\cos\psi\end{bmatrix} \qquad \textbf{(17)}$$

Since the coil moves with the eye, the normal to the frontal coil can be expressed as (0, -1, 0) in eye coordinates, independent of eye orientation. This vector can be obtained in head coordinates by multiplying it by the rotation matrix given in Eq. 17.

Therefore, in head coordinates, the vector is given by $\hat{n}_f = (\sin\phi\cos\theta, -\cos\phi\cos\theta, -\sin\theta)$. The top coil normal is given by (0, 0, 1) in eye coordinates. This vector can similarly be transformed by Eq. 8 to head coordinates to a vector, $\hat{n}_t = (\cos\phi\sin\psi+\sin\phi\sin\theta\cos\psi, \sin\phi\sin\psi-\cos\phi\sin\theta\cos\psi, \cos\theta\cos\psi)$. The voltage output for the coil system, scaled to values between [-1, 1], can be represented as inner products of the coil vectors, $\hat{n}_f$ and $\hat{n}_t$, with unit vectors along the field coil axes. Because, in this study, the horizontal, vertical and roll voltages were recorded as positive for movements to the right, up and clockwise from the animal's point of view, the negative of the voltages V_{fx}, V_{fz}, and V_{tx}, are the inner products of $\hat{n}_f$ with e_x, $\hat{n}_f$ with e_z, and $\hat{n}_t$ with e_x, respectively. In terms of Euler angles, this can be expressed as follows:

$$\begin{aligned} -V_{fx} &= \sin\phi\cos\theta \\ -V_{fz} &= \sin\theta \\ -V_{tx} &= \cos\phi\sin\psi+\sin\phi\sin\theta\cos\psi \end{aligned} \qquad \textbf{(Eq.18)}$$

The derivatives of these voltages can be expressed in terms of the Euler angles and their derivatives as follows:

$$\begin{aligned} -\dot{V}_{fx} &= (-\sin\phi\sin\theta)\dot{\theta}+(\cos\theta\cos\phi)\dot{\phi} \\ -\dot{V}_{fz} &= (\cos\theta)\dot{\theta} \\ -\dot{V}_{tx} &= (\sin\theta\cos\phi\cos\psi-\sin\psi\sin\phi)\dot{\phi}+(\sin\phi\cos\psi\cos\theta)\dot{\theta}+(\cos\phi\cos\psi-\sin\phi\sin\theta\sin\psi)\psi \end{aligned} \qquad \textbf{(Eq.19)}$$

A simple algorithm can be derived to compute the components of eye velocity in

head coordinates, ω, from the coil voltages at each instance of time as follows:

From Eq. 18, the Euler angles representing eye orientation can be obtained sequentially from the coil voltages as follows:

$$\theta = \sin^{-1}(-V_{fz})$$
$$\phi = \sin^{-1}\left(\frac{-V_{fx}}{\cos\theta}\right) \qquad \textbf{(Eq.20)}$$
$$\psi = \sin^{-1}\frac{-V_{tx}}{\sqrt{\cos^2\phi + \sin^2\phi\sin^2\theta}} - \tan^{-1}\frac{\sin\phi\sin\theta}{\cos\phi}$$

Using the Euler angles computed in Eq. (20), the derivatives of the Euler angles can be obtained sequentially from Eq. 19 as follows:

$$\dot{\theta} = -\frac{\dot{V}_{fz}}{\cos(\theta)}$$
$$\dot{\phi} = -\dot{V}_{fx} + \frac{\sin\phi\sin\theta}{\cos\phi\cos\theta}\dot{\theta} \qquad \textbf{(21)}$$
$$\dot{\psi} = \frac{-\dot{V}_{tx} - (\sin\theta\cos\phi\cos\psi - \sin\psi\sin\phi)\dot{\phi} - (\sin\phi\cos\psi\cos\theta)\dot{\theta}}{\cos\phi\cos\psi - \sin\phi\sin\theta\sin\psi}$$

The components of the angular velocity vector along the pitch (X), roll(Y), and yaw (Z) axes of the head are given in terms of the Euler angles and their derivatives by (Goldstein, 1980):

$$\omega_x=(\cos\phi)\dot{\theta}-(\sin\phi\cos\theta)\psi$$
$$\omega_y=(-\sin\phi)\dot{\theta}+(\cos\phi\cos\theta)\psi \qquad \textbf{(Eq.22)}$$
$$\omega_z=\dot{\phi}+(\sin\theta)\psi$$

where the ω_x, ω_y, and ω_z are the components of angular velocity of the eyes in head coordinates, and $\dot{\phi}$, $\dot{\theta}$, and $\dot{\psi}$ are the derivatives of the Euler angles. Substituting the values obtained in equations 20 and 21 into equation 22 generates the components of the angular velocity, ω_x, ω_y, and ω_z, in head coordinates at each instant in time. It should be noted that for small angles ($< 15°$), the angular velocity in head coordinates is approximately equal to the derivatives of the Euler angles which are in turn approximately equal to the derivatives of the coil voltages. That was tested with the program written in BASIC 7.1 (Appendix D). A sample of processed data is shown on Fig 3.5. The same measurements were performed based on voltage derivatives and on derivatives of the Euler angles. The result demonstrate that there are no significant differences between the two types of data for four monkeys tested after surgery.

APPENDIX B:
PREDICTION OF THE NORMAL aVOR GAINS AND RESULTS OF THE SEMICIRCULAR CANAL PLUGGING.

This program is written in BASIC 7.1 based on the model of how individual semicircular canals contribute to the three dimensional gain of the aVOR (Yakushin et al. 1995).

```
'*************************************************************************
' * This Program can calculate gains of the Horizontal, Vertical and      *
' * Torsional aVOR During Sine (or velocity-step) rotation for the normal *
' * animals and for animals with complementary canal plugging. That is    *
' * animals can have lateral canals plugged (VC-animal), Right Anterior and*
' * Left Posterior canal intact (RALP), Left Anterior and Right           *
' * Posterior Canal intact (LARP) or any combination of these three       *
' * cases. It suggests initial (default) gains and coupling coefficients, *
' * that can be modified according to any particular responses. Tilt can  *
' * occur in Forward-Backward of Left-Right Directions. Final gain        *
' * can be downloaded on the floppy disk (b:\) an ASCII format            *
'  *************************************************************************

REM *** Reserving data arrays for the Gains matrix (Gain!(2,2)) for values of shift in
REM *** Vertical eye position (VertEyePos(18)), Eigenvalues (egn(2, 18))
DIM Gain!(2, 2), VertEyePos(18), egn(2, 18), A!(2, 2), M(2, 2)
DIM eyegn(2, 19), inva(3, 3), agl(18)

REM *** Declaring the SUB programms that will be in use ***
DECLARE SUB Definitions (VertEyePos(), FileName1$)
DECLARE SUB Gmatrix (Gain!())
DECLARE SUB Graph (FileName2$, egn(), Gain!())
DECLARE SUB WriteFile (FileName2$, egn())

DEFSNG A-Z
SCREEN 12
CLS

REM ********** Parameters Used for Simulation **********
ThetaVert! = -40: ThetaHor! = -30
R                                   E                                   M
*************************************************************************

REM ** If Effect of the Vertical Eye Position Shift is NOT Counting,  ****
REM ** Then "VertEyePos()" array must be filed with zero               ****
```

```
Definitions VertEyePos(), FileName1$

R                                                                    E                                                                    M
**********************************************************************

REM ** Defining Tilt Direction ***************************************
LOCATE 5, 1
COLOR 2
PRINT "Tilt in Which Direction?";
COLOR 10
PRINT "  Enter ";
COLOR 4
PRINT "<F>";
COLOR 10
PRINT " for FRONTAL or ";
COLOR 4
PRINT "<L>";
COLOR 10
1 INPUT " for LATERAL"; Q4$
IF Q4$ = "F" OR Q4$ = "f" THEN Flag1 = 0: GOTO 3
IF Q4$ = "L" OR Q4$ = "l" THEN Flag1 = 1: GOTO 3
GOTO 1 ' In error go to the beginning of the cycle

REM ** Information about canal plugging ******************************
3 LOCATE 8, 10
INPUT "Enter Monkey ID Number"; FileName2$
IF FileName2$ = "" THEN GOTO 3
5 COLOR 5
LOCATE 10, 10
10 INPUT "Is Right Horizontal Canal Plugged "; Q1$
IF Q1$ = "Y" OR Q1$ = "y" THEN PlugLatRight = 0: GOTO 20
IF Q1$ = "N" OR Q1$ = "n" THEN PlugLatRight = 1: GOTO 20
GOTO 10
20 LOCATE 11, 10
INPUT "Is Left Horizontal Canal Plugged "; Q1$
IF Q1$ = "Y" OR Q1$ = "y" THEN PlugLatLeft = 0: GOTO 30
IF Q1$ = "N" OR Q1$ = "n" THEN PlugLatLeft = 1: GOTO 30
GOTO 20
30 LOCATE 12, 10
INPUT "Is Right Anterior Canal Plugged  "; Q1$
IF Q1$ = "Y" OR Q1$ = "y" THEN PlugAntRight = 0: GOTO 40
IF Q1$ = "N" OR Q1$ = "n" THEN PlugAntRight = 1: GOTO 40
GOTO 30
40 LOCATE 13, 10
```

```
INPUT "Is Left Anterior Canal Plugged    "; Q1$
IF Q1$ = "Y" OR Q1$ = "y" THEN PlugAntLeft = 0: GOTO 50
IF Q1$ = "N" OR Q1$ = "n" THEN PlugAntLeft = 1: GOTO 50
GOTO 40
50 LOCATE 14, 10
INPUT "Is Right Posterior Canal Plugged  "; Q1$
IF Q1$ = "Y" OR Q1$ = "y" THEN PlugPostRight = 0: GOTO 60
IF Q1$ = "N" OR Q1$ = "n" THEN PlugPostRight = 1: GOTO 60
GOTO 50
60 LOCATE 15, 10
INPUT "Is Left Posterior Canal Plugged   "; Q1$
IF Q1$ = "Y" OR Q1$ = "y" THEN PlugPostLeft = 0: GOTO 70
IF Q1$ = "N" OR Q1$ = "n" THEN PlugPostLeft = 1: GOTO 70
GOTO 60
70 REM
Gmatrix Gain!()

REM ********************** Theoretical Pitch Gain's **********************
PRINT "       Tilt "; "     Pitch   "; "    Roll    "; "     Yaw    "
FOR I% = 0 TO 18
ThetaV! = ((ThetaVert! - VertEyePos(I%)) / 57.29
ThetaH! = ((ThetaHor! - VertEyePos(I%)) / 57.29
Psi! = 45 / 57.29
A!(0, 0) = COS(Psi!)
A!(0, 1) = SIN(Psi!) * COS(ThetaV!)
A!(0, 2) = SIN(Psi!) * SIN(ThetaV!)
A!(1, 0) = -SIN(Psi!)
A!(1, 1) = COS(Psi!) * COS(ThetaV!)
A!(1, 2) = COS(Psi!) * SIN(ThetaV!)
A!(2, 0) = 0
A!(2, 1) = -SIN(ThetaH!)
A!(2, 2) = COS(ThetaH!)

REM ***************** Defining Direction of the Tilt **********************
W! = 1!
Alpha! = (I% - 9) * 10) / 57.29
IF Flag1 = 0 THEN Wroll! = W! * SIN(Alpha!)
IF Flag1 = 1 THEN Wroll! = 0
IF Flag1 = 0 THEN Wpitch! = 0
IF Flag1 = 1 THEN Wpitch! = W! * SIN(Alpha!)
Wyaw! = W! * COS(Alpha!)

WantLeft! = A!(0, 0) * Wpitch! + A!(0, 1) * Wroll! + A!(0, 2) * Wyaw!
WpostLeft! = A!(1, 0) * Wpitch! + A!(1, 1) * Wroll! + A!(1, 2) * Wyaw!
```

```
WlatLeft! = A!(2, 0) * Wpitch! + A!(2, 1) * Wroll! + A!(2, 2) * Wyaw!
WpostRight! = -WantLeft!
WantRight! = -WpostLeft!
WlatRight! = -WlatLeft!
Want! = ((PlugAntLeft * WantLeft!) - (PlugPostRight * WpostRight!)) / 2
Wpost! = ((PlugPostLeft * WpostLeft!) - (PlugAntRight * WantRight!)) / 2
Wlat! = ((PlugLatLeft * WlatLeft!) - (PlugLatRight * WlatRight!)) / 2

REM ******* Canal's Projection Head Coordinates to Calculate Eye Velocity **
PantPitch! = Gain!(0, 0) * COS(Psi!)
PantRoll! = (Gain!(1, 0) * COS(ThetaH!) * SIN(Psi!)) / COS(ThetaV! - ThetaH!)
PantYaw! = (Gain!(2, 0) * SIN(ThetaH!) * SIN(Psi!)) / COS(ThetaV! - ThetaH!)
PposPitch! = -Gain!(0, 1) * SIN(Psi!)
PposRoll! = (Gain!(1, 1) * COS(ThetaH!) * COS(Psi!)) / COS(ThetaV! - ThetaH!)
PposYaw! = (Gain!(2, 1) * SIN(ThetaH!) * COS(Psi!)) / COS(ThetaV! - ThetaH!)
PlatPitch! = 0
PlatRoll! = -(Gain!(1, 2) * SIN(ThetaV!)) / COS(ThetaV! - ThetaH!)
PlatYaw! = (Gain!(2, 2) * COS(ThetaV!)) / COS(ThetaV! - ThetaH!)

REM ********************************** Eye Velocity ********************
EvelPitch! = PantPitch! * Want! + PposPitch! * Wpost!
EvelRoll! = PantRoll! * Want! + PposRoll! * Wpost! + PlatRoll! * Wlat!
EvelYaw! = PantYaw! * Want! + PposYaw! * Wpost! + PlatYaw! * Wlat!
egn(0, I%) = EvelPitch!
egn(1, I%) = EvelRoll!
egn(2, I%) = EvelYaw!
Angle = (I% - 9) * 10
PRINT USING "#########.##"; Angle; EvelPitch!; EvelRoll!; EvelYaw!
agl(I%) = Angle
NEXT I%
PRINT "Negative= Tilt Backward"; "Positive=Tilt Forward"
INPUT "Press any key to plot:"; Q
Graph FileName2$, egn(), Gain!()
LOCATE 30, 1
INPUT "Anything to Change"; Q5$
IF Q5$ = "Y" OR Q5$ = "y" THEN CLS : GOTO 5
WriteFile FileName2$, egn()
END

SUB Definitions (VertEyePos(), FileName1$)
*****************************************************************************
' * These SUB program create temporary file which contain information about *
' * values of the Gain Matrix ("GMATRIX.DAT") and temporary file with       *
' * information about vertical eye position. The first one can be modify at *
```

```
' * any time. The second one is fixed.                                    *
'*************************************************************************
CHDRIVE "C:"
CHDIR "c:\plug"
OPEN "C:\PLUG\GMATRIX.DAT" FOR RANDOM AS #1
FOR I% = 0 TO 8
IF I% = 0 THEN G! = .83
IF I% = 1 THEN G! = .83
IF I% = 2 THEN G! = 0!
IF I% = 3 THEN G! = .52
IF I% = 4 THEN G! = .52
IF I% = 5 THEN G! = .52
IF I% = 6 THEN G! = .87
IF I% = 7 THEN G! = .87
IF I% = 8 THEN G! = .87
PUT #1, , G!
NEXT I%
CLOSE #1
LOCATE 1, 1
COLOR 14
INPUT "Do You Want To Create File for Vertical Eye Position's (Y/N)"; Q3$
IF Q3$ = "N" OR Q3$ = "n" THEN COLOR 2: FILES "*.pos": COLOR 14
IF Q3$ = "N" OR Q3$ = "n" THEN INPUT "Enter File Name with vertical Eye
Position's (*.pos)"; FileName1$
IF Q3$ = "N" OR Q3$ = "n" THEN GOTO 80

REM ********************** Writting File for Vertical Eye Positions ******
COLOR 10
FILES "*.pos"
COLOR 14
INPUT "Enter File Name with vertical Eye Position's (*.pos)"; FileName1$
COLOR 5
85 PRINT "Enter Vertical Eye Positions for Different Tilt Angles:"
PRINT "Negative Value = Tilt Back"
OPEN FileName1$ FOR OUTPUT AS #2
Ang = -100
FOR I% = 0 TO 18
Ang = Ang + 10
PRINT "Tilt Angle="; Ang;
INPUT ""; VertPos!
WRITE #2, VertPos!
NEXT I%
CLOSE #2
CLS
```

```
80 REM ***************************** Reading File Contence **************
OPEN FileName1$ FOR INPUT AS #3
FOR I% = 0 TO 18
INPUT #3, Posit!
VertEyePos(I%) = Posit!
NEXT I%
CLOSE #3

90 REM
COLOR 2
FOR I% = 0 TO 18
PRINT VertEyePos(I%);
NEXT I%
PRINT
COLOR 5
INPUT "Do You Want to make Any Changes (Y/N)"; Q4$
IF Q4$ = "Y" OR Q4$ = "y" THEN CLS : GOTO 85
END SUB


SUB Gmatrix (Gain!())
'*************************************************************************
' * These SUB program modified temporary file which contain information  *
' * about values of the Gain Matrix ("GMATRIX.DAT").                      *
' *************************************************************************
CLS
OPEN "C:\PLUG\GMATRIX.DAT" FOR RANDOM AS #1
FOR I% = 0 TO 8
GET #1, , G!
IF I% = 0 THEN Gain!(0, 0) = G!
IF I% = 1 THEN Gain!(0, 1) = G!
IF I% = 2 THEN Gain!(0, 2) = G!
IF I% = 3 THEN Gain!(1, 0) = G!
IF I% = 4 THEN Gain!(1, 1) = G!
IF I% = 5 THEN Gain!(1, 2) = G!
IF I% = 6 THEN Gain!(2, 0) = G!
IF I% = 7 THEN Gain!(2, 1) = G!
IF I% = 8 THEN Gain!(2, 2) = G!
NEXT I%
100 LOCATE 1, 1
COLOR 4
PRINT "Original Gain's Matrix"
COLOR 3
FOR I% = 0 TO 2
```

```
PRINT Gain(I%, 0); Gain(I%, 1); Gain(I%, 2)
NEXT I%

First = 5: Second = 3
COLOR 4
LOCATE 12, 1
PRINT "Enter Coupling Paramethors:"
COLOR First
LOCATE 14, 1
PRINT "From Anterior to Pitch", "G(0,0)=";
COLOR Second: PRINT Gain!(0, 0);
COLOR First
INPUT "Change it (Y/N)"; Q2$
IF Q2$ = "Y" OR Q2$ = "y" THEN LOCATE 14, 59: INPUT "New is ="; Q3!:
Gain!(0, 0) = Q3!

LOCATE 15, 1
PRINT "From Posterior to Pitch", "G(0,1)=";
COLOR Second: PRINT Gain!(0, 1);
COLOR First
INPUT "Chang it (Y/N)"; Q2$
IF Q2$ = "Y" OR Q2$ = "y" THEN LOCATE 15, 59: INPUT "New is ="; Q3!:
Gain!(0, 1) = Q3!

LOCATE 16, 1
PRINT "From Lateral to Pitch", "G(0,2)=";
COLOR Second: PRINT Gain!(0, 2);
COLOR First
INPUT "Chang it (Y/N)"; Q2$
IF Q2$ = "Y" OR Q2$ = "y" THEN LOCATE 16, 59: INPUT "New is ="; Q3!:
Gain!(0, 2) = Q3!

LOCATE 17, 1
PRINT "From Anterior to Roll", "G(1,0)=";
COLOR Second: PRINT Gain!(1, 0);
COLOR First
INPUT "Chang it (Y/N)"; Q2$
IF Q2$ = "Y" OR Q2$ = "y" THEN LOCATE 17, 59: INPUT "New is ="; Q3!:
Gain!(1, 0) = Q3!

LOCATE 18, 1
PRINT "From Posterior to Roll", "G(1,1)=";
COLOR Second: PRINT Gain!(1, 1);
COLOR First
```

```
INPUT "Chang it (Y/N)"; Q2$
IF Q2$ = "Y" OR Q2$ = "y" THEN LOCATE 18, 59: INPUT "New is ="; Q3!:
Gain!(1, 1) = Q3!

LOCATE 19, 1
PRINT "From Lateral to Roll", "G(1,2)=";
COLOR Second: PRINT Gain!(1, 2);
COLOR First
INPUT "Chang it (Y/N)"; Q2$
IF Q2$ = "Y" OR Q2$ = "y" THEN LOCATE 19, 59: INPUT "New is ="; Q3!:
Gain!(1, 2) = Q3!

LOCATE 20, 1
PRINT "From Anterior to Yaw", "G(2,0)=";
COLOR Second: PRINT Gain!(2, 0);
COLOR First
INPUT "Chang it (Y/N)"; Q2$
IF Q2$ = "Y" OR Q2$ = "y" THEN LOCATE 20, 59: INPUT "New is ="; Q3!:
Gain!(2, 0) = Q3!

LOCATE 21, 1
PRINT "From Posterior to Yaw", "G(2,1)=";
COLOR Second: PRINT Gain!(2, 1);
COLOR First
INPUT "Chang it (Y/N)"; Q2$
IF Q2$ = "Y" OR Q2$ = "y" THEN LOCATE 21, 59: INPUT "New is ="; Q3!:
Gain!(2, 1) = Q3!

LOCATE 22, 1
PRINT "From Lateral to Yaw", "G(2,2)=";
COLOR Second: PRINT Gain!(2, 2);
COLOR First
INPUT "Chang it (Y/N)"; Q2$
IF Q2$ = "Y" OR Q2$ = "y" THEN LOCATE 22, 59: INPUT "New is ="; Q3!:
Gain!(2, 2) = Q3!

LOCATE 24, 1
COLOR 4
PRINT "New Gain's Matrix"
COLOR 5
FOR I% = 0 TO 2
PRINT Gain(I%, 0); Gain(I%, 1); Gain(I%, 2)
NEXT I%
COLOR Second
```

```
LOCATE 25, 17
INPUT "Do You Want to Change Any Paramethor (Y/N)"; Q$
IF Q$ = "Y" OR Q$ = "y" THEN CLS : GOTO 100
CLOSE #1
END SUB


SUB Graph (FileName2$, egn(), Gain!())
CLS
REM ************* Drowing Graph for Horizontal aVOR Gain *****************
DRAW "C0"
X = 35: Y = 200
DRAW "M 35, 200"
DRAW "C2"
DRAW "U 171"
DRAW "R 231"
DRAW "D 171"
DRAW "L 231"
COLOR 2
BX = X - 4: BY = Y: EX = X + 230: EY = Y
FOR I% = 0 TO 19
IF I% = 9 THEN COLOR 10
LINE (BX, BY)-(EX, EY)
BY = BY - 9: EY = EY - 9: COLOR 2
NEXT I%

BX = X: BY = Y + 4: EX = X: EY = Y - 171
FOR I% = 0 TO 21
IF I% = 10 THEN COLOR 10
LINE (BX, BY)-(EX, EY)
BX = BX + 11: EX = EX + 11: COLOR 2
NEXT I%
COLOR 3

FOR J% = 0 TO 10
LOCATE X - 22 - J%, Y - 199
PRINT USING "##.#"; 1 - J% * .2
NEXT J%
LOCATE X - 21, Y - 199
FOR I% = 0 TO 4
PRINT USING "######."; 100 - I% * 50;
NEXT I%
LOCATE X - 34, Y - 190
```

```
COLOR 5
PRINT "Horizontal Gain"
COLOR 14
FOR I% = 0 TO 18
Xcircle% = 46 + I% * 11
Ycircle% = INT(-egn(2, I%) * 85.5 + 119)
CIRCLE (Xcircle%, Ycircle%), 3, 14
IF I% > 0 THEN LINE (Xcircle%, Ycircle%)-(X2, Y2)
X2 = Xcircle%: Y2 = Ycircle%
NEXT I%


REM ************ Drowing Graph for Roll aVOR Gain *****************
DRAW "C0"
X = 350: Y = 200
DRAW "M 350, 200"
DRAW "C2"
DRAW "U 171"
DRAW "R 231"
DRAW "D 171"
DRAW "L 231"
COLOR 2
BX = X - 4: BY = Y: EX = X + 230: EY = Y
FOR J% = 0 TO 19
IF J% = 9 THEN COLOR 10
LINE (BX, BY)-(EX, EY)
BY = BY - 9: EY = EY - 9: COLOR 2
NEXT J%

BX = X: BY = Y + 4: EX = X: EY = Y - 171
FOR J% = 0 TO 21
IF J% = 10 THEN COLOR 10
LINE (BX, BY)-(EX, EY)
BX = BX + 11: EX = EX + 11: COLOR 2
NEXT J%
COLOR 3

FOR J% = 0 TO 10
LOCATE X - 337 - J%, Y - 160
PRINT USING "##.#"; 1 - J% * .2
NEXT J%
LOCATE X - 336, Y - 159
FOR I% = 0 TO 4
PRINT USING "######."; 100 - I% * 50;
```

```
NEXT I%
LOCATE X - 349, Y - 146
COLOR 5
PRINT "Roll Gain"
COLOR 14
FOR I% = 0 TO 18
Xcircle% = 361 + I% * 11
Ycircle% = INT(-egn(1, I%) * 85.5 + 119)
CIRCLE (Xcircle%, Ycircle%), 3, 14
IF I% > 0 THEN LINE (Xcircle%, Ycircle%)-(X2, Y2)
X2 = Xcircle%: Y2 = Ycircle%
NEXT I%


REM ************ Drowing Graph for Vertical aVOR Gain ****************
DRAW "C0"
X = 350: Y = 420
DRAW "M 350, 420"
DRAW "C2"
DRAW "U 171"
DRAW "R 231"
DRAW "D 171"
DRAW "L 231"
COLOR 2
BX = X - 4: BY = Y: EX = X + 230: EY = Y
FOR I% = 0 TO 19
IF I% = 9 THEN COLOR 10
LINE (BX, BY)-(EX, EY)
BY = BY - 9: EY = EY - 9: COLOR 2
NEXT I%

BX = X: BY = Y + 4: EX = X: EY = Y - 171
FOR I% = 0 TO 21
IF I% = 10 THEN COLOR 10
LINE (BX, BY)-(EX, EY)
BX = BX + 11: EX = EX + 11: COLOR 2
NEXT I%
COLOR 3

FOR J% = 0 TO 10
LOCATE X - 323 - J%, Y - 380
PRINT USING "##.#"; 1 - J% * .2
NEXT J%
LOCATE X - 322, Y - 379
```

```
FOR I% = 0 TO 4
PRINT USING "######."; 100 - I% * 50;
NEXT I%
LOCATE X - 335, Y - 368
COLOR 5
PRINT "Vertical Gain"
COLOR 14
FOR I% = 0 TO 18
Xcircle% = 361 + I% * 11
Ycircle% = INT(-egn(0, I%) * 85.5 + 339)
CIRCLE (Xcircle%, Ycircle%), 3, 14
IF I% > 0 THEN LINE (Xcircle%, Ycircle%)-(X2, Y2)
X2 = Xcircle%: Y2 = Ycircle%
NEXT I%

LOCATE 20, 1
PRINT "   Monkey:"; FileName2$
PRINT "   Gain Metrix"
COLOR 13
FOR I% = 0 TO 2
PRINT USING "##.##"; Gain!(I%, 0); Gain!(I%, 1); Gain!(I%, 2)
NEXT I%
COLOR 4
END SUB


SUB WriteFile (FileName2$, egn())
' ************************************************************
' * Writing Gain Values in to the ASCII File                 *
' ************************************************************
SHELL "D:"
OPEN FileName2$ FOR OUTPUT AS #3
FOR I% = 0 TO 18
Tilt% = (I% - 9) * 10
WRITE #3, Tilt%, egn(0, I%), egn(1, I%), egn(2, I%)
NEXT I%
CLOSE #3
END SUB
```

APPENDIX C:
COMPARING COIL VOLTAGES RELATED TO THE EYE POSITION WITH EULER ANGLES AND DERIVATIVES OF BOTH OF THEM.

This program is written in BASIC 7.1 to compare coil voltages to computed Euler angles for eye orientation. The program reads an ASCII file, detects the number of channels recorded in the file and writes each channel as a separate file on a RAM drive. The program has one buffer file "Temp1#(K)" which holds the currently used channel. The intermediate results of the channel transformation in some cases are written as a temporary file and then reloaded back to the buffer file. After converting voltages related to horizontal, vertical and roll eye movement into eye movements represented by Euler angles (see **SUB Recalc (K)**). The pregram saves three output channels on the RAM drive as well. Eye velocity is computed from the coil voltages and eye orientation signals. Any of the channels that are the results of computation can also be saved as an ASCII file.

```
' ** This Program computes eye velocity in head coordinate based on the coil
' ** Voltages recorded by the "Neurodata" that recorded eye movement related
' ** signal in the coordinates of the recording system's magnetic field. The main
' ** approximation for calibration of eye position was that in-light
' ** rotation with constant velocity, eye velocity is equal to the stimulus
' ** velocity. Based on that assumption for eye velocity we calibrated
' ** eye position and than calculated real eye velocity to be compared
' ** with original one.

DECLARE SUB ReadFile (FileName$, K, HBios#, VBios#, RBios#)
DECLARE SUB ReadFileToArray (FileName4$, Temp1#(), Reversing#)
DECLARE SUB Plot1 (K, Temp1#(), CallValue#)
DECLARE SUB Plot2 (K, Temp1#(), CallValue#)
DECLARE SUB PlotScreen (Temp1#(), BB#, Gain, Col, Dec, K, FlagClear, Mesage$)
DECLARE SUB PlotScreenLine (Temp1#(), BB#, Gain, Col, Dec, K, FlagClear,
Mesage$)
DECLARE SUB Desaccading (K, Temp1#(), Saccades())
DECLARE SUB Differ (Temp1#(), K)
DECLARE SUB Smooth (Temp1#(), K, NS1)
DECLARE SUB WriteFile (FileName1$, K, Temp1#(), NS1)
DECLARE SUB WriteFile2 (K)
DECLARE SUB Recalc (K)
DECLARE SUB BiosSubtract (K, HBios#, VBios#, RBios#, Temp1#())
DECLARE SUB CallStim (K, Temp1#(), CallValue#)
DECLARE SUB PlotCall (CallValue#)
DEFSNG A-Z
SCREEN 12
DIM Saccades(200, 2)
```

```
CLS
REM ****************** REQUEST FOR INFORMATION ********************
LOCATE 11, 15'                                                  *
COLOR 9'                                                       *
INPUT "Enter File Name that is on C:\TMP\", FileName$'                  *
LOCATE 12, 15'                                                  *
COLOR 9'                                                       *
INPUT "Do You Want to Enter Bios Levels"; q1$'                        *
IF q1$ = "N" OR q1$ = "n" THEN HBios# = 0: VBios# = 0: RBios# = 0: GOTO
15'*
IF q1$ = "Y" OR q1$ = "y" THEN COLOR 3'                                 *
LOCATE 14, 15'                                                 *
INPUT "Enter Horizontal Bios"; HBios#'                            *
LOCATE 15, 15'                                                 *
INPUT "Enter Vertical Bios  "; VBios#'                            *
LOCATE 16, 15'                                                 *
INPUT "Enter Roll Bios      "; RBios#'                            *
R                                   E                                   M
**********************************************************************

15 ReadFile FileName$, K, HBios#, VBios#, RBios#

DIM Temp1#(K)

CallStim K, Temp1#(), CallValue#

IF q1$ = "N" OR q1$ = "n" THEN BiosSubtract K, HBios#, VBios#, RBios#,
Temp1#()
LOCATE 18, 15
PRINT "Enter Horizontal Bios"; HBios#
LOCATE 19, 15
PRINT "Enter Vertical Bios  "; VBios#
LOCATE 20, 15
PRINT "Enter Roll Bios      "; RBios#
LOCATE 21, 15
COLOR 4
INPUT "Press ENTER When Ready"; q

Plot1 K, Temp1#(), CallValue#

Recalc K

Plot2 K, Temp1#(), CallValue#
```

```
Desaccading K, Temp1#(), Saccades()

WriteFile2 K

STOP
END

SUB BiosSubtract (K, HBios#, VBios#, RBios#, Temp1#())
REM  ************************* HORIZONTAL EYE MOVEMENT ********
SHELL "D:"
OPEN "HOR1.DAT" FOR INPUT AS #1
K3 = 0
REM _____________________ Reading Data From File to the Array _______
DO UNTIL EOF(1)
INPUT #1, M#
Temp1#(K3) = M# - HBios#
K3 = K3 + 1
LOOP
CLOSE #1'_____________________ End of Reading ____________________

OPEN "HOR1.DAT" FOR OUTPUT AS #1
FOR I% = 0 TO K - 1
WRITE #1, Temp1#(I%)
NEXT I%
CLOSE #1

REM ************** VERTICAL EYE MOVEMENT ************************
SHELL "D:"
OPEN "VERT1.DAT" FOR INPUT AS #1
K3 = 0
REM _____________________ Reading Data From File to the Array _______
DO UNTIL EOF(1)
INPUT #1, M#
Temp1#(K3) = M# - VBios#
K3 = K3 + 1
LOOP
CLOSE #1'_____________________ End of Reading ____________________

OPEN "VERT1.DAT" FOR OUTPUT AS #1
FOR I% = 0 TO K - 1
WRITE #1, Temp1#(I%)
NEXT I%
CLOSE #1
```

```
REM ****************** ROLL EYE MOVEMENT ************************
SHELL "D:"
OPEN "ROLL1.DAT" FOR INPUT AS #1
K3 = 0
REM _____ Reading Data From File to the Array _____
DO UNTIL EOF(1)
INPUT #1, M#
Temp1#(K3) = M# - RBios#
K3 = K3 + 1
LOOP
CLOSE #1'_____ End of Reading _____

OPEN "ROLL1.DAT" FOR OUTPUT AS #1
FOR I% = 0 TO K - 1
WRITE #1, Temp1#(I%)
NEXT I%
CLOSE #1
END SUB

SUB CallStim (K, Temp1#(), CallValue#)
REM  ************************ STIMULUS VELOCITY **********
SHELL "D:"
OPEN "STIM1.DAT" FOR INPUT AS #1
K3 = 0: Max# = -999999: Min = 999999: StBios# = 0
REM _____ Reading Data From File to the Array _____
DO UNTIL EOF(1)
INPUT #1, M#
Temp1#(K3) = M# - HBios#
IF Temp1#(K3) > Max# THEN Max# = Temp1#(K3)
IF Temp1#(K3) < Min# THEN Min# = Temp1#(K3)
StBios# = StBios# + Temp1#(K3)
K3 = K3 + 1
LOOP
AverStim# = AverStim# / K: CallValue# = (Max# - Min#) / 120
CLOSE #1'_____ End of Reading _____

OPEN "STIM1.DAT" FOR OUTPUT AS #1
FOR I% = 0 TO K - 1
Temp1#(I%) = (Temp1#(I%) - StBios#) / CallValue#
WRITE #1, Temp1#(I%)
NEXT I%
CLOSE #1
END SUB
```

```
SUB Desaccading (K, Temp1#(), Saccades())
FOR I% = 0 TO 200
FOR J% = 0 TO 2
Saccades(I%, J%) = 0
NEXT J%
NEXT I%

FileName4$ = "HVEL1.DAT": Reversing# = 1
ReadFileToArray FileName4$, Temp1#(), Reversing#
Flag7 = 0: LMax# = -99999: Tresh = 70: Saccade = -1

FOR I% = 0 TO K - 1
IF Flag7 = 1 THEN GOTO 620
IF Flag7 = 0 AND ABS(Temp1#(I%)) < Tresh THEN GOTO 680
Flag7 = 1
620 IF ABS(Temp1#(I%)) > LMax# THEN LMax# = ABS(Temp1#(I%)): Tmax = I%
IF ABS(Temp1#(I%)) < Tresh - 10 THEN Flag7 = 0: LMax# = -99999: Saccade =
Saccade + 1: Saccades(Saccade, 0) = Tmax: I% = I% + 10
680 NEXT I%

FileName4$ = "HOR1.DAT": Reversing# = 1
ReadFileToArray FileName4$, Temp1#(), Reversing#

FOR Dec = 1 TO 1000' _____ Counting Decriment for Data Plotting _____
IF K / Dec < 640 THEN GOTO 725
NEXT Dec
725 CLS

REM _____ Plotting Horizontal Chanel _____
Mesage$ = "THIS IS ORIGINAL HORIZONTAL POSITION"
BB# = 200: Gain = 5: Col = 15: FlagClear = 0
PlotScreen Temp1#(), BB#, Gain, Col, Dec, K, FlagClear, Mesage$
FOR S% = 0 TO Saccade
LINE (Saccades(S%, 0) / Dec, 100)-(Saccades(S%, 0) / Dec, 380), 3
LINE ((Saccades(S%, 0) - 10) / Dec, 200)-((Saccades(S%, 0) + 10) / Dec, 200), 4
NEXT S%
INPUT ""; q
CLS
FileName4$ = "HVEL1.DAT": Reversing# = 1
ReadFileToArray FileName4$, Temp1#(), Reversing#
Mesage$ = "THIS IS ORIGINAL HORIZONTAL VELOCITY"
BB# = 200: Gain = 2: Col = 15: FlagClear = 1
PlotScreen Temp1#(), BB#, Gain, Col, Dec, K, FlagClear, Mesage$
```

```
S% = 0: Trig = 20

FOR I% = 0 TO K - 1
IF S% > Saccade THEN GOTO 790
IF I% < (Saccades(S%, 0)) THEN GOTO 790
IF I% = (Saccades(S%, 0)) THEN Tbeg = I% - 1: Tend = I% + 1
750 IF Tbeg < 0 THEN Tbeg = 0: GOTO 760
IF I% - Tbeg > 15 THEN Tbeg = I% - 15: GOTO 760
IF ABS(Temp1#(Tbeg) - Temp1#(Tbeg + 1)) > Trig THEN Tbeg = Tbeg - 1: GOTO
750
760 IF ABS(Temp1#(Tend) - Temp1#(Tend - 1)) > Trig THEN Tend = Tend + 1
IF Tend > K - 1 THEN Tend = K - 1: GOTO 770
IF ABS(Temp1#(Tend) - Temp1#(Tend - 1)) > Trig THEN GOTO 760
IF Tend - I% > 15 THEN Tend = I% + 15: GOTO 770
770 Tbeg = Tbeg - 1: Tend = Tend + 1
IF Tbeg < 0 THEN Tbeg = 0
IF Tend > K - 1 THEN Tend = K - 1
Saccades(S%, 1) = Tbeg: Saccades(S%, 2) = Tend
I% = Tend
780 S% = S% + 1
IF S% > Saccade THEN GOTO 790
IF Saccades(S%, 0) < Tend THEN GOTO 780
790 NEXT I%

FOR I% = 0 TO Saccade - 1
Tbeg = Saccades(I%, 1): Tend = Saccades(I%, 2)
IF Saccades(I%, 0) = 0 THEN GOTO 805
Durat = Tend - Tbeg: DelAmp# = (Temp1#(Tend) - Temp1#(Tbeg)) / Durat
FOR J% = 0 TO Durat - 2
Temp1#(Tbeg + J%) = 0'Temp1#(Tbeg) + DelAmp# * J%
NEXT J%
PRINT I%; Tbeg; Tend; DelAmp#
805 NEXT I%

REM _____ Plotting Horizontal Chanel _____
Mesage$ = "THIS IS DESACCADED HORIZONTAL VELOCITY"
BB# = 200: Gain = 2: Col = 13: FlagClear = 1
PlotScreenLine Temp1#(), BB#, Gain, Col, Dec, K, FlagClear, Mesage$

FOR I% = 0 TO Saccade - 1
Tbeg = Saccades(I%, 1): Tend = Saccades(I%, 2)
LINE (Saccades(I%, 1), 50)-(Saccades(I%, 1), 400), 3
LINE (Saccades(I%, 2), 50)-(Saccades(I%, 2), 400), 4
NEXT I%
```

```
INPUT ""; q
END SUB

SUB Differ (Temp1#(), K)
FOR I% = 0 TO K - 1
M1# = Temp1#(I%) * 10000
IF I% <> K - 1 THEN M2# = Temp1#(I% + 1) * 10000
IF I% = K - 1 THEN M2# = M1#
Temp1#(I%) = -(M2# - M1#) / 64
NEXT I%
END SUB

SUB Plot1 (K, Temp1#(), CallValue#) STATIC
FlagClear = 0
REM ************************ HORIZONTAL EYE MOVEMENT **********
20 Flag1 = 0
FileName4$ = "HOR1.DAT": Reversing# = 1
ReadFileToArray FileName4$, Temp1#(), Reversing#

FOR Dec = 1 TO 1000' _____ Counting Decriment for Data Plotting _____
IF K / Dec < 640 THEN GOTO 25
NEXT Dec
25 CLS

REM _____ Plotting Horizontal Chanel _____
Mesage$ = "THIS IS ORIGINAL HORIZONTAL POSITION"
BB# = 200: Gain = 5: Col = 15
PlotScreen Temp1#(), BB#, Gain, Col, Dec, K, FlagClear, Mesage$
Differ Temp1#(), K' _____ Calculating Horizontal Velocity _____
Count = 0
27 CLS
IF Count = 2 THEN GOTO 20
REM _____ Plotting Horizontal Velocity _____
Mesage$ = "THIS IS ORIGINAL HORIZONTAL VELOCITY"
BB# = 200: Gain = 2: Col = 15
PlotScreen Temp1#(), BB#, Gain, Col, Dec, K, FlagClear, Mesage$
PlotCall CallValue#
28 IF Count = 0 THEN NS1 = 5: Count = Count + 1: GOTO 45
LOCATE 2, 15
COLOR 4
30 INPUT "Do You Want to Smooth This Data"; q1$
IF q1$ = "Y" OR q1$ = "y" THEN Count = Count + 1: GOTO 40
IF q1$ = "N" OR q1$ = "n" THEN GOTO 60
GOTO 30
```

```
40 INPUT "Enter the Number of Data Point for Smoothing"; NS1
45 IF NS1 <= 0 THEN NS1 = 1
IF NS1 / 2 = INT(NS1 / 2) THEN NS1 = NS1 + 1
Smooth Temp1#(), K, NS1
GOTO 27
60 FileName1$ = "HVEL1.DAT"
WriteFile FileName1$, K, Temp1#(), NS1

REM ************** VERTICAL EYE MOVEMENT ************************
120 FileName4$ = "VERT1.DAT": Reversing# = 1
ReadFileToArray FileName4$, Temp1#(), Reversing#
CLS
REM ______________ Plotting Vertical Chanel _____________________
Mesage$ = "THIS IS ORIGINAL VERTICAL POSITION"
BB# = 200: Gain = 5: Col = 15
PlotScreen Temp1#(), BB#, Gain, Col, Dec, K, FlagClear, Mesage$
Differ Temp1#(), K' __________ Calculating Vertical Velocity _________
Count = 0
127 CLS
IF Count = 2 THEN GOTO 120
REM ____________________ Plotting Vertical Velocity __________
Mesage$ = "THIS IS ORIGINAL VERTICAL VELOCITY"
BB# = 200: Gain = 2: Col = 15
PlotScreen Temp1#(), BB#, Gain, Col, Dec, K, FlagClear, Mesage$
PlotCall CallValue#
IF Count = 0 THEN NS1 = 5: Count = Count + 1: GOTO 145
LOCATE 2, 15
COLOR 4
130 INPUT "Do You Want to Smooth This Data"; q1$
IF q1$ = "Y" OR q1$ = "y" THEN Count = Count + 1: GOTO 140
IF q1$ = "N" OR q1$ = "n" THEN GOTO 160
GOTO 130
140 INPUT "Enter the Number of Data Point for Smoothing"; NS1
145 IF NS1 <= 0 THEN NS1 = 1
Smooth Temp1#(), K, NS1
GOTO 127
160 FileName1$ = "VVEL1.DAT"
WriteFile FileName1$, K, Temp1#(), NS1

REM *************** ROLL EYE MOVEMENT ************************
320 FileName4$ = "ROLL1.DAT": Reversing# = 1
ReadFileToArray FileName4$, Temp1#(), Reversing#
CLS
REM ______________ Plotting Roll Chanel _____________________
```

```
Mesage$ = "THIS IS ORIGINAL ROLL POSITION"
BB# = 200: Gain = 5: Col = 15
PlotScreen Temp1#(), BB#, Gain, Col, Dec, K, FlagClear, Mesage$
Differ Temp1#(), K' _____ Calculating Roll Velocity _____
Count = 0
327 CLS
IF Count = 2 THEN GOTO 320
REM _____ Plotting Roll Velocity _____
Mesage$ = "THIS IS ORIGINAL ROLL VELOCITY"
BB# = 200: Gain = 2: Col = 15
PlotScreen Temp1#(), BB#, Gain, Col, Dec, K, FlagClear, Mesage$
PlotCall CallValue#
IF Count = 0 THEN SN1 = 5: Count = Count + 1: GOTO 345
LOCATE 2, 15
COLOR 4
330 INPUT "Do You Want to Smooth This Data"; q1$
IF q1$ = "Y" OR q1$ = "y" THEN Count = Count + 1: GOTO 340
IF q1$ = "N" OR q1$ = "n" THEN GOTO 360
GOTO 330
340 INPUT "Enter the Number of Data Point for Smoothing"; NS1
345 IF NS1 <= 0 THEN NS1 = 1
Smooth Temp1#(), K, NS1
GOTO 327
360 FileName1$ = "RVEL1.DAT"
WriteFile FileName1$, K, Temp1#(), NS1
END SUB

SUB Plot2 (K, Temp1#(), CallValue#)
REM  ********** HORIZONTAL EYE MOVEMENT **********
FileName4$ = "HVEL1.DAT": Reversing# = -1
ReadFileToArray FileName4$, Temp1#(), Reversing#

FOR Dec = 1 TO 1000' _____ Counting Decriment for Data Plotting _____
IF K / Dec < 640 THEN GOTO 1025
NEXT Dec
1025 CLS

REM _____ Plotting Horizontal Velocity _____
Mesage$ = "THIS IS ORIGINAL HORIZONTAL VELOCITY"
BB# = 200: Gain = 2: Col = 15: FlagClear = 1
PlotScreen Temp1#(), BB#, Gain, Col, Dec, K, FlagClear, Mesage$
PlotCall CallValue#

FileName4$ = "HVEL2.DAT": Reversing# = 1
```

```
ReadFileToArray FileName4$, Temp1#(), Reversing#
NS1 = 5: Smooth Temp1#(), K, NS1

REM _____ Plotting Horizontal Velocity _____
Mesage$ = "THIS IS RECALCULATED HORIZONTAL VELOCITY"
BB# = 200: Gain = 2: Col = 14: FlagClear = 1
PlotScreen Temp1#(), BB#, Gain, Col, Dec, K, FlagClear, Mesage$
LOCATE 30, 15
COLOR 5
INPUT "Are You Ready to See Next"; q$
CLS

REM ********** VERTICAL EYE MOVEMENT **********
FileName4$ = "VVEL1.DAT": Reversing# = -1
ReadFileToArray FileName4$, Temp1#(), Reversing#
REM _____ Plotting Vertical Velocity _____
Mesage$ = "THIS IS ORIGINAL VERTICAL VELOCITY"
BB# = 200: Gain = 2: Col = 15: FlagClear = 1
PlotScreen Temp1#(), BB#, Gain, Col, Dec, K, FlagClear, Mesage$
PlotCall CallValue#
FileName4$ = "VVEL2.DAT": Reversing# = 1
ReadFileToArray FileName4$, Temp1#(), Reversing#
NS1 = 5: Smooth Temp1#(), K, NS1

REM _____ Plotting Vertical Velocity _____
Mesage$ = "THIS IS RECALCULATED VERTICAL VELOCITY"
BB# = 200: Gain = 2: Col = 14: FlagClear = 1
PlotScreen Temp1#(), BB#, Gain, Col, Dec, K, FlagClear, Mesage$
LOCATE 30, 15
COLOR 5
INPUT "Are You Ready to See Next"; q$
CLS

REM ********** ROLL EYE MOVEMENT **********
FileName4$ = "RVEL1.DAT": Reversing# = -1
ReadFileToArray FileName4$, Temp1#(), Reversing#

REM _____ Plotting Vertical Velocity _____
Mesage$ = "THIS IS ORIGINAL ROLL VELOCITY"
BB# = 200: Gain = 2: Col = 15: FlagClear = 1
PlotScreen Temp1#(), BB#, Gain, Col, Dec, K, FlagClear, Mesage$
PlotCall CallValue#
FileName4$ = "RVEL2.DAT": Reversing# = 1
ReadFileToArray FileName4$, Temp1#(), Reversing#
```

```
NS1 = 5: Smooth Temp1#(), K, NS1

REM _____ Plotting ROLL Velocity _____
Mesage$ = "THIS IS RECALCULATED ROLL VELOCITY"
BB# = 200: Gain = 2: Col = 14: FlagClear = 1
PlotScreen Temp1#(), BB#, Gain, Col, Dec, K, FlagClear, Mesage$
REM ************************************************************
END SUB

SUB PlotCall (CallValue#)
COLOR 0
LINE (440, 350)-STEP(190, 120), , BF'step(620,470)
LINE (620, 370)-(620, 370 + 30 * CallValue# * 2), 4
LINE (450, 450)-(606, 450), 4
LOCATE 28, 64
COLOR 6
PRINT "1 sec"
LOCATE 26, 67
COLOR 6
PRINT "30 deg/sec"
END SUB

SUB PlotScreen (Temp1#(), BB#, Gain, Col, Dec, K, FlagClear, Mesage$)
IF FlagClear = 1 THEN GOTO 777
COLOR 1
LINE (0, 40)-STEP(640, 440), , BF' (0,0)-(640,480)
777 IF FlagClear = 0 THEN LOCATE 1, 15: COLOR 6
IF FlagClear = 1 THEN LOCATE 2, 15: COLOR 3
PRINT Mesage$
FOR I% = 0 TO K - 1 STEP Dec
Ycoord# = Temp1#(I%)
REM LINE (I% / Dec, Ycoord# * Gain + BB#)-((I% + 1) / Dec, Ycoord# * Gain +
BB#), Col
PSET (I% / Dec, Ycoord# * Gain + BB#), Col
NEXT I%
END SUB

SUB PlotScreenLine (Temp1#(), BB#, Gain, Col, Dec, K, FlagClear, Mesage$)
IF FlagClear = 1 THEN GOTO 877
COLOR 1
LINE (0, 40)-STEP(640, 440), , BF' (0,0)-(640,480)
877 IF FlagClear = 0 THEN LOCATE 1, 15: COLOR 6
IF FlagClear = 1 THEN LOCATE 2, 15: COLOR 3
PRINT Mesage$
```

```
FOR I% = 0 TO K - 1 STEP Dec
Ycoord1# = Temp1#(I%)
IF I% + Dec < K - 1 THEN Ycoord2# = Temp1#(I% + Dec)
IF I% + Dec >= K - 1 THEN Ycoord2# = Temp1#(I%)

LINE (I% / Dec, Ycoord1# * Gain + BB#)-(I% / Dec + 1, Ycoord2# * Gain + BB#),
Col
NEXT I%
END SUB

SUB ReadFile (FileName$, K, HBios#, VBios#, RBios#) STATIC

'************************************************
'* IMPORTANT!!!                                 *
'*                                              *
'*                                              *
'*                                              *
'* This SUB identified the lenght of the file   *
'* that only one thing that can varied, because *
'* file itself must have all three eye POSITION *
'* chanels, atherwise, all computetion are      *
'* miningless.                                  *
'*                                              *
'*                                              *
'*                                              *
'*      K     - Lense of the File               *
'************************************************
CHDRIVE "C:"
CHDIR "\TMP"
OPEN FileName$ FOR INPUT AS #1
OPEN "D:/TMP1.DAT" FOR OUTPUT AS #2
OPEN "D:/ROLL1.DAT" FOR OUTPUT AS #3
OPEN "D:/TIME1.DAT" FOR OUTPUT AS #4
OPEN "D:/STIM1.DAT" FOR OUTPUT AS #5
OPEN "D:/HOR1.DAT" FOR OUTPUT AS #6
OPEN "D:/VERT1.DAT" FOR OUTPUT AS #7
K = 0: K1 = -1: K2 = 0: BiosHor# = 0: BiosVert# = 0: BiosRoll# = 0
DO UNTIL EOF(1)
INPUT #1, M#
K = K + 1
K2 = K2 + 1: IF K2 > 4 THEN K2 = 0
WRITE #2, M#
IF K2 = 0 THEN WRITE #3, (M# - RBios#)
IF K2 = 1 THEN WRITE #4, M#
```

```
IF K2 = 2 THEN WRITE #5, M#
IF K2 = 3 THEN WRITE #6, (M# - HBios#)
IF K2 = 4 THEN WRITE #7, (M# - VBios#)

IF K2 = 0 THEN BiosRoll# = BiosRoll# + M# - RBios#
IF K2 = 3 THEN BiosHor# = BiosHor# + M# - HBios#
IF K2 = 4 THEN BiosVert# = BiosVert# + M# - VBios#


LOOP
K = K / 5
HBios# = BiosHor# / K: VBios# = BiosVert# / K: RBios# = BiosRoll# / K
CLS
COLOR 4
LOCATE 20, 20
PRINT "The Program Has Detected:"
COLOR 3
LOCATE 22, 15
PRINT "The Lenght of One Chanel in the File is:";
COLOR 6
PRINT K
BEEP
CLOSE #1
CLOSE #2
CLOSE #3
CLOSE #4
CLOSE #5
CLOSE #6
CLOSE #7
END SUB

SUB ReadFileToArray (FileName4$, Temp1#(), Reversing#)
SHELL "D:"
OPEN FileName4$ FOR INPUT AS #1
K3 = 0
REM _____ Reading Data From File to the Array _____
DO UNTIL EOF(1)
INPUT #1, M#
Temp1#(K3) = M# * Reversing#
K3 = K3 + 1
LOOP
CLOSE #1'_____ End of Reading _____
END SUB
```

```
SUB Recalc (K)
' This SUB recalculate Euler angles of eye movement based on the ' coil voltages signals!
CONST PI = 3.14159265#
SHELL "D:"
OPEN "D:\HOR1.DAT" FOR INPUT AS #1
OPEN "D:\VERT1.DAT" FOR INPUT AS #2
OPEN "D:\ROLL1.DAT" FOR INPUT AS #3
OPEN "D:\HVEL1.DAT" FOR INPUT AS #4
OPEN "D:\VVEL1.DAT" FOR INPUT AS #5
OPEN "D:\RVEL1.DAT" FOR INPUT AS #6

OPEN "D:/HVEL2.DAT" FOR OUTPUT AS #7
OPEN "D:/VVEL2.DAT" FOR OUTPUT AS #8
OPEN "D:/RVEL2.DAT" FOR OUTPUT AS #9

DO UNTIL EOF(1)
INPUT #1, HOR1#
INPUT #2, VERT1#
INPUT #3, ROLL1#
INPUT #4, HVEL1#
INPUT #5, VVEL1#
INPUT #6, RVEL1#

REM ********************************************************
REM COMPUTING EULER ANGLES FROM EYE POSITION COIL VOLTAGES
REM ********************************************************

REM                         **** First Angle ****
Theta# = (PI * (-VERT1#)) / 180'        Equation is Theta=ArcSin(-Vfz)
REM                         **********************

REM ************************************************
CosTheta# = COS(Theta#)
IF CosTheta# = 0 THEN CosTheta# = .000001
REM _____________________________________________

REM                         **** Second Angle ****
Phi# = (SIN(((-HOR1#) * PI) / 180)) / CosTheta#
REM                         **********************

REM ************************************************
Sin1# = SIN(Phi#) * SIN(Theta#)
Cos1# = COS(Phi#) * COS(Theta#)
```

```
IF Sin1# = 0 THEN Sin1# = .000001
IF Cos1# = 0 THEN Cos1# = .000001
SqRoot1# = SQR(ABS(COS(Phi#) * COS(Phi#) + SIN(Phi#) * SIN(Phi#) * SIN(Theta#)
* SIN(Theta#)))
IF SqRoot1# = 0 THEN SqRoot1# = .000001
Num1# = ((-ROLL1# * PI) / 180) / SqRoot1#
LOCATE 20, 10
COLOR 7
IF Num1# = 0 THEN Num1# = .000001
ArcSinR# = ATN(Num1# / SQR(ABS(1 - Num1# * Num1#)))

Cos2# = COS(Phi#)
IF Cos2# = 0 THEN Cos2# = .000001
ArcTanR# = ATN(SIN(Phi#) * SIN(Theta#) / Cos2#)
REM _____________________________________________

REM                          **** Third Angle (Psi)****
Psi# = ArcSinR# - ArcTanR#
REM IF ABS(Psi#) > .26 THEN HOR2# = 0: VERT2# = 0: ROLL2# = 0: GOTO
3000
REM IF ABS(Theta#) > .26 THEN HOR2# = 0: VERT2# = 0: ROLL2# = 0: GOTO
3000
REM IF ABS(Phi#) > .26 THEN HOR2# = 0: VERT2# = 0: ROLL2# = 0: GOTO
3000

REM                          **********************

VTheta# = (((PI * (-VVEL1#)) / 180)) / CosTheta#

VPhi# = (((-HVEL1#) * PI) / 180 + Sin1# * VTheta#) / Cos1#

Part1# = ((-RVEL1#) * PI) / 180
Part2# = VPhi# * (SIN(Theta#) * COS(Phi#) * COS(Psi#))
Part3# = SIN(Psi#) * SIN(Phi#)
Part4# = VTheta# * (SIN(Phi#) * COS(Psi#) * COS(Theta#))
Part5# = COS(Phi#) * COS(Psi#) - SIN(Phi#) * SIN(Theta#) * SIN(Psi#)
IF Part5# = 0 THEN Part5# = .000001

VPsi# = (Part1# / Part5#) - (Part2# / Part5#) - (Part3# / Part5#) - (Part4# / Part5#)


REM VPsi# = NumVPsi# / Part5#

OmegaX# = COS(Phi#) * VTheta# - SIN(Phi#) * COS(Theta#) * VPsi#
```

```
OmegaY# = -SIN(Phi#) * VTheta# + COS(Phi#) * COS(Theta#) * VPsi#
OmegaZ# = VPhi# + SIN(Theta#) * VPsi#
VERT2# = (OmegaX# * 180) / PI
ROLL2# = (OmegaY# * 180) / PI
HOR2# = (OmegaZ# * 180) / PI
3000 REM
WRITE #7, HOR2#
WRITE #8, VERT2#
WRITE #9, ROLL2#
LOOP
BEEP
CLOSE #1
CLOSE #2
CLOSE #3
CLOSE #4
CLOSE #5
CLOSE #6
CLOSE #7
CLOSE #8
CLOSE #9
END SUB

SUB Smooth (Temp1#(), K, NS1)
REDIM SPoint#(NS1)
FOR I% = 0 TO K - 1
FOR J% = 0 TO NS1 - 1
IF I% + J% > K - 1 THEN SPoint#(J%) = 0: GOTO 200
SPoint#(J%) = Temp1#(I% + J%)
200 NEXT J%
Sum1# = 0
FOR JJ% = 0 TO NS1 - 1
Sum1# = Sum1# + SPoint#(JJ%)
NEXT JJ%
Temp1#(I%) = Sum1# / NS1
NEXT I%
END SUB

SUB WriteFile (FileName1$, K, Temp1#(), NS1)
SHELL "D:"
OPEN FileName1$ FOR OUTPUT AS #2
FOR I% = 0 TO K - 1
IF I% < (NS1 + 1) / 2 THEN WRITE #2, 0
IF I% >= (NS1 + 1) / 2 THEN WRITE #2, Temp1#(I% - (NS1 + 1) / 2)
NEXT I%
```

```
CLOSE #2
END SUB

SUB WriteFile2 (K) STATIC
I1 = -1: N2% = N2% + 1: n% = N2%: F% = N0%
REM CLS
LOCATE 20, 15
COLOR 9
INPUT "Enter Ouptut File Name"; FileName3$
SHELL "D:"
OPEN "D:\STIM1.DAT" FOR INPUT AS #1
OPEN "D:\HOR1.DAT" FOR INPUT AS #2
OPEN "D:\VERT1.DAT" FOR INPUT AS #3
OPEN "D:\ROLL1.DAT" FOR INPUT AS #4
OPEN "D:\HVEL1.DAT" FOR INPUT AS #5
OPEN "D:\VVEL1.DAT" FOR INPUT AS #6
OPEN "D:\RVEL1.DAT" FOR INPUT AS #7
OPEN "D:\HVEL2.DAT" FOR INPUT AS #8
OPEN "D:\VVEL2.DAT" FOR INPUT AS #9
OPEN "D:\RVEL2.DAT" FOR INPUT AS #10

OPEN FileName3$ FOR OUTPUT AS #11
D0$ = "Time"
D1$ = "Stim": D2$ = "HorPos": D3$ = "VertPos": D4$ = "RollPos"
D5$ = "HorVel1": D6$ = "VertVel1": D7$ = "RollVel1": D8$ = "HorVel2"
D9$ = "VertVel2": D10$ = "RollVel2"
WRITE #11, D0$, D1$, D2$, D3$, D4$, D5$, D6$, D7$, D8$, D9$, D10$
I1 = 0: D0# = 0
DO UNTIL EOF(1)
D0# = I1 * 6.4
INPUT #1, D1#'      STIM1#
INPUT #2, D2#'      HOR1#
INPUT #3, D3#'      VERT1#
INPUT #4, D4#'      ROLL1#
INPUT #5, D5#'      HVEL1#
INPUT #6, D6#'      VVEL1#
INPUT #7, D7#'      RVEL1#
INPUT #8, D8#'      HVEL2#
INPUT #9, D9#'      VVEL2#
INPUT #10, D10#'     RVEL2#
WRITE #11, D0#, D1#, D2#, D3#, D4#, D5#, D6#, D7#, D8#, D9#, D10#
I1 = I1 + 1
LOOP
```

```
BEEP
CLOSE #1
CLOSE #2
CLOSE #3
CLOSE #4
CLOSE #5
CLOSE #6
CLOSE #7
CLOSE #8
CLOSE #9
CLOSE #10
CLOSE #11
END SUB
```

APPENDIX D:
MEASUREMENT OF aVOR GAIN FOR CONSTANT VELOCITY OF ROTATION.

This program was written in BASIC 7.1 to analyze aVOR gain when the head is rotated with a constant velocity. It reads an ASCII file, detects number of channels recorded in the file and writes each channel as a separate file onto a RAM drive. The program has two buffer files (CH0!() and CH1!()). Eye position related signals are transformed to velocity related signals. The beginning of the head rotation of each trial is detected. Saccades are detected and eliminated. Each channel is synchronized to the beginning of the head rotation. Average value of the eye velocity and aVOR gain of each trial is determined for a chosen time interval and average values and 1 SD calculated.

```
DIM MARK(9), MIN%(9, 9), MAX%(9, 9), AvVOR!(3), SDVOR!(3)
DIM AvVORG!(3), SDVORG!(3), MU(33)
DIM CH0!(9, 3, 299), CH1!(9, 3, 299), NNS%(9, 9), NKS%(9, 9)
DECLARE SUB MESSAGE1 (FileName$)
DECLARE SUB ReadFile (FileName$, CH1!(), CH0!())
DECLARE SUB BegStim (CH0!(), CH1!(), MARK(), FlPr1)
DECLARE SUB RewriteArray (CH0!(), CH1!(), MARK())
DECLARE SUB Exstrem (MAX%(), MIN%(), CH1!(), NN, NK, R, S, SN, F%, FlPr1,
CHI)
DECLARE SUB Maxsimum (MAX%(), MIN%(), CH1!(), R, S, NNS%(), NKS%(),
FlPr1)
DECLARE SUB Plot (CH1!(), CHI, NN, NK, BB, F%)
DECLARE SUB Music (MU())
DECLARE SUB PrintFile (CH1!(), M%)
DECLARE SUB PlotAll (CH1!(), NN, NK)
DECLARE SUB VOR (CH1!(), NNS%(), NKS%(), AvVOR!(), SDVOR!(),
AvVORG!(), SDVORG!(), FlPr1)
DECLARE SUB PrGain (AvVOR!(), SDVOR!(), AvVORG!(), SDVORG!(), FileName$,
FlPr)
DECLARE SUB PrSaccades (NNS%(), NKS%())
DECLARE SUB Plot1 (CH0!(), CHI, NN, NK, BB!, F%)
DECLARE SUB VertLine (M!, COL!)
DECLARE SUB WriteFile (FileName$, CH1!())
DECLARE SUB Music1 (MU())
DEFSNG A-Z
SCREEN 12
CLS
LOCATE 12, 15
INPUT "Do you want to print out data on a PRINTER (Y/N)?", Q$
FlPr = 0
IF Q$ = "Y" THEN FlPr = 1
```

```
LOCATE 13, 15
INPUT "Do you want to PLOT all data on a SCREEN (Y/N)?", Q$
FlPr1 = 0
IF Q$ = "Y" THEN FlPr1 = 1
LOCATE 14, 15
INPUT "Do you want to WRITE FILE on a B:\ (Y/N)?", Q$
FlPr2 = 0
IF Q$ = "Y" THEN FlPr2 = 1
Music1 MU()
8 COLL
MESSAGE1 FileName$
ReadFile FileName$, CH1!(), CH0!()
IF FlPr1 = 1 THEN Music MU()
100 CLS
BegStim CH0!(), CH1!(), MARK(), FlPr1
RewriteArray CH0!(), CH1!(), MARK()
NN = 0: NK = 299: PlotAll CH1!(), NN, NK
Maxsimum MAX%(), MIN%(), CH1!(), R, S, NNS%(), NKS%(), FlPr1
REM PrSaccades NNS%(), NKS%()
VOR CH1!(), NNS%(), NKS%(), AvVOR!(), SDVOR!(), AvVORG!(), SDVORG!(),
FlPr1
PrGain AvVOR!(), SDVOR!(), AvVORG!(), SDVORG!(), FileName$, FlPr
CLOSE #1
IF FlPr2 = 0 THEN GOTO 4444
WriteFile FileName$, CH1!()
4444 GOTO 8
END

SUB BegStim (CH0!(), CH1!(), MARK(), FlPr1)
BB! = -250
IF CH0!(1, 0, 200) - CH0!(1, 0, 2) > 0 THEN BB! = -450
FOR F% = 0 TO 9
AV! = 0: NVAL = 0: SUM! = 0: AV1! = 0: SD = 0: SD1 = 0
IF FlPr1 = 1 THEN NN = 0: NK = 299: CHI = 0: Plot1 CH0!(), CHI, NN, NK,
BB!, F%
FOR I% = 0 TO 299
SUM! = SUM! + CH0!(F%, 0, I%): NVAL = NVAL + 1: AV! = SUM! / NVAL:
SD = SQR(ABS(((CH0!(F%, 0, I%) - AV!) * (CH0!(F%, 0, I%) - AV!)) / NVAL))
IF I% < 5 THEN GOTO 1300
IF I% > 290 THEN GOTO 1300
IF BB! = -250 AND (CH0!(F%, 0, I%) + 2) < AV! THEN MARK(F%) = I% - 1:
GOTO 1303
IF BB! = -250 THEN GOTO 1300
IF CH0!(F%, 0, I%) > (AV! + 2) THEN MARK(F%) = I% - 2: GOTO 1303
```

```
1300 NEXT I%
1303 AV1! = AV!: SD1 = SD
ADbeg = 0: ADend = -20 '+10,0
IF BB! = -250 THEN ADbeg = 0: ADend = -20
FOR I% = MARK(F%) + ADbeg TO MARK(F%) + ADend STEP -1
IF BB! <> -250 THEN GOTO 1301
IF CH0!(F%, 0, I%) - CH0!(F%, 0, I% + 1) >= 0 THEN MARK(F%) = I% - 1:
GOTO 1400
1301 IF CH0!(F%, 0, I% + 1) - CH0!(F%, 0, I%) <= 0 THEN MARK(F%) = I%
+ 1: GOTO 1400
NEXT I%
1400 IF FlPr1 = 1 THEN LINE (MARK(F%) * 2 + 1, 0)-(MARK(F%) * 2 + 1, 500),
1
1500 IF FlPr1 = 1 THEN GOTO 1600
1520 INPUT "NEXT? (Y/N)?", X$
1530 IF X$ = "Y" THEN CLS : GOTO 1600
1560 IF X$ = "N" THEN GOTO 1601
1580 GOTO 1520
1600 NEXT F%
1601 REM
END SUB

SUB Exstrem (MAX%(), MIN%(), CH1!(), NN, NK, R, S, SN, F%, FlPr1, CHI)
MA! = 5000: MI! = -5000: IMA = -1: IMI = -1: FlagR = -1: FlagL = -1
IF SN > 0 THEN R = R + 1
IF SN < 0 THEN S = S + 1
FOR I% = NN TO NK
IF I% > 297 THEN GOTO 3005
AV1! = (CH1!(F%, CHI, I%) + CH1!(F%, CHI, I% + 1) + CH1!(F%, CHI, I% +
2)) / 3
IF SN > 0 AND AV1! < MA! THEN MA! = AV1!: IMA = I% + 1
IF SN < 0 AND AV1! > MI! THEN MI! = AV1!: IMI = I% + 1
3005 NEXT I%
IF SN > 0 THEN MAX%(F%, R) = IMA
IF SN < 0 THEN MIN%(F%, S) = IMI
END SUB

SUB Maxsimum (MAX%(), MIN%(), CH1!(), R, S, NNS%(), NKS%(), FlPr1)
FOR I% = 0 TO 9
FOR J% = 0 TO 9
MAX%(I%, J%) = 0: MIN%(I%, J%) = 0
NNS%(I%, J%) = 0: NKS%(I%, J%) = 0
NEXT J%
NEXT I%
```

```
COL = 1: SN = -1: FlSN = 2
IF FlPr1 = 0 THEN GOTO 333
330 INPUT "Whitch Chanel Use FOR Detection (1-Hor,2-Ver,3-Roll"; CHI
IF CHI = 0 THEN GOTO 330
IF CHI > 3 THEN GOTO 330
333 IF (CH1!(0, 1, 100) + CH1!(0, 1, 120) + CH1!(0, 1, 140)) / 3 > (CH1!(0, 1, 0)
+ CH1!(0, 1, 3) + CH1!(0, 1, 5)) / 3 THEN SN = 1
334 FOR F% = 0 TO 9
R = -1: S = -1
IF FlPr1 = 1 THEN CLS
IF FlPr1 = 1 THEN BB = 150: NN = 0: NK = 299: Plot CH1!(), CHI, NN, NK, BB,
F%
335 NN = -1: NK = -1: FlagMax = -1
FOR I% = 0 TO 299
IF I% > 294 THEN GOTO 350
AV2! = (CH1!(F%, CHI, I%) + CH1!(F%, CHI, I% + 1) + CH1!(F%, CHI, I% +
2)) / 3
IF SN < 0 AND FlagMax = -1 AND AV2! > 10 THEN NN = I% - 5: FlagMax =
0
IF SN > 0 AND FlagMax = -1 AND AV2! < -10 THEN NN = I% - 5: FlagMax =
0
IF FlagMax = -1 THEN GOTO 350
IF NN < 0 THEN NN = 0
IF SN < 0 AND FlagMax = 0 AND AV2! < 10 THEN NK = I% + 5: FlagMax =
-1: Exstrem MAX%(), MIN%(), CH1!(), NN, NK, R, S, SN, F%, FlPr1, CHI: GOTO
340
IF SN > 0 AND FlagMax = 0 AND AV2! > -10 THEN NK = I% + 5: FlagMax =
-1: Exstrem MAX%(), MIN%(), CH1!(), NN, NK, R, S, SN, F%, FlPr1, CHI: GOTO
341
GOTO 350
340 IF SN < 0 THEN N = S
341 IF SN > 0 THEN N = R
NNS%(F%, N) = NN: NKS%(F%, N) = NK
IF FlPr1 = 1 THEN LINE (NN * 2, 150)-(NK * 2, 150), 4
NN = -1: NK = -1
COL = COL + 1: IF COL > 15 THEN COL = 1
IF SN > 0 THEN M = MAX%(F%, R)
IF SN < 0 THEN M = MIN%(F%, S)
IF M = 0 THEN GOTO 350
IF FlPr1 = 1 THEN VertLine M, COL
350 NEXT I%
IF FlSN < 2 THEN GOTO 360
355 PRINT FlSN: INPUT "Is It Correct (Y/N)?"; Q$
IF Q$ = "N" THEN SN = -SN: FlSN = -1: GOTO 334
```

```
IF Q$ = "Y" THEN FlSN = -1: GOTO 360
GOTO 355
360 LOCATE 1, 5
COLOR 14
IF FlPr1 = 1 THEN INPUT "Drow the next one for you?", Y$
NEXT F%
END SUB

SUB MESSAGE1 (FileName$)
CLS
COLOR 3
LINE (0, 0)-STEP(640, 480), , BF
COLOR 0
LINE (10, 50)-STEP(520, 350), , BF
COLOR 2
DRAW "C0"
DRAW "M 10, 400"
DRAW "C2"
DRAW "U 350"
DRAW "R 520"
DRAW "D 350"
DRAW "L 520"
COLOR 2       'Print in Green Color
LOCATE 5, 10
PRINT "This Program Will Prepared Data Array For the MAC"
LOCATE 8, 10
PRINT "Input File Must Have "
LOCATE 9, 33
COLOR 6
PRINT "Yaw"
LOCATE 10, 33
PRINT "Vertical"
LOCATE 11, 33
PRINT "Roll"
LOCATE 12, 33
COLOR 2
PRINT "Eye Velocity For 10 VOR Steps"
LOCATE 15, 10
PRINT "The input Files Mast be on Drive";
COLOR 4       'Print in Red Color
PRINT "   a:"
LOCATE 16, 10
COLOR 2       'Print in Green Color
PRINT "Output will Produce on Drive";
```

```
COLOR 4        'Print in Red Color
PRINT "        b:"
LOCATE 18, 15
COLOR 4        'Print in Red Color
PRINT "Press ENTER when ready...";
INPUT Y$
CLS
DRAW "C0"
DRAW "M 0, 220"
DRAW "C2"
DRAW "U 120"
DRAW "R 580"
DRAW "D 120"
DRAW "L 580"
DRAW "C0"
DRAW "M 0, 400"
DRAW "C2"
DRAW "U 140"
DRAW "R 580"
DRAW "D 140"
DRAW "L 580"
LOCATE 5, 1
COLOR 2      'Print in Green Color
PRINT "Disk A: contains the following files:"
LOCATE 7, 40
COLOR 15       'Print in Bright White Color
FILES "a:\*.*"
LOCATE 16, 1
COLOR 2        'Print in Green Color
PRINT "Disk B: alrady have following files:"
LOCATE 17, 40
COLOR 15       'Print in Bright White Color
FILES "b:\*.*"
COLOR 3
LINE (0, 0)-STEP(640, 40), , BF
LOCATE 1, 20
COLOR 12         'Print in Red Color
PRINT "Which file would you like to load?";
COLOR 4: INPUT "      ", FileName$
LOCATE 5, 15
COLOR 2          'Print in Green Color
PRINT "                                          "
Flag = 0
CLS
```

```
LOCATE 20, 20
COLOR 4
PRINT "Wait for opening:", FileName$
END SUB

SUB Music (MU())
FOR I% = 0 TO 16
note% = MU(I% * 2): duration% = MU(I% * 2 + 1)
   SOUND note%, duration%
NEXT I%
END SUB

SUB Music1 (MU())
MU(0) = 392: MU(1) = 8: MU(2) = 659: MU(3) = 8: MU(4) = 587: MU(5) = 8
MU(6) = 523: MU(7) = 8: MU(8) = 587: MU(9) = 8: MU(10) = 523:MU(11) = 8
MU(12)= 440: MU(13)= 8: MU(14)= 392: MU(15) =8: MU(16)=330: MU(17)= 32
MU(18)= 392: MU(19)= 8: MU(20)= 659: MU(21)= 8: MU(22)= 587:MU(23)= 8
MU(24)= 523: MU(25)= 8: MU(26)= 523: MU(27)= 8: MU(28)= 494:MU(29)= 8
MU(30) = 523: MU(31) = 8: MU(32) = 587: MU(33) = 40
END SUB

SUB Plot (CH1!(), CHI, NN, NK, BB, F%)
CLS
COLOR 2
LOCATE 1, 60
PRINT "RESPONSE = ";
COLOR 4
PRINT F%
FOR J% = NN TO NK
PSET (J% * 2, (CH1!(F%, CHI, J%) + BB)), 7
NEXT J%
END SUB

SUB Plot1 (CH0!(), CHI, NN, NK, BB!, F%)
CLS
FOR J% = NN TO NK
PSET (J% * 2, (CH0!(F%, CHI, J%) * 5 + BB!)), 7
NEXT J%
END SUB

SUB PlotAll (CH1!(), NN, NK)
CLS
COR! = 0
IF CH1!(0, 0, 2) - CH1!(0, 0, 100) < 0 THEN COR! = -200
```

```
FOR M% = 0 TO 3
COLOR 4
LOCATE 1, 30
IF M% = 0 THEN DRAW "P1, 1": PRINT "Stimulus"; : BB = -250 + COR!
IF M% = 1 THEN DRAW "P1, 2": PRINT "YAR velocity"; : BB = 350 + COR!
IF M% = 2 THEN DRAW "P1, 6": PRINT "VERTICAL velocity";: BB = 250 +
                                                    COR!
IF M% = 3 THEN DRAW "P1, 8": PRINT "ROLL velocity"; : BB = 250 + COR!
FOR F% = 0 TO 9
FOR J = NN TO NK
PSET (J * 2, (CH1!(F%, M%, J) * 5 + BB)), 7
NEXT J
NEXT F%
LOCATE 29, 40
COLOR 2
PRINT "Press <ENTER> for continuation";
LOCATE 29, 25
COLOR 4
INPUT "Next ?"; Q
CLS
NEXT M%
END SUB

SUB PrGain (AvVOR!(), SDVOR!(), AvVORG!(), SDVORG!(), FileName$, FlPr)
CLS
PRINT "The File that have been prosessed is-", FileName$
PRINT : PRINT : PRINT
IF FlPr = 1 THEN LPRINT "The File that have been prosessed is-", FileName$
IF FlPr = 1 THEN LPRINT : LPRINT : LPRINT
FOR M% = 0 TO 3
COLOR 2
IF M% = 0 THEN GOTO 500
IF M% = 1 THEN PRINT "Velocity of YAW:": PRINT ""
IF M% = 2 THEN PRINT "Velocity of VERTICAL:": PRINT ""
IF M% = 3 THEN PRINT "Velocity of ROLL:": PRINT ""
COLOR 3
PRINT "Average Velocity=";
COLOR 6
PRINT USING "###.####"; AvVOR!(M%);
PRINT "", CHR$(241); ' +/-
PRINT USING "###.####"; SDVOR!(M%)
COLOR 3
PRINT "Average Gain    =";
COLOR 6
```

```
PRINT USING "##.####"; AvVORG!(M%);
PRINT "", CHR$(241); ' +/-
PRINT USING "###.####"; SDVORG!(M%)
PRINT ""
500 NEXT M%
IF FlPr = 0 THEN GOTO 501
FOR M% = 0 TO 3
IF M% = 0 THEN GOTO 502
IF M% = 1 THEN LPRINT "Velocity of YAW:": LPRINT ""
IF M% = 2 THEN LPRINT "Velocity of VERTICAL:": LPRINT ""
IF M% = 3 THEN LPRINT "Velocity of ROLL:": LPRINT ""
LPRINT "Average Velocity=";
LPRINT USING "###.####"; AvVOR!(M%);
LPRINT " +/-";
LPRINT USING "###.####"; SDVOR!(M%)
LPRINT "Average Gain    =";
LPRINT USING "##.####"; AvVORG!(M%);
LPRINT " +/-";
LPRINT USING "###.####"; SDVORG!(M%)
LPRINT ""
502 NEXT M%
501 REM M% = 1: PrintFile CH1!(), M%
LPRINT CHR$(12)
END SUB

SUB PrintFile (CH1!(), M%)
FOR I = 0 TO 299
LPRINT I, CH1!(0, M%, I), CH1!(1, M%, I), CH1!(2, M%, I), CH1!(3, M%, I)
NEXT I
END SUB

SUB PrSaccades (NNS%(), NKS%())
'       This SUB program printing out on a screen
'       numder of saccades for each response in that File
CLS
FOR F% = 0 TO 9
FOR I% = 0 TO 9
PRINT "F="; F%; "Saccade N="; I%, "T begin="; NNS%(F%, I%); "T end=";
NKS%(F%, I%)
NEXT I%
INPUT Q
NEXT F%
END SUB
```

```
SUB ReadFile (FileName$, CH1!(), CH0!())
SHELL "A:"
OPEN FileName$ FOR INPUT AS #1
J = 0: K = 0: K1 = -1
10 FOR I = 0 TO 12299
IF I / 42 = INT(I / 42) THEN K1 = K1 + 1
IF I = K1 * 42 OR I = K1 * 42 + 1 THEN GOTO 120
40 K = INT((I - 1) / 42)
50 IF I - 42 * K = 0 GOTO 180
60 L = INT(ABS((I - 42 * K) - 2) / 4)
70 M = (((I - 42 * K) - 2) - 4 * L)
90 GOTO 140
120 INPUT #1, CH1!(L, M, K): GOTO 180
140 INPUT #1, CH0!(L, M, K)
180 NEXT I
200 BEEP
END SUB

SUB RewriteArray (CH0!(), CH1!(), MARK())
COLOR 2              'Print in Green Color
PRINT "I,m cleaning data array"
FOR F% = 0 TO 9
FOR M% = 0 TO 3
FOR I% = 0 TO 299
CH1!(F%, M%, I%) = 0
NEXT I%
NEXT M%
LOCATE 2, 10
COLOR 15             'Print in Yellow Color
PRINT F% + 1, "of 10 is cleaned"
NEXT F%
FOR F% = 0 TO 9
FOR I% = 0 TO 299
IF I% < MARK(F%) - 5 THEN GOTO 2500
FOR R% = 0 TO 3
CH1!(F%, R%, I% - (MARK(F%) - 5)) = CH0!(F%, R%, I%)
NEXT R%
2500 NEXT I%
NEXT F%
CLS
END SUB

SUB VertLine (M, COL)
LINE (M * 2, 20)-(M * 2, 480), COL
```

```
END SUB

SUB VOR (CH1!(), NNS%(), NKS%(), AvVOR!(), SDVOR!(), AvVORG!(),
SDVORG!(), FlPr1)

' ************************************************************************
' *  Average and SD                                                      *
' *          SD=SQR((N*Sum(Xi*Xi)-Sum(Xi)*Sum(Xi))/N*(N-1))              *
' *                  VELOCITY                                            *
' *              Average      =AvVOR#                                    *
' *              N            =CountAV                                   *
' *              Xi           =AverVOR#                                  *
' *              Xi*Xi        =SqAv#                                     *
' *              Sum(Xi*Xi)   =SumSqAv#                                  *
' *              Sum(Xi)      =SumAverVOR#                               *
' *              Sum(Xi)*Sum(Xi)=SumSqAvVOR#                             *
' *                  GAIN                                                *
' *              Average      =AvVORG#                                   *
' *              N            =CountAV                                   *
' *              Xi           =AverVORG#                                 *
' *              Xi*Xi        =SqAvG#                                    *
' *              Sum(Xi*Xi)   =SumSqAvG#                                 *
' *              Sum(Xi)      =SumAverVORG#                              *
' *              Sum(Xi)*Sum(Xi)=SumSqAvVORG#                            *
' ************************************************************************
FOR M% = 0 TO 3
CountAV = 0: SumAverVOR# = 0: SumSqAv# = 0: SumSqAvVOR# = 0
SumAverVORG# = 0: SumSqAvG# = 0: SumSqAvVORG# = 0
FOR F% = 0 TO 9
SumVOR# = 0: CountVOR = 0
SumVORG# = 0
NN = 30: NK = NNS%(F%, 0)
IF NK - NN < 0 THEN NN = 30: NK = NNS%(F%, 1)
IF NKS%(F%, 0) > 30 AND NK = NNS%(F%, 1) THEN NN = NKS%(F%, 0)
IF NN < 30 THEN NK = NNS%(F%, 2): NN = NKS%(F%, 1)
REM IF NK < 50 THEN NN = NKS%(F%, 0): NK = NNS%(F%, 1)
IF NN > NK THEN NN = NKS%(F%, 1): NK = NNS%(F%, 2)
IF NK - NN < 2 THEN GOTO 4105
IF NK - NN > 40 THEN NK = NN + 20
I1% = NN: I2% = NK
FOR I = 0 TO 299
IF I < NN THEN GOTO 4100
IF I > NK THEN GOTO 4100
SumVOR# = SumVOR# + CH1!(F%, M%, I): CountVOR = CountVOR + 1
```

```
SumVORG# = SumVORG# + CH1!(F%, M%, I) / 60
4100 NEXT I
AverVOR# = (SumVOR# / CountVOR): CountAV = CountAV + 1
AverVORG# = (SumVORG# / CountVOR)
SqAv# = AverVOR# * AverVOR#
SqAvG# = AverVORG# * AverVORG#
SumSqAv# = SumSqAv# + SqAv#
SumSqAvG# = SumSqAvG# + SqAvG#
SumAverVOR# = SumAverVOR# + AverVOR#
SumAverVORG# = SumAverVORG# + AverVORG#
CLS
IF FlPr1 = 1 AND M% > 0 THEN GOTO 4105
IF FlPr1 = 0 THEN GOTO 4105
NN = 0: NK = 299: CHI = 3: BB = 250: Plot CH1!(), CHI, NN, NK, BB, F%
M = I1%: COL = 2: VertLine M, COL
M = I2%: COL = 4: VertLine M, COL
INPUT ; Q
4105 NEXT F%
AvVOR!(M%) = SumAverVOR# / CountAV
AvVORG!(M%) = SumAverVORG# / CountAV
SumSqAvVOR# = SumAverVOR# * SumAverVOR#
SumSqAvVORG# = SumAverVORG# * SumAverVORG#
SDVOR!(M%) = SQR((CountAV * SumSqAv# - SumSqAvVOR!) / (CountAV *
(CountAV - 1)))
SDVORG!(M%) = SQR(ABS((CountAV * SumSqAvG# - SumSqAvVORG#) /
(CountAV * (CountAV - 1))))
NEXT M%
END SUB

SUB WriteFile (FileName$, CH1!())
I1 = -1
SHELL "B:"
PRINT FileName$
OPEN FileName$ FOR OUTPUT AS #2
D0$ = "TIME"
D1$ = "S1": D2$ = "H1": D3$ = "V1": D4$ = "R1"
D5$ = "S2": D6$ = "H2": D7$ = "V2": D8$ = "R2"
D9$ = "S3": E0$ = "H3": E1$ = "V3": E2$ = "R3"
E3$ = "S4": E4$ = "H4": E5$ = "V4": E6$ = "R4"
E7$ = "S5": E8$ = "H5": E9$ = "V5": F0$ = "R5"
F1$ = "S6": F2$ = "H6": F3$ = "V6": F4$ = "R6"
F5$ = "S7": F6$ = "H7": F7$ = "V7": F8$ = "R7"
F9$ = "S8": G0$ = "H8": G1$ = "V8": G2$ = "R8"
G3$ = "S9": G4$ = "H9": G5$ = "V9": G6$ = "R9"
```

```
G7$ = "S10": G8$ = "H10": G9$ = "V10": H0$ = "R10"
WRITE #2, I1, D0$, D1$, D2$, D3$, D4$, D5$, D6$, D7$, D8$, D9$, E0$, E1$, E2$,
E3$, E4$, E5$, E6$, E7$, E8$, E9$, F0$, F1$, F2$, F3$, F4$, F5$, F6$, F7$, F8$,
F9$, G0$, G1$, G2$, G3$, G4$, G5$, G6$, G7$, G8$, G9$, H0$
I1 = 0
FOR I = 0 TO 299
I2 = I1 * 6.4
D0 = I2: D1 = CH1!(0, 0, I): D2 = CH1!(0, 1, I): D3 = CH1!(0, 2, I): D4 =
CH1!(0, 3, I)
D5 = CH1!(1, 0, I): D6 = CH1!(1, 1, I): D7 = CH1!(1, 2, I): D8 = CH1!(1, 3, I)
D9 = CH1!(2, 0, I): E0 = CH1!(2, 1, I): E1 = CH1!(2, 2, I): E2 = CH1!(2, 3, I)
E3 = CH1!(3, 0, I): E4 = CH1!(3, 1, I): E5 = CH1!(3, 2, I): E6 = CH1!(3, 3, I)
E7 = CH1!(4, 0, I): E8 = CH1!(4, 1, I): E9 = CH1!(4, 2, I)
F0 = CH1!(4, 3, I): F1 = CH1!(5, 0, I): F2 = CH1!(5, 1, I): F3 = CH1!(5, 2, I)
F4 = CH1!(5, 3, I): F5 = CH1!(6, 0, I): F6 = CH1!(6, 1, I): F7 = CH1!(6, 2, I)
F8 = CH1!(6, 3, I): F9 = CH1!(7, 0, I)
G0 = CH1!(7, 1, I): G1 = CH1!(7, 2, I): G2 = CH1!(7, 3, I): G3 = CH1!(8, 0, I)
G4 = CH1!(8, 1, I): G5 = CH1!(8, 2, I): G6 = CH1!(8, 3, I): G7 = CH1!(9, 0, I)
G8 = CH1!(9, 1, I): G9 = CH1!(9, 2, I): H0 = CH1!(9, 3, I)
WRITE #2, I1, D0, D1, D2, D3, D4, D5, D6, D7, D8, D9, E0, E1, E2, E3, E4, E5,
E6, E7, E8, E9, F0, F1, F2, F3, F4, F5, F6, F7, F8, F9, G0, G1, G2, G3, G4, G5,
G6, G7, G8, G9, H0
I1 = I1 + 1
NEXT I
CLOSE #2
END SUB
```

BIBLIOGRAPHY:

Albus, J. S. (1971). A theory of cerebellar function. Math. Biosci, **10**: 25-61.

Alley, K., R. Baker and J. I. Simpson (1975). Afferents to the vestibulo - cerebellum and the origin of the visual climbing fibers in the rabbit. Brain Res., **98**: 582-589.

Angelaki, D., B. J. M. Hess and J.-I. Suzuki (1995). 3-D organization before and after adaptation to lateral semicircular canal inactivation. Three-Dimensional Kinematic Principles of Eye-, Head-, and Limb Movements in Health and Disease, Tübingen, Germany, 11.

Baker, J., J. Goldberg, B. Peterson and R. Schor (1982). Oculomotor reflexes after semicircular canal plugging in cats. Brain Res., **252**: 151-155.

Baker, J., C. Wickland and B. Peterson (1987). Dependence of cat vestibulo-ocular reflex direction adaptation on animal orientation during adaptation and rotation in darkness. Brain Res., **408**: 339-343.

Baker, J. F., N. Isu, C. R. Wickland and B. W. Peterson (1986). Dynamics of adaptive change in vestibulo-ocular reflex directions. II. Sagittal plane rotation. Brain Res., **371**: 166-170.

Baker, J. F. and B. W. Peterson (1991). Excitation of the extraocular muscles in decerebrate cats during the vestibulo-ocular reflex in three-dimensional space. Exp. Brain Res., **84**: 266-278.

Barmack, N. H. and V. E. Pettorossi (1988a). The otolithic origin of the vertical vestibuloocular reflex following bilateral blockage of the vertical semicircular canal in the rabbit. J. Neurosci., **8**: 2827-2835.

Barmack, N. H. and V. E. Pettorossi (1988b). The induction and compensation of asymmetric eye movements following unilateral blockage of a horizontal semicircular canal in the rabbit. J. Neurosci., **8**: 2836-2843.

Berthoz, A., G. Melvill Jones and A. E. Begue (1981). Differential visual adaptation of vertical canal-dependent vestibulo-ocular reflexes. Exp. Brain Res., **44**: 19-26.

Bizzi, E., R. E. Kalil and P. Morasso (1972). Two modes of active eye-head coordination in monkeys. Brain Res., **40**: 45-48.

Bizzi, E., R. E. Kalil and V. Tagliasco (1971). Eye-head coordination in monkeys: evidence for centrally patterned organization. Science, **173**: 452-454.

Blanks, R. H. I., I. S. Curthoys, M. Bennet and C. H. Markham (1985). Planar relationships of the semicircular canals in rhesus and squirrel monkeys. Brain Res., **340**: 315-324.

Blanks, R. H. I., I. S. Curthoys and C. H. Markham (1972). Planar relationships of semicircular canals in the cat. Am. J. Physiol., **223**: 55-62.

Blanks, R. H. I., I. S. Curthoys and C. H. Markham (1975). Planar relationships of the semicircular canals in man. Acta Oto-Laryngol., **80**: 185-196.

Blanks, R. H. I., W. Precht and Y. Torigoe (1983). Afferent projections to the cerebellar flocculus in the pigmented rat demonstrated by retrograde transport of horseradish peroxidase. Exp. Brain Res., **52**: 293-306.

Böhmer, A., V. Henn and J.-I. Suzuki (1985). Vestibulo-ocular reflex after selective plugging of the semicircular canals in the monkey - Response Plane determinations. Brain Res., **326**: 291-298.

Brodal, A., O. Pompeiano and F. Welberg (1962). The vestibular nuclei and their connections anatomy and functional correlations. Illinois, Springfield.

Büttner, U. and W. Waespe (1981). Vestibular nerve activity in the alert monkey during vestibular and optokinetic nystagmus. Exp. Brain Res., **41**: 310-315.

Büttner-Ennever, J. A. (1992). Patterns of connectivity in the vestibular nuclei. Sensing and controlling motion. Vestibular and sensorimotor function. New York, NY Acad. Press. 363-378.

Camis, M. (1930). The Physiology of the Vestibular Apparatus. Oxford, UK, Clarendon.

Cannon, S. C. and D. A. Robinson (1987). Loss of the neural integrator of the oculomotor system from brain stem lesions in monkey. J. Neurophysiol, **57**: 1382-1409.

Chubb, C. M., A. F. Fuchs and C. A. Scudder (1984). Neural activity in monkey vestibular nuclei during vertical vestibular stimulation and eye movements. J. Neurophysiol., **52**: 724-742.

Cohen, B., D. Helwig, T. Raphan, J.-I. Suzuki, K. Kaga and A. Eden (1988). Changes in visual and vestibular function after canal plugging in the monkey. Society for Neuroscience, 18th annual meeting, Nov. 13-18, Toronto, Ontario, Canada, 173, 74.5.

Cohen, B., V. Henn, T. Raphan and D. Dennett (1981). Velocity storage, nystagmus, and visual vestibular interactions in humans. Ann. N.Y. Acad. Sci., **374**: 421-433.

Cohen, B., I. B. Kozlovskaya, T. Raphan, D. Solomon, D. Helwig, N. Cohen, M. G. Sirota and S. B. Yakushin (1992). Vestibuloocular reflex of rhesus monkeys after spaceflight. J.Appl. Physiol., **73**: 121S-131S.

Cohen, B., T. Raphan, D. Solomon, D. Helwig, N. Cohen, I. B. Kozlovskaya, M. G. Sirota and S. B. Yakushin (1991). Effects of spaceflight in the "Cosmos" biosatellite 2044 on the VOR of Rhesus Monkey. International Meeting "Biosatellite Cosmos", Leningrad 12-15 August, 113.

Cohen, B., J. Suzuki and M. B. Bender (1965). Nystagmus induced by electric stimulation of ampullary nerves. Acta Otolaryngol., **60**: 422-436.

Cohen, B., J.-I. Suzuki and M. B. Bender (1964). Eye movements from semicircular canal nerve stimulation in the cat. Annals of Otology, Rhinology and Laryngology, **73**: 153-169.

Cohen, B., J.-I. Suzuki and Raphan, T. (1983). Role of the otolith organs in generation of horizontal nystagmus: effects of selective labyrinthine lesions. Brain Res., **276**: 159-164.

Cohen, H., B. Cohen, T. Raphan and W. Waespe (1992). Habituation and adaptation of the vestibulo-ocular reflex: A model of differential control by the vestibulo-cerebellum. Exp. Brain Res., **90**: 526-538.

Collewijn, H. (1972). An analog model of the rabbit's optokinetic system. Brain Res., **36**: 71-88.

Collewijn, H. (1976). Impairment of optokinetic (after-)nystagmus by labyrinthectomy in the rabbit. Exp. Neurol, **52**: 146-156.

Collewijn, H., L. Ferman and A. V. Van Den Berg (1988). The behavior of human gaze in three dimensions. Representation of three-dimensional space in the vestibular, oculomotor, and visual systems. New York, NY Acad. of Sci. 105-127.

Collewijn, H. and A. F. Grootendorst (1979). Adaptation of optokinetic and vestibulo-ocular reflexes to modified visual input in the rabbit. Prog. Brain Res, **50**: 772-781.

Collins, W. E. (1962). Effects of mental set upon vestibular nystagmus. J. Exp. Psychol., **63**: 191-197.

Correia, M. J. and K. E. Money (1970). The effect of all six semicircular canal ducts on nystagmus produced by linear acceleration in the cat. Acta Otolaryngol., **69**: 7-16.

Correia, M. J., A. A. Perachio, J. D. Dickman, I. B. Kozlovskaya, M. G. Sirota, S. B. Yakushin and I. N. Beloozerova (1990a). The effects of 14 days of microgravity on post-flight semicircular canal primary afferent and horizontal eye movement responses. XV Barany Society Meeting, 87.

Correia, M. J., A. A. Perachio, J. D. Dickman, I. B. Kozlovskaya, M. G. Sirota, S. B. Yakushin and I. N. Beloozerova (1990b). Vestibular primary afferent and vestibulo-ocular changes in rhesus monkey following 14 day of microgravity. XII Ann. Meeting Commission of Gravitational Physiology, Leningrad 14-19 October, 1990, 124.

Correia, M. J., A. A. Perachio, J. D. Dickman, I. B. Kozlovskaya, M. G. Sirota, S. B. Yakushin and I. N. Beloozerova (1991). Reprogramming of horizontal semicircular canals in Rhesus monkey following 14 days of microgravity. International Meeting "Biosatellite Cosmos", Leningrad, 12-15 August 1991, 180-181.

Correia, M. J., A. A. Perachio, J. D. Dickman, I. B. Kozlovskaya, M. G. Sirota, S. B. Yakushin and I. N. Beloozerova (1992a). Changes in monkey horizontal semicircular canal afferent responses after spaceflight. J. Appl. Physiol., **73**: 112S-120S.

Correia, M. J., A. A. Perachio, J. D. Dickman, I. B. Kozlovskaya, M. G. Sirota, S. B. Yakushin and I. N. Beloozerova (1992b). Post-flight changes in yaw responses of horizontal semicircular canal afferents in rhesus monkey following 14 days of microgravity. XVIIth Barany Society Meeting, Czechoslovakia, June 1-5, 188-189.

Crawford, J. D. and T. Vilis (1991). Axes of eye rotation and Listing's law during rotations of the head. J Neurophysiol., **65**: 407-23.

Curthoys, I. S., R. H. I. Blanks and C. H. Markham (1977). Semicircular canal functional anatomy in cat, guinea pig and man. Acta Otolaryngol., **83**: 258-265.

Curthoys, I. S. and G. M. Halmagyi (1995). Vestibular compensation: a review of the oculomotor, neural, and clinical consequences of unilateral vestibular loss. J. Vestib. Res., **5**: 67-107.

Dai, M., L. McGarvie, I. Kozlovskaya, T. Raphan and B. Cohen (1994). Effects of spaceflight on ocular counterrolling and spatial orientation of the vestibular system. Exp. Brain Res., **102**: 45-56.

Dai, M. J., T. Raphan, B. Cohen and C. Schnabolk (1991). Spatial orientation of velocity storage during post-rotatory nystagmus. Soc. for Nuerosc. Abstr. New Orleans, Louisiana, 314.

Dichgans, J., E. Bizzi, P. Morasso and V. Tagliasco (1973). Mechanisms underlying recovery of eye-head coordination following bilateral labyrinthectomy in monkeys. Exp.

Brain Res., **18**: 548-562.

Duensing, F. and K.-P. Schaefer (1958). Die Aktivitat einzelner Neurone im Bereich der Vestibulariskerne bei Horizontal-beschleunigungen unter besonderer Berucksichtigung des vestibularen Nystagmusw. Arch. Psychiat. Nervenkr., **198**: 225-252.

Dufosse, M., M. Ito, P. J. Jastreboff and Y. Miyashita (1978). A neuronal correlate in rabbit's cerebellum to adaptive modification of the vestibulo-ocular reflex. Brain Res., **150**: 511-616.

Epema, A. H., N. M. Gerrits and J. Voogd (1988). Commissural and intrinsic connections of the vestibular nuclei in the rabbit: a retrograde labeling study. Exp. Brain Res., **71**: 129-146.

Ewald, J. R. (1892). Physiologische Untersuchungen uber das Endorgan des Nervus Octavus. Weisbaden.

Ezure, K. and W. Graf (1984a). A quantitative analysis of the spatial organization of the vestibulo-ocular reflexes in lateral- and frontal-eyed animals -I. Orientation of semicircular canals and extraocular muscles. Neuroscience, **12**: 85-93.

Ezure, K. and W. Graf (1984b). A quantitative analysis of the spatial organization of the vestibulo-ocular reflexes in lateral- and frontal-eyed animals -II. Neuronal networks underlying vestibulo-oculomotor coordination. Neuroscience, **12**: 95-109.

Ferman, L., H. Collewijn, T. C. Jansen and A. V. Van den Berg (1987a). Human gaze stability in the horizontal, vertical and torsional direction during voluntary head movement, evaluated with a three-dimentional scleral induction coil technique. Vision Res., **5**: 811-828.

Ferman, L., H. Collewijn and A. V. Van den Berg (1987b). A direct test of Listing's law: II. Human ocular torsion measured under dynamic conditions. Vision Res., **27**: 939-951.

Fernandez, C. and J. M. Goldberg (1971). Physiology of peripheral neurons innervatingsemicircular canals of the squirrel monkey. II Response to sinusoidal stimulation and dynamics of peripheral vestibular system. J. Neurophysiol, **34**: 661-675.

Fetter, M., H. Misslisch, D. Sievering and D. Tweed (1995). Effects of full-field visual input on the three-dimensional properties of the human vestibuloocular reflex. J. Vestib. Res., **5**: 201-209.

Fetter, M. and D. S. Zee (1988). Recovery from unilateral labyrinthectomy in rhesus monkey. J. Neurophysiol., **59**: 370-393.

Frens, M. A. and A. J. van Opstal (1994). Transfer of short-term adaptation in human saccadic eye movements. Exp. Brain Res., **100**: 293-306.

Gacek, R. R. (1969). The course and central termination of the first order neurones supplying vestibular endorgans in the cat. Acta Oto-laryngol., **254**: 1-66.

Gacek, R. R. and M. Lyon (1974). Localization of vestibular efferent neurones in the kitten with horseradish peroxidase. Acta Oto-laryngol., **77**: 92-101.

Gauthier, G. M. and D. A. Robinson (1975). Adaptation of the human vestibulo-ocular reflex to magnifying lenses. Brain Res., **92**: 331-335.

Goldberg, J., M. and C. Fernandes (1975). Responses of peripheral vestibular neurons to angular and linear accelerations in the squirrel monkey. Acta Otolaryngol. (Stockh), **80**: 101-110.

Goldberg, J. M. and C. Fernandez (1971). Physiology of peripheral neurons innervating semicircular canals of the squirrel monkey. I. Resting discharge and response to angular accelerations. J. Neurophysiol., **34**: 676-684.

Goldberg, J. M. and C. Fernandez (1980). Efferent vestibular system in the squirrel monkey: anatomical location and influence on afferent activity. J. Neurophysiol., **43**: 986-1025.

Gonshor, A. and G. Melvill-Jones (1976a). Short-term adaptive changes in the human vestibulo-ocular reflex arc. J. Physiol. (L), **256**: 361-379.

Gonshor, A. and G. Melvill-Jones (1976b). Extreme vestibulo-ocular adaptation induced by prolonged optical reversal of vision. J. Physiol. (L), **256**: 381-414.

Graf, W. and K. Ezure (1986). Morphology of vertical canal related second order vestibular neurones in the cat. Exp. Brain Res., **63**: 35-48.

Grossman, G. E., R. J. Leigh, E. N. Bruce, W. P. Huebner and D. Lanska (1989). Performance of the human vestibuloocular reflex during locomotion. J. Neurophysiol., **62**: 264-272.

Harrison, R. E. W., J. F. Baker, N. Isu, C. R. Wickland and B. W. Peterson (1986). Dynamics of adaptive changes in vestibulo-ocular reflex directions. I. Rotations in the horizontal plane. Brain Res., **371**: 162-165.

Henn, V., D. Straumann, B. J. M. Hess, T. Haslwanter and N. Iida (1992). Three dimensional transformation from vestibular and visual input to oculomotor output. Ann. N.Y. Acad. of Sci., **656**: 166-180.

Highstein, S. H. and R. Baker (1985). Action of the efferent vestibular system on primary afferents in the toadfish, *Opsanus tau*. J. Neurophysiol., **54**: 370-384.

Hudspeth, A. J. and D. P. Corey (1977). Sensitivity, polarity and conduction change in the response of vertebrate hair cells to controlled mechanical stimuli. Proc. Nat. Acad. Sci., **746**: 2407-2411.

Igarashi, M., T. Himi, W. B. Kulecz and S. Patel (1987). The role of saccular afferents in vertical optokinetic nystagmus in primates. A study in relation to optokinetic nystagmus in microgravity. Arch Otorhinolaryngol., **244**: 143-146.

Ito, M. (1970). Neurophysiological aspects of the cerebellar motor control system. Int. J. Neurol., **7**: 162-176.

Ito, M. (1972). Neural design of the cerebellar motor control system. Brain Res., **40**: 81-84.

Ito, M. (1974). The control mechanisms of cerebellar motor systems . The neurosciences: Third study program. Cambridge Mass., Cembridge Mass.M.I.T. Press. 293-303.

Jäger, J. and V. Henn (1981). Vestibular habituation in man and monkey during sinusoidal rotation. Ann. N.Y. Acad. Sci., **374**: 330-339.

Judge, S. J., B. J. Richmond and F. C. Chu (1980). Implantation of magnetic search coils for measurement of eye position: an improved method. Vision Res., **20**: 535-538.

Keller, E. L. (1978). Gain of the vestibulo-ocular reflex in monkey at higher rotational frequencies. Vision Res., **18**: 311-315.

Keller, E. L. and W. Precht (1979). Adaptive modification of central vestibular neurons in response to visual stimulation through reversing prism. J. Neurophysiol., **42**: 896-911.

Keppel, G. (1991). Design and analysis: A researcher's handbook. Englewood Cliffs, NJ, Prentice Hall, pp 594.

Khalsa, S. B., R. D. Tomlinson, D. W. Schwarz and J. P. Landolt (1987). Vestibular nuclear neuron activity during active and passive head movement in the alert rhesus monkey. J. Neurophysiol., **57**: 1484-1497.

Kimura, M. and K. Maekawa (1981). Activity of flocculus Purkinje cells during passive eye movements. J.Neurophysiol., **46**: 1004-1017.

Kozlovskaya, I. B., B. M. Babaev, V. A. Barmin, I. N. Beloozerova, M. G. Sirota, S.

B. Yakushin and L. N. Kornilova (1990). Results of vestibular function studying in space flight in man and animals. 4 Europium Meeting ECA, Triest,Italy, 28 May - 1 June, 353-357.

Kozlovskaya, I. B., M. B. Babaev, V. A. Barmin, I. I. Beloozerova, Y. V. Kreidich and M. G. Sirota (1984). The effect of weightlessness on motor and vestibulo-motor reactions. The Physiologist, **27**: 111-114.

Kozlovskaya, I. B., V. A. Barmin, Y. V. Kreidich and A. A. Repin (1985). The effects of real and simulated microgravity on vestibulo-oculaomotor interaction. The Physiologist, **28**: 51-56.

Kozlovskaya, I. B., E. A. Ilyin, M. G. Sirota, V. I. Korolkov, B. M. Babaev, I. N. Beloozerova and S. B. Yakushin (1989). Studies of space adaptation syndrome on board of Soviet biosattelite "Cosmos 1887". The Physiologist, **32**: 45-48.

Kozlovskaya, I. B., M. G. Sirota, I. N. Beloozerova and S. B. Yakushin (1991). Vestibulo-motor interaction in microgravity. International Meeting "Biosatellite Cosmos", Leningrad 12-15 August, 52 (in Russian).

Langer, T., A. F. Fuchs, M. C. Chubb, C. A. Scudder and S. G. Lisberger (1985). Afferents to the flocculus of the cerebellum in the rhesus macaque as revealed by retrograde transport of horseradish peroxidase. J. Comp. Neurology, **235**: 1-25.

Lisberger, S. F. and A. F. Fuchs (1978). Role of primate flocculus during rapid behavioral modification of vestibuloocular reflex. I. Purkinje cell activity during visually guided horizontal smooth-pursuit eye movements and passive head rotation. J. Neurophysiol., **41**: 733-763.

Lisberger, S. F., T. A. Pavelko, H. M. Bronte-Stewart and L. S. Stone (1994b). Neural basis for motor learning in the vestibuloocular reflex of primates. II. Changes in the responses of horizontal gaze velocity Purkinje cells in the cerebellar flocculus and ventral paraflocculus. J. Neurophysiol., **72**: 954-973.

Lisberger, S. F., T. A. Pavelko and D. M. Broussard (1994a). Neural basis for motor learning in the vestibuloocular reflex of primates. I. Changes in the responses of brain stem neurons. J. Neurophysiol., **72**: 928-953.

Lisberger, S. G. and F. A. Miles (1980). Role of primate medial vestibular nucleus in long-term adaptive plasticity of vestibuloocular reflex. J. Neurophysiol., **43**: 1725-1745.

Lisberger, S. G., F. A. Miles and D. S. Zee (1984). Signals used to compute errors in monkey vestibuloocular reflex: Possible role of flocculus. J Neurophysiol., **52**: 1140-1153.

Lorente de No, R. (1933). Vestibulo-ocular reflex arc. Arch Neurol Psychiat., **30**: 245-291.

Maekawa, K. and J. A. Simpson (1973). Climbing fiber responses evoked in the vestibulo-cerebellum of rabbit from visual system. J.Neurorhysiol., **36**: 649-666.

Maekawa, K. and J. I. Simpson (1972). Climbing fiber activation of Purkinje cells in the flocculus by impulses transferred through the visual pathway. Brain Res., **39**: 245-251.

Maekawa, K. and T. Takeda (1975). Mossy fiber responses evoked in the cerebellar flocculus of rabbits by stimulation of the optic pathway. Brain Res., **98**: 590-595.

Marr, D. (1969). A theory of cerebellar cortex. J.Physiol. (L), **202**: 437-470.

Melvill-Jones, G., A. Berthoz and B. Segal (1984). Adaptive modification of the vestibulo-ocular reflex by mental effort in darkness. Exp. Brain Res., **56**: 149-153.

Miles, F. A. and D. J. Braitman (1980b). Long-term adaptive changes in vestibulo-ocular reflex. II. Electrophysiological observations on semicircular canal primary afferents. J Neurophysiol, **43**: 1426-1436.

Miles, F. A. and B. B. Eighmy (1980a). Long-term adaptive changes in primate vestibuloocular reflex. I. Behavioral observations. J. Neurophysiol., **43**: 1406-1425.

Miles, F. A. and J. H. Fuller (1974). Adaptive plasticity in the vestibulo-ocular responses of the rhesus monkey. Brain Res., **80**: 512-516.

Miles, F. A., J. H. Fuller, D. J. Braitman and B. M. Dow (1980c). Long-term adaptive changes in primate vestibuloocular reflex. III. Electrophysiological obsevations in flocculus of normal monkeys. J. Neurophysiol., **43**: 1437-1476.

Miles, F. A., J. H. Fuller, D. J. Braitman and B. M. Dow (1980d). Long-term adaptive changes in primate vestibuloocular reflex. IV. Electrophysiological obsevations in flocculus of adapted monkeys. J. Neurophysiol, **43**: 1477-1493.

Miles, F. A. and S. G. Lisberger (1981). Plasticity in the vestibulo-ocular reflex: A new hypothesis. Ann. Rev. Neurosci., **4**: 273-299.

Miller, J. M., J. L. Demer and A. L. Rosenbaum (1993). Effect of transposition surgery on rectus muscle paths by magnetic resonance imaging. Ophthalmology, **100**: 475-487.

Minor, L. B. and J. M. Goldberg (1990). Influence of static head position on the horizontal nystagmus evoked by caloric, rotational and optokinetic stimulation in the squirrel monkey. Exp. Brain Res., **82**: 1-13.

Minor, L. B. and J. M. Goldberg (1991). Vestibular-nerve inputs to the vestibulo-ocular reflex: a functional-ablation study in the squirrel monkey. J Neurosci, **11**: 1636-1648.

Misslisch, H., D. Tweed, M. Fetter, D. Sievering and E. Koenig (1994). Rotational kinematics of the human vestibuloocular reflex. III. Listing's law. J. Neurophysiol., **72**: 2490-2502.

Money, K. E. and J. W. Scott (1962). Functions of separate sensory receptors of non-auditory labyrinth of the cat. Amer. J. Physiol., **202**: 1211-1220.

Nagao, S. (1989). Behavior of floccular Purkinje cells correlated with adaptation of vestibulo-ocular reflex in pigmented rabbits. Exp. Brain Res., **77**: 531-540.

Paige, G. D. (1983). Vestibuloocular reflex and its interactions with visual following mechanisms in the squirrel monkey. II. Response characteristics and plasticity following unilateral inactivation of horizontal canal. J. Neurophysiol., **49**: 152-168.

Paige, G. D. and D. L. Tomko (1991). Eye movement responses to linear head motion in the squirrel monkey. II. Visual-vestibular interactions and kinematic considerations. J Neurophysiol., **65**: 1183-1196.

Peng, G. C. Y., J. F. Baker and B. W. Peterson (1994). Dynamics of directional plasticity in the human vertical vestibulo-ocular reflex. J. Vest. Res, **4**: 453-460.

Peterson, B. W., J. F. Baker and J. C. Houk (1991). A model of adaptive control of vestibuloocular reflex based on properties of cross-axis adaptation. Ann. NY Acad Sci, **627**: 319-337.

Press, W. H., S. A. Teukolsky, W. T. Vetterling and B. P. Flannery (1992). Numerical recepes in C. The art of scientific computing. Cambridge University Press, pp 994.

Raphan, T. (1995). Comparing models of velocity-position integration in three dimensions. Three-Dimensional Kinematic Principles of Eye-, Head-, and Limb Movements in Health and Disease, Tübingen, Aug 28-30, 1995, 45.

Raphan, T., B. Cohen and V. Henn (1981). Effects of gravity on rotatory nystagmus in monkeys. Ann. NY. Acad. Sci., **374**: 44-55.

Raphan, T., B. Cohen and V. Henn (1983). Nystagmus generated by sinusoidal pitch while rotating. Brain Res., **276**: 165-172.

Raphan, T., M. Dai and B. Cohen (1992). Spatial orientation of the vestibular system. Ann. N.Y. Acad. Sci. 140-157.

Raphan, T., V. Matsuo and B. Cohen (1977). A velocity storage mechanism responsible for optokinetic nystagmus (OKN), optokinetic after-nystagmus (OKAN), and vestibular nystagmus. Control of Gaze by Brain Stem Neurons. Amsterdam, Elsevier/North Holland. 37-47.

Raphan, T., V. Matsuo and B. Cohen (1979). Velocity storage in the vestibulo-ocular reflex (VOR). Exp. Brain Res., **35**: 229-248.

Raphan, T. and D. Sturm (1991). Modelling the spatio-temporal organization of velocity storage in the vestibulo-ocular reflex (VOR) by optokinetic studies. J. Neurophysiol., **66**: 1410-1421.

Reisine, H. and V. Henn (1984). Transformation in three dimensions between primary and secondary vestibular neuronal signals in the rhesus monkey. Neurosci. Abstr., **10**: 49.7.

Reisine, H. and T. Raphan (1992). Neural basis for eye velocity generation in the vestibular nuclei during off-vertical axis rotation (OVAR). Exp. Brain Res., **92**: 209-226.

Reisine, H., J. I. Simpson and V. Henn (1988). A geometric analysis of semicircular canals and induced activity in their peripheral afferents in the rhesus monkey. Ann. N.Y Acad. of Sci., **545**: 10-20.

Reisine, H., J. I. Simpson, D. Rudinger and V. Henn (1985). Combined anatomical and physiological study of semicircular canal orientation in the rhesus monkey. Neurosci. Abstr., **11**: 97.2.

Robinson, D. A. (1963). A method of measuring eye movement using a scleral search coil in a magnetic field. IEEE Trans. Bio-Med. Electrn., **10**: 137-145.

Robinson, D. A. (1975). A quantitative analysis of extraocular muscle cooperation and squint. Investigative Ophthalmology, **14**: 801-825.

Robinson, D. A. (1976). Adaptive gain control of vestibulo-ocular reflex by the cerebellum. J. Neurophysiol., **39**: 954-969.

Robinson, D. A. (1982). The use of matrices in analyzing the three-dimensional behavior of the vestibulo-ocular reflex. Biol. Cybern., **46**: 53-66.

Schultheis, L. W. and D. A. Robinson (1981). Directional plasticity of the vestibulo-ocular reflex in the cat. Ann. N.Y. Acad. Sci., **374**: 504-512.

Schultheis, L. W. and D. A. Robinson (1982). The brain-stem matrix of the vestibulo-ocular reflex. Physiological and pathological aspects of eye movements. The

Hague-Boston-London, Dr. W. Junk Publishers. 121-125.

Shimazu, H. and W. Precht (1965). Tonic and kinetic responses of cat's vestibular neurons to horizontal angular acceleration. J. Neurophysiol., **28**: 991-1013.

Simonsz, H. J. (1990). The mechanics of squint surgery. Paris, CERES, pp 148.

Simpson, J. I. and W. Graf (1981). Eye muscle geometry and compensatory eye movements in lateral eyed and frontal eyed animals. Vestibular and Oculomotor Physiology. International Meeting of the Barany Society. 20-30.

Singh, A., F. E. Thau, T. Raphan and B. Cohen (1981). Detection of saccades by a maximum likelihood ratio criterion. 34 ACEMB . Houston Texas, 136.

Sirota, M. G., B. M. Babaev, I. N. Beloozerova, A. N. Nyrova, S. B. Yakushin and I. B. Kozlovskaya (1988). Neuronal activity of nucleus vestibularis during coordinated movement of eyes and head in microgravitation. The Physiologist, **31**: 8-9.

Sirota, M. G., B. M. Babayev, I. B. Beloozerova, A. N. Nyrova, S. B. Yakushin and I. B. Kozlovskaya (1987). Characteristic of vestibular reactions to canal and otolith stimulation at an early stage of exposure to microgravity. The Physiologist, **30**: S82-S84.

Sirota, M. G., I. N. Beloozerova, B. M. Babaev, S. B. Yakushin and I. B. Kozlovskaya (1989b). Effects of microgravity on vestibular function in monkey. Results of space flight studies. Eleventh Ann. Meeting IUPS Commission on Gravitational Physiology, Lion, France, 25-27 Sept., 2.

Sirota, M. G., I. N. Beloozerova, S. B. Yakushin, B. M. Babaev and I. B. Kozlovskaya (1990b). Influence of microgravity to vestibular function of monkey. XII International Meeting of gravitational physiology, Leningrad 14-19 October, 63-64 (in Russian).

Sirota, M. G., I. N. Beloozerova, S. B. Yakushin, B. M. Babaev and I. B. Kozlovskaya (1990c). Changes in neuronal activity of vestibular nuclei during active head movements in microgravity. XII International Meeting of gravitational physiology, Leningrad 14-19 October, 63 (in Russian).

Sirota, M. G., I. N. Beloozerova, S. B. Yakushin, A. M. Ivanov and I. B. Kozlovskaya (1990a). Vestibulo-motor interaction of monkey in microgravity. Eye-head coordination test. XI Meeting in space biology and medicine, Kaluga, 342-343 (in Russian).

Sirota, M. G., I. N. Beloozerova, S. B. Yakushin, A. M. Ivanov and I. B. Kozlovskaya (1991a). Kinematic of saccades and head movement in eye-head coordination test of monkey. Experiment on biosatellite "Cosmos-2044" board. International Meeting "Biosatellite Cosmos", Leningrad 12-15 August, 113 (in Russian).

Sirota, M. G., I. N. Beloozerova, S. B. Yakushin, A. M. Ivanov and I. B. Kozlovskaya (1991b). Gain of vestibulo-ocular reflex of monkey in microgravity. Experiment on biosatellite "Cosmos-2044" boarad. International Meeting "Biosatellite Cosmos", Leningrad 12-15 August, 114 (in Russian).

Sirota, M. G., I. N. Beloozerova, S. B. Yakushin and I. B. Kozlovskaya (1989a). Eye-head coordination during adaptation to microgravity. Regulation of sensor-motor functions, Vinniza, USSR, 140 (in Russian).

Skavenski, A. A. and D. A. Robinson (1973). Role of abducens neurons in vestibuloocular reflex. J. Neurophysiol., **36**: 724-738.

Snedecor, G. W. and W. G. Cochran (1967). Statistical methods. Iowa, The Iowa State University Press, pp 593.

Stein, B. M. and M. B. Carpenter (1967). Central projections of portions of the vestibular ganglia innervating specific parts of the labyrinth in the rhesus monkey. Am. J. Anat., **120**: 281-318.

Steinhausen (1933). Über die Beobachtung der Cupula in den Bogengansampullen des Labyrinths des lebenden Hechts. Arch Ges Physiol, **232**: 500-512.

Suzuki, J., B. Cohen and M. B. Bender (1964). Compensatory eye movements induced by vertical semicircular canal stimulation. Exp. Neurol., **9**: 137-160.

Suzuki, J.-I. and B. Cohen (1966). Integration of semicircular canal activity. J.Neurophysiol., **29**: 981-995.

Suzuki, J.-I., A. Kodama, Y. Arai, V. Henn and B. Cohen (1995). Paired and unpaired pluggings of the semicircular canals in monkeys related with physiological and pathological findings. Three-Dimensional Kinematic Principles of Eye-, Head-, and Limb Movements in Health and Disease, Tübingen, Aug 28-30, 1995, 54.

Suzuki, J.-I., A. Kodame, B. Cohen and V. Henn (1991). Canal-plugging in the rhesus monkey: A tool to study the contribution of individual canals to nystagmus generation. Acta Otolaryngol (Suppl), **481**: 91-93.

Szentagothai, J. (1950). The elementary vestibulo-ocular reflex arc. J. Neurophysiol., **13**: 395-407.

Szentagothai, J. and M. A. Arbib (1974). Conceptual models of neural organization. A report based on an NRP Work Session held October 1-3, 1972 and updated by participants. Boston, Homsy.

Tokumasu, K., K. Goto and B. Cohen (1965). Eye movements produced by the superior oblique muscle. Archives of Ophtalmology, **73**: 851-862.

Tweed, D., D. Sievering, H. Misslisch, M. Fetter, D. Zee and E. Koenig (1994). Rotational kinematics of the human vestibuloocular reflex. I. Gain matrices. J. Neurophysiol., **72**: 2467-2479.

Uemura, T. and B. Cohen (1975). Loss of optokinetic after-nystagmus (OKAN) after dorsal medullary reticular formation (MRF) lesions. Proceedings of the Barany Society. 101-105.

Virre, E., D. Tweed, K. Milnor and T. Vilis (1986). A reexamination of the gain of the vestibuloocular reflex. J. Neurophysiol., **56**: 439-450.

Waespe, W., U. Buttner and V. Henn (1981). Visual-vestibular interaction in the flocculus of the alert monkey I. Input activity. Exp.Brain Res., **43**: 337-348.

Watanabe, E. (1984). Neuronal events correlated with long-term adaptation of horizontal vestibuloocular reflex in the primate flocculus. Brain Res., **297**: 169-174.

Wilson, V. J. and G. Melvill-Jones (1979). Mammalian vestibular physiology. New York, Plenum Press.

Yakushin, S. B., I. N. Beloozerova, M. G. Sirota and I. B. Kozlovskaya (1989). Cerebellar and brain stem structures activity during semicircular canals stimulation in microgravity. Regulation of sensomotor functions, Vinniza, USSR, 179 (in Russian).

Yakushin, S. B., M. Dai, J.-I. Suzuki, T. Raphan and B. Cohen (1992b). Contribution of the vertical semicircular canals to the horizontal and roll components of the vestibulo-ocular reflex. XVIIth Barany Society Meeting, Czechoslovakia, June 1-5, 162.

Yakushin, S. B., M. Dai, J.-I. Suzuki, T. Raphan and B. Cohen (1995). Semicircular canal contributions to the three-dimensional vestibuloocular reflex: A model-based approach. J. Neurophysiol., **74**: 2722-2738.

Yakushin, S. B., M. G. Sirota, I. N. Beloozerova, B. M. Babaev and I. B. Kozlovskaya (1992a). Eye-head coordination of monkey (Macaca mulatta) in gaze fixation reaction during "Cosmos" biosatellites flight. XVIIth Barany Society Meeting, Czechoslovakia, June 1-5,

Yamamoto, M. (1979). Topographical representation in rabbit cerebellar flocculus for various inputs from the brainstem investigated by means of retrograde axonal transport of horseradish peroxidase. Neurosci. Lett., **12**: 29-34.

Yue, Q., D. Straumann and V. Henn (1994). Three-dimensional characteristics of rhesus monkey vestibular nystagmus after velocity steps. J. Vestib. Res., **4**: 313-323.

Zee, D. S., A. Yamazaki, P. H. Butler and G. Gucer (1981). Effects of ablation of flocculus and paraflocculus on eye movements in primate. J. Neurophysiol., **46**: 878-899.